



CISM COURSES AND LECTURES NO. 316
INTERNATIONAL CENTRE FOR MECHANICAL SCIENCES

ADVANCED PROBLEMS IN BRIDGE CONSTRUCTION

EDITED BY

G. CREAZZA/M. MELE

SPRINGER-VERLAG WIEN GMBH



INTERNATIONAL CENTRE FOR MECHANICAL SCIENCES

COURSES AND LECTURES - No. 316



ADVANCED PROBLEMS
IN BRIDGE CONSTRUCTION

EDITED BY

G. CREAZZA

UNIVERSITY OF VENICE

M. MELE

UNIVERSITY OF ROME



SPRINGER-VERLAG WIEN GMBH

Le spese di stampa di questo volume sono in parte coperte da
contributi del Consiglio Nazionale delle Ricerche.

This volume contains 243 illustrations.

This work is subject to copyright.

All rights are reserved,

whether the whole or part of the material is concerned
specifically those of translation, reprinting, re-use of illustrations,
broadcasting, reproduction by photocopying machine
or similar means, and storage in data banks.

© 1991 by Springer-Verlag Wien

Originally published by Springer Verlag Wien-New York in 1991

In order to make this volume available as economically and as
rapidly as possible the authors' typescripts have been
reproduced in their original forms. This method unfortunately
has its typographical limitations but it is hoped that they in no
way distract the reader.

ISBN 978-3-211-82318-7

ISBN 978-3-7091-2614-1 (eBook)

DOI 10.1007/978-3-7091-2614-1

PREFACE

The volume collects the lecture notes of a course held at the Department of Structural Engineering and Geotechnics of the International Centre for Mechanical Sciences dealing with the most and modern topical problems of bridge design.

The topics presented allow to tackle both theoretical-analytical as well as technical-constructive aspects of the design problem, pointing out how in the case of bridges, specifically for long span bridges, the two aspects are absolutely inseparable.

In modern bridges, reasons of technical and economic feasibility oblige an extreme parceling of the construction process, with the consequent need to revise, with respect to the past, both design concepts as well as the theoretical apparatus of analysis that governs it.

All this can clearly be derived from reading the present volume, in which the different contributions stress theoretical and technical questions of particular interest and topicality, without claiming to approach them systematically, but offering clear procedural rules and trend indications.

With reference to the theoretical approach, some topics of particular importance are reviewed, such as the possibility of using limit analysis, the simplification of the design process for bridges, durability, and computer aided design.

These topics are presented with the aim of providing design tools and not specific analytical verification procedures, for which it is necessary to consult specialized texts.

For what concerns the bridge typologies and the corresponding construction problems, the emphasis is mostly on the ones still in an evolutionary phase, that is long span suspended/stayed bridges and cantilever built bridges with prefabricated segments.

Giuseppe Creazza

Michele Mele

CONTENTS

	Page
Preface	
Bridges: some problems and some solutions <i>G. Macchi</i>	1
New trends and developments in bridge construction <i>R. Walther</i>	1 1
Cantilever built bridges with prefabricated segments <i>R. Lacroix</i>	2 7
Composite bridges: new developments in Europe <i>P. Dubas</i>	5 5
Structural systems for cable suspended bridges <i>N. J. Gimsing</i>	6 7
Some basic problems in the design of long span cable stayed bridges <i>F. De Miranda</i>	9 1
On the durability of reinforced and prestressed concrete structures <i>M. Mele, E. Siviero</i>	1 2 1
Cracking due to thermal effects on bridges <i>H. Falkner</i>	1 6 1
Structural effects of time dependent behaviour of concrete <i>F. Mola</i>	1 7 5
Technological factors in the design of foundation piles <i>C. Viggiani</i>	2 2 3
Computer based structural analysis of bridges <i>S. Odorizzi</i>	2 5 7

**BRIDGES
SOME PROBLEMS
AND SOME SOLUTIONS**

**G. Macchi
University of Pavia, Pavia, Italy**

This introduction to the course is not emphasizing such applications of the modern technique which are at the frontier of the present possibilities as the bridge of the Messina strait or the Gibraltar strait, fascinating problems certainly reserved to very exclusive groups of engineers.

Nevertheless, a vaste field of activities for the engineers is appearing in new roles: both the repair works and the reconstruction of new bridges in the special environment formed in the last decades require a substantial change of the disciplinar bases for our profession.

1. A NEW ROLE FOR THE ENGINEERS: DIAGNOSIS AND STRENGHTENING

The new roles do not require a further sofistication of statics and dynamics of the great structural systems, but rather the improvement of the knowledge of the properties of construction materials, their behaviour in time, particularly on the chemical attack of the environment and under the fatigue effects. They require the analysis of structural elements much more complex than the usual ones, the study of different associations between steel and concrete, and a more systematic use of the non-linear analysis of structures in which steel and concrete are associated.

The engineer is often called to study existing structures and therefore he needs an education on such diagnostic techniques which have been so far rarely useful to him, simply called to design new works whith perfectly known materials and with freely selected techniques.

The 3 Arch Bridge in Venice is a personal experience in the field of restoring bridges, it is for me a symbol of this new role prepared for engineers; the monument is in this case not only a "monument", but also an important resisting structure to be analyzed and to be strengthened according to the rules of our scientific and technical knowledge.

The tools to be used in such occasions are not rigorously the same of our daily profession. It is necessary a further development of the knowledge of materials nearly unknown to us until yesterday, as the ancient masonry, improve the knowledge of the degradation processes, analyze structures having a so high complexity that our usual analysis methods cannot be used: structures nevertheless very familiar to the engineers living four hundred years ago.

The problems are not very different when often we are called to assess the stability or the residual life of reinforced concrete works built in the first decades of this century or even in the fifties or sixties. In such cases the traditional strength of materials helps very little and the need arises of improving our knowledge of the corrosion processes of reinforcement within concrete, transformed by chemical processes due to the environment, and extrapolate from our still scarce knowledge of the development in time of such phenomena a prognosis and proposals for strengthening.

On the bow-string bridge of the Polyclinic in Pavia I had the opportunity of completely live the problems posed by this new situation created by a rapid increase of the effects of the environment on the structures.

The discussion of the alternatives between demolition and repair, unfortunately took place in the absence of precise parameters allowing to judge (in a suitable cost-benefit analysis) the advantages of one or the other of the two alternative solutions.

The chemistry of materials is helping, but the development in time of these phenomena, their dependency on several environmental quantities, the real transformation of the resistance mechanisms in presence of reinforcements in advanced phase of corrosion, are still basically unknown. The engineer is therefore often forced to take a decision with insufficient information.

Nevertheless, this will be our fundamental role in the years to come, all the owners of roads and railways in the world agree in thinking that the highest percentage of available resources will be devoted in the next decades to the maintenance and repair, or even to replacement of existing structures instead of construction of new infrastructures.

The International Association for Bridge and Structural Engineering IABSE will held next September in Lisbon an International Symposium on this subject, in general on the subject of the durability of structures, which is today one of the fundamental items for the structural engineering.

I will report there on the events of the bridge in Pavia, which led to the decision of demolition and rebuilding of the works, and I will indicate the decisional process which took place; this type of decision is now current practice even on our highways.

Fatigue stresses monitoring under traffic has been recently performed on the Pecora Vecchia Viaduct of the Autostrada Florence-Bologna; the measurements took place in view of the demolition of the bridge.

Such studies are performed under the belief that the degradation phenomena which took place on the viaducts of our highways and which are generally attributed to the chemical attack (particularly from the salts used to avoid frost effects) are in reality more complex physical and chemical phenomena on concrete. On such a degradation an important role seems to have the mechanical effect of the dynamic repeated action due to the transit of more and more heavy vehicles at more and more higher speed. The results of such measurements are not yet complete and have not been published. In cooperation with Professor Radogna and his co-workers, nevertheless, it seems to us that the degradation of the concrete structures takes place under a combined and synergetic action of chemical degradation and mechanical action.

The transits of vehicles are considerably increased since the time of design of such works; the load per axle of the vehicles is also considerably increased, most of the heavy vehicles are very near to the limit of the bearing capacity of the bridges; the transit speed is considerably higher than the speeds usual at the time of the construction. From measures recorded in few hours it is possible to extrapolate to several millions the number of the significant excursions in order to study the effects of fatigue during a life of thirty years; they explain the high level of degradation presently observed and the necessity of essential intervention or even the demolition of the structure.

A difficult and sophisticated professional work is open now for the engineer: it is dealing with the interventions for strengthening and repair, an extremely difficult profession. A multiplicity of materials is on the market, not always fit to the case, and not always easy to control. Further problems are posed by interaction processes with the existing materials of the structure.

2. HOW BUILD DURABLE BRIDGES IN THE FUTURE?

The experience done in the field of degradation leads to the problem of techniques suitable for building in the future structures more durable than done thirty years ago. In lack of more sophisticated scientific approaches we may learn from the most frequently observed phenomena. The most damaged structural elements are the slabs: they are thin, they are reinforced with small diameter steel, directly subject to the action of chemical corrosion and to the fatigue action of heavy traffic.

Carbonation of concrete reaches to 50 or 100 mm in the thin webs of structural elements and produced the corrosion of the transversal reinforcement before that of the longitudinal reinforcement.

Those considerations should lead to conceive compact structures, with reinforcements concentrated at a considerable distance from the external surface and with reinforcement less sensitive to corrosion, that is large diameter bars.

A second important cause of degradation have been the anchorages of prestressing reinforcement when they are applied outside the structure. The elimination, as long as possible, of such anchorages is surely a good measure for higher durability. Finally, expansion joints and moving bearings showed to be among the most vulnerable elements of our bridges.

The joints between adjacent decks did not find adequate solutions for water-proofing, and were a cause of penetration of water, of de-icing salts, and therefore of considerable corrosion.

Even the construction joints, which have been then closed (so that through them the prestressing bars have a continuity) have been incorrectly executed for the lack of precompression in the joint itself, and then formation of cracks and further corrosive actions.

The supports of decks on the piles were also subject to frequent and systematic damages with necessity of substitution. The question arises whether, instead of creating ideally rational and simple boundary conditions, particularly difficult or excessively expensive, is it not preferable to create a continuity between supports and deck. In such a way supporting devices and expansion joints may be reduced, and used where they are strictly necessary, and where it is possible to guarantee the best quality and durability by adequate (even expensive) devices.

At the FIP Congress in New York, nearly twenty years ago, I indicated such development lines for the durable construction of bridges. After a tiring and difficult work of restoration on just executed works on the Autostrada between Venice and Trieste, I succeeded in convincing the owners to realize a first viaduct along my new ideas: the bridge on the river Meduna. It was a solid prestressed slab, continuous along its complete length; this bridge has been a prototype which has been later on repeated several times with excellent results, even from the economic point of view.

One of such works is the viaduct Cadore, here in Udine.

Then, when possible, in the central part of the work the deck has been built solidly connected with the piles, so that the supporting devices have been eliminated.

The prestressing reinforcement is done with 40 mm diameter bars, continuous for the complete length, without external intermediate anchorages, therefore without possibility of chemical attack.

A further element of knowledge has been achieved more recently: carbonation of concrete, and all the corrosion phenomena of the reinforcement, may be considerably reduced by a more compact external surface of the structure. The porosity of concrete may be reduced in such a way that the penetration of water and CO₂ may be sensibly reduced with the new technique of high strength concrete. This option has to be seriously considered today, not in view of reducing the resisting sections of the structures, but in order to realize more durable concrete.

3. BRIDGES WITH UNBONDED CABLES

If considered from the point of view of durability, the solutions for bridges recently suggested by our French colleagues are surprising: they suggest truss structures with extremely thin members, caisson decks with very thin webs, prestressing cables out of the section.

Such solutions are justified in the following way:

- i) : prestressing cables within the concrete section hinder the perfect execution and the perfect compaction, so that to put outside the large sections of prestressing cables may be better
- ii) : prestressing cables may better be protected outside by different means, and may be subject to an easier control of their possible deterioration; substitution is easy when their corrosion appears.

Such a philosophy, which is just opposite to that previously described, has its own logic and its own conception of maintenance.

The merits of the two opposite attitudes may be judged only case by case; the French solution, which is based on an efficient maintenance and on a continuous diagnosis of the degradation of reinforcement, is not suitable for cases well known to our experience.

Continuous monitoring and sudden intervention in case of necessity are certainly possible in the case of great engineering works; more difficult is to imagine that such a perfect organization would work in that net of roads of tens of thousand kilometers which is the ordinary net.

The bridges with external unbonded prestress lead me to the second subject which was intended to be treated in this lecture; that is the necessity of new methods of analysis for new types of structures, in particular the systematic use of nonlinear analysis. I am confident that no Italian engineer is convinced to be allowed to calculate the ultimate safety of such bridges with the usual methods suggested by our national code. The bond between steel and concrete, which is the essential assumption of our method of verification, is lacking in this case; it is therefore necessary to take account of the independence of the two materials in a nonlinear analysis which takes rigorously account of the compatibility of deformation.

The consequence of the lack of bond is that concrete deforms locally without a similar local strain in the steel; the strain of steel is distributed along a great length and therefore the stress in steel may increase very little (or nothing at all) at the moment of collapse of the structure. This mechanism is not difficult to be followed for relatively simple structures, but requires to abandon the old methods of analysis and to use rather sophisticated nonlinear methods.

4. SLENDER MEMBERS

Another problem more and more frequently appearing in the design of bridges is that of slender members, and also in this field nonlinear analysis is a technique without alternatives. The problem arises for the tall and very flexible piles of viaducts and bridges and for the very long stays of the most modern cable-stayed bridges; they are the most specific field of application of the nonlinear methods of analysis of reinforced concrete.

Classic methods of analysis for instability cannot be applied to such structures, and the analysis may only be performed with methods taking into account the geometrical nonlinearity and nonlinearities of materials.

In this field the limit states analysis of reinforced concrete led in the last decades to substantial improvements. Slenderness may be extremely high, so that the check of stability would be impossible without adequate consideration of two fundamental factors having an impact on the second order effects: the value of the axial force and the quantity of longitudinal reinforcement. The Eulerian slenderness is not a sufficient parameter even for preliminary design of slender members. Effects of reinforcement on second order effects cannot be neglected.

Furthermore, under the action of permanent loads it is not allowed to neglect the effects of creep; it seems therefore worth to remember how in the field of such problems a precious help may be found in the use of parametric methods, which have been developed in the last 10 years for reinforced concrete sway frames. The available numeric testing is very sophisticated and allows the extension of results to a large number of cases, taking into account: tensile strength, cracking of the section, tension-stiffening, nonlinear behaviour of concrete, creep: for all of them the most modern models have been used.

The first diagram shows how the second order effects may be reduced, at a constant value of the axial load, by increasing the reinforcement, which is represented by the geometrical percentage: it is very easy to understand that under an increase of flexural moments the best way to resist them is an increase of reinforcement.

The second diagram shows how even very slender members may be subject to rather limited second order moments if the axial load is limited. This concept is easy to understand. Very slender members may result well acceptable, if subject to small axial loads. All these concepts may be synthesized in the third diagram here presented, in which the abscissa is a newly proposed equivalent slenderness λ^* in which the Eulerian slenderness λ is modified taking into account the geometrical percentage of reinforcement ρ , and the value of the reduced axial load, ν , that is the ratio between the existing axial load and the maximum which may be sustained by the section.

Such two parameters, together with a correction taking into account the resistance of concrete (in comparison with a conventional resistance) may easily be assumed as criteria for design of very slender elements to be subject afterwards to a more complete and sophisticated analysis when the final project has to be established.

5. NONLINEAR ANALYSIS

The mentioned problems are not the only ones in which a nonlinear analysis is useful. I will only mention the necessity to know the real safety margins of the great cable-stayed bridges, which usually are analyzed in extremely sophisticated way for the service conditions, but for which the safety is very rarely analyzed.

According to the usual criteria of limit states, it would be necessary to contemporarily operate the reduction of the strength of materials, an increase of the external actions and a correction on the unfavorable way of the state of coaction introduced by the tensioning of the stays, which are subject to a very important model uncertainty. It is certain that the great designers of the most important of such bridges are perfectly aware of this necessity, but in the technical literature very seldom this kind of considerations are found.

I think that more care should be given in the future to these problems, and that ultimate state verifications of cable-stayed bridges should be systematically required and performed.

REFERENCES

1. G.MACCHI, G.NOCCA - Assessment of a Bow-String Bridge 50 Years Old in Pavia - Estratto dai Proc. of IABSE Symp. on Durability of Concrete Structures, Lisbon, 1989
2. G.MACCHI, E.F.RADOGNA, A.L.MATERAZZI - Synergetic Effects of Environmental Actions and Fatigue - Estratto dai Proc. of IABSE Symp. on Durability of Concrete Structures, Lisbon, 1989
3. A.CAUVIN, G.MACCHI - Définition modifiée d'éclatement des colonnes dans les ossatures en béton armé à noeuds déplaçables - Estratto da FESTSCHRIFT Prof. Dr. Bruno Thürlimann zum 60 - Geburtstag 1983
4. G.MACCHI - A Model for Unbonded Tendons Prestressed Structures - Int. Symp. on Fundamental Theory of Reinforced and Prestressed Concrete, NIT, Nanjing, Cina, Sept. 18-20, 1986, pp.46-53
5. G.MACCHI - Design Philosophy of the CEB-FIP Model Code With Respect to Non-Linearity - Estratto dai Proc. of FIP Symp., Jerusalem, Sept. 4-9, 1988



**Fig.1. Three Arch Bridge
in Venice (16th century).**

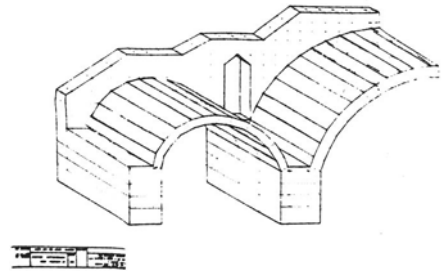


**Fig.2. Three Arch Bridge
in Venice (FEM model)**



**Fig.3. Bow-string r.c.
bridge in Pavia(1935)
corrosion of reinforcement.**



**Fig.4. Corrosion of prestressing
strands in a bridge to be
demolished.**

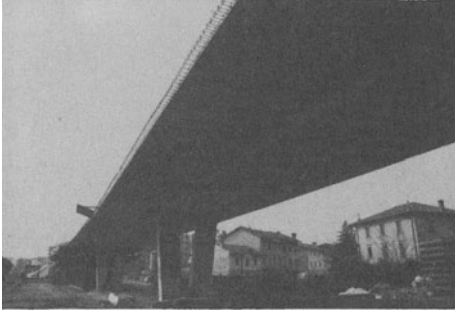


Fig.5. Continuous slab viaduct in Udine (Viadotto Cadore).

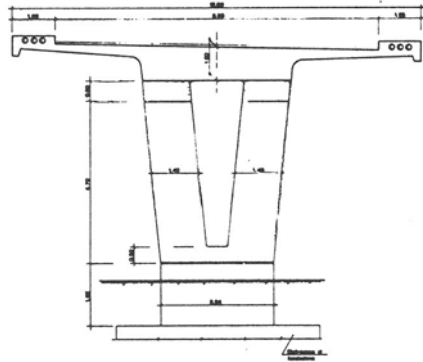


Fig.6. View of Cadore Viaduct.

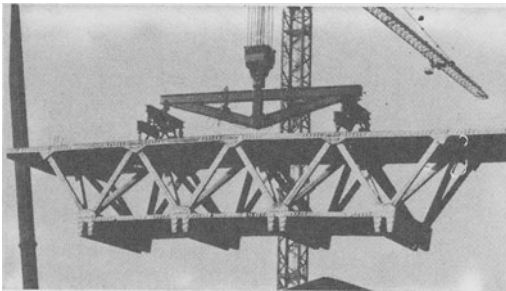


Fig.7. Truss bridge with external unbonded prestress.

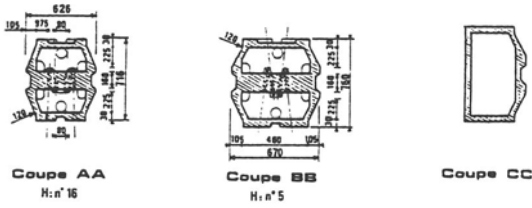


Fig. 8. A slender structure: the mast of a cable-stayed bridge.

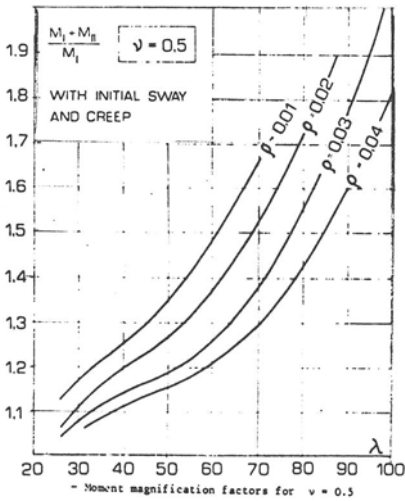
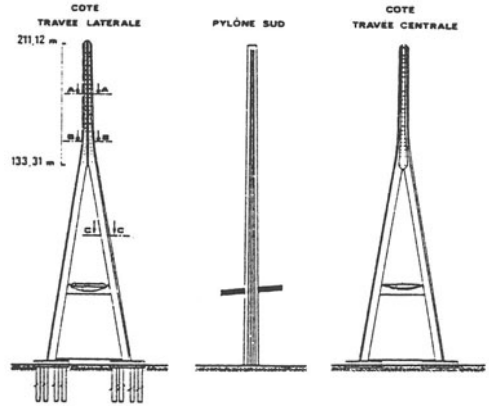


Fig. 9. Effect of reinforcement (ρ) on second order effects of slender r.c. frames.

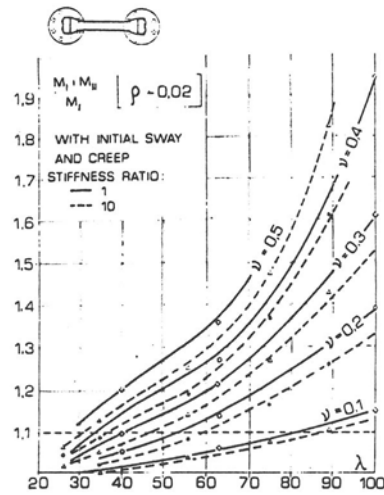


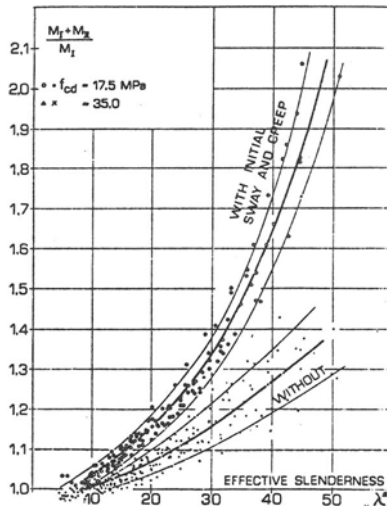
Fig. 10. Effect of the axial load (ν) on second order effects.

Fig. 11. Second order effect

$$\frac{M_I + M_{II}}{M_I}$$

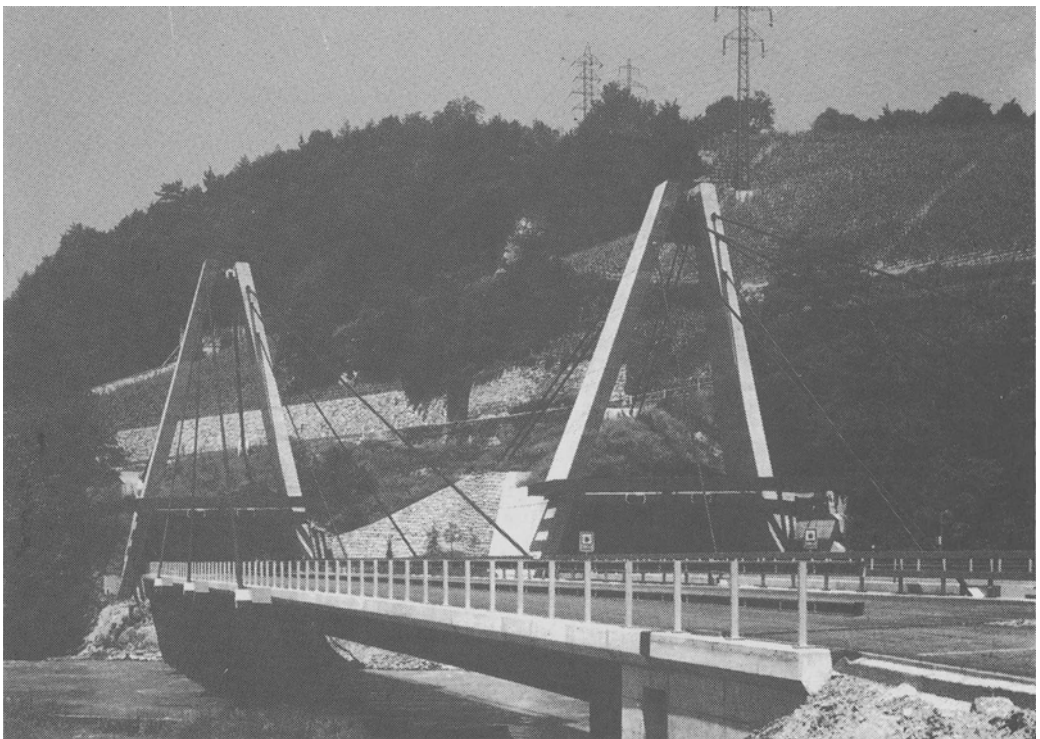
as a function of the equivalent slenderness

$$\lambda^* = \lambda \frac{\nu^{0.6}}{1 + 15\nu} \left(\frac{f_{cd}}{17.5} \right)^{0.5} \text{ (MPa)}$$



**NEW TRENDS AND DEVELOPMENTS
IN BRIDGE CONSTRUCTION**

**R. Walther
EPFL, Lausanne, Switzerland**



1. General remarks.

In recent years a great many innovative developments have taken place in modern bridge construction, as will be described in the following. However, it has to be pointed out that important and noteworthy as they are, they hardly constitute an outright revolution as for example the invention of prestressing did some fifty years ago. The most striking development can undoubtedly be found in the surge of cable-stayed bridge construction with concrete decks and towers, which are nowadays being built in great numbers almost anywhere in the world. The idea of supporting structures by stays is indeed quite old the first application dating back some 200 years and it seems rather surprising that the actual break-through had to wait for so long a time. These important aspects of modern bridge construction will be dealt with at the end of this presentation. New developments which are likely to improve and innovate bridge design in the coming years will now be discussed.

2. Design philosophy and analysis.

Our generation has certainly been decisively marked by the explosive entry of modern computer techniques used in the design process. Highly sophisticated and reliable programs of Computer Aided Design (CAD) are now operational and widely used in practice. While this does indeed greatly facilitate the daily work and allows complicated structures to be analysed relatively easily and precisely, it may be rightly questioned, whether in the long run it will really help to further the innovation and creation of new structures. One should never lose sight of the fact that by far the most decisive and challenging part of good engineering, which governs all other aspects, is and will always be, the search for the most appropriate basic concept, an art which no computer can assume and one which is incidentally very difficult to teach and to master. As an example the still beautiful Brooklyn Bridge built over one hundred years ago by John Roebling may be cited. At that time the available theoretical tools did not permit the analysis of such a complicated highly indeterminate static system correctly, yet due to his intuition and ingenuity

Roebing was able to imagine and localize a novel load carrying concept made up of a skilful combination of suspension and stay cables.

For the design he used a greatly simplified but appropriate approach which today would be termed the statical method of the theory of plasticity. He attributed one part of the loads to be carried by the suspension cables, which could already then be analysed by the catenary equation and the other part by the stays, the forces of which he determined by simple equilibrium considerations.

It took nearly a century to recognize the potential advantages of the theory of plasticity, which is the simplest and most appropriate method of assessing the inherent structural safety of statically indeterminate systems. Most modern codes today require separate verifications, one to guarantee the serviceability (SLS; serviceability limit state according to the CEB terminology) and the other to satisfy the safety requirements (ULS, ultimate limit state).

The clear distinction of the purpose of these two verifications permits us to choose the appropriate method for each, which was not really the case with the ancient concept of allowable stresses. Since at service loads prestressed concrete structures behave more or less elastically, it seems only logical to rely on the theory of elasticity. In many cases, especially in bridge design, the SLS is the determining criterion and the fear that the application of the theory of plasticity might lead to unsatisfactory or even dangerous structures is thus wholly unwarranted. In the case of the free cantilever or incrementally launched bridges the governing criterion are the prevention of cracks and the limitation of deformations during the critical erection phases, both of which have to be checked on the basis of elastic or quasi-elastic analysis by taking into account all the relevant phenomena including shrinkage, creep, relaxation and temperature effects.

It is however of prime importance to recognize that those particular effects just mentioned have in general no or only insignificant influence on structural safety, as the theory of plasticity or any other non-linear analysis clearly reveals and what can also be verified experimentally. Thus there is really no need to consider the effects due to shrinkage, creep and temperature, sometimes even increased by arbitrary load factors, for the ULS check.

The recognition of these facts often permits structural elements such as columns, piers or pylons to be built more elegantly and more importantly to

avoid expansion joints and mechanical bearing devices, which are always susceptible to premature deterioration.

The theory of plasticity gives also a clear answer to the often discussed question of how to treat the hyperstatical moments of prestress for the ULS check. Even today many codes stipulate formulae of the type:

$$M_u > \gamma_Q M_Q + \gamma_p M_p^h$$

where:

M_u ultimate moment at the section considered

$\gamma_Q M_Q$ moment due to load effects increased by the load factor (1.6-1.9)

M_p^h hyperstatical (secondary) moment of prestress.

γ_p load factor of M_p^h (varying between 0.8 and 1.3 depending on the code considered).

Again it has to be stressed that the hyperstatical moments pertain to the elastic state and can no longer be clearly defined at the ultimate limit state due to the considerable moment redistribution which will have taken place. While the formula just mentioned may yield satisfactory results in most cases, there are others (inverted T-beams for example) fig 1, where the shifting of the moment closure line stipulated by the term $\gamma_p M_p^h$ goes in the wrong direction. The resulting sectional safety factors g , calculated backwards by assuming $\gamma_p = 1$ (first line in the table of figure 1) and $\gamma_p = 1,3$ (second line) clearly show the inconsistency of such approaches. Furthermore it is sometimes recommended to take $\gamma_p = 0.8$ if M_p acts favourably and $\gamma_p = 1.2$ in the unfavourable case, which means that the global system would not even satisfy the equilibrium conditions and the resulting global safety, which is identical for a T-beam and an inverted T-beam (last line in the table of figure 1). No such ambiguities are met if one performs the ULS check by the statical method of the theory of plasticity, which clearly assesses the effective distribution of internal forces.

3. Materials.

By applying advanced concrete technology it is now possible to obtain very high strength concretes of about 100 N/mm² or even more under field conditions, and without exorbitant costs. It is true that compressive strength values of 120 N/mm² have been obtained experimentally under laboratory

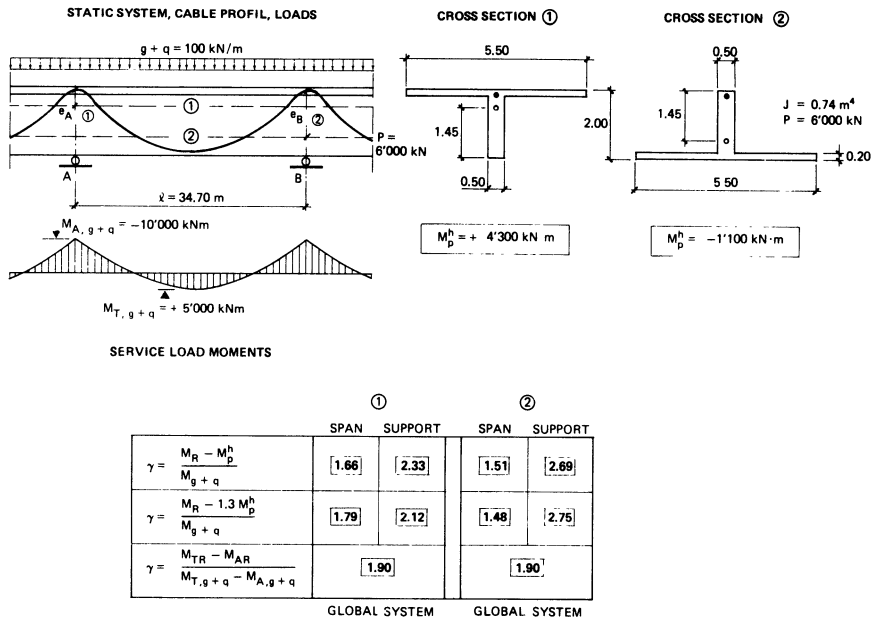


Fig 1

conditions before, but it is only recently that these concretes have become commercially available.

For concrete bridges of short or medium span the necessary dimensions are often dictated by serviceability and detailing requirements (deflection, cover, durability etc) rather than by the concrete compressive strength and therefore one might feel that the use of high strength concrete is not really relevant for bridges, except for members heavily subjected to compression such as columns, piers, pylons or compression chords of cantilever bridges.

There are however, other properties of these concretes which are potentially of great interest in structural engineering, namely :

- very high strength concretes can reduce creep and shrinkage up to 50% compared with normal concrete.
- considerable improvement to the resistance to chemical aggression, notably greater protection against corrosion of the reinforcement.
- improved freeze-thaw resistance.
- greater abrasion resistance.

The main problem with high strength concretes is that their ductility is decreased appreciably and this creates many problems (fig 2).

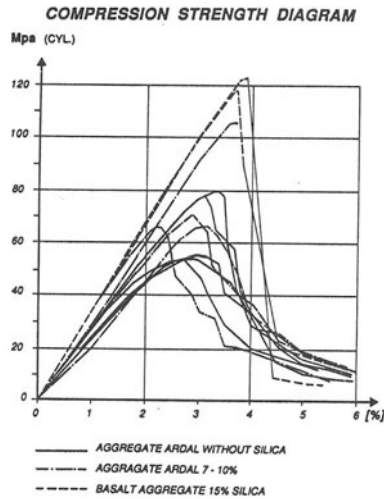


Fig. 2. Stress strain diagram for concretes of different strengths.

This fact is all the more crucial as modern design concepts are based on the theory of plasticity or other non-linear methods, which are only applicable for ductile materials. However it should be noted that one way of increasing the ductility of high strength concretes is by proper detailing. A good example of this is tightly wrapped transverse reinforcement. Also it has been shown experimentally that decreasing the stirrup spacing means that the lateral deformations which a column could sustain without any loss of compression capacity increases substantially. There is on the other hand, a limit to the amount of transverse reinforcement lest not to impair the necessary compaction.

Composite construction is another way of producing the concrete as ductile as possible. By placing the deformable steel section at the surface of the concrete member and then encasing the two as a monolithic section the ductility of the concrete is increased.

This solution was recently proposed by Prof. Schlaich and the author in their prize winning project of the new Williamsburg Bridge in New York (fig. 3). The slender pylons were considered as a composite stiff steel casing filled with very high strength concrete.

A good example of composite construction is high strength concrete filled steel tubes. In this case the ductility, load bearing capacity and compacting of



Fig. 3. Proposal for the new Williamsburg Bridge.

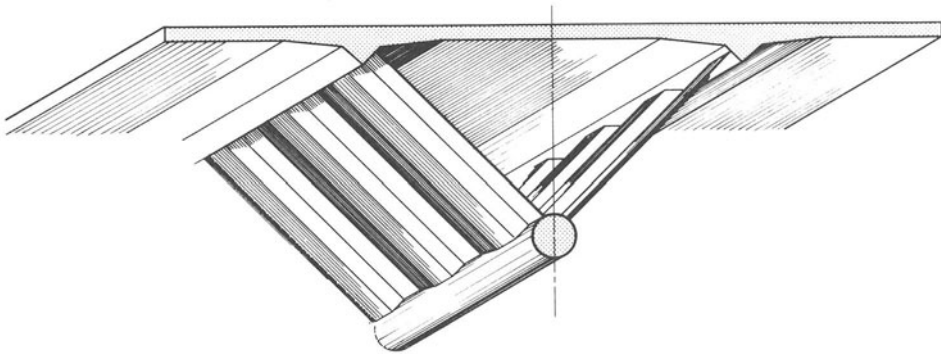


Fig. 4

concrete are all improved. French engineers have recently adopted this idea in bridge construction by using a concrete filled steel tube as the lower cord of a bridge section as shown in fig 4.

4. Skew slabs.

Urban conditions for overpasses and underpasses quite often require that skew bridges of moderate spans be used for which solid prestressed concrete slabs are usually best suited. For such slabs the customary distinction between primary and hyperstatic load effects due to prestress cannot be applied since their internal hyperstaticity is infinite.

In principle, the serviceability limit state is checked by an elastic analysis. However, even small micro-cracking can already lead to considerable redistribution of stresses which has to be accounted for in the analysis. The real deflections often become larger than the calculated values, while theoretical moment peaks, e.g. in obtuse angles, are of little significance since neither are they necessary for equilibrium, nor do they appreciably affect the general crack development. A minimum reinforcement according to detailing rules will in general be sufficient in these regions.

Unfortunately, the statical method of the theory of plasticity does not readily lend itself to ULS-checks of skew slabs. Even relatively modern finite element calculations yield only the elastic distribution of stresses, which do not adequately reproduce the actual conditions of the ultimate limit state. In reality, this can only be achieved satisfactorily by using non-linear finite elements, which are not readily available and whose application for daily practice is still somewhat tedious and expensive. In the meantime one can easily use the kinematic method, also called the yield line theory. Since this results in an upper bound limit, thus leading to an over estimation of the load-carrying capacity, one should be very prudent in choosing the assumed mechanism. The true mechanism can easily be found by relatively small and inexpensive model tests.

As an example, some pertinent results of a large series of tests conducted at the Swiss Federal Institute of Technology at Lausanne are presented in Fig. 5 together with a sketch of the appropriate mechanism. Among others, the following conclusions can be drawn from this type of investigation:

- by selecting a realistic mechanism, the ultimate load can be accurately predicted.
- transverse prestressing can greatly improve the behaviour of simple skew slabs at the ultimate, as well as at the serviceability limit state.
- no significant passive reinforcement is needed at obtuse angles or at any other singular point.

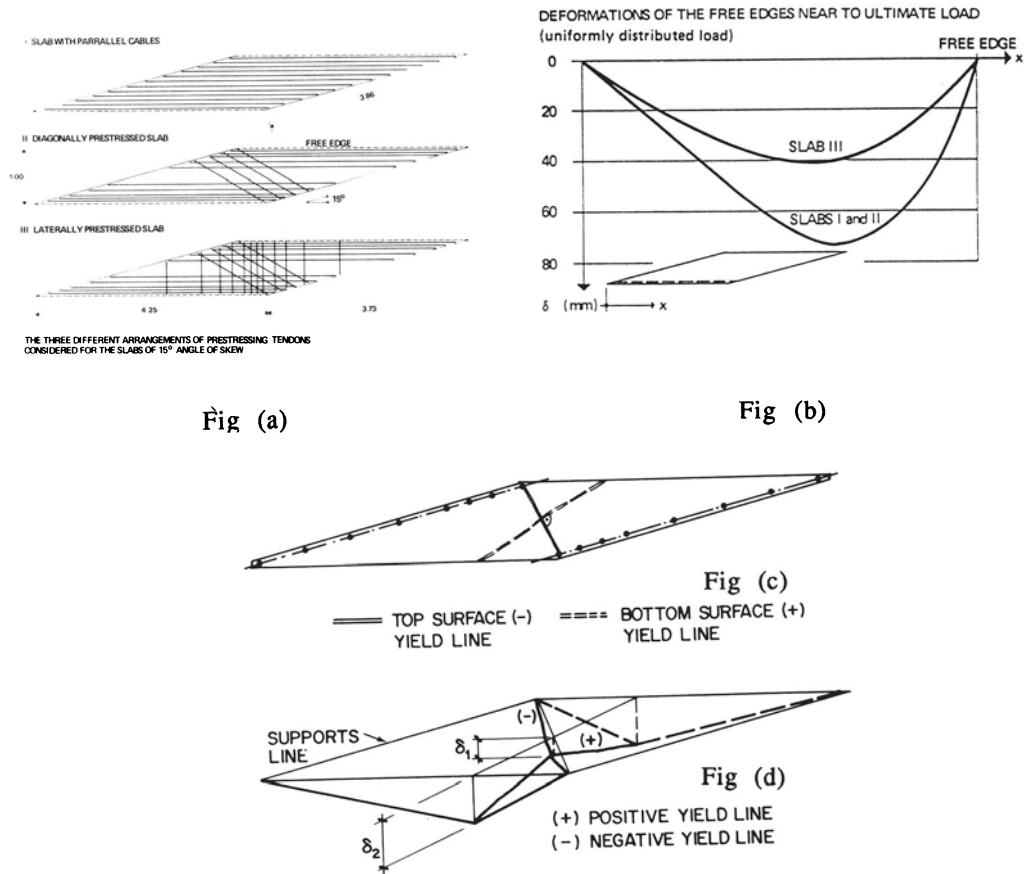


Fig 5. Skew slabs in micro-concrete tested at the Swiss Federal Institute of Technology, Lausanne.

- a) cable arrangements and dimensions.
- b) deflection at the free edge under service load (the transverse prestressing reduces deflections significantly).
- c) yield lines.
- d) failure mechanism.

5. Cable stayed bridges with slender concrete decks.

As has been mentioned above, cable stayed bridges undoubtedly represent one of the most rapidly developing fields in modern bridge design. The structural configuration of this type of bridge has led to the more recent development of cable stayed bridges with slender concrete decks.

For multiple cable stayed bridges with close cable spacing the longitudinal bending moments in the deck due to permanent loads remain very small, while the ones due to live loads increase with the bending stiffness of the deck. Hence for small and medium span cable stayed bridges there is no need to choose stiff decks, on the contrary a relatively slender concrete slab may often prove to be the best solution. The main advantage of this type of bridge is its structural

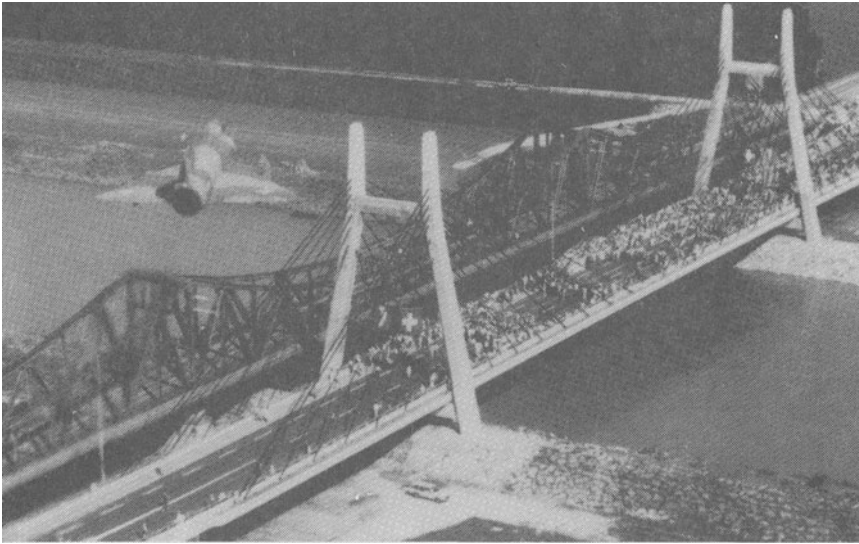


Fig. 6 Diepoldsau Bridge, Switzerland.

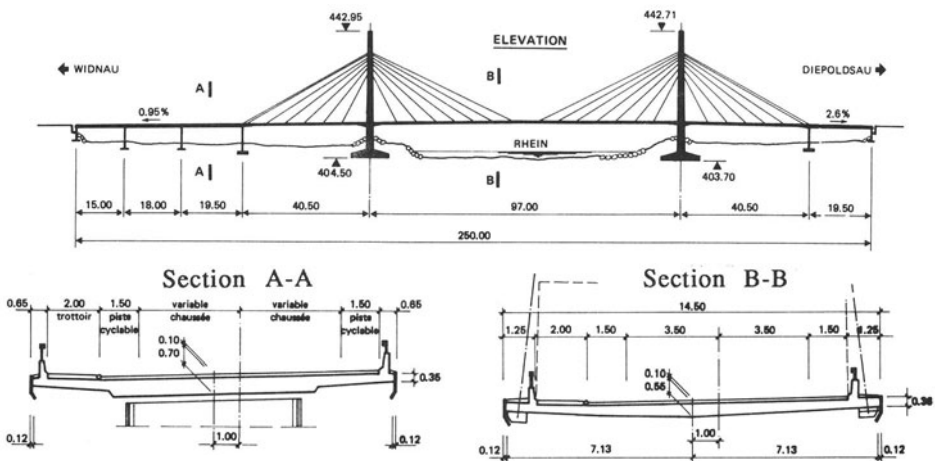


Fig. 7 Elevation and cross-sections of the Diepoldsau Bridge.

simplicity and easy erection which renders it very economical and elegant. The first time these ideas were put into action was with the Diepoldsau Bridge over the Rhine in Switzerland Fig 6 and 7. This bridge consisted of a main span of 97m supported by a multiple cable stayed system, the average deck thickness being 0.45m. In spite of the deck slenderness, the global stiffness and the sensitivity of the system to vibrations are quite similar to those observed for more traditional bridges.

Theoretical and experimental work has also shown that these concepts are equally applicable to longer spans. An example of this is the project of the La Dala bridge in Switzerland, with a span of some 210m and an average deck thickness equal to 0.42m and with a width of 13m, Fig 8 and 9.

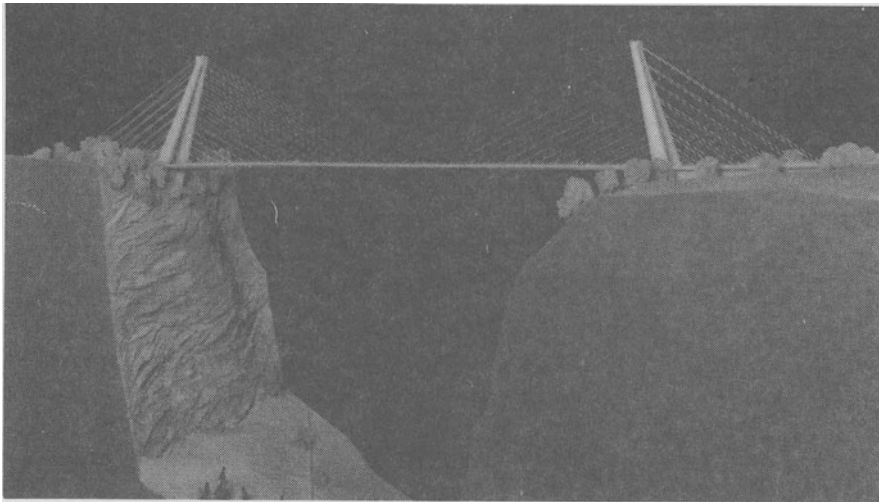
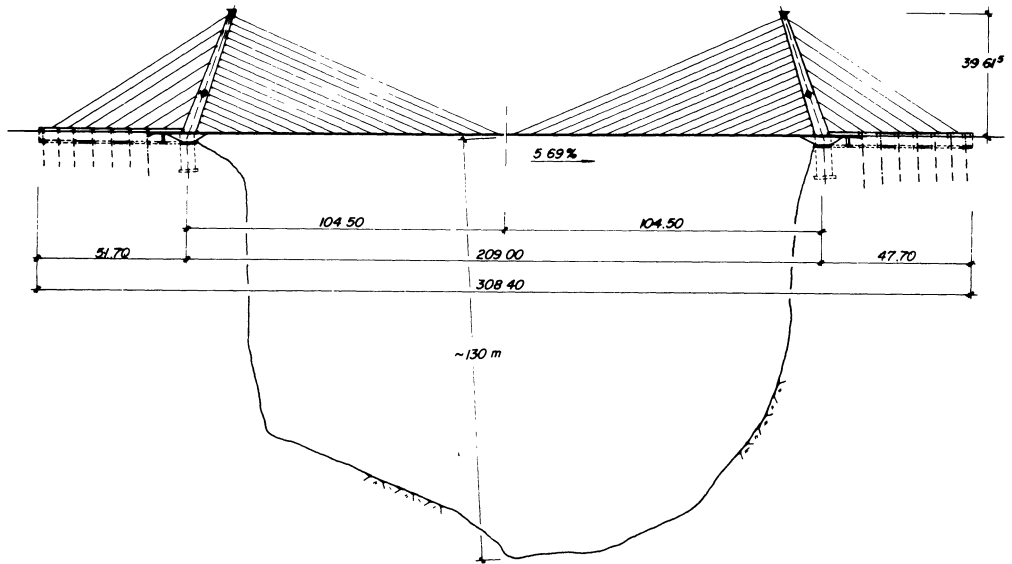


Fig. 8. Project of the La Dala Bridge, Switzerland.

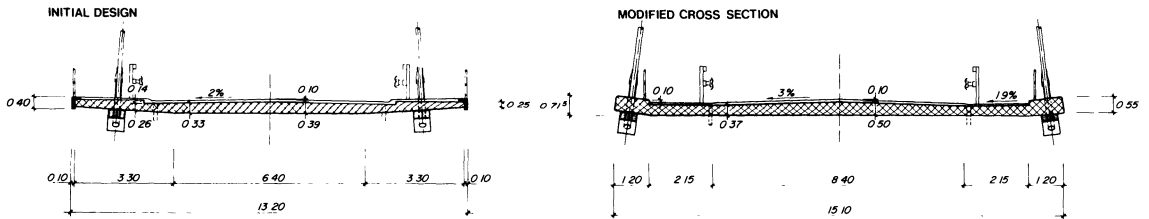
The main problem with such a bridge is its resistance against flutter due to high wind forces. A thorough dynamic analysis and wind tunnel tests have shown that the initially conceived cross-section (fig 9 left) did not guarantee a sufficient safety against flutter; thus it proved necessary to shift the cable-stays further out to the edges (fig 9 right).

6. Experimental work.

Even though the static and dynamic behaviour of cable stayed bridges can nowadays be analyzed by modern non-linear computer programs, it was deemed desirable to verify the feasibility of choosing very slender concrete decks by a



Elevation.



Cross sections

Fig. 9. Elevation and cross-section of the La Dala Bridge, Switzerland.

thorough experimental investigation on a fairly large scale model. Such a study has been successfully completed at the Swiss Federal Institute of Technology.(4).

The main dimensions and the set-up of these tests are shown in the figures 10 and 11. In addition the aerodynamic properties of this type of bridge were determined on sectional and global models in wind-tunnel tests.



Fig. 10. Test set-up of the experimental investigation.

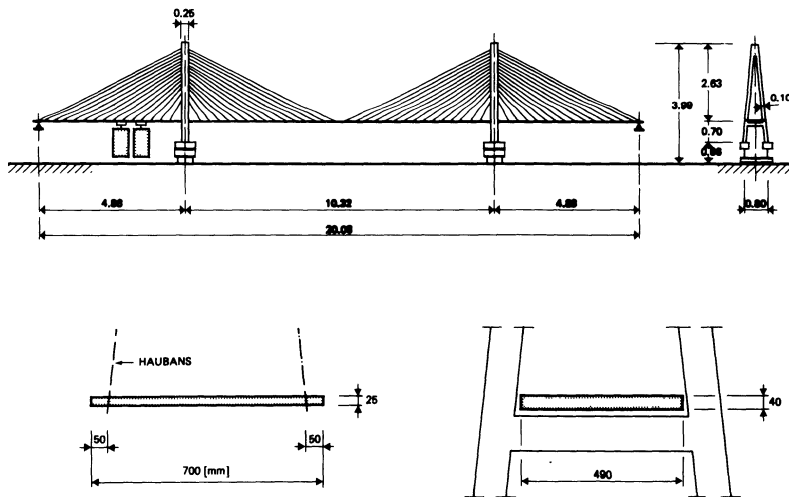


Fig. 11. Main dimensions of the test bridge.

The following main conclusions can be drawn from the theoretical and experimental investigations:

The buckling stability of bridges with relatively narrow spacing of the stays (5 to 10 m) becomes hardly ever critical. The failure load is usually determined by the yield strength of the stays.

The horizontal forces introduced into the deck by the stays effectively prevent cracking of the concrete deck. Small cracks occurred only at mid-span and close to the end support.

Such bridges are rather flexible structures and the displacements are relatively important. For the main model the ratio between maximum deflection and span length is about 1/600 under service load distributed over the entire structure (1/300 for loads distributed over the central span only). As can be seen from figure 12 the non-linearity of geometry and material have clearly to be considered in calculating the displacements.

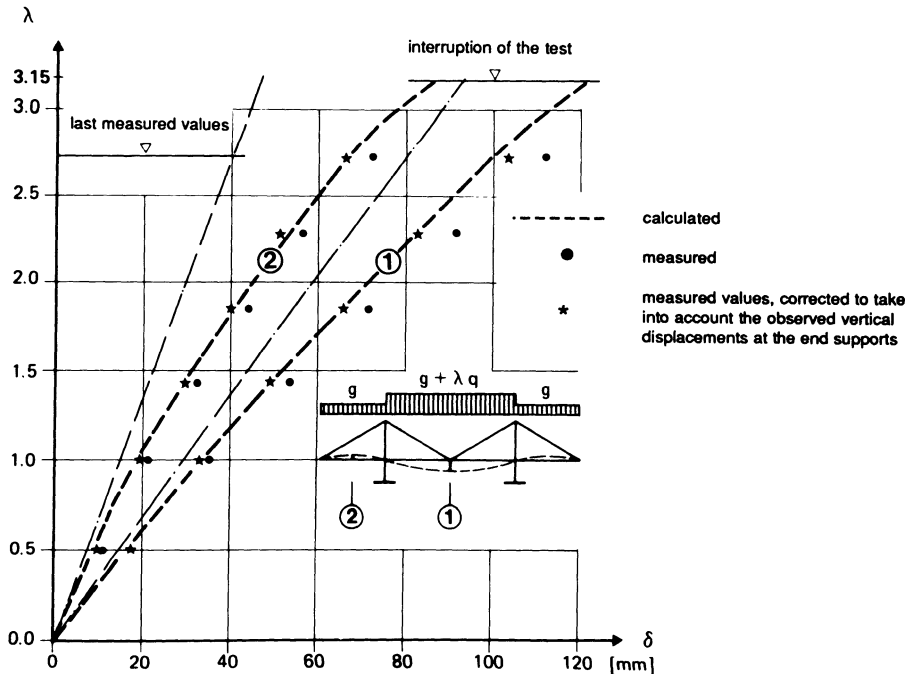


Fig. 12.

As far as the dynamic and aerodynamic behaviour is concerned four phenomena have to be considered:

- vibrations under traffic loads.
- galloping.
- vortex-shedding
- flutter.

Vibrations due to traffic loads do not impair the safety of such structures (the stress-variations are way too small to produce fatigue problems), but they may cause undesirable physiological effects for the pedestrians. The study has however shown that vibrations remain in the fully acceptable range according to all the pertinent recommendations.

Galloping of the deck can only occur if the diagram of vertical loads induced by wind versus angle of attack have regions of negative slopes ($\delta C_N / \delta \alpha < 0$), however, this is never the case for slender decks.

Vortex-shedding may in certain cases give raise to potentially dangerous vibrations even though one of the determining parameters, that is the ratio of the deck width (B) to the depth (h) is usually greater than $B/h > 10$ and thus in a rather favourable range. In order to limit the vortex-shedding phenomena the deck should be given a streamline shape, if necessary deflectors have to be provided to channel the air flow around angles. At any rate sectional wind tunnel tests have to be conducted for important structures beyond the known range of experience.

However, by far the most critical aerodynamic phenomenon is undoubtedly the flutter, that is a combination of bending and torsional movements with rapidly increasing amplitudes, which may occur if the torsional and flexural natural frequencies are similar. Unfortunately the best method to prevent flutter, choosing a high torsional rigidity, is contrary to the very concepts of bridges with slender decks. This fact limits the range of feasible applications of this type of structure to bridges of small and medium spans (up to 250m) or to bridges of greater deck width.

In the case of the Skarnsund Bridge, actually under construction in Norway, with a central span of 530m and a width of only about 12m this concept was clearly no longer feasible and for this reason a torsionally rigid deck (triangular box-section) had to be chosen (fig 13).

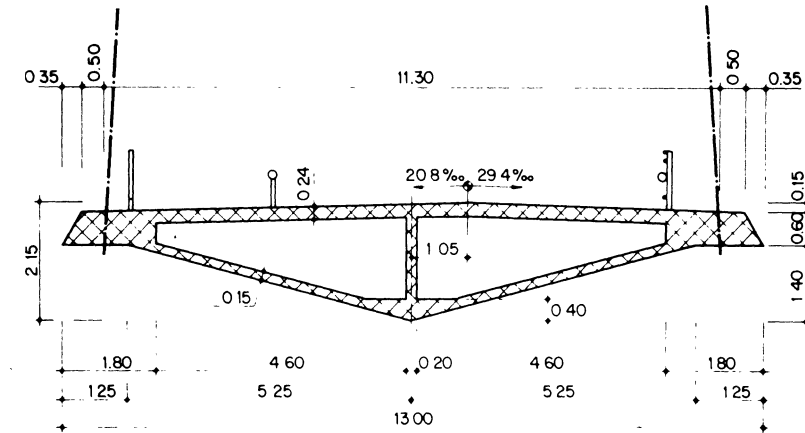


Fig. 13.

Cross section of the Skarnsund Bridge in Norway with a central span of 530m.

References.

- (1) Walther R., Houriet B., Isler W., Moia P.:
Cable-Stayed Bridges.
Thomas Telford, London, 1989.
- (2) Almeida J.:
Non-linear problems in Cable-Stayed Concrete Bridges.
Swiss Federal Institute of Technology
Pre stressed and Concrete Institute-IBAP. Lausanne September 1988.
- (3) Klein J.F.:
Comportement et stabilité des tabliers minces dans les ponts haubanés.
Thèse de doctorat en cours de rédaction à l'IBAP-EPFL.
The behaviour and stability of cable stayed bridges with slender decks.
PhD Thesis, in the process of completion at the Swiss Federal Institute of Technology, EPFL, Lausanne, Switzerland.
- (4) Cable-Stayed Bridges with Slender Decks.:
Test Report.
Swiss Federal Institute of Technology
Pre stressed and Concrete Institute-IBAP. Lausanne September 1988.

**CANTILEVER BUILT BRIDGES
WITH PREFABRICATED SEGMENTS**

**R. Lacroix
Freyssinet, Boulogne, Francia**

1. INTRODUCTION

Bridges with cast-in-situ segments come up against certain limitations, particularly as far as large structures are concerned, or at least have certain drawbacks.

The first consists of a relatively lengthy construction schedule, caused by the casting cycle of segments : the normal cycle lasts one week, in order to allow for the hardening of concrete on days off ; an average segment length of 2.50 m, will mean a construction of 5 m a week on each side of the pier, and for a very long bridge, the contractor may have to increase the number of carriage form travellers to maintain an adequate program.

In certain cases, a cycle of two segments a week could be attained, by means of either a high strength concrete, or a thermal treatment to increase the concrete's early strength. However, such achievements are not easy, and the difficulty in controlling the arms' deflections is increased, due to the concrete being so recently cast at the time of the prestress tensioning.

From a quality point of view, the cantilever built bridge with cast-in-situ segments runs another risk due to the fact that the strength of the concrete is only known after 28 days ; if the results of the control samples prove to be insufficient, one must then choose between either the demolition of all the concrete already cast, or the acceptance of a derogation, provided that a few extra precautions are taken.

Finally, statistically, a higher frequency of disorders has been noticed on bridges with cast-in-situ segments because of early stressing of the concrete and the obviously difficult casting conditions.

The design of prefabricated segment bridges makes these problems avoidable, and is therefore an actual improvement despite a few inconveniences which will be described below.

2. THE DESIGN PRINCIPLE FOR PREFABRICATED SEGMENTS

Prestressing is an excellent means of assembly, thanks to the compression exerted on the faces in contact with the prefabricated pieces ; but to achieve this tightening without any problems, the mutual contact must be perfect.

The solution to this problem was thought up in the late fifties by Campenon-Bernard, for the construction of the Choisy-Le-Roi Bridge on the Seine River (near Paris).

This solution consists of casting the n th segment with its contact face with $(n-1)$ segment cast directly in contact with the latter. A perfect similarity of the contiguous faces is therefore achieved; these faces are said to be match-cast, and provided that incidental deformations do not appear between the casting of concrete and the assembling of segments, an excellent mutual contact at the joints is obtained.

Generally, immediately prior to assembling two contiguous segments, the contact faces are coated with a multi-purpose epoxy resin which :

- firstly guarantees the joint's watertightness, an important characteristic, especially if prestressing ducts embedded in concrete pass through the joint ;
- secondly, ensures a better contact by evening out any slight imperfections in the segments' match casting, with the thickness of the resin ;
- lastly, facilitates assembly with the lubrication of the contact faces, the friction coefficient of the resin before polymerization being quite small.

In some cases the segments have been assembled without resin. For reasons mentioned earlier, this method would seem inadvisable.

When the joint between two segments is obliquely crossed by prestressing reinforcements, apart from the exceptional case when the component of the prestressing force in the joint's plane is strictly balanced by the shear force exerted at the joint, a tangential force is applied along the contact area, and because of the small value of the friction coefficient of the resin, the segments tend to slide one against the other. This sliding is generally avoided by fitting the faces in contact with shear keys (ref. fig 1), thick enough to withstand the shear force.

These keys, useful in avoiding the mutual sliding of two contiguous segments, are also placed in the slabs, where their purpose is different : they insure the mechanical assembling of two pieces of slab belonging to adjacent segments (ref. fig 2), and allow a better distribution of the traffic load.

3. FABRICATION, STOCKING AND ERECTION OF SEGMENTS

One of the main advantages of construction with prefabricated segments is in the quality achieved, thanks to the industrial casting of concrete . Especially as far as large bridge are concerned, the fabrication unit for segments may be conceived with a stiff steel frame, with means of important vibration, and if the need arises, heating equipment for concrete, without the weight of the installation being a drawback, as is the case with cast-in-situ segments.

This unit can be located near the batching plant, thus shortening the actual casting time, and facilitating the use of superplasticizers (since the effect of superplasticizers on fresh concrete is short term, and can disappear 30 to 45 minutes after mixing).

As explained above, the n th segment is cast directly in contact with the $(n-1)$ segment, the face of the latter simply being coated with a form oil type product.

A well equipped unit can produce one segment every other day with a setting and hardening time of the concrete of 36 hours, and even one segment per day, provided that the early strength of concrete is sufficient.

Incidentally, one must note that the requirement of a very short fabrication cycle justifies the use of a high strength concrete, far more than mechanical requirements : for bridges, the concrete usually considered must have a characteristic strength on cylinders of about 35 MPa at 28 days, and it is quite rare that the structural analysis demands a strength higher than 40 or 45 MPa. Although for a long span bridge, it might be more economical to increase the concrete quality, rather than increase the number of fabrication cells ; for example, such was the case with the Ré Island Bridge, over 3 km long. This structure was built with a concrete with a characteristic strength of 55 MPa, whereas the project only required 40 MPa. The use of high strength concrete therefore enabled a considerable amount of time to be saved, the opening of the bridge could take place before the start of the tourist season (the bridge was completed within 18 months, including foundations). Another important side effect of the use of strength concrete must also be noticed : this material, due to its compactness, actually gives the structure a better durability : the action of superplasticizers on concrete is achieved through an impressive reduction of its water content ; the W/C ratio, i.e. water weight over cement weight, the value of which amounts to 0.45 to 0.50 for a typical concrete, diminishes to 0.32 or 0.35 for a plasticized concrete, hence a very small free water content in the hardened material. Many tests proved that the water or air permeability of a plasticized concrete was 10 to 100 times smaller than that of a normal concrete. The carbonation, or the ingress of chlorides in a marine atmosphere, is therefore much slower.

The last but not least advantage of the prestressed concrete bridge must be added, as far as high strength concrete is concerned : again because of its low content of free water, its creep is 30 to 40 % less than that of a normal concrete, which also diminishes the prestressed losses, and the re-allocation of forces.

After fabrication, the storage of the segments, which are often quite cumbersome, is in the open air. The only precaution to take concerns the stacking of segments on top of each other ; the early concrete may be submitted to an important creep, and it is then advisable to avoid any flexions caused by the weight they carry.

It is also useful to set up a data base which records the fabrication date, the respective position in the storage area, and the waiting period of each segment ; this will ensure the correct match-casting of the joints, and also keeping account of the concrete creep parameters, (particularly, age at first loading), for the determination of the camber to be given to the arms during construction. The same data is also useful for calculating the re-allocation of forces due to creep.

The handling of segments can be done in various ways : when the deck is to be built entirely over a navigable waterway, or an accessible area, a transportation on barge or flat bed trailer can be considered ; the end of the arm is then equipped with a derrick in order to lift the segments, and to bring them into contact with the previous ones. However, when the ground below deck is not uniform, which is generally the case, it is strongly advised to use a launching gantry resting on the piers and to erect the segments progressively. Launching gantries are costly investments, but, if well conceived, can be redeemed and used again on several successive sites.

The actual adjustment of the arms' profile during their erection, up to the profile desired for the service life, must be carried out before hand, prior to the segments' fabrication, and cannot be subjected to any modification during the construction of the deck.

In other words, prefabrication implies, contrary to cast-in-situ bridges, a perfect previous knowledge of the concrete's rheological properties, and of the sitework schedule. An interruption of work, caused by a strike for example, means a modification of the segments' bonding age, and therefore modifies the alignment of the profile.

After the erection of the prefabricated segments, the arms' continuity is obtained by casting in situ a special closing piece, which does not cause any particular difficulty.

4. CONCEPTION AND INSTALLATION OF PRESTRESSING TENDONS

As for bridges with cast-in-situ segments, the prefabricated segment bridge contains isostatic tendons, meant to ensure the stability of the structure during construction, and continuous tendons.

As far as the deck's analysis hypothesis is concerned, one must note that prefabrication excludes partial prestressing : with cast-in-situ segments, and with a rather complicated alteration of the formwork, some reinforcing bars can be laid across the segments' joints ; this allows tensile stress under the effect of short lasting actions. This is ruled out with prefabricated segments.

The anchoring of isostatic tendons also differs : with cast-in-situ bridges, these tendons are usually anchored at the ends of the webs. This disposition is inadvisable in the case of prefabricated segments, because the immediate and long term deflection of compressed concrete behind the anchor plates tends to destroy the geometrical match-casting of the segments' contact faces.

The tendons are preferably anchored in concrete blocks or ribs protruding from the concrete, inside the box-girder formed by the deck.

The watertightness of the ducts' coupling across the joints is another delicate matter, for prefabricated segments as well as those cast-in-situ. The ducts, made of spiral steel sheets, are joined end to end with threaded sleeves screwed to the ducts fillets. The watertightness is achieved by applying a supple, compressible product around the opening of the duct, similar to that used in building construction. Whatever the precautions taken, it is important to check, by blowing air for example, that watertightness is perfect, and that the ducts are not blocked by resin.

As far as all cantilever built bridges are concerned, the areas behind the prestressing anchor plates must be very carefully treated, since their concrete is submitted to an often considerable tensile stress ; after tensioning, tensile cracks are sometimes noticed, of a small width (about 0.1 mm), along the ducts' outline ; the starting point of these cracks is located a few decimetres behind the prestressing anchor plate, and their length may vary from a few decimetres up to one metre. These cracks do not jeopardize the structure's safety, and often vanish after completion of the works, due to the sheer force exerted by the loads applied to the arm. They can be avoided, especially if the detailing rules prescribed by the French prestressed concrete code are followed : Code BPEL83.

Lastly, one must note the risk of disorders induced by the installation of longitudinal prestressing tendons in the lower slab of a box girder of-variable height : the height of the girder being variable, the slab is curved, which induces a radial force from the prestressing tendons ; during tensioning, no disorder arises, since this radial force is balanced by an opposing force, induced by the curve of the compressed concrete.

But when the bending moment increases, due to the effect of live loads, to a thermal gradient, or to the re-allocation of load effects due to creep, then the concrete of the lower slab is no longer compressed, and the radial force of prestressing tendons is no longer opposed, and could trigger the rupture of the slab, through excessive flexion.

5. EXTERNAL PRESTRESSING

As explained above, the layout of prestressing tendons and anchorages demands many special precautions. There are other constraints related to the project itself : for example, for the checking of shear force, the web's thickness cannot be taken into account as a whole : one must deduct either the diameter or half the diameter of the embedded prestressing ducts, according to the code followed.

For all of these reasons, and under the leadership of French engineers, a real "external prestressing school" has been developed, with the construction of many long span bridges.

In fact, the feature of tendons outside the concrete has other advantages :

- construction is simplified,
- casting of beams is more easily carried out,
- provided that certain precautions are taken, the tendons can if necessary be replaced during the life of the structure,
- lastly, external prestressing allows the installation of high capacity tendons without any risk of cracks in the concrete behind the anchor plates.

To the detriment of external prestressing, one must however note a lower resistance to flexion at the ultimate limit state, due to the tendon not being bonded to the concrete (for a detailed study of the mechanical properties of girders fitted with external tendons, the reader can refer to the many articles pertaining to this subject).

The different types on external prestressing reinforcement are as follows :

1. The bars wires or naked strands, galvanized. Such re-inforcement has been used on several bridges ; the guarantee of durability they offer does not seem satisfactory, except in the case of a very dry climate (and even then one must check the absence of condensation inside the box-girder).
2. The wires or strands, laid within a sheath made of a smooth steel tube, filled with a cement grout. This arrangement is preferable, and has been especially chosen for many repairs using additional prestressing. However, the steel tube, even when painted, is exposed to corrosion.
3. The wires or strands, laid within a high density polyethylen duct (HDPE), filled with a cement grout. This solution is preferable, as the duct within the box-girder, is not exposed to the UV radiations, which could induce ageing and cracking of the polyethylen.
4. The wires or strands, laid within an HDPE duct, filled with a soft material, either grease or wax. This solution, slightly more costly, is advisable, since it allows the possible retensioning or replacement of a tendon if the need arises.

5. The strand, individually protected by an HDPE duct, with an interposition of grease or wax. This latter solution is the best as it allows an extreme pliability for re-tensioning or replacing the reinforcement, as well as an excellent protection against corrosion.

6. CONCLUSION ; A FEW CONSIDERATION

Bridges constitute a very special kind of structure : their statical scheme is clearly determined and their structural analysis is more simple than most building frames. However, if the latter can accomodate approximative calculations, as far as bridges are concerned, mistakes are fatal.

The reasons for the particular sensitivity of engineering structures are multiple :

- First of all they are submitted to actual loads closer to nominal loads than those of many other structures, and, in spite of taking into account the dynamic coefficient, the probably underestimated.

- The effects of climatic conditions are also underestimated in many cases : the thermal gradient, between the road surface covered with a black bituminous layer exposed to the sun, and the underface of the deck in the shade, quite often exceeds the prescribed value of 10° C.

The effects of frost and de-icing salts are also dangerous. For a long time, experts have been looking for a technique to prevent the pouring of buckets of sodium chloride onto concrete, the sworn enemy of reinforcing bars and tendons.

- One must lastly note an unfortunate practice, under the pretext of presenting a clever alternative, of economising as much as possible on materials whilst abiding with the regulations, in order to built as light a structure as possible.

This practice is detrimental to the owners, who may buy bridges with a far lower durability than expected ; it is also detrimental to the consultants and contractors, whose global reputation can be damaged.

A more detailed analysis of the present situation leads us to believe that it results from three independent factors, which are :

* The development of stronger and stronger competition, leading to an excessive dissection of projects, often means exceeding the operation's budget, the difficulties in carrying out the works according to the chosen method outweighing any saving on materials.

* The popularization of computer science, with the appearance of powerful and effective programs on the market, facilitates working out voluminous supporting calculations at a moderate price ; many are misled by this presentation, forgetting that a machine can only give back what it has been fed, and that man remains responsible for conception : the best computer in the world, even fitted with the best "CAD", will only work out a second-rate project if controlled by a poor designer.

* Lastly, the third factor is the decreasing technical knowledge of owners, who are less and less capable of estimating a project's worth, and therefore of weeding out the hazaruous and dangerous offers.

Often restricted by over strict rules regarding tenders and competition, the owners tend to award to the lowest bidding consulting engineer, a study which represents only a slight percentage of the construction cost ; this is why the studies are sometimes slap-dash, entrusted to a young engineer or a trainee, "cheaper" than an experienced engineer.

In order to restore the qualities of durability to bridges, which used to be theirs, it is necessary for the owners to be held accountable for their structures,; they must realize the importance of the structure's global cost. This global cost includes not only the cost of studies and construction, but also maintenance, possible repairs and eventual replacement of the structure. The optimization of global costs will give priority in each case to an elaborate preliminary study of the structure, which is the only way to prevent disorders during the structure's life.

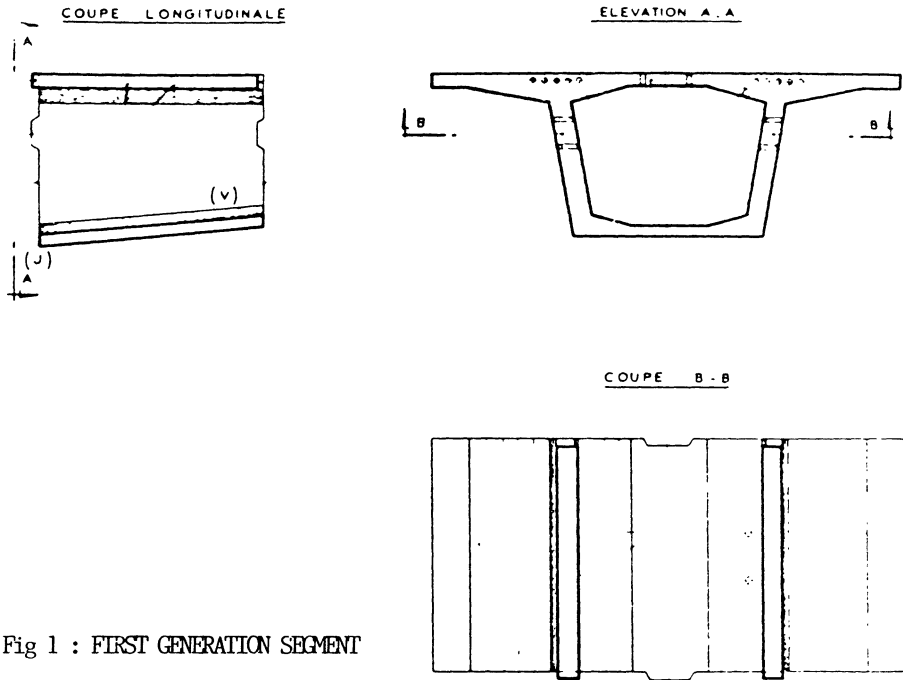


Fig 1 : FIRST GENERATION SEGMENT

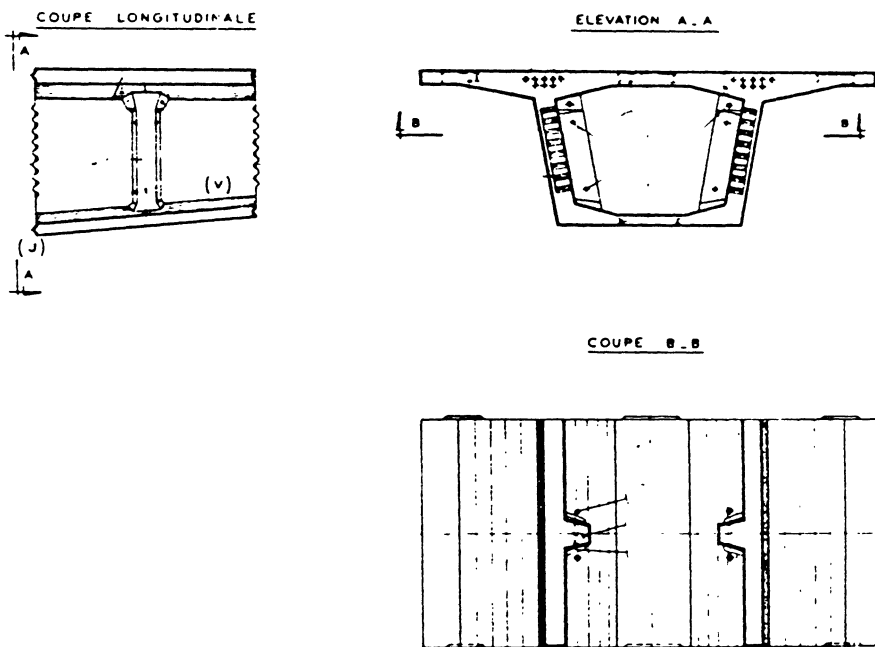
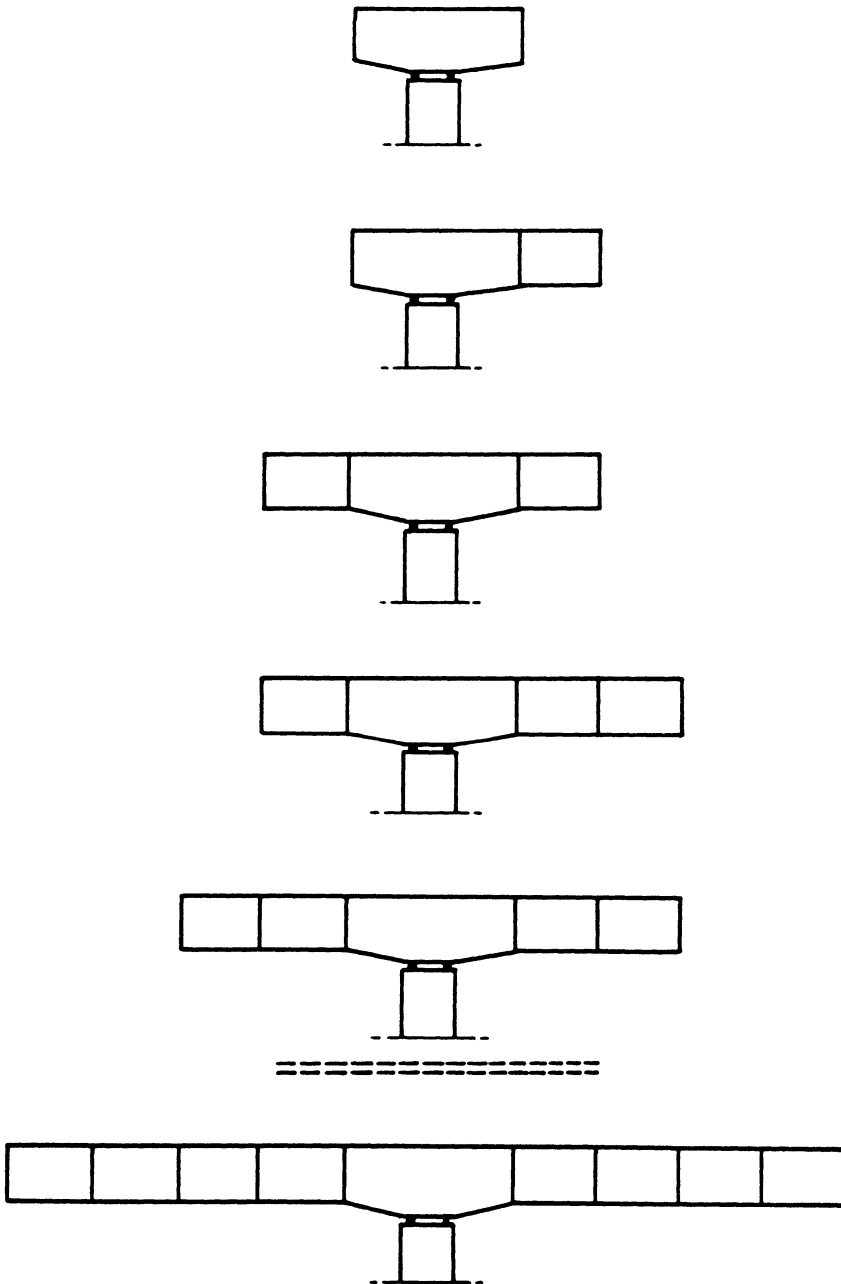
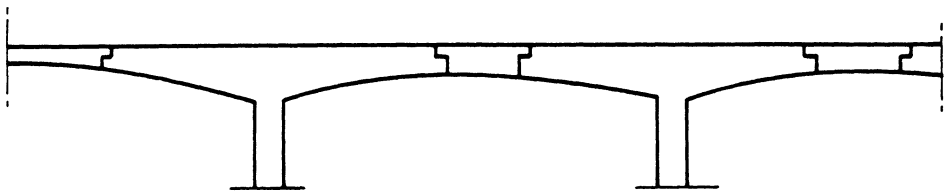
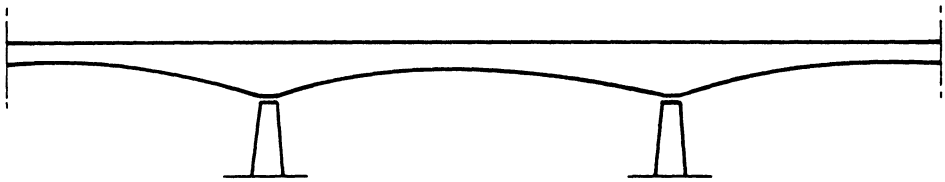
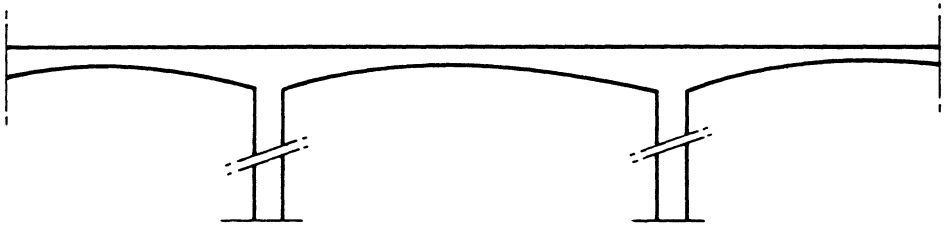
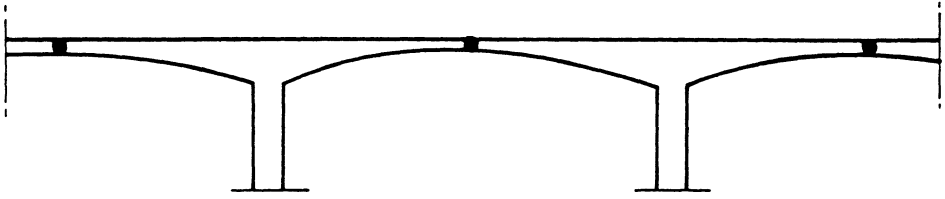


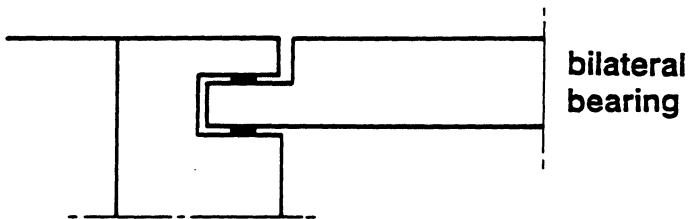
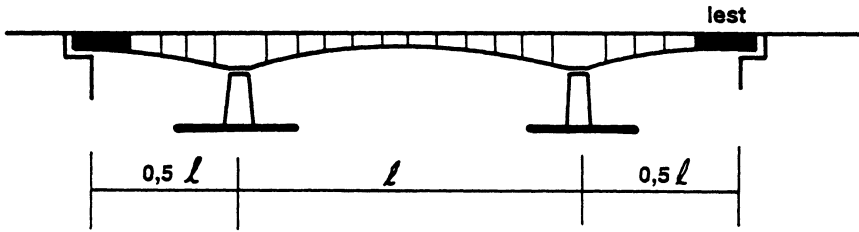
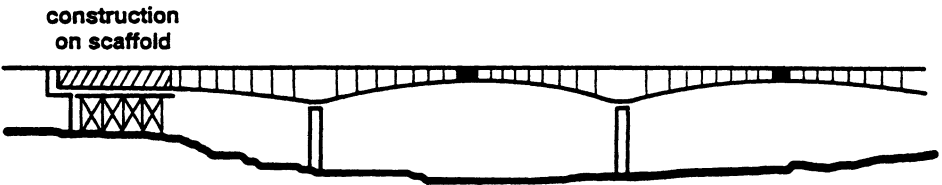
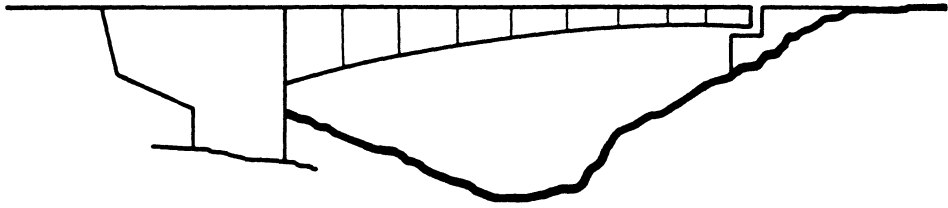
Fig 2 : SECOND GENERATION SEGMENT



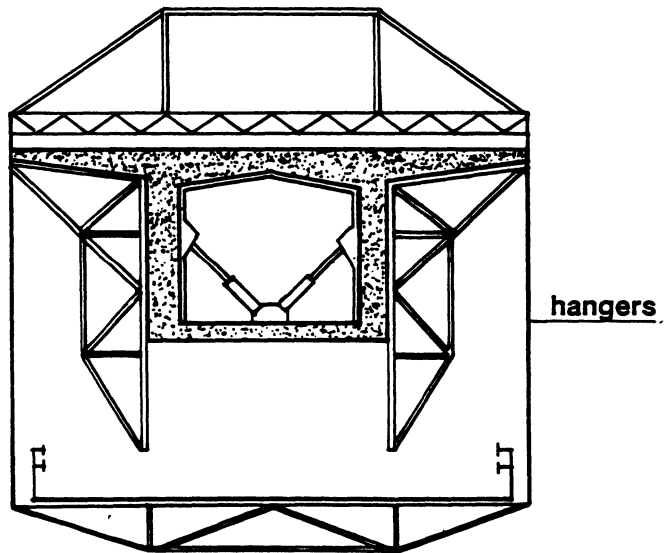
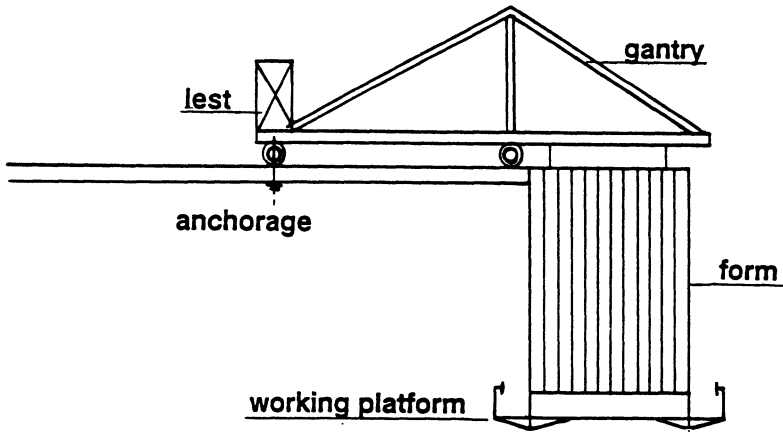
PRINCIPLE OF CONSTRUCTION



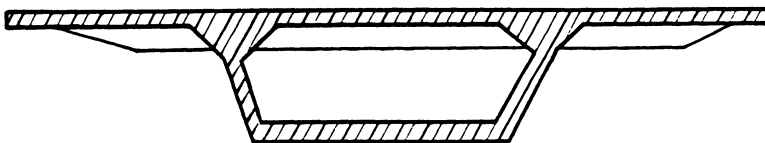
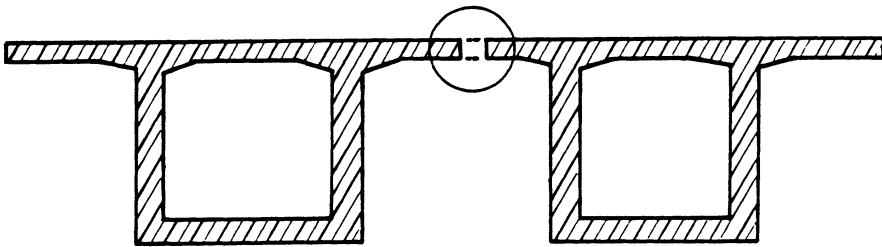
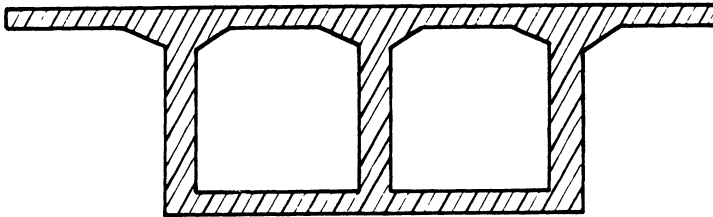
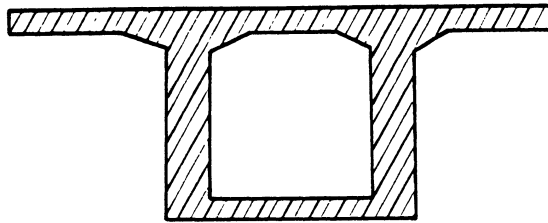
STRUCTURAL SCHEMES



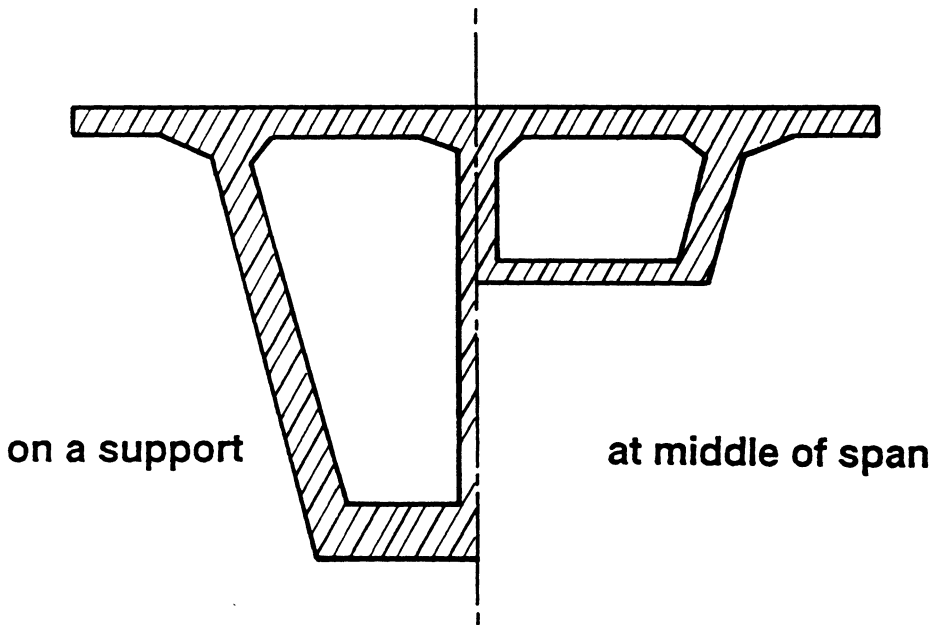
STRUCTURAL DETAILS



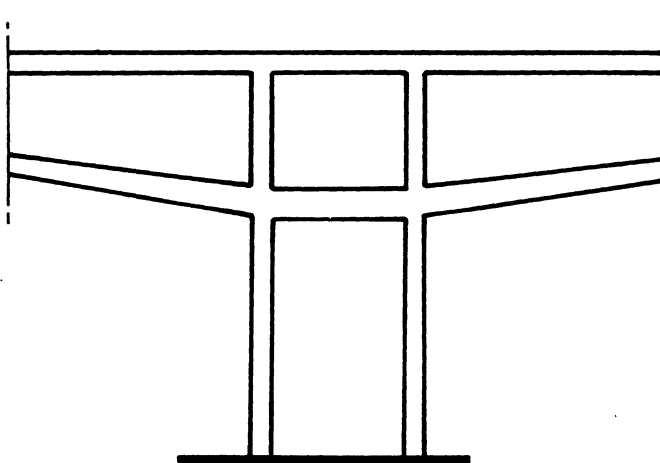
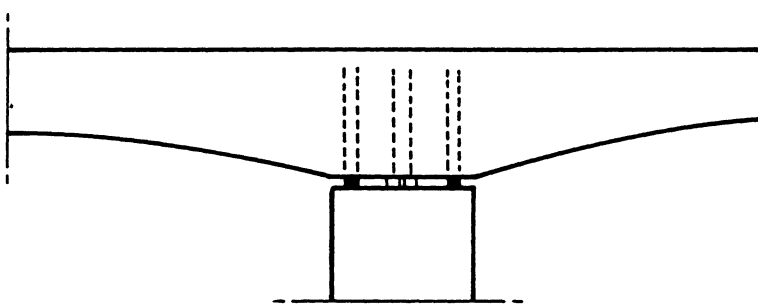
PRINCIPLE OF A MOBILE GANTRY



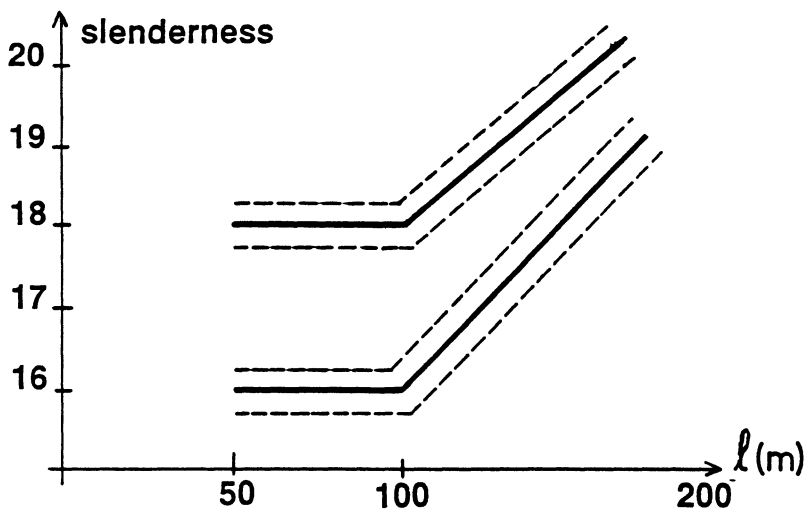
EXAMPLES OF TRANSVERSE SECTIONS



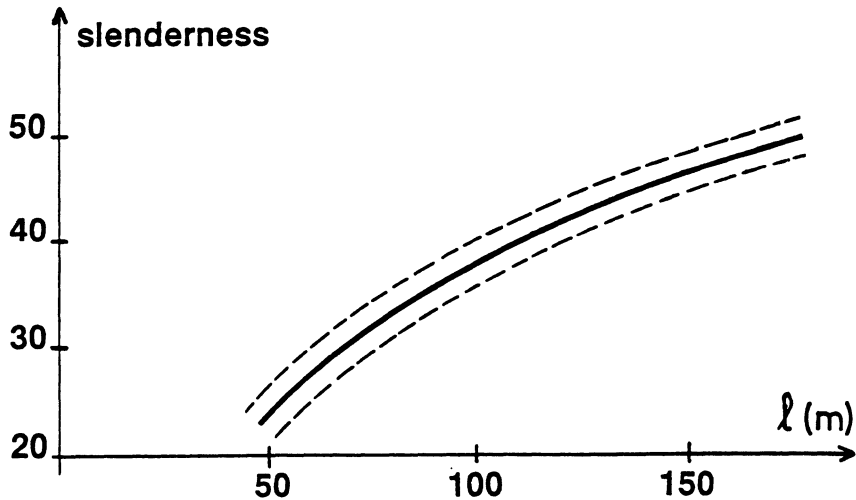
VARIABLE HEIGHT - INCLINED WEBS



LIAISON DECK – SUPPORT

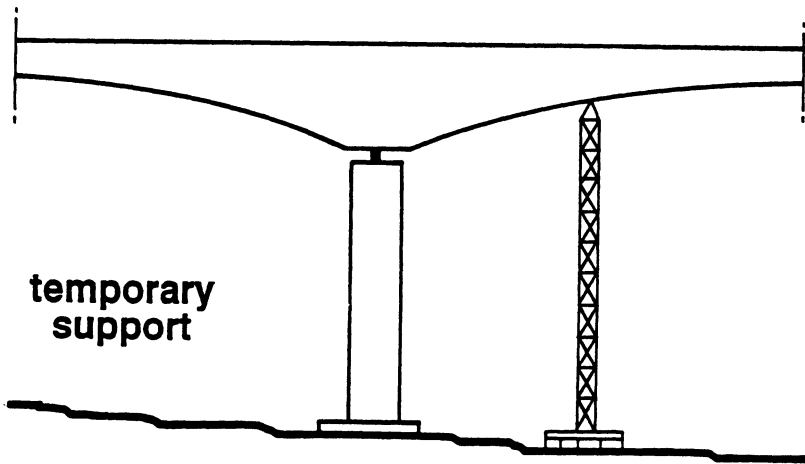
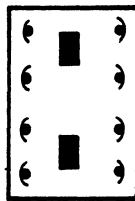
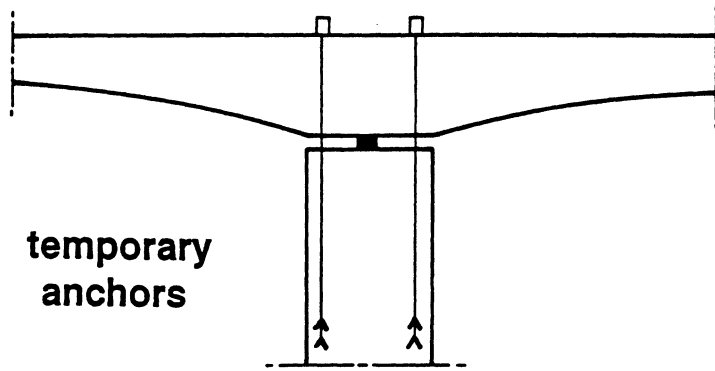


deck height on support

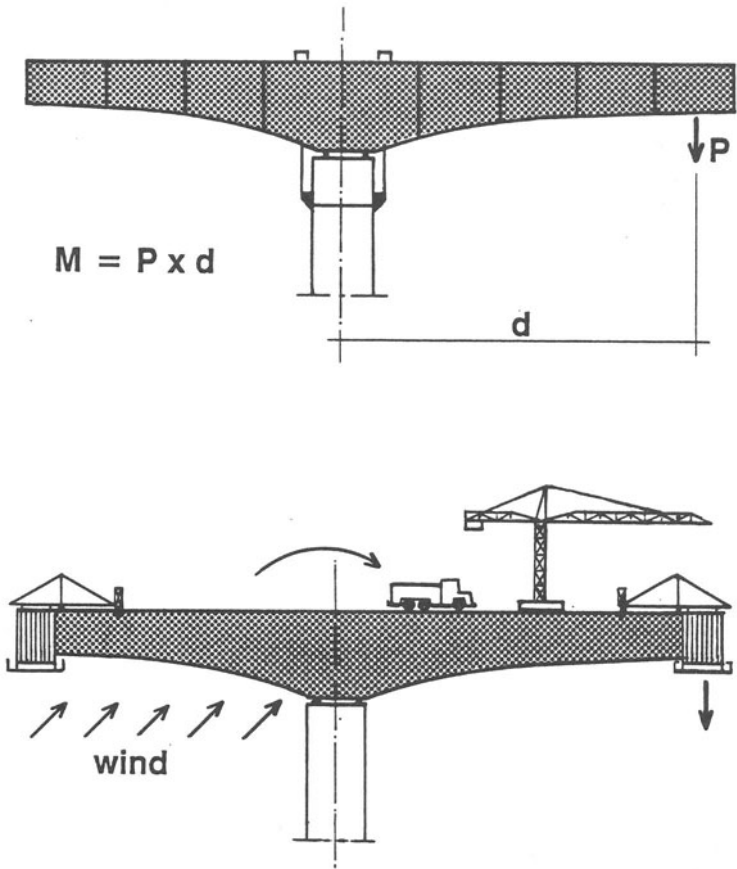


height at middle span

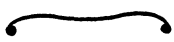
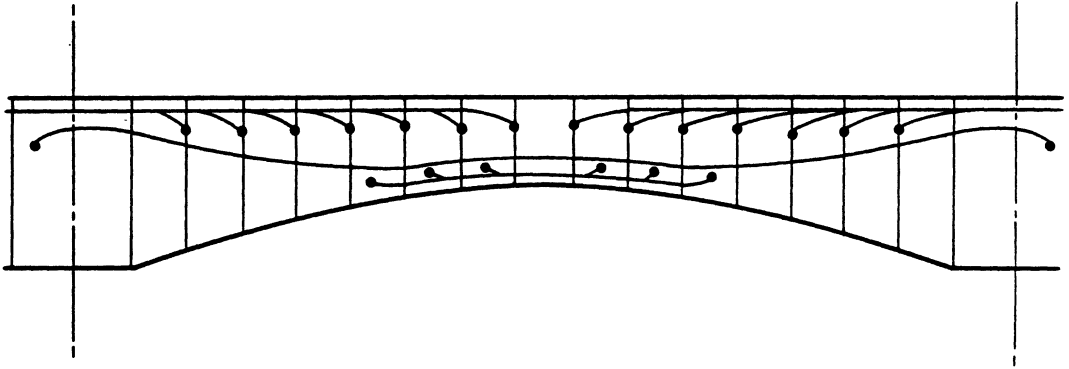
RATIO HEIGHT/SPAN



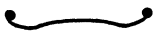
STABILITY DURING CONSTRUCTION



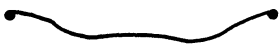
OPERATING AND CLIMATIC ACTIONS



isostatic tendons ($M < 0$)



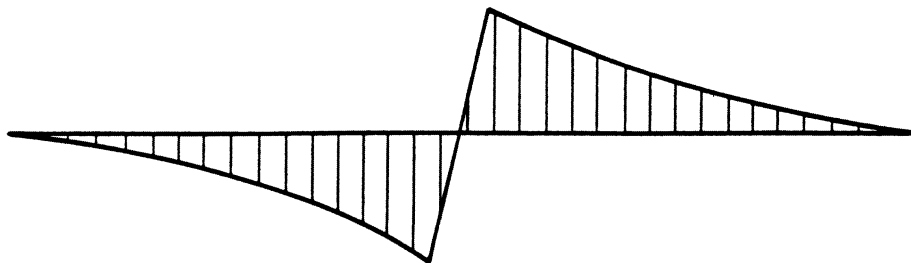
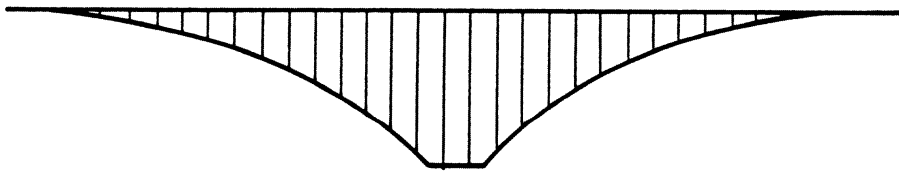
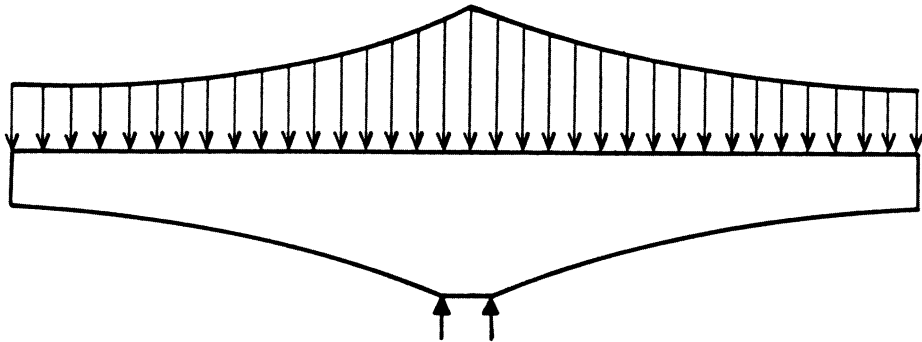
linking tendons ($M > 0$)



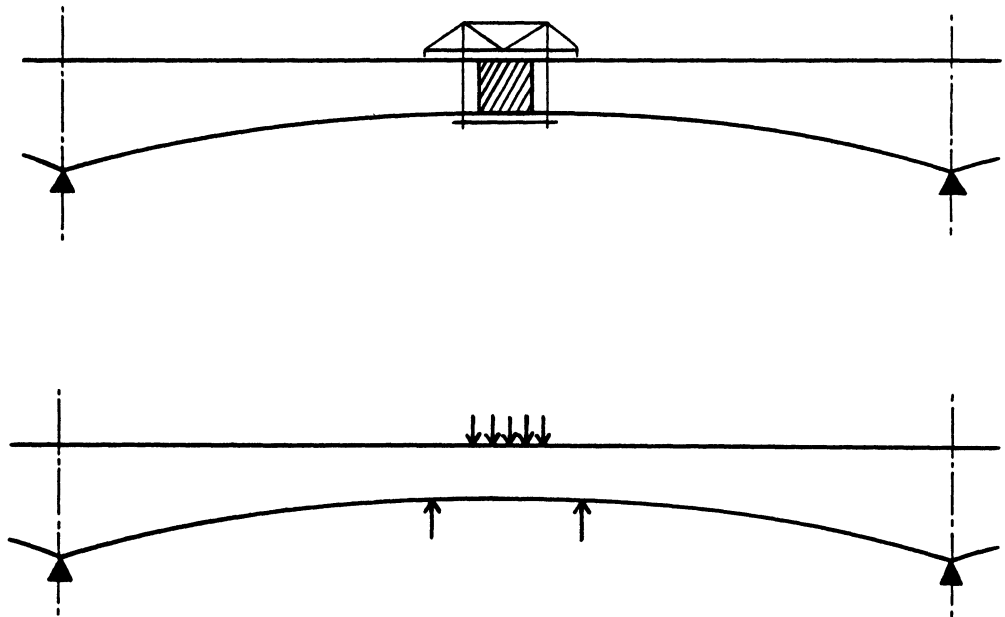
continuity tendons

WEIGHT OF THE DECK

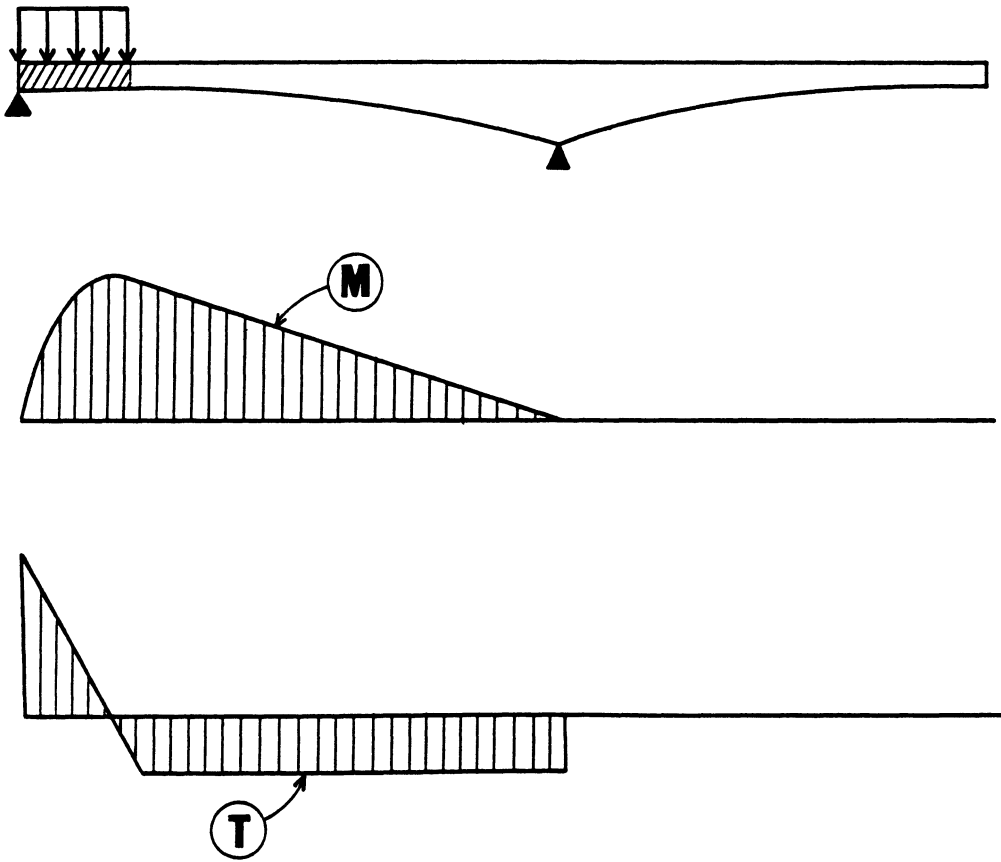
$$\delta = 2,5 \text{ t/m}^3 \quad \text{major. 2 to 3 \%}$$



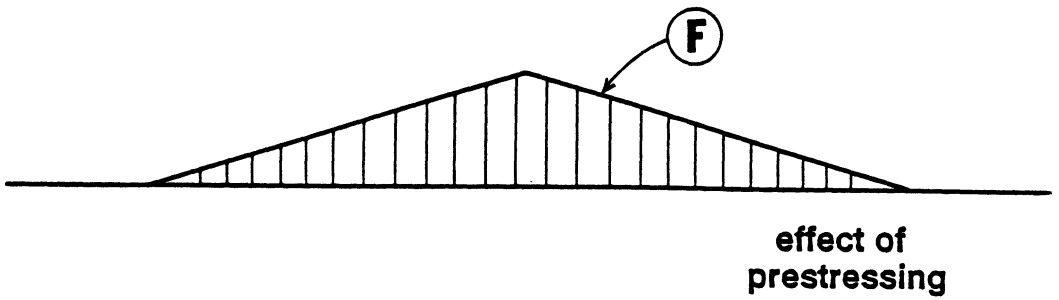
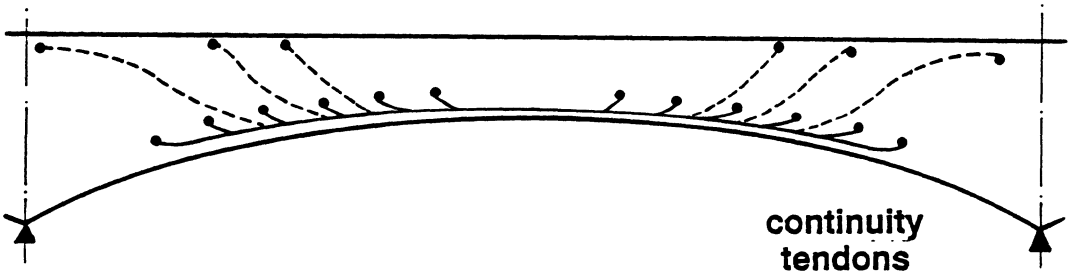
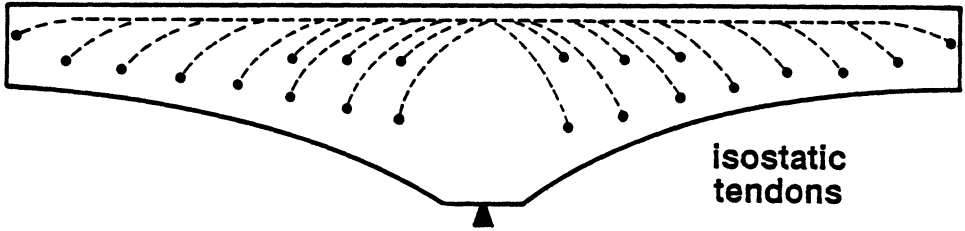
JUNCTION AT MIDDLE SPAN



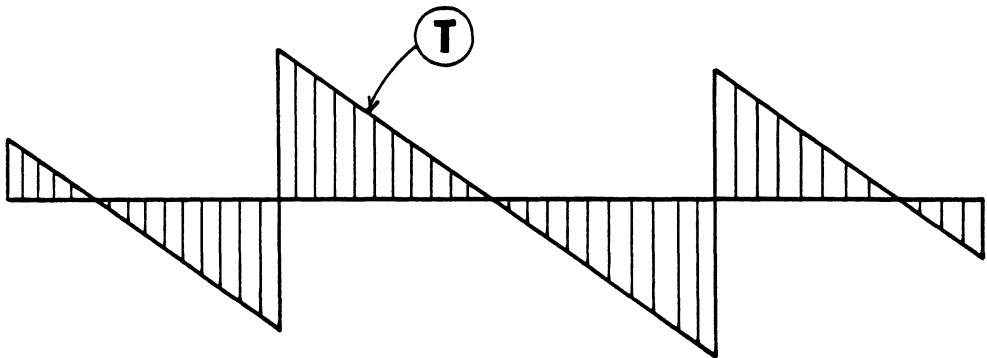
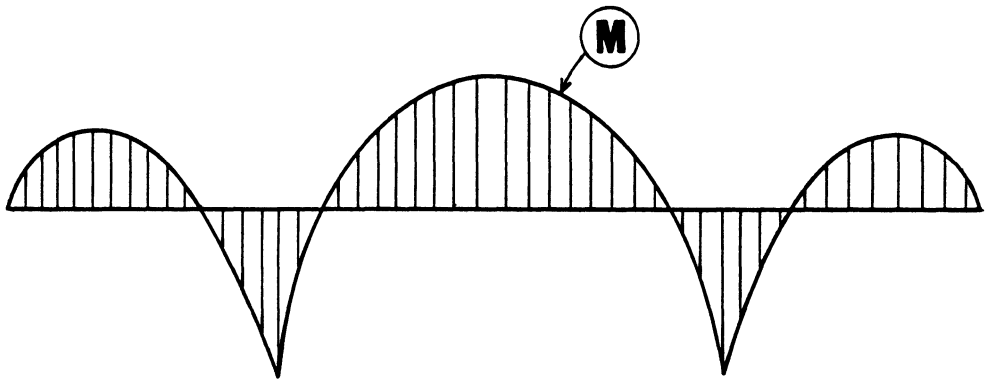
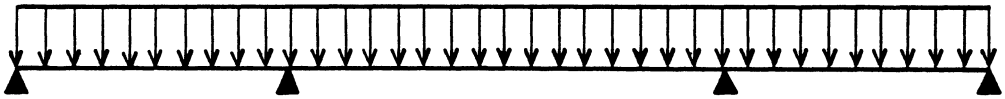
CONSTRUCTION OF END SPANS



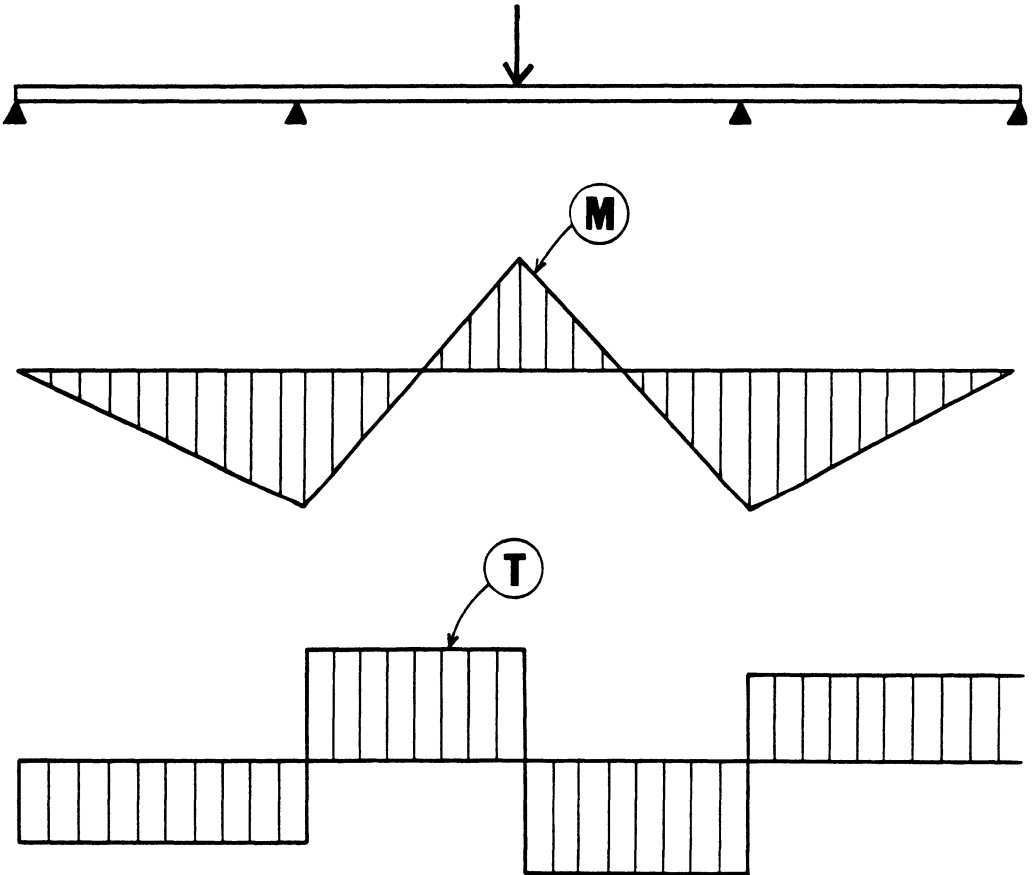
ACTION OF PRESTRESSING TENDONS



EFFECT OF PERMANENT LOADS

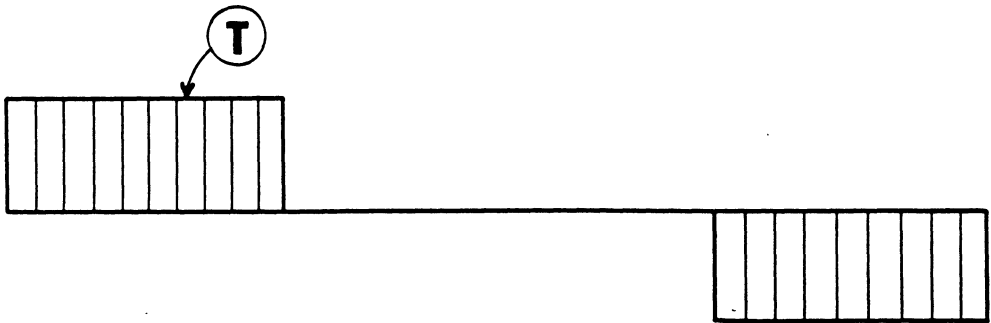
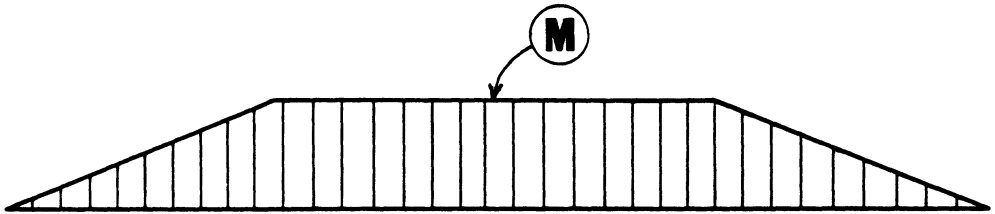
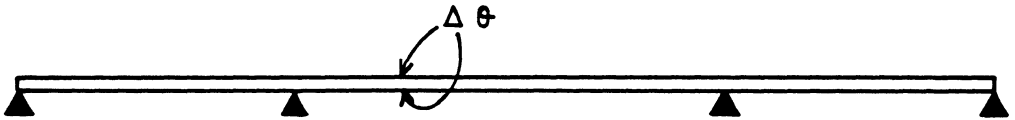


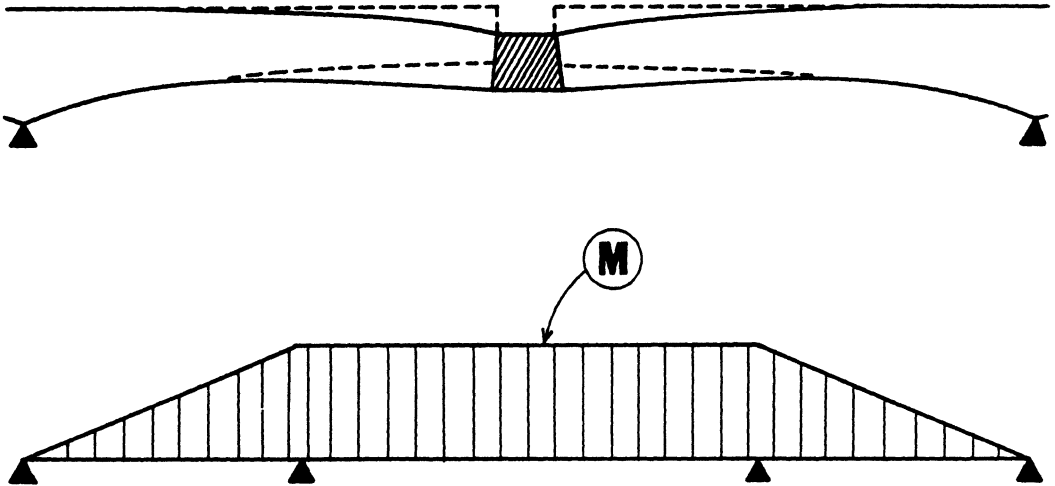
EFFECT OF OPERATING LOADS



EFFECT OF THERMAL GRADIENT

$$\left. \begin{array}{l} 5^{\circ} \text{ C} + \text{G} + \text{Q} \\ 10^{\circ} \text{ C} + \text{G} \end{array} \right\} \text{ with } E_i$$





EFFECT OF CONCRETE CREEP

$$S_t = \frac{1}{2} (S_2 - S_1)$$

compression margin $\left\{ \begin{array}{l} 1 \text{ MPa prefa} \\ 1.5 \text{ MPa in situ} \end{array} \right.$

**COMPOSITE BRIDGES
NEW DEVELOPMENTS IN EUROPE**

P. Dubas

Swiss Federal Institute of Technology, Zurich, Svizzera

ABSTRACT

The present paper deals with new developments for composite bridges, as they have been opened recently to traffic. Firstly some indications are given for the materials used, i.e. weathering steel as an example for structural steel, and concrete e.g. lightweight concrete. The main part of the paper is devoted to the structural arrangement of composite bridges, both with deck at lower flange level and at upper flange level. For this second arrangement the relative advantages of structures with open framing or closed framing respectively (particularly for bridges curved in plane) are described and illustrated by existing composite bridges. Some aspects of the design procedures, especially concerning the web behaviour in the postcritical plate buckling range, are considered. The usual methods for the construction of composite bridges, more precisely for the concreting of the deck (deck slab cast in situ, precast deck slabs, stage-deck jacking along the steel girders) are mentioned. The last short section of the paper deals with the possible widening of existing composite bridges, due to increased traffic.

1. INTRODUCTION

The paper deals with new developments for composite girder bridges. The range of spans considered is therefore limited to about 150 m. Composite construction, however, is also applied for cable stay bridges, for example the Annacis Bridge in the Vancouver area with a 465 m main span [1]. For further information to such structures reference can also be made to the contribution of R. Walther.

The following paper concerns mainly highway or motorway bridges opened recently to traffic. Railway bridges require special considerations, due to heavier loading and to the reduced deck width.

2. MATERIALS

2.1 Structural steel

In some countries weathering steel is widely used: the reduction in maintenance costs is mostly higher than the increase in steel price. Fig. 1 shows as an application the elevation of the main span of the Napoléon Bridge near Brig (outside girder). In the hogging moment region a high strength weathering steel with a yield stress of 410 N/mm^2 , made in Italy, has been used, allowing a reduction of the cross-sectional area of the flanges and of the corresponding welding labour. The webs are relatively thick for the reason explained in section 4.2.

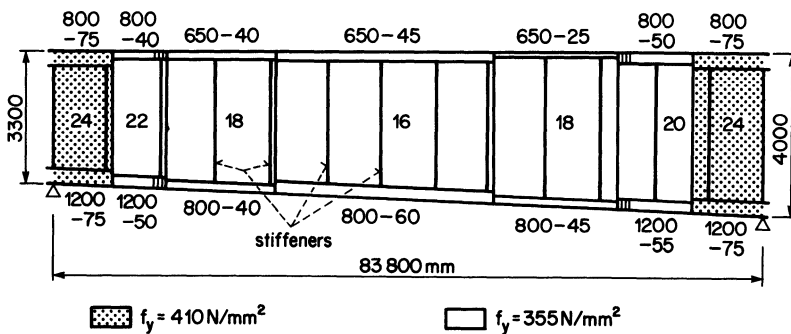


Fig. 1, Elevation of the main span of the Napoléon Bridge (CH)

During the formation of the protective layer brownish trail may make the concrete piles dirty. This can be avoided by lateral guidance and water moulding on the bottom flanges.

2.2 Concrete

For the deck slab a concrete with a 28-day cube strength of $40\text{--}45 \text{ N/mm}^2$ is generally used. Lightweight concrete, with an air dry density of 1800 kg/m^3 (reinforcement included) is seldom competitive, due to the higher price of lightweight aggregate. Such a concrete may be interesting for long spans, e.g. 174 m for the Tay bridge at Friarton

(1977), for which the 30% decrease in self weight of the deck takes a prominent part. For the bridge at Eptingen (CH) a concrete structure destroyed during construction by a landslide had to be rebuilt without one of the two piles. This results in two very different spans of 71 m and 37 m. The concrete deck of the new composite structure is therefore pre-stressed by jacking up at the abutment (37 m span).

3. STRUCTURAL ARRANGEMENT

3.1 Deck at lower flange level

A deck at lower flange level is required when the height as disposal is limited. Fig. 2 shows a simply supported bridge with a 41 m span. The structure, also here in weathering steel, comprises two tapered main girders and composite cross-girders. Profiled steel sheeting acts as both formwork and tensile reinforcement. This solution is widely used for composite floor construction in buildings. For bridges, however, fatigue must be included – specially for the connection between steel and concrete – so that this solution may be applied rather for minor roads.

For higher span lengths, e.g. 88 m for the combined railway and highway bridge over the Rhone shown in Fig. 3, a bowstring (Langer girder) is interesting. The footways are located outside of the girders so that the span of the cross-girders is reduced. No upper bracing is provided: the arch boxes, rigidly connected to stiff end cross-girders are wide enough to insure their lateral stability. The composite cross-girders guarantee the required vertical stiffness with a limited deck depth. The concrete slab acts also as tie-rod for a part of the horizontal component of the arch forces.

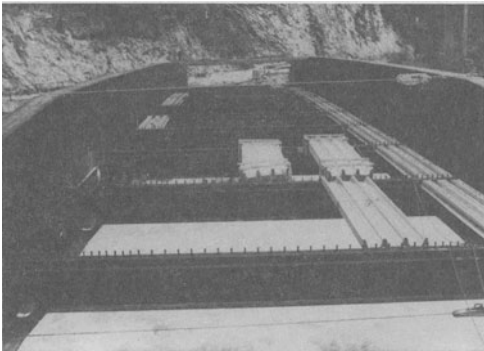


Fig. 2, Girder bridge over the Sarine river (CH)

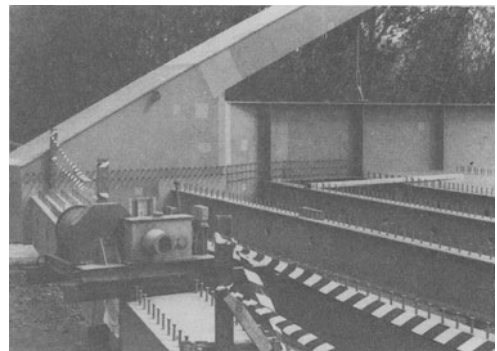


Fig. 3, Arch bridge over the Rhone (CH)

For a similar bridge, some kilometers upstream, the structure comprises steel arches and a deck with concrete lateral beams acting as stiffening system. This hybrid solution, with steel in compression and concrete in tension, may seem odd. The advantage is the easy erection of the arches, without expensive shuttering.

3.2 Deck at upper flange level

For bridges with composite main girders the deck is always located at upper flange level. The structure comprises generally two main girders only, even for a wide deck. In

the beginning, the slab was supported also in transverse direction by closely spaced cross-girders. Over interior supports this arrangement leads to tensile stresses in concrete due both to the hogging moments of the main girders and to the local plate bending. A longitudinal prestressing is then often required.

At the present time the concrete deck spans between the main girders only. This arrangement is possible also for wide highway bridges, e.g. 20 m for the bridge over the river Oise shown in Fig.12, with a 250 mm thick slab in the central region. With due regard to the large cantilevers, a transverse prestressing is provided which reduces the deflection due to creep and also the crack wide under the dead load; for economic reasons this solution is generally provided only for decks cantilevering more than 4 m. The cross-girders act here as cross-frames only, i.e. they prevent a distortion of the bridge sections and transmit the wind blowing on the lower girder part to the deck acting as wind brace.

For straight bridges an **open-framed** system is mostly adequate and more economic. The torques due to a traffic loading on a half wide of the deck are balanced mostly by an anti-symmetric bending of the two girders, i.e. by warping torsion. For a simply supported structure with a span l , a bending stiffness EI_x for one of the two main girders and a torsional stiffness GK of the deck, the straight line giving the transverse load distribution derives from the following two ordinates in the axis of the girders, spaced with a distance $2c$:

$$0.5 \pm 0.5/(1 + 4\omega^2/\pi^2) \quad \text{with} \quad \omega^2 = (GK/2EI_x) \cdot (l/2c)^2$$

This relation applies exactly for a sinusoidal longitudinal loading, but is also appropriate for a uniform loading (see for comparison the exact formula in [2]). For a negligible torsional stiffness GK the distribution follows obviously from the level principle, with the ordinates 1.0 and 0. Fig. 4 shows as an application the distribution line for a continuous motorway bridge with a 60 m span, i.e. about 50 m for the equivalent simply supported structure.

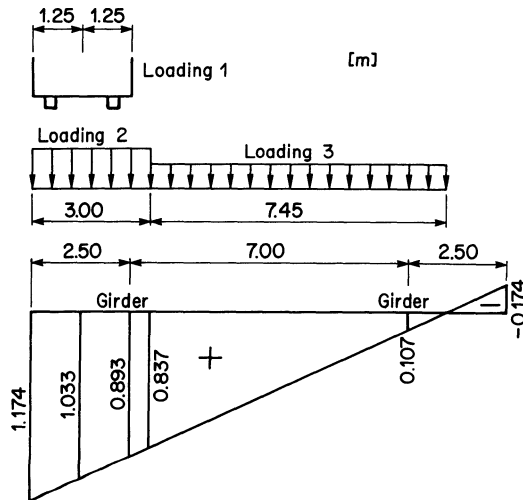


Fig. 4, Transverse load distribution for a composite bridge

The loading corresponds to the new Swiss Code SIA 160/1989. The decrease in girder bending, in comparison with a distribution according to the level principle, is of the order of 10% for the sagging moments. The corresponding torsional moments in the deck plate require generally no increase for the reinforcement.

3.3 Bridges curved in plane with open framing

For curved bridges built some twenty years ago in Switzerland a closed framing was generally adopted, even for relatively high ratios of the radius of curvature to the span length. For moderate spans, less than say 100 m, a torsional brace at bottom level was provided, whereas a proper box section is economic for higher spans only. The increase in labour costs in construction, however, is important, mainly due to the gussets welded to the bottom flanges which require a well-finished fabrication to avoid fatigue cracking.

For this reason, open framing is adopted at the present time even for low values of the radius of curvature. The distributed torque (kN·m/m) M/r generated by the tangential component of the bending moments M are also here (see section 3.2) balanced by an increased loading on the outside girder and a decreased loading on the inside girder (for sagging moments). When the length of the two concentric main girders is nearly the same, i.e. when the spacing $2c$ between the girders is low in comparison with the radius r , the additional girder load due to the bending moment M_o of the outside girder and the corresponding value M_i for the inside girder is given as

$$\Delta q = \pm (M_o + M_i)/2cr$$

The primary bending moments and the secondary moments due to the curvature are shown in Fig. 5, both for a simply supported structure and for a continuous bridge with equal spans and a uniform load. The ratio of the additional moments to the primary moments depends obviously on the non-dimensional parameter $l^2/2cr$. For the continuous structure, however, the additional moments are very small because the forces Δq change the sign at the points of contraflexure. For the limit of application of the approximate analysis given in Fig. 5 reference can be made to [3].

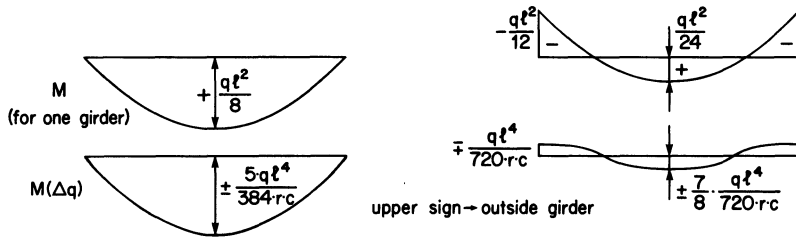


Fig. 5, Bending moments of open-framed curved bridges

Fifteen years ago a value $l^2/2cr \leq 1$ was considered as a limit for a curved open-framed structure. For the Napoléon bridge shown on Fig. 6, with a main span of 83 m, a radius of curvature of 400 m and a girder spacing $2c$ of only 5 m dictated mainly by geotechnical conditions, the parameter takes the value 3.4. The simplified method given in Fig. 5 is obviously not applicable here and the structure has been calculated as girder grillage.

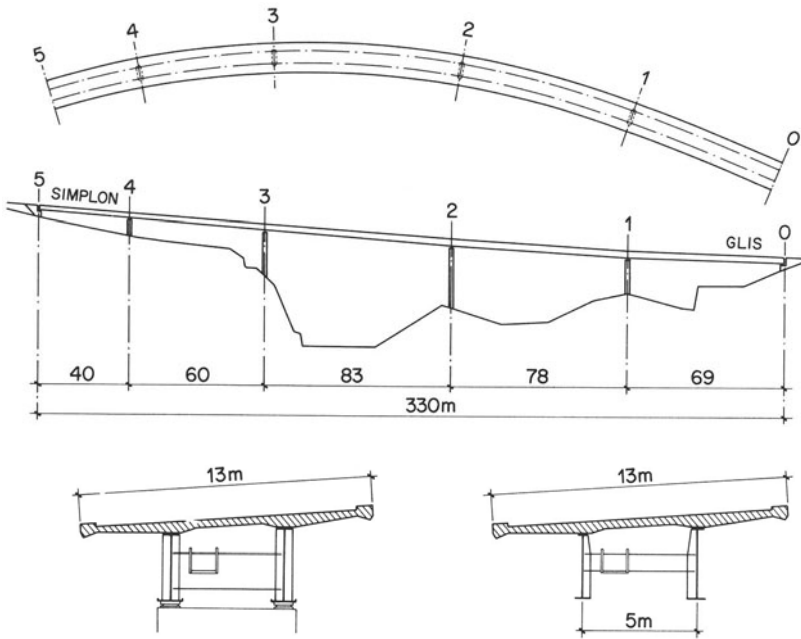


Fig. 6, Napoléon Bridge near Brig

The same model has been adopted for the bridge shown in Fig. 7, with a 32 m main span and an average radius of curvature of 130 m. The axis of the structure is S-shaped, with skew supports and a junction for a minor road in the main span. The cross-frames are rolled profiles arranged radially to simplify their connection to the main girders, located at different levels in each cross-section according to the transverse deck slope.



Fig. 7, Maladeire Bridge (CH)



Fig. 8, La Tine Bridge (CH)

3.4 Bridges curved in plane with closed framing

For another bridge in a mountainous region (see Fig. 8) the main span reaches 47.5 m, with a radius $r = 100$ m and a girder spacing of 5 m. The torques due to curvature are therefore relatively high so that a closed-framed structure was required, with strong bracing diagonals at bottom level and cross braces.

For the Goldswil viaduct near Interlaken (Fig. 9) mainly aesthetic reasons have led to a "trough" type of box with trapezoidal section and a constant height in spite of the span lengths varying between 81 m over the river Aare, 71 m over the railway station and 45 m for the intermediate spans. During erection a top bracing equilibrates the shear flow due to the torques M/r mentioned in section 3.3, with a radius $r = 680$ m. The need for easy longitudinal placement of the interior part of the shuttering for the slab has led to a plane of the bracing located at about 0.5 m below the level of the top flanges. For the corresponding calculation of the transverse braces reference can be made to [3].

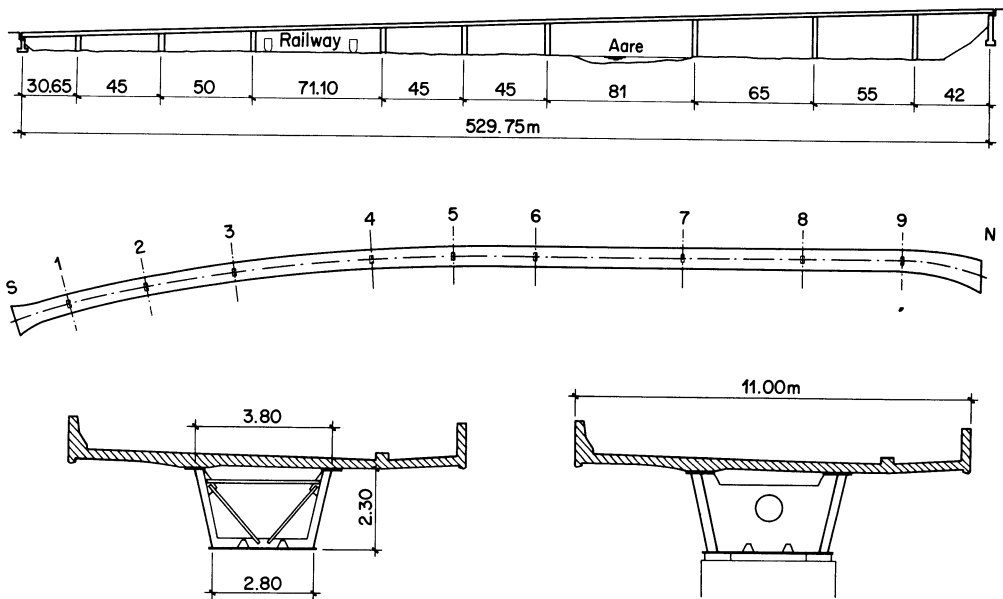


Fig. 9, Goldswil viaduct near Interlaken (CH)

3.5 Bridges with several main girders

An arrangement with more than two girders may be adequate for very large bridges, e.g. for the bridge over the Limmat river at Zurich (Fig. 10). The new structure is more or less a duplicate of the old one, a solution required by a public voting. The structure forms a girder grillage, well adapted for the relatively heavy loading due to the tramway lines. The erection was made by a transverse launching of the new and the old structure tied together, so that only a very short traffic interruption was needed.

For the replacement of an old trussed bridge spanning the river Ticino the new composite structure has been built in two stages, each half-bridge consisting of two steel girders with the corresponding precast concrete deck.

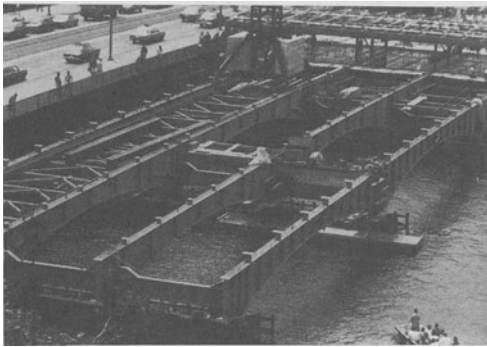


Fig. 10, Bridge over the Limmat river at Zurich

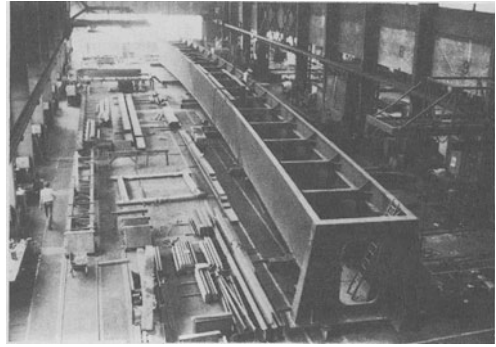


Fig. 11, Railway bridge near Disentis

3.6 Railway bridges

When the height at disposal is very limited, a "trough" box girder with a relatively large bottom flange plate gives an adequate solution for a railway bridge, in spite of the higher labour costs. Fig. 11 shows a simply supported structure with a 54 m span during construction. At the abutments the width of the trapezoidal box is increased to insure the stability of this curved structure considered as a rigid body. For a "trough" box as a combined railway-highway bridge with large span lengths reference can be made to [4].

The bridge over the Limmat river below Zurich replaces two old trussed bridges [5]. The arrangement with only two girders for a double track railway leads on the one hand to a reduced steel weight, on the other hand to an increased depth of the deck slab (400 mm). The structure is open-framed, mainly owing to the fatigue requirements for the bottom flanges (no gussets required).

In Germany also some composite **truss** girder bridges have been built for the high speed new railways lines, due to severe deflection requirements. Such conditions can be satisfied even by simply supported truss girders, a solution avoiding cracks in the concrete deck at support. For more details reference can be made to [6].

4. DESIGN PROCEDURES

4.1 Analysis of structures

In general both the internal force resultants and the section capacities are calculated by elastic theory. The cross-sections are indeed too slender and allow no plastic hinge rotation, furthermore a negligible stress redistribution only. EUROCODE 4 will give some indications for the modified moment distribution due to concrete cracking in hogging moment regions.

In sagging moment regions the steel girder is in the tension zone so that no buckling problem occurs: the cross-sections are therefore compact and the bending capacity may be determined here by simple plastic theory when the increase of hogging moments due to fully plastified cross-sections in sagging moment regions is considered in design [7]. This

solution is economic because the loading history must not be taken into account, i.e. a differentiation between loads applied to the steel section prior to the development of composite action and those applied to the composite section is no more needed.

4.2 Postcritical behaviour of thin-webbed plate girders

A design based on the classical plate buckling theory requires longitudinal stiffeners for a girder depth of say more than 2 m and an adequate web thickness. When the postcritical plate behaviour is accounted for, on the contrary, Fig. 1 shows that webs with transverse stiffeners only are suitable even for girders up to 4 m (for a bridge in Luxemburg with a main span of 92 m and a girder depth of 4 m, designed as well according to the Swiss code SIA 161/1979, see [8]). The web thickness is obviously higher than for a longitudinally stiffened web but the labour costs are largely lower.

The bending capacity of such girders can be calculated by replacing the compression zone b_c of the web by an effective width b_e which is inversely proportional to the plate reference slenderness $\bar{\lambda}_p = \sqrt{f_y/\sigma_{cr}}$ (f_y = yield stress; σ_{cr} = critical plate bending stress according linear theory, i.e. $\sigma_{cr} = k_\sigma \cdot 0.9 \cdot E \cdot (t_w/b)^2$ for a web depth b). This method considers therefore implicitly a shedding of the bending stresses from the web to the compression flange, so that the flange capacity is the leading factor for the ultimate strength. The classical buckling theory, on the contrary, evaluates the bending capacity of the whole girder by considering the critical stress σ_{cr} of the web only.

Similarly the shear capacity of thin webs is given by a tension field model, with the transverse stiffeners acting as compression posts. For more details concerning the postcritical plate behaviour reference can be made to ECCS publication no. 44 [9] and to EUROCODE 3. Composite girders require special considerations; they will be given in the final draft of EUROCODE 4, not available at the present time.

4.3 Spacing of transverse stiffeners

The spacing between the transverse stiffeners is very important from an economic point of view. Both for the Napoléon bridge (Fig. 6) and for the Goldswil viaduct (Fig. 9) it was intended at the beginning to have relative low aspect ratios, in the order of 1.0, i.e. to introduce intermediate transverse stiffeners between the cross-braces. Comparative studies conducted for the two bridges have proved that an arrangement with thicker webs, say 2 mm more on an average to reach the required shear strength, and an aspect ratio of at least 2 is better: the decrease in the labour costs is namely higher than the increase of material supply.

5. CONSTRUCTION OF COMPOSITE BRIDGES

5.1 Deck slab cast in situ

The choice of an optimum method for the concreting of the deck is essential for the economic efficiency of a composite bridge. A conventional wooden scaffolding over the full length may be interesting for particular conditions. In situ concrete, however, is generally poured using a movable scaffolding, as shown in Fig 12 for the bridge over the river Oise already mentioned in section 3.2 (span lengths 45 m). The interior part of the shuttering will be slid on the flanges of the cross-frames to that these elements must be located at a suitable level. A deck length of about 15 m can be concreted each week.

When the deck is poured continuously in this manner the problem of concrete cracking in the hogging moment region needs careful consideration: the part of the slab

cast one or more weeks before is green and has a very small tension strength, so that the hogging moments due to the concrete weight in the span may cause cracking.



Fig. 12, Bridge over the river Oise (F) with movable scaffolding

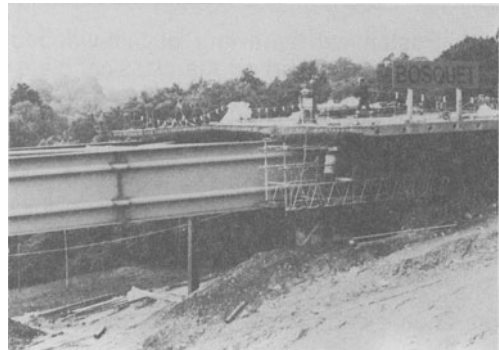


Fig. 13, Stage deck jacking for the Sorge bridge (CH)

For the Goldswil viaduct (Fig. 9) two measures have been adopted to avoid cracks as much as possible and therefore to increase serviceability. On the one hand the connectors are arranged in groups and the corresponding zones in the slab are not concreted immediately. All 60 m transverse joints remain open to allow for shrinkage and other movements. On the other hand the deck is prestressed in the longitudinal direction, especially over the intermediate supports, with an initial concrete compression in the order of 2–4 N/mm². The transverse joints are poured after as long as possible a time so that the prestressing decrease due to creep with corresponding hyperstatic moments can be limited.

5.2 Precast deck slabs

Precast deck slabs are today less utilized than twenty years ago. The advantages are well-known, especially the concrete weight will surely be supported by the steel girders only, avoiding therefore cracking during concreting. The presence of many transverse joints between the slabs (spacing 2-3 m), however, complicates the compliance with the serviceability requirements in the hogging moment region. This solution remains interesting for special conditions, e.g. for the two bridges in mountainous regions shown in Fig. 7 and 8 (see also [4]). For various laying procedures reference can be made to [10].

5.3 Stage-deck jacking along the steel girders

The concreting area is located here generally behind the abutment – for a long bridge on the span. In the first case the adjacent span must be propped to reduce the slope at the abutment (Fig. 13); moreover equilibrium conditions for the friction forces require that the steel structure and the formwork are connected together.

The launching method for the deck combines the advantages of in situ concreting (no transverse joints) with those of precasting. Obviously all possible hazard scenarios must be considered. The main problems to be solved are the stability of the top flanges, taking into account transverse forces during launching, and the effect of possible eccentricities of the vertical loads. Last but not least the friction behaviour has to be carefully investigated. On the one hand sliding devices must be provided at the interface, e.g. pads introduced in

some of the openings for the connectors. A lubrication consisting of colloidal graphite suspension allows to reduce the friction according to the jack capacity. For bridges with a longitudinal slope, however, the friction must be sufficient to stabilize the deck. An accident has shown that the friction coefficient can be as low as 6% (see for example [11]).

5.4 Erection of the steel girders

The erection procedures for the girders are the same as for steel bridges: the composite action obviously does not play a role in this topic. For the viaduct at Goldswil (see Fig. 9), as an example, the curved southern part has firstly be launched over the railway station, without any traffic interruption, and the two adjacent 45 m spans have been assembled at ground level and erected by crane, each span as a unit (Fig. 14). Finally the northern part has been also erected by launching, using the end span, curved and skew, as assembly site.

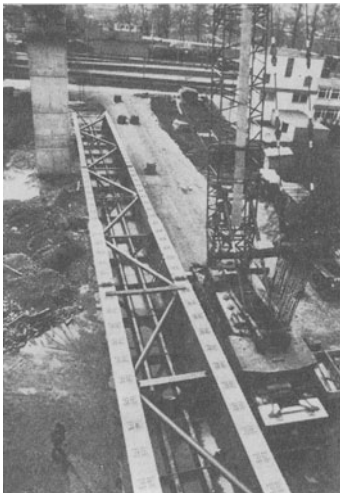


Fig. 14, Erection of the viaduct at Goldswil
(Figure on the right)



Fig. 15, Demolishment of the old deck

6. WIDENING OF EXISTING BRIDGES

Due to increased traffic bridges must in some circumstances be widened, as this was required for the Austrian section of the Brenner motorway. Fig. 15 shows the demolition of the old concrete deck of the Gschnitztal viaduct (span lengths about 80 m) during winter time, the traffic being then supported by the parallel bridge only. The new deck is widened on the outside part of the section so that a special lane for heavy vehicles can be provided. With the use of transverse prestressing its weight is not increased in comparison to the old one. Only the torsional brace at under flange level has to be strengthened due to the increased torques resulting from the eccentricity between the new deck and the axis of the steel structure. The new slab has been concreted using a movable scaffolding as mentioned in section 5.1, with the area in the hogging moment region poured in a final stage to surely avoid cracks due to the self-weight.

FINAL REMARKS

The present paper is a kind of extended summary of the conference presented in French on 15th June 1989 at Udine. Specially the number of figures compared with the slides shown during the conference has been drastically reduced due to the allowed number of pages. For some of these cancelled figures, references have been included which give detailed information together with illustration. Moreover reference can be made to the publication series "Bauen in Stahl" edited by "Schweizerische Zentralstelle für Stahlbau", CH-8034 Zürich. See for example the numbers 5/1982 (Brücke über den Tessin bei Quartino), 14/1983 (Viadukt Goldswil), 23/1985 (Napoleonsbrücke Brig), 14/1988 (Pont sur le Rhône à Saint-Triphon).

REFERENCES

1. Stiemer, S.F., Taylor, P. and D.H.C. Vincent: Full scale dynamic testing of the Annacis Bridge. IABSE Proceedings P-122/88 (1988).
2. Dubas, P.: Développements suisses récents en matière de ponts mixtes acier-béton. *Costruzioni metalliche* 21 (1969) n. 1, 1-15.
3. Dubas, P.: Some remarks concerning the design of composite bridges. *J. Construct. Steel Research* 7 (1987) 233-251.
4. Mason, J.: Verbundbrücke über den Fluss Tocantins in Nordbrasilien. *Stahlbau* 58 (1989) 129-135.
5. Gut, H. und E. Graf: Neubau Obere Limmatbrücke der SBB. *Schweizer Ingenieur und Architekt* 107 (1989) 240-244.
6. Keller, N., Kahmann, R. und M. Krips: Fuldabrücke Kragenhof. *Bauingenieur* 63 (1988) 443-454.
7. Roik, K., Bode, H. and J. Haensel: Erläuterungen zu den "Richtlinien für die Bemessung und Ausführung von Stahlverbundbrücken" - Anwendungsbeispiele". Institut für konstruktiven Ingenieurbau, Ruhr-Universität Bochum, Mitt. Nr. 75-11, 1975.
8. Molitor, Ley et Geisen: Viaduc sur le Sernigerbach (Luxembourg). *IABSE Structures* C-33/85 (1985) 16-17.
9. European Convention for Constructional Steelwork, TWG 8.3: Behaviour and design of steel plated structures. Publication no. 44, Edited by P. Dubas and E. Gehri, Zurich, Swiss Federal Institute of Technology, 1986.
10. Dubas, P.: Problèmes relatifs à la conception et à la réalisation des ponts mixtes acier-béton. *Revue Technique Luxembourgeoise* 80 (1978) 89-100.
11. Bourquin, G.H.: Composite bridge decking by stage-deck jacking. *Journal of the Structural Division, ASCE* 104 (1978) No. ST1, 171-189.
12. Tschemmernegg, F., Passer, H. und O. Neuber: Verbreiterung und Sanierung von Stahlbrücken. *Stahlbau* 58 (1989) 289-298.

STRUCTURAL SYSTEMS FOR CABLE SUSPENDED BRIDGES

N.J. Gimsing

Technical University of Denmark, Copenhagen, Danimarca

ABSTRACT

The paper describes a number of the features related to the choice of the structural system for cable suspended bridges, i.e. cable stayed bridges and suspension bridges.

For the cable stayed bridges most of the text deals with the conventional three span arrangement found in the major part of the existing cable suspended bridges, whereas the problems related to a multispans arrangement are treated for both the cable stayed and the suspension system.

INTRODUCTION

During its three decade history of evolution the cable stayed bridge has probably appeared in a larger variety of forms than any other bridge type. This is due to the large degree of geometrical freedom associated with the cable stayed system.

In recent years the many variants have, however, shown a tendency to crystalize into a limited number of basic types that have proven to be superior to many of the early concepts.

1. THREE SPAN CABLE STAYED BRIDGES

The major part of the existing cable stayed bridges are of the three span configuration with a large main span flanked by two smaller side spans, e.g. the same span arrangement as found in most suspension bridges.

1.1 General Arrangement of Cable Planes

The aim of the cable system is to assist the girder in transmitting the loads acting on the structure to the supports.

The loads that have to be considered when choosing the arrangement of the cable planes are : The vertical loads P_v , the lateral loads P_l and the torsional moments M_t , as shown on Figure 1.

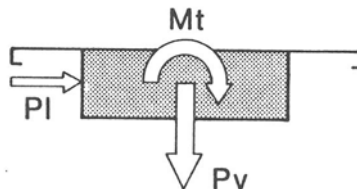


Figure 1. Resulting forces acting on the stiffening girder.

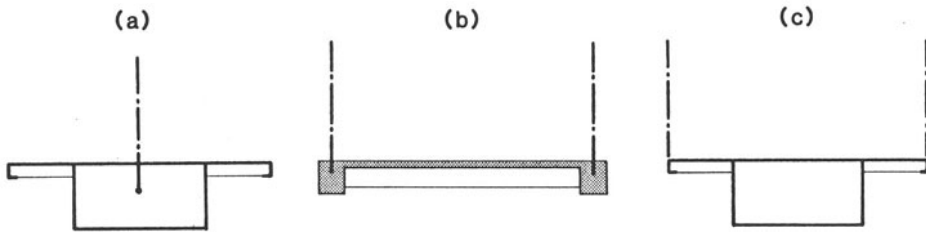


Figure 2. Bridges with one or two cable planes and with or without torsional stiffness of the girder.

For road bridges with dual carriageways a single, central cable plane has frequently been applied (Figure 2(a)). With this arrangement the cable system only contributes by carrying the vertical loads P_v globally, whereas the girder has to transfer the entire lateral load P_l and the torsional moments M_t . Consequently, the system with a central cable plane requires a girder with large lateral and torsional rigidity.

With two vertical cable planes attached along the edges of the roadway both the vertical loads P_v and the torsional moments M_t can be transferred by the cable system, so that only the lateral loads P_l have to be carried by the girder (Figure 2(b)). Consequently, no torsional stiffness is required and an open cross section is therefore adequate.

If, however, a double cable plane system is combined with a torsionally rigid girder (Figure 2(c)) the torsional moment M_t will be partly transferred by the cable system and partly by the girder. The vertical and lateral loads will be transferred in the same way as for the system with no torsional stiffness of the girder.

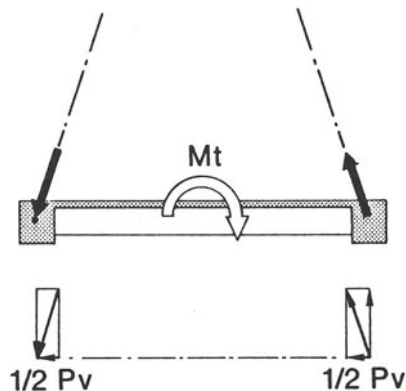


Figure 3. Lateral forces induced by torsional moment transferred by inclined cable planes.

With two laterally inclined cable planes the transmission of the vertical loads P_v will basically be as for the system with two vertical cable planes.

For a bridge with no torsional girder stiffness the lateral loads P_l will have to be carried by the girder, and the torsional moments M_t by the cable system. However, due to the inclination of the cable planes the transfer of torsional moments by the cable system will induce additional lateral loads in the girder, as illustrated in Figure 3.

Finally, if the laterally inclined cable planes are combined with a torsionally rigid girder the transmission of the lateral loads P_l and the torsional moments M_t becomes more complex. Thus, the lateral load P_l will partly be carried by lateral bending of the girder and partly by the cable system due to the resistance against rotation offered by the girder (Figure 4). Similarly, the torsional moments will also induce lateral loads.

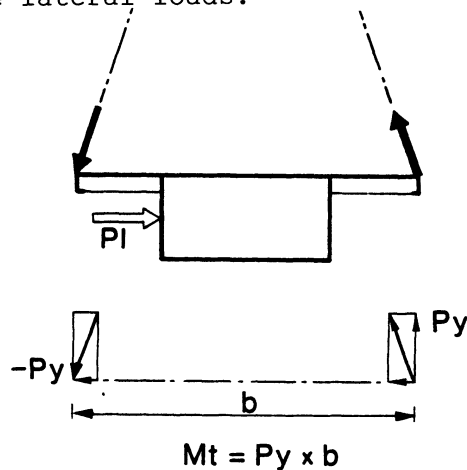


Figure 4. Torsional moment induced by transmission of lateral forces to inclined cable planes.

As described above the participation of the cable system in transmitting the loads acting on the girder depends to a large extent on the arrangement of the cable planes.

This feature is further illustrated in Figure 5 showing systems ranging from the pure box girder bridge where all loads naturally have to be transferred by the girder, to a system with four inclined cable planes allowing all the loads P_v , P_l and M_t to be carried by the cable system.

So far the cable systems able to transmit the lateral load P_l has not been used in road bridges but only in a limited number of pipeline bridges. However, cable systems

adding lateral stiffness could also be attractive for road bridges with a modest width-to-span ratio.

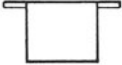




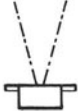
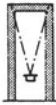
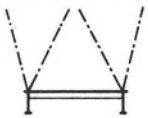

TYPE OF STRUCTURE	LOAD TRANSFER BY		PYLON SHAPE (TYPICAL)
	CABLE SYSTEM	GIRDER	
 PURE BOX GIRDER		Pv, Pl, Mt	
 CENTRAL CABLE PLANE	Pv	Pl, Mt	
 TWO VERTICAL CABLE PLANES	Pv, Mt	Pl	
 TWO INCLINED CABLE PLANES	Pv, Pl	Mt	
 FOUR INCLINED CABLE PLANES	Pv, Pl, Mt		

Figure 5. Force transfer and cable plane arrangement.

1.2 Configuration of the Cable System

In the early cable stayed bridges from the 1950.es and 1960.es the cable systems generally contained a very limited number of stay cables (Figure 6(a)). This led to large forces in each stay cable and consequently a multi-strand cross section was required. In the present practice the preference is for a multi cable system (Figure 6(b)) comprising mono-strand stay cables. This is partly due to the advantages of a more continuous support of the girder by the cable system and partly to the easier installation and replacement of stay cables. However, the indisputable advantages gained by introducing the multi cable system has also been followed by some drawbacks. Thus, the problems

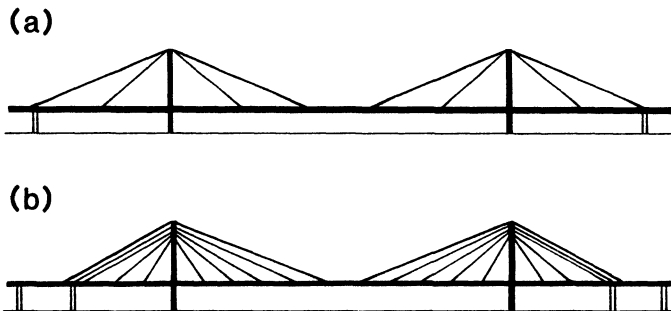


Figure 6. Cable systems with few or many stay cables.

related to wind induced oscillations of the individual stay cables have become more pronounced for mono-strand cables than for multi-strand cables.

The preferred cable configuration is the modified fan shown in Figure 6(b). Here the cable anchorages in the pylon are concentrated at the pylon top and spaced as closely as the installation and force transmission allow. By concentrating the cable anchorages at the pylon top it is achieved that the moments in the pylon due to transmission of unbalanced horizontal forces are kept at a minimum (Figure 7).

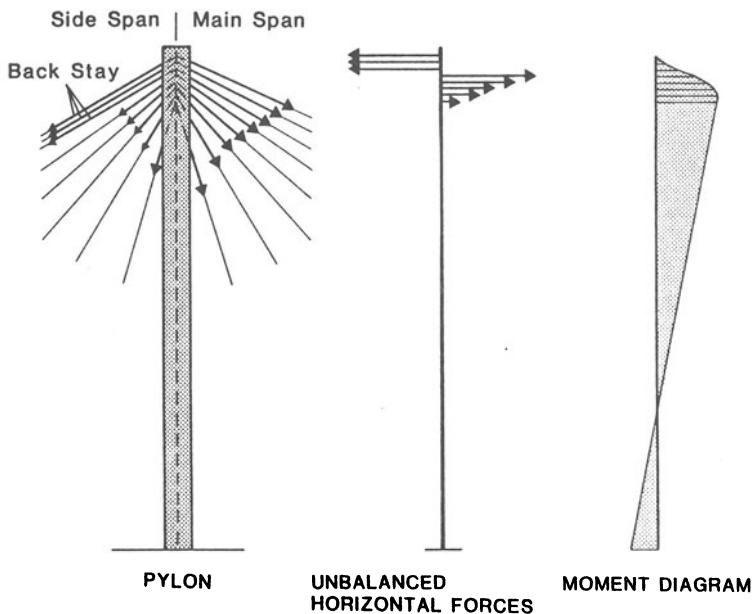


Figure 7. Moments in the pylon induced by unbalanced horizontal cable components.

To ensure a reasonable tension in the backstay cable, the length of the side span has to be chosen to somewhat less than half of the main span length. With a constant spacing of the cable anchorages in the girder this implies that the number of cables leading to the side span will be smaller than the number leading to the corresponding main span half. To counteract this difference the back stay cable is in most cases composed of a number of parallel mono-strand cables, as shown in Figure 8(c). Alternatively, the two fans radiating from the pylon can be made symmetrical by extending the cable anchorages into the span adjacent to the side span, as shown in Figure 8(d). However, with this system the girder will be subjected to a substantial bending in the region at the anchor pier.

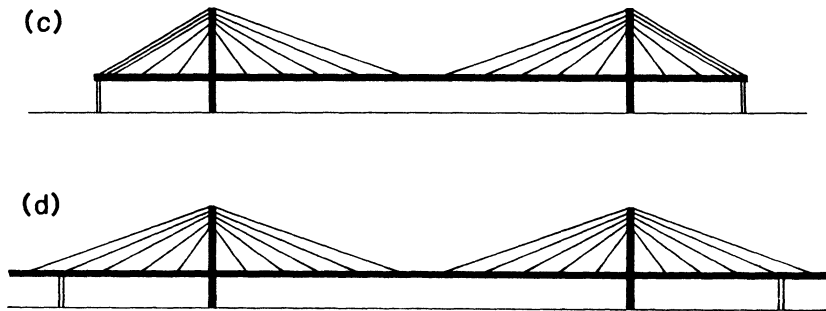


Figure 8. Asymmetrical and symmetrical fan arrangement.

The harp system comprising parallel stay cables - and therefore a spreading of the pylon anchorages over the entire pylon height - might be preferred if the pylon is made with a large bending stiffness in the longitudinal direction (Figure 9(e)) or if the girder has intermediate supports in the side span (Figure 9(f)). As the purpose of the intermediate supports is to eliminate vertical deflections of the side span cable anchorages, they must be

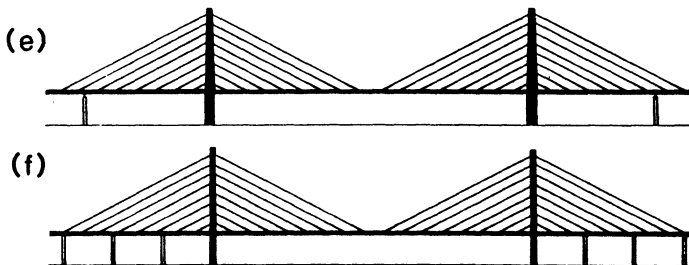


Figure 9. Harp shaped cable systems stabilized by stiff pylons or intermediate supports.

placed so closely that the girder only deflects insignificantly between the supporting points. This requirement will be fulfilled if the distance between intermediate supports is chosen to be less than approximately 20 times the girder depth.

In the modern cable stayed bridges the stay cables will always be fixed both vertically and horizontally to the pylon whether the cable system is of the modified fan or the harp configuration.

2. LIMITING SPAN OF CABLE STAYED BRIDGES

Since its introduction in the 1950s the cable-stayed bridge has gradually increased its free span from 183m in the Stromsund Bridge to 465m in the Annacis Island Bridge, and at present several cable-stayed bridges with spans around 500m are under construction.

Having witnessed this evolution it is natural to ask: What is the maximum span that can be reached with the cable-stayed bridge?

To answer this question it is necessary to consider each structural element and determine which ones will ultimately determine the maximum length of the free span.

2.1. The Stay Cable

The stay cable is the structural element that primarily characterizes the cable stayed bridge and it is therefore reasonable to first consider how this element behaves with increasing span length.

First of all, the load-carrying capacity of a stay cable is influenced by the sag - illustrated to the left in Figure 10 - and as the relative sag increases with the length of the stay cable the load carrying capacity will decrease.

This is illustrated to the right in Figure 10 where the efficiency ratio (defined as the ratio between the force T_0 in a straight cable and the force T in the real, sagging cable) is plotted against the horizontal cable projection.

The ultimate length of the stay cable is obviously the length where the efficiency ratio becomes zero, which corresponds to a case where the cable tangent at the bottom is horizontal.

Based on realistic assumptions regarding design stress level and density of the cable material the ultimate lengths

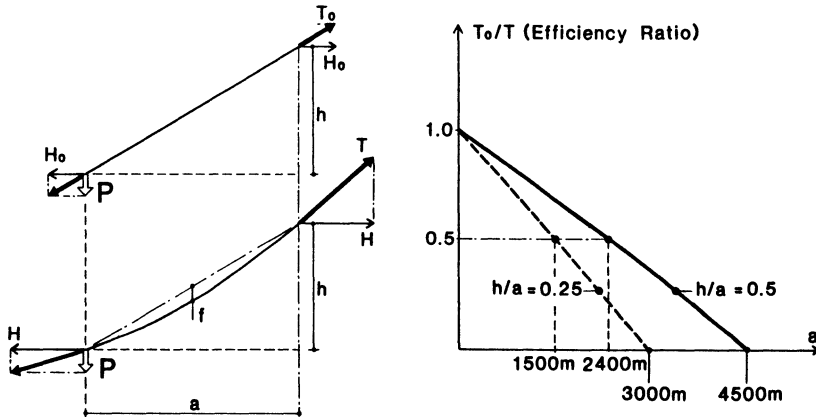


Figure 10. Load carrying capacity of a stay cable as expressed by the efficiency ratio T_o/T .

will be approximately 3000m for a chord inclination of 0.25 and 4500m for a chord inclination of 0.5.

In real structures it will probably not be acceptable to have cables with an efficiency ratio of less than 0.5 as the stay cable naturally also has to carry other loads than its own weight. But even for an efficiency ratio of 0.5 the maximum horizontal stay cable length becomes 1500-2400m, which corresponds to main span lengths of 3000-4800m. Thus, the load carrying capacity of the stay cables allows a most significant extension of the present cable stayed bridge spans.

The sag also results in a reduction of the axial stiffness of the stay cable as it can be expressed by the ratio between the equivalent modulus E_{eq} (Ref.3) and the real modulus of elasticity E (Figure 11).

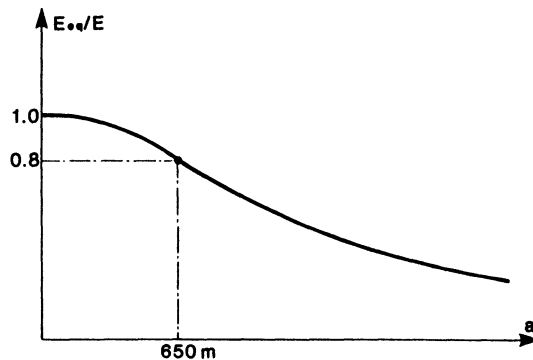


Figure 11. Stiffness of a stay cable expressed by the ratio E_{eq}/E .

It is in general difficult to specify the allowable reduction in axial stiffness for a given case, as the static and dynamic behaviour of the entire structure is influenced by the flexibility of the cables.

If the limiting ratio between E_{eq} and E is stipulated at 0.8 the maximum horizontal stay cable length becomes approximately 650m corresponding to a main span length of 1300m. Thus, the stiffness requirements can easily be more restrictive than the strength requirements.

The stay cable length might also be limited by considerations regarding dynamic behaviour, and already in some of the existing cable-stayed bridges the stay cable oscillations have presented a problem. However, in the span range found to-day the undesirable dynamic actions have been eliminated by introducing relatively simple stabilizing or damping devices.

Serious dynamic effects would undoubtedly occur if the natural frequencies of the lower modes of the individual stay cable oscillations coincided with the natural frequency of the total system characterized by vibrations of the entire stiffening girder and the towers.

As the natural frequency of the individual stay cable decreases with the span length, resonance will inevitably occur for a certain cable length. With typical values the frequencies of the first individual mode and the global mode will coincide for cable lengths between 600m and 1200m (Figure 12). Consequently, also the dynamic action might easily be more decisive than the load-carrying capacity of the stay cable.

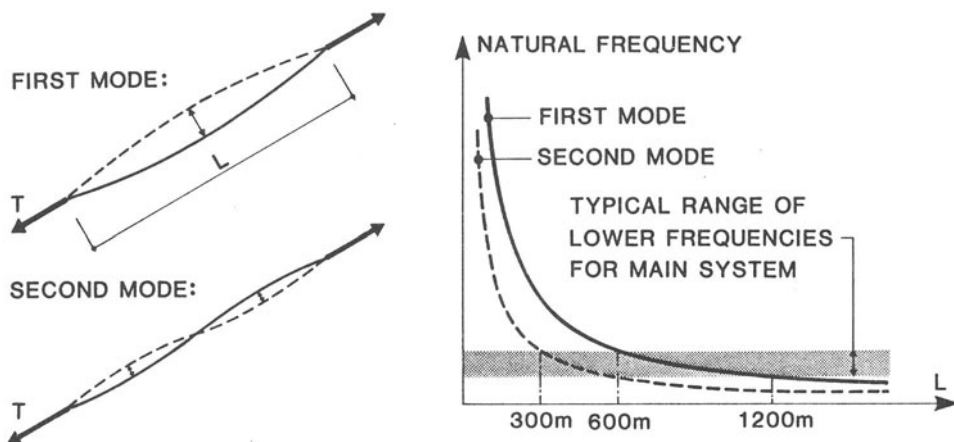
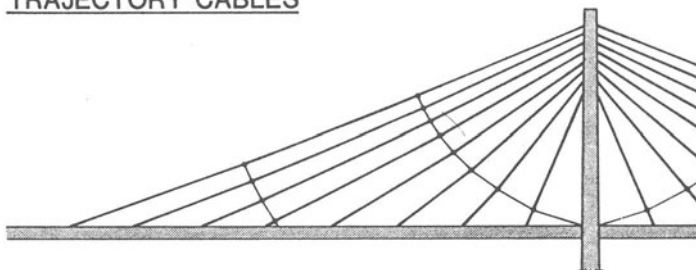


Figure 12. Resonance between oscillation of the individual stays and the global system.

An overall improvement of the system can therefore be achieved by adding secondary trajectory cables, as shown in Figure 13. Such secondary cables will significantly reduce the sag variations of the primary stay cables under varying axial forces and they will restrain free oscillations of the single cable. Consequently, both the axial stiffness and the dynamic behaviour of the single cable will benefit from an addition of the trajectory cables.

TRAJECTORY CABLES



IMPROVES:

STIFFNESS OF STAY CABLES

REDUCES:

OSCILLATION OF INDIVIDUAL STAYS

LOAD CARRING CAPACITY OF STAYS

Figure 13. Application of secondary trajectory cables.

To be efficient the trajectory cables have to pull down the stay cables which involves a reduction of inclination of the stay cable tangent at the bottom and an increased tangent inclination at the top. This will unfavourably influence the load-carrying capacity of the stay cable, but this effect is of minor importance due to the fact that this parameter is less restrictive than the other two.

2.2. The Stiffening Girder

In the cable stayed bridge the stiffening girder contributes to the global load transfer by transmitting the horizontal stay cable components as axial forces, and by carrying the lateral wind load by bending to the supports.

The maximum axial force in the stiffening girder obviously increases with the span length so that for larger spans the cross sectional area A_s of the girder at the pylon have to be chosen larger than the area A_o in the midspan region.

If it is assumed (more or less arbitrarily) that it is acceptable to have a 2,5 times larger girder cross section at the pylon than at midspan, then the limiting length of

the half span (=horizontal stay cable length) will be approximately 370m for a concrete bridge and 940m for a steel bridge (Figure 14) - again based on realistic values for densities and stress levels.

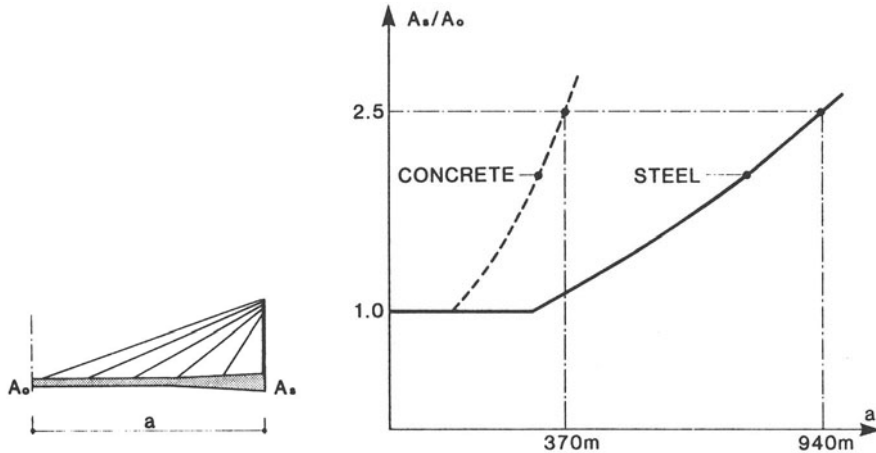


Figure 14. Increase in the cross sectional area of the girder to allow transfer of axial forces.

Consequently, the axial strength of the stiffening girder might be the limiting factor for a concrete bridge, whereas it is less likely to be decisive for a steel bridge.

The lateral stability of the stiffening girder will generally limit the free length of the cantilever arm during erection (Figure 15). Thus, the length-to-width ratio of the cantilever must be limited to a value between 15 and 25 to avoid unacceptable dynamic actions. For a bridge with a

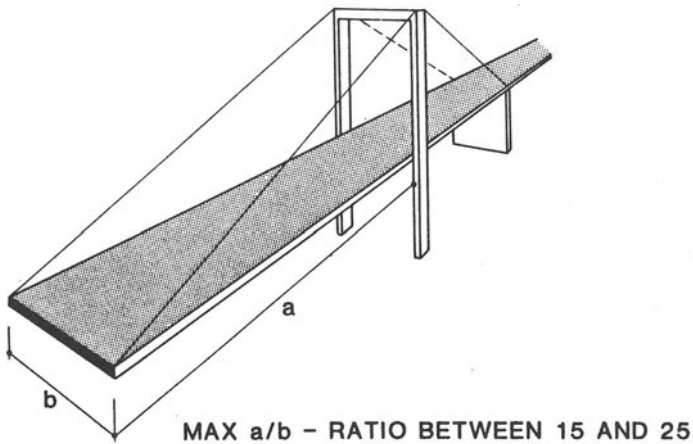


Figure 15. Lateral stability of the stiffening girder.

roadway width of 12m this requirement might limit the span length to as little as 360m.

The limiting length-to-width ratio mentioned above can not be stipulated at a fixed value as it will depend on a number of factors such as the local wind climate, the efficiency of the temporary fixation to the pylon pier, the moment of inertia of the stiffening girder and its degree of streamlining.

To overcome the problem related to the lateral stability of the stiffening girder a twin box arrangement as shown in Figure 16 might be introduced. Here the total deck width b is split in two parts each with a width of $b/2$ and joined by transverse beams and horizontal cable diagonals. Thus, in the lateral direction the stiffening girder will act as a truss with the two boxes forming the chords.

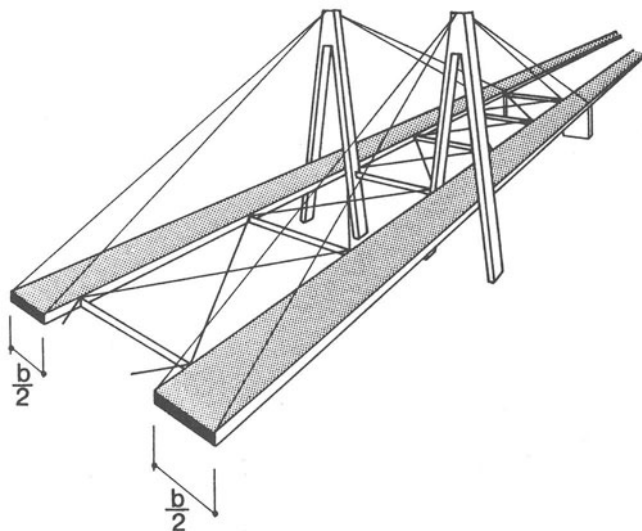


Figure 16. Twin box arrangement to improve the lateral stability.

The twin box concept was originally proposed by Richardson (Ref.4) as a mean to improve the aerodynamic stability of long span suspension bridges but it might very well be even more efficient in improving the lateral stability of of a cable stayed bridge where the cable system (at least in the self anchored case) does not render any lateral support to the girder.

3. STRUCTURAL SYSTEMS FOR MULTISPAN SUSPENDED BRIDGES.

The majority of all cable suspended bridges built so far are made as three-span structures with a large main span flanked by two shorter side spans.

In the cases where more than three cable suspended spans have been required, it has often been chosen to apply two (or more) conventional three-span structures in a row. This was the case for the West Bay Crossing of the San Francisco-Oakland Bay Bridge, and the same principle has recently been used also in two of the Honshu-Shikoku Bridges: The Bisan Seto Suspension Bridges and the Hitsuishijima and Iwagurojima Cable Stayed Bridges.

The main reason for using three-span structures as a basic element also for bridges with a larger number of spans is undoubtedly that special problems arise if a true multispan cable suspended bridge shall be designed.

A true multispan bridge will comprise a number of consecutive main spans of equal size and shorter side spans at the extreme ends only, as illustrated at the bottom of Figure 17.

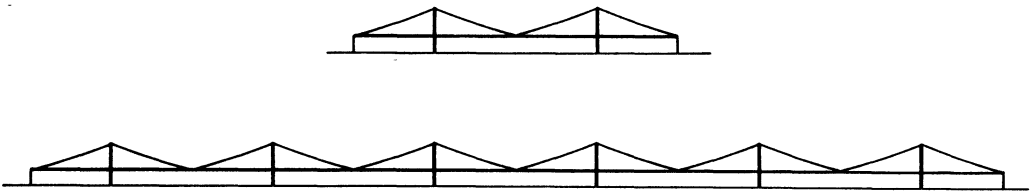


Figure 17. Three span and multi span cable suspended bridges.

From a structural viewpoint the largest problems relate to the lack of efficient longitudinal support of the inner pylon tops, as they are not restrained by an anchor cable leading to a point where the girder is supported vertically.

Generally, it can be stated that in multispan cable suspended bridges the main effort must be concentrated at achieving sufficient stiffness, as adequate strength is easier obtained. However, the flexibility that will result if the multispan structure is not carefully designed might also have some side effects that influence the safety. Thus, a flexible structure is more vulnerable to aerodynamic actions and might easier be subjected to fatigue due to larger stress variations under moving traffic loads.

3.1. Multispan Cable Stayed Bridges.

To improve the deformational characteristics of a multispan cable stayed bridge two basic approaches can be followed. One is to increase the bending stiffness of the girder or the pylons, and the other to modify the cable system.

If it is chosen to increase the bending stiffness of the girder, significantly larger depth-to-span ratios than found in the normal three-span bridges have to be used (Figure 18(b)), typically approx. three times larger ($1/40$ instead of less than $1/100$). This inevitably leads to a larger dead load influencing unfavourably the dimensions of the stay cables, the pylons and the substructure. Consequently, to choose a larger stiffness of the girder often constitutes the most expensive way to limit deflections of a multispan cable stayed bridge.

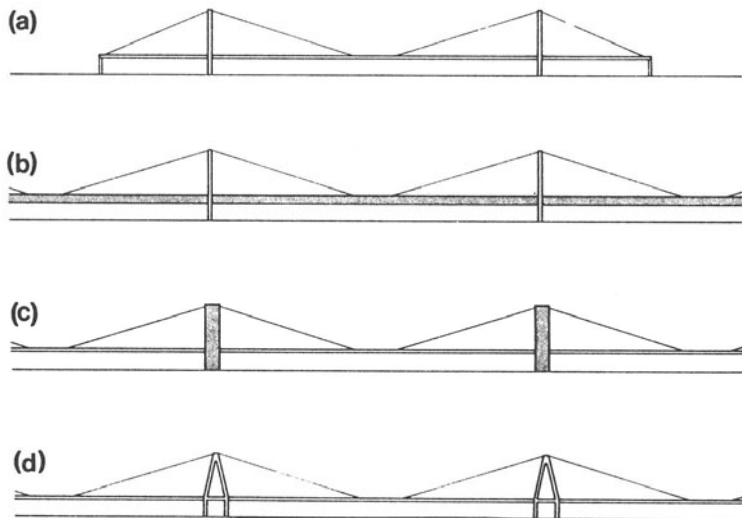


Figure 18. Multispan cable stayed bridges stabilized by increased stiffness of the girder or the pylons.

For systems with pylons fixed to the piers the required overall stiffness can be achieved by increasing the bending stiffness of the inner pylons. This offers the advantage that the girder depth can be kept unchanged, but as shown in Ref.(1) the width of the pylons have to be increased by a factor of approx. 5 (Figure 18(c)).

As this leads to disharmonic proportions it will often be preferred to apply triangular pylon structures, as shown in Figure 18(d).

Note that for a self-anchored system, as generally used in cable stayed bridges, the inner pylons should have their

legs inclined only above the girder, whereas the legs below should be vertical. This is in contrast to the earth anchored case where the pylon legs should be inclined all the way down to the top of the bridge pier.

Modifications of the cable system to give a more efficient restraint of the inner pylon tops can be made as shown in Figure 19(e)-(g).

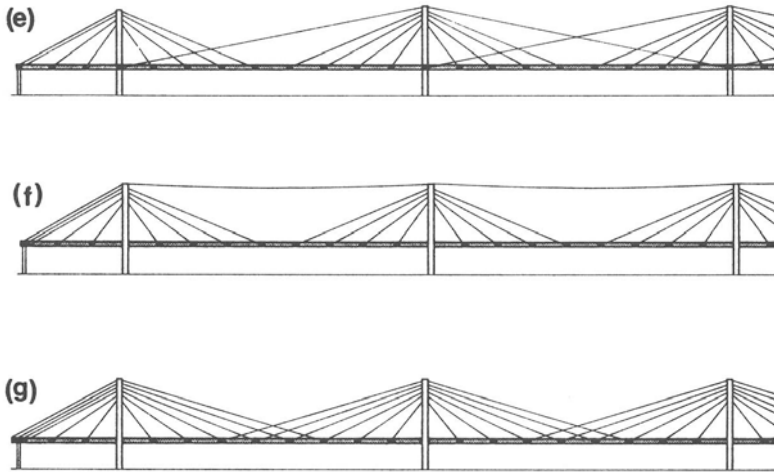


Figure 19. Modified cable systems to stabilize multispan cable stayed bridges.

System (e) is characterized by long anchor cables leading from the tops of the inner pylons to the girder at the two adjacent pylons, i.e. to points with efficient vertical support.

Alternatively, the inner pylons might be restrained by a horizontal tie cable connecting all tops, as indicated for system (f).

Finally, the necessary stiffness might be achieved by overlapping the fans at midspan, as shown in system (g). This solution requires, however, that the number of main spans is limited, probably to less than three.

If the systems (e)-(g) are made as self-anchored systems, they all have to be made with a continuous stiffening girder from one end to the other. This is due to the fact that there are no regions between the two end supports where the axial force in the girder is zero. Consequently, the distance between expansion joints might end up to be unattractively large.

If partially anchored systems are used, both systems (f) and (g) will allow expansion joints to be inserted in the

intermediate spans. Thus, if the continuous tie cable of system (f) is earth anchored at the ends of the side spans, the stiffening girder will in the dead load condition have zero axial force at the center of all main spans.

Among the systems shown in Figures 18 and 19, system (d) appears to be the easiest to erect as the partially erected superstructure will be efficiently supported by the double columns of the pylon structure (Figure 20). For the systems (e), (f) and (g) a (costly) temporary fixation of the superstructure to the pier is required as the cables stabilizing the inner pylon tops can not be erected until the entire stiffening girder is in place.

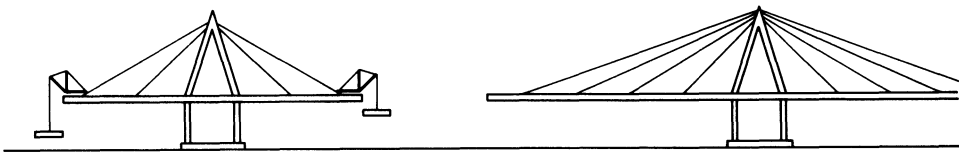


Figure 20. Erection of a multispan cable stayed bridge with triangular pylon structures.

3.2 Traditional Single-cable Suspension Systems.

It is a wellknown fact that an earth anchored cable system possesses an ability to deform into a configuration

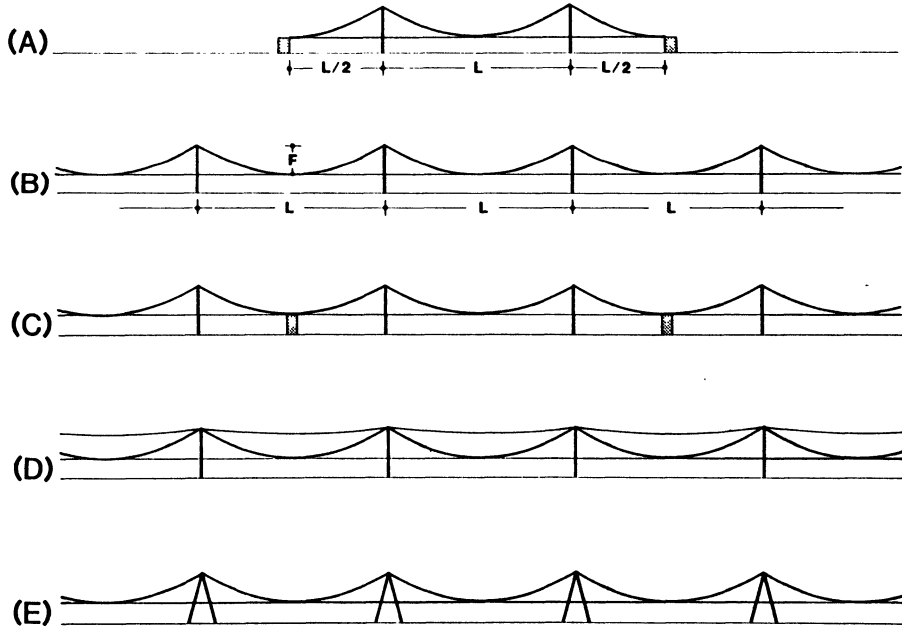


Figure 21. Structural systems for multispan suspension bridges.

that will allow it to carry any applied load - as long as all active cable elements are in tension. For a bridge with a large number of consecutive spans a solution as shown under (B) in Figure 21 would, therefore, at first glance seem appropriate. In this system, all pylons are of the traditional column-type rendering only vertical support to the cable system.

However, the deformations required to create equilibrium in a loading case with traffic load in one main span only are unrealistically large. For a bridge with a large number of spans the sag of the traffic loaded span will increase to $F(p+g)/g$, where F is the sag in the dead load condition, p the traffic load per unit length, and g the dead load per unit length. Consequently, the deflection under maximum traffic load will be $(p/g)F$, and this value becomes unacceptably large with realistic sag ratios, e.g. with $p=0.2g$ and $F=100$ meters the deflection would be 20 meters!

This feature is illustrated in Figure 22 showing the midspan deflection as a function of the sag ratio for the system (B) and for the reference system (A). It is seen that in the actual case the sag ratio of system (B) should be chosen to approx. 0.03 or 1/33 to arrive at the same midspan deflection as for system (A) with the traditional sag ratio of 1/10. Such a reduction of the sag ratio would, however, for a bridge with spans of 1000 meters imply an increase of the cable steel quantity per unit length by a factor of approx. 4.5, which must be regarded as unacceptable due to the associated cost increase.

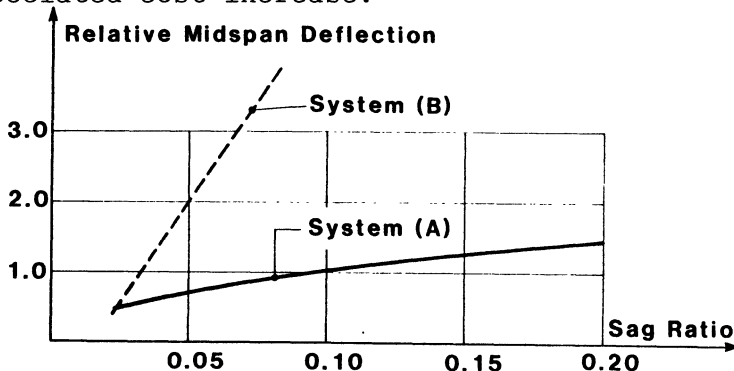


Figure 22. Relative flexibility of systems (A) and (B) in figure 21.

Considerations along these lines probably have been decisive for the additional anchor pier in the central span of the existing bridges mentioned in the introduction. For a multispan bridge the principle of adding intermediate anchor piers is illustrated in system (C) of Figure 21.

Elimination of the intermediate anchor piers can be achieved - as in the cable stayed case - by stabilizing the inner pylon tops in the longitudinal direction of the bridge by a horizontal tie cable, as shown in system (D). However, this solution is only applicable in bridges with moderate spans as the horizontal cable otherwise will be characterized by a too small equivalent modulus of elasticity.

For large multispan suspension bridges with a single-cable system the only solution left seems to be to apply triangular pylon structures comprising two inclined legs, as shown in system (E). Provided the main dimensions of the pylon structures are chosen to give adequate rigidity, this system can lead to deformational characteristics that are even more favourable than those of the reference system (A).

The fixation of the pylon tops in the longitudinal direction of the bridge significantly increases the frequency of the first symmetrical mode of vibration that is often critical for bridges with long side spans. Actually, by fixing the pylon tops the first antisymmetrical mode will often turn out to be the most critical. Thus, it might also prove advantageous to take measures to increase the frequency of the first antisymmetrical mode, such as clamping the main cable to the girder at midspan and restraining the stiffening girder at the pylons by hydraulic dampers (shock absorbers). These devices would allow slow movements due to temperature change but exclude fast movements due to wind excited oscillations or moving traffic loads.

The main disadvantage of system (E) is the increase in the quantities to go into the pylon structures. Under maximum horizontal force, occurring for one-sided traffic load, the resulting force from the cable system will have to be transferred almost entirely by the legs leaning towards the loaded span, due to the inclination of the resulting force from the cable system. It is, therefore, to be expected that the quantities to go into the pylon structure will be almost doubled when changing from a vertical column-type pylon to a triangular pylon structure.

Despite the disadvantages regarding the quantities of the pylons, system (E) must be regarded as the most promising among the traditional single-cable suspension systems.

3.3 Untraditional Double-cable Suspension Systems.

To improve the ability of the suspension system to transfer nonuniform loading, it has in some cases been proposed to use systems where each cable plane contains two (or more) main cables with different geometrical configurations.

A system as shown in Figure 23(J) has earlier been proposed. The main attraction of this system should be that each of the two continuous cables can be anchored to every second pylon at the level of the bridge deck (point B in the figure). However, this advantage must be paid by a considerable increase in the quantity of cable steel compared to the traditional system (I).

In the dead load condition there will be no forces acting between the cable and the pylon at the anchor point B as the horizontal force in the cable is constant and there is no break in the cable curve at the pylon. Therefore, for dead load the cable A-B-C will be equivalent to a free cable A-B with a length that is twice the span of the bridge! At the same time the sag ratio of this cable ($F/2L$) is only half the sag ratio of the traditional cable (F/L). These features make the system extremely unfavourable to carry the very decisive dead load.

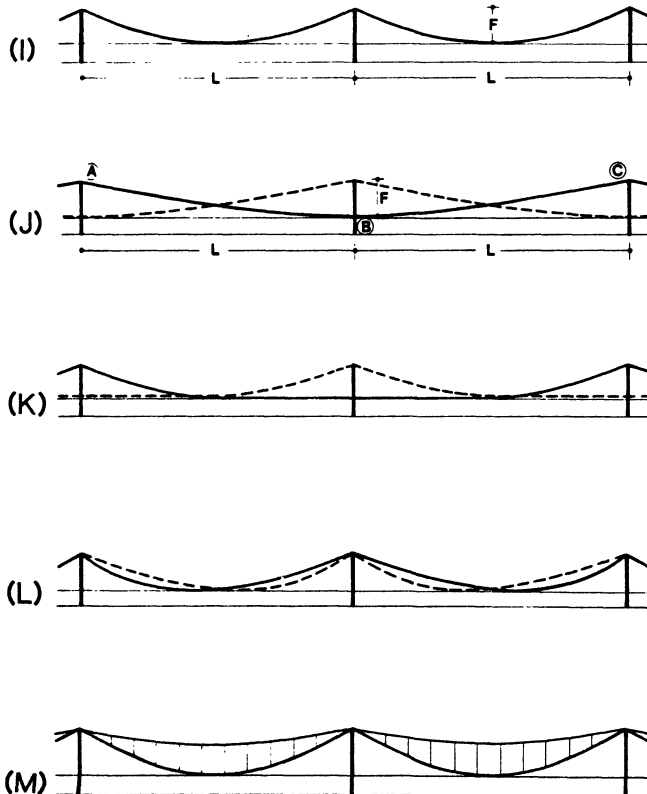


Figure 23. Double-cable suspension systems.

For a bridge with spans of 1000 meters each with a sag of 100 meters (=vertical distance between pylon top and bridge deck), the cable stress from the self weight of the cables

will for system (J) amount to approx. 50% of the allowable cable stress, leaving only the other 50% for carrying the dead load of the stiffening girder and the traffic load. For the traditional system, the cable stress from the self weight will be equal to approx. 12% of the allowable cable stress - a much more acceptable value.

The improved stiffness under traffic load that can be observed for system (J) is mainly due to the reduced sag ratios of the cables. Thus, under traffic load, where the cables can be regarded as supported also at point B, the sag of the cable A-B (and B-C) is $F/4$, e.g. a fourth of the sag ratio of the traditional system (I). In this connection it is interesting to note that if system (B) in Figure 21 is made with a sag ratio of $1/40$ then this system will also be sufficiently stiff, and at the same time be characterized by simpler and cheaper pylons than those of system (J).

Double-cables each with a cable curve coinciding with the funicular curve of an asymmetrical loading (as shown under (K)) have been proposed - and in a few cases even built - primarily to limit the deflections under traffic load acting in only one half of the span.

In the case of a multi-span bridge, the system does not immediately indicate any special advantages in relation to the critical loading case with traffic load confined to one span. But with triangular pylons, as those of Figure 21(E), the system could show some deformational benefits. This could especially be the case if the two main cables were clamped to the stiffening girder at midspan, as indicated on Figure 24. Here the central cable clamp is at the top of the stiffening girder and the adjacent portions of the girder supported directly through brackets onto the lower cable. To assure that the lowest point of the cable is above the bottom of the stiffening girder (which is essential from an aesthetical point of view) the girder depth has to be larger than approx. 0.03 times the cable sag, i.e. around 3 meters for a 100 meter sag.

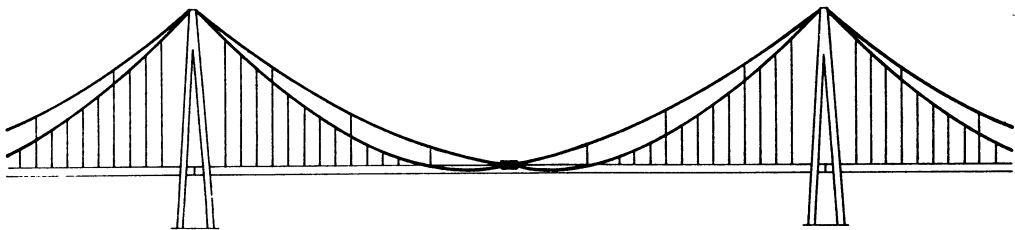


Figure 24. Double-cable system with triangular pylon structures.

The double-cable system of Figure 24 will be characterized by having favourable dynamic properties. Thus, the configuration of the main cables increases the frequency

of the first asymmetrical mode and the fixation of the pylon tops has a similar influence on the first symmetrical mode. Also, the system renders an efficient longitudinal restraint to the stiffening girder so that it is unnecessary to apply any special centering devices.

In relation to the double-cable system of Figure 24, it shall be emphasized that the required cable geometry can be achieved automatically during erection by suspending each half of the stiffening girder from its own cable.

The evaluation of the double-cable suspension systems shall be concluded by the system shown in Figure 23(L). In this system, shown in more detail in Figure 25, the two symmetrical main cables are arranged with different sags. This makes the system able to carry loads of different intensities in the individual spans without changing the total horizontal force. Thus, in the dead load condition the top cable will be subjected to its maximum tension, whereas the bottom cable will have its largest force in the dead+traffic load condition. In other words the single span can adjust to different loadings by changing the distribution of forces between the two cables.

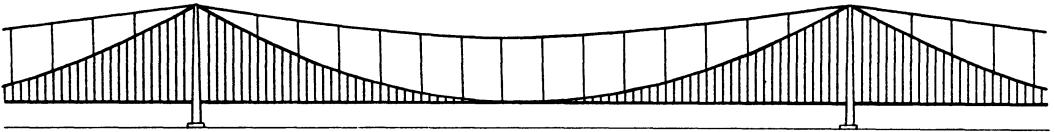


Figure 25. Double-cable system with two interconnected cables with different sags.

For this reason, system (M) does not require pylons with a large rigidity in the longitudinal direction of the bridge, so that conventional column-type pylons can be applied. On the other hand, the pylons have to be higher to assure a reasonable sag of the top cable and a reasonable difference in sag between the two cables - both features being of importance for the cable steel quantity. For a 1000 meter span, a sag of 50-70 meters for the top cable and 150-200 meters for the bottom cable seem realistic.

In a comparative investigation between a conventional three-span bridge with a sag of 150 meters and spans of 750, 1500, 750 meters, and a double-cable suspension bridge in accordance with system (L), with an infinite number of spans each 1500 meters long, and cable sags of 225 meters and 75 meters, respectively, it has been shown that the maximum midspan deflection for the two systems is practically the same (less than 2.5% difference). This result is based on the assumption that the pylons are completely flexible in the longitudinal direction of the bridge. In the actual comparative investigation, it was furthermore found that the

quantity of cable steel per unit length would be approx. 20% higher for system (L) than for the three-span bridge.

A comparison between system (E) of Figure 21 and system (L) indicates that the latter will lead to a saving of approx. 15% in the quantities of the pylons, but an increase of approx. 20% in the quantity of cable steel. With these values, the superstructure of system (L) will, undoubtedly, be more costly than that of system (E). Therefore, the possible savings in the substructure have to be taken into account to arrive at a conclusion on which system is to be preferred.

REFERENCES

- Ref. 1 : Gimsing, N.J.: "Multispan Stayed Girder Bridges", Journal of the Structural Division ASCE, October 1976
- Ref. 2 : Gimsing, N.J. and J. Gimsing: "Analysis of Erection Procedures for Bridges with Combined Cable Systems - Cable Net Bridge Concept", Techn. Univ. of Denmark, Dept. of Structural Engineering, Report No. R 128, 1980.
- Ref. 3 : Gimsing, N.J.: "Cable Supported Bridges - Concept and Design", Wiley, Chichester 1983.
- Ref. 4 : Richardson, J.R.: "Aerodynamic Stability of Twin Suspension Bridge Concept", IABSE 12th Congress, Final Report 1984.

SOME BASIC PROBLEMS IN THE DESIGN OF LONG SPAN CABLE STAYED BRIDGES

F. de Miranda
Politecnico di Milano, Milano

Summary:

Design criteria for increasing the stiffness of long span cable stayed bridges are recalled and discussed. Some new technical innovative solutions are proposed and analyzed.

1. Introduction

If one pauses for a moment to consider certain modern typologies of bridges over the past 40 years, such as cable stayed bridges (Fig.1), the attentive critic will be struck by an evolution that is so rich and variegated that it might almost be considered a revolution. This revolutionary process, with the help of new construction and assembly techniques, and new technologies for the use of materials, has brought results that are objectively of very great interest in the field of long span bridges, even from a formal point of view. And this is just the case of cable stayed bridges.

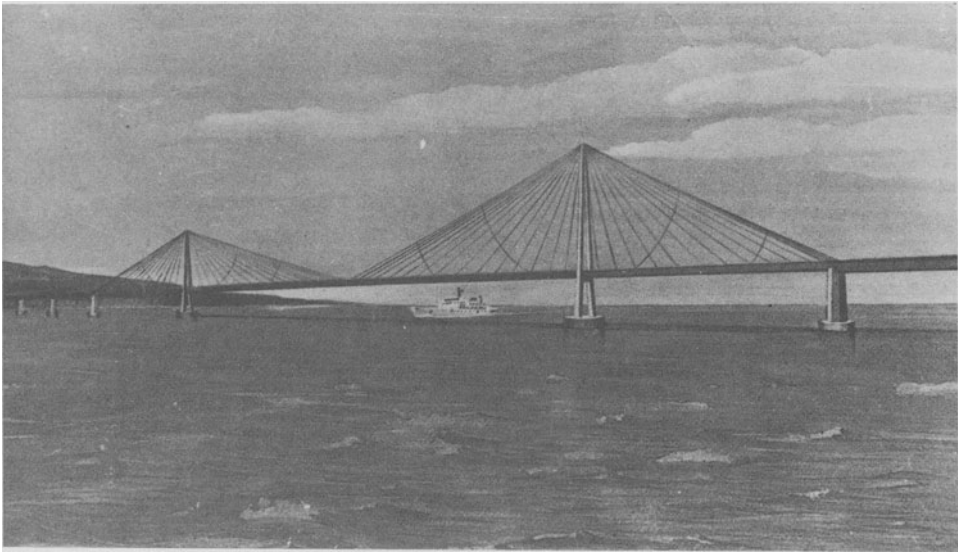
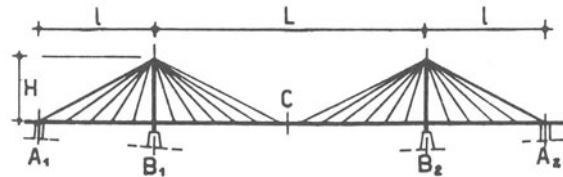
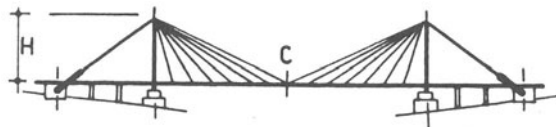


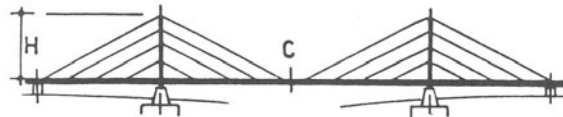
Fig.1 : Messina Bridge - Design of "Gruppo Lambertini" (1969)



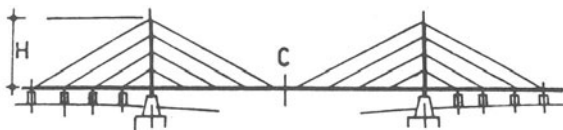
a) Three span cable stayed bridge - fan system



b) Single large span cable stayed bridges - fan system.



c) Three span cable stayed bridge - harp system



d) Cable stayed bridge-harp system with cables anchored to fixed points in the side spans.

Fig. 2 : Structural systems of cable stayed bridges

The construction of bridges has gone on to face structural problems of growing importance so that the bridge designer has been able to express and realize his ideas in terms of statics. So in bridge design the analytical type of problem has assumed a dominant role, with the result that for some time now most of the technical and scientific publications in this field have concentrated on the development of new calculation methods. However, during the last 30 years enormous progress in automatic processing has largely changed the situation, so much so that more thorough structural analyses for bridge design can now be developed through programs dealing with the static and dynamic behaviour of three dimensional structures.

So the overcoming of the analytical type of problem with the introduction of the computer, should also lead to a reevaluation of the importance of synthesis in the process of designing long span bridges. In fact, much of the quality of a bridge depends on the first design phase, which is really the creative moment.

The conception of a load-bearing system is a creative act which is based only in part on scientific data. It also depends on a sensibility to statics, which remains, like the sensibility to aesthetics, a capacity to understand and assimilate physical laws needed for any good design.

The constructional aspects, together with the more strictly theoretical and analytical side, is of fundamental importance for the design of long span bridges.

2. Cable stayed bridges

The cable stayed system (Fig.2) contains straight cables connecting the stiffening girder to the pylons. In the fan system all stay cables radiate from the pylon top, whereas parallel stay cables are used in the harp system.

Besides the two basic cable stayed systems (the fan and the harp system), intermediate systems can also be found; thus, in the modified fan system the cable anchor points as the pylon top are spread sufficiently to separate each cable anchorage.

For cable stayed bridges the trend has been to move from systems with relatively few heavy stay cables to multi-cable systems with a large number of stay cables supporting the stiffening girder more continuously.

For the concept and design of cable stayed bridges too, aspects related to erection have a very strong influence, as is the case for any structure of considerable size. Thus, the structural systems and materials, as well as the design of details, must be chosen with due regard to the erection procedure.

A straightforward solution is to erect the entire stiffening girder on temporary supports before adding the cables, as illustrated in Fig.3 for a fan cable stayed bridge with a Earth Anchored Cable System, where four main stages are indicated.

This erection procedure offers the advantage that the girder can be erected continuously by cantilevering from one end to the other, allowing the transportation of men, equipment, and material on the completed part of the deck (Fig.4).

Also, the procedure leads to an efficient control of the geometry and cable tension. The disadvantage is related to the temporary supports that must be used. In many cases clearance requirements during the construction period, or deep water under the main span, will exclude the installation of the necessary number of temporary supports, and the procedure will not be feasible. Temporary supports can be completely avoided if the bridge is being erected by the free cantilever method, as illustrated in Fig.5, where four main stages are involved.

With this procedure it is essential to have a very efficient fixity of the superstructure to the main piers throughout the construction period, as the entire stability depends on this fixity until the end pier is reached. Also, the lateral bending stiffness of the girder must be sufficient to ensure the stability of the cantilever arm with a length corresponding to half of the main span.

Thus, the procedure is especially advantageous in bridges with a large width-to span ratio of the girder (Fig.6). The cantilevering of a cable stayed bridge requires that all girder joints are closed as soon as the girder units are in place, to allow the transmission of the axial forces and the bending moments induced in the deck during the subsequent tensioning of the stay cables.

Fig. 3 :
Self-anchored cable stayed bridge erected on temporary supports.

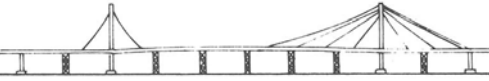
Stage 1: Construction of the main piers and temporary supports.



Stage 2: Erection of the stiffening girder.



Stage 3: Installation of stay cables, moderately tensioned.



Stage 4: Removing of the temporary supports and self tensioning of the cable.

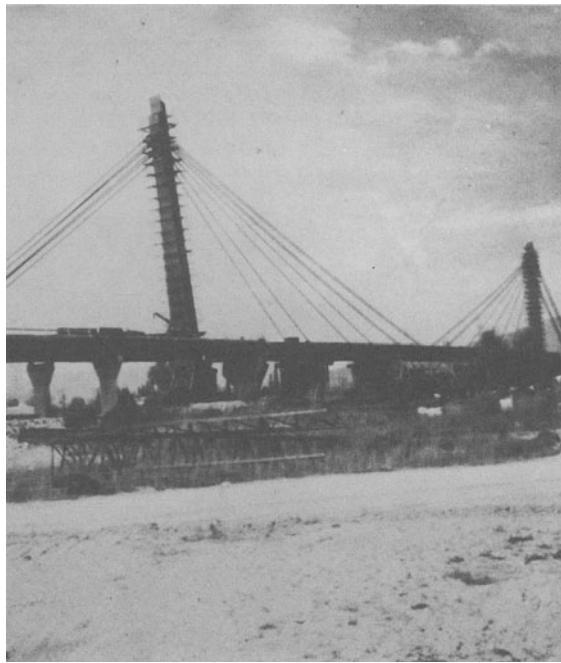
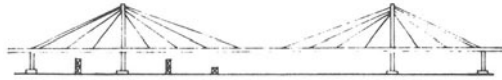
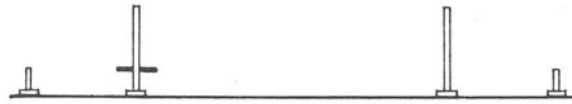
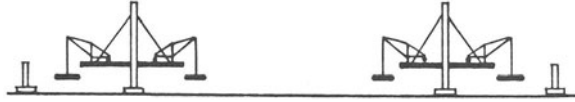


Fig.4a: Indiano Bridge (Florence) during deck erection by longitudinal launching.

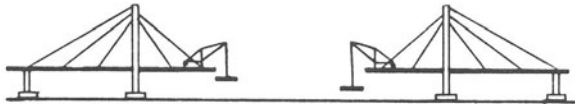
Fig.4b: Indiano Bridge in the stage of tensioning of cables.



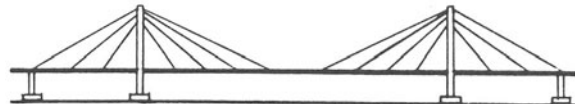
Stage 1: Construction of piers and pylons- The girder units above the main piers are erected (temporarily) fixed to the piers.



Stage 2: Erection of deck and cables by balanced free cantilevering.



Stage 3: Erection of central part of the bridge



Stage 4: Closing of main span central additional dead loads from wearing surface, etc... are applied.

Fig. 5 : Self-anchored cable stayed bridge erected by double-sided free cantilevering from the pylons.



Fig.6: Zarate Brazo Largo Bridges during erection.

3. Structural Analysis of Cable Stayed Bridges

Reference is to a continuous three span stayed bridge with the fan system and with a continuous distribution of cables along the girder, which is the most suitable system for long spans. It is assumed that construction, by regulating the tension in the cable, will ensure a practically straight final configuration with no bending moments in the deck. The structural analysis due to permanent loads can be carried out starting from the equilibrium equations of a beam element in the left half of the bridge (Fig.7):

$$\begin{aligned} \frac{dN}{dz} + \bar{n} \cos \alpha &= 0 \\ g - \bar{n} \sin \alpha &= 0 \end{aligned} \quad ; \quad \bar{n} = \frac{N_s}{\Delta} \quad , \quad (1)$$

in which z is the abscissa of the cross-section considered, N is the axial force in the deck, N_s the axial force in the cable. With reference to the adimensional abscissa $\zeta = z/H$, and considering that:

$$\operatorname{tg} \alpha = \frac{1}{\zeta} \quad ; \quad \cos \alpha = \frac{\zeta}{\sqrt{1+\zeta^2}} \quad ; \quad \sin \alpha = \frac{1}{\sqrt{1+\zeta^2}} \quad ,$$

then the second equation of system (1) gives:

$$\bar{n} = g \sqrt{1+\zeta^2} \quad ; \quad N_s = \frac{g \cdot \Delta}{\sqrt{1+\zeta^2}} \quad , \quad (2)$$

which, when substituted in the first of the equations (1), gives:

$$\frac{dN}{d\zeta} = -gH\zeta \quad .$$

From this, taking into account that at the centre ($\xi = L/2H$), because of the erection procedure, it can be assumed that $N = 0$, on finally we obtain:

$$N(\xi) = -g \frac{H}{2} \left\{ \left(\frac{L}{2H} \right)^2 - \xi^2 \right\} \quad (3)$$

The action of the live loads modifies the initial equilibrium corresponding to the permanent loads, and sets up an additional stress-strain state. The stress state already existing before the action of the live loads is made up of tensile stresses in the stayes and of compression stresses in the pylons and in the girder. Furthermore, the action of the dead loads fixes the equilibrium configuration of the cables, and thus controls their reactions through the value of Dischinger's virtual modulus of elasticity (Fig.8):

$$E_* = \frac{E}{1 + \frac{\gamma^2 l_0^2 E}{12\sigma^3}} \quad (4)$$

where:

- γ = specific weight of steel in the cable
- l_0 = horizontal projection of the length of the cable
- E = modulus of longitudinal elasticity of the cable
- σ = tension of the cable.

The additional strain in the bridge is further indentified (Fig.9) by the vertical displacements $v(z)$ of the girder, by the rigid horizontal displacement w of the girder itself, and by the elastic horizontal displacement u of the tops of the pylons.

Structural analysis for evaluating static effects due to live loads, after the first simple applications in the 1950's, has been studied theoretically by various authors with approximation methods that are very interesting, but tend to be rather laborious and complex.

At the same time, however, the complete and exact structural analysis of the stress-strain state has been carried out systematically by means of a discrete model which also takes into account the effects of non linearity due to strains in the cables and variations in the geometry of the structure.

The discrete model can be obtained either by the analysis with a computer of a system with a given number of cables, or by solving with a numerical method (e.g. the finite element method) the equations of the continuous model.

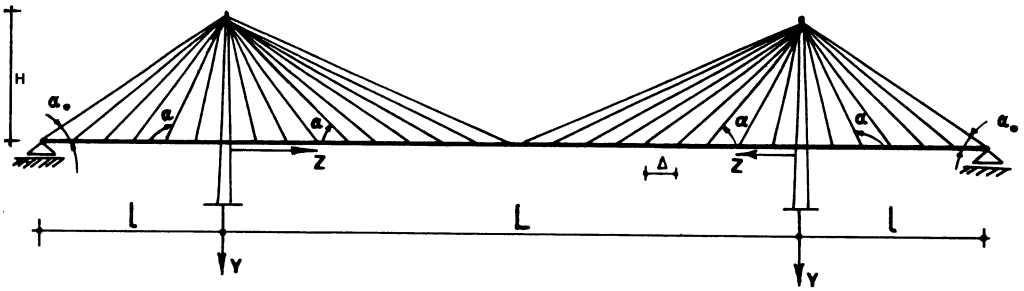


Fig.7: Typical structural system of wide span cable stayed bridges.

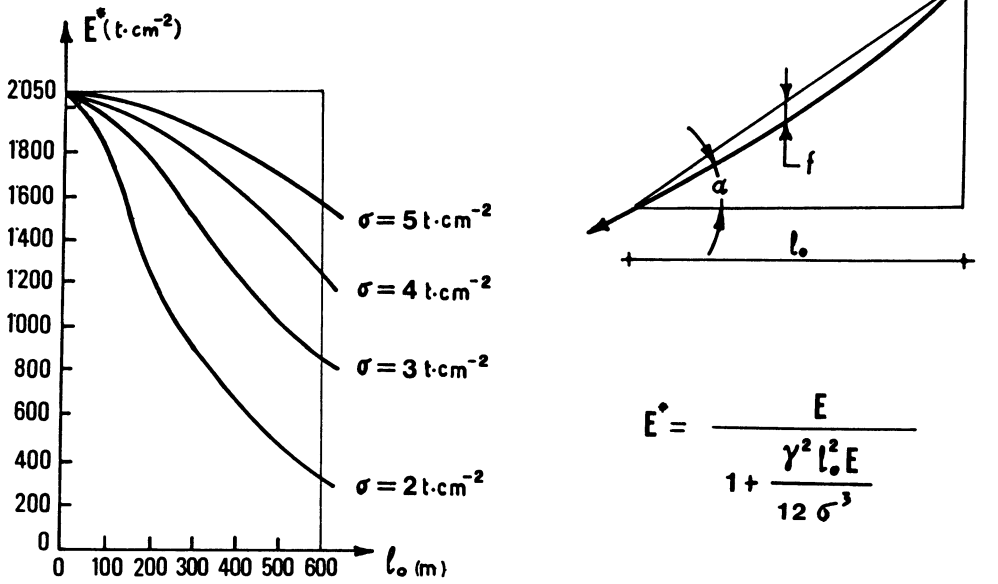


Fig.8: Virtual modulus of elasticity of the cable.

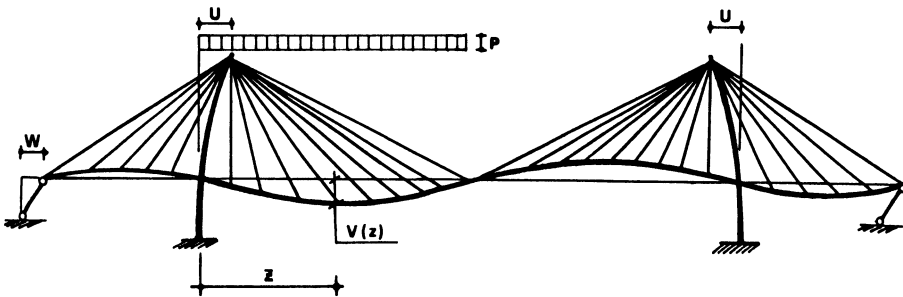


Fig.9: Distorted system under live loads on half central span

The results obtained in this way are very precise and make it possible to state that the earlier analytical obstacles, considerable though they were, have now been overcome, obstacles that were responsible for the initial distrust in the cable stayed bridge and its late development.

In fact, computers have made it possible also to conduct investigations and reasearch on stiffening systems of cable stayed bridges for application to long spans, or to very heavy live loaded (railway double track bridges), as will be illustrated later.

4. The Stiffening of Cable Stayed Bridges

A three span cable stayed bridge with a fan system of cables of the type shown in Fig.7 is already in itself one of the stiffest structural systems for bridges.

But, first of all, we have to outline how to the optimum values of the H/L ratio (concerning the weight of the steel required for the cables) also an average optimum case of rigidity is corresponding; this means that, in relation to such values, are minimized the differences between rigidity (in the same plane of the structure) of the zones near the towers and of the zones near the centerline, as well as the absolute rigidity values.

The elastic deflections in the central zones of the span due to live loads on the central span are also influenced, and quite considerably, by the value of the horizontal longitudinal displacements of the tops of the towers, and by the angle formed by the generic cable with the axis of the deck.

Referring to Fig.10, for the generic stay (i) loaded like shown in Fig.11, the vertical displacement $\delta_{v(i)}$ is:

$$\delta_{v(i)} = \frac{\delta_{ii}}{\text{sen} \alpha_i} = \frac{\frac{q\Delta}{\text{sen} \alpha_i} \cdot \frac{H}{\text{sen} \alpha_i}}{E_i A_i} = \frac{q\Delta H}{E_i A_i} \cdot \frac{1}{\text{sen}^3 \alpha_i} ;$$

Furtherly, because it is:

$$A_i = \frac{N}{\sigma_{ai}} = \frac{q\Delta}{\sigma_{ai} \operatorname{sen}\alpha_i} ,$$

the value of becomes:

$$\delta_{v(i)} = \frac{q\Delta H}{E_i} \frac{1}{\operatorname{sen}^3\alpha_i} \frac{\sigma_{ai}}{q\Delta} = \frac{\sigma_{ai} H}{E_i} \frac{1}{\operatorname{sen}^2\alpha_i}$$

The function $\delta_v = f(\alpha_i)$ is represented in Fig.12, where clearly appears that for $\alpha = 90^\circ$ is:

$$\delta_v = |\min\delta_v| = \frac{\sigma_a H}{E} ,$$

while, with the same value of δ_a , for $\alpha = 30^\circ$ the value of becomes $4\delta_{\min}$

Then, for low values of H/L , while the vertical displacements δ_v of cables near to the towers are smaller, contemporarely the values of δ_v for the cables near the center of the bridge will increase very much, because increases itself the geometric coefficient:

$$\operatorname{sen}^2\alpha_{\min} = \left(1 + \frac{\alpha_{\min}^3}{3!} + \dots\right)^{-2}$$

Practically, in order to not differenziate too much the local flexibility of the bridge around the center of the span, it is necessary to limit the value of α_{\min} .

For the type of structure considered, if we adopt for the ratio H/L , values between 0,21 and 0,24, we can consider to give a high stiffness to the structure itself.

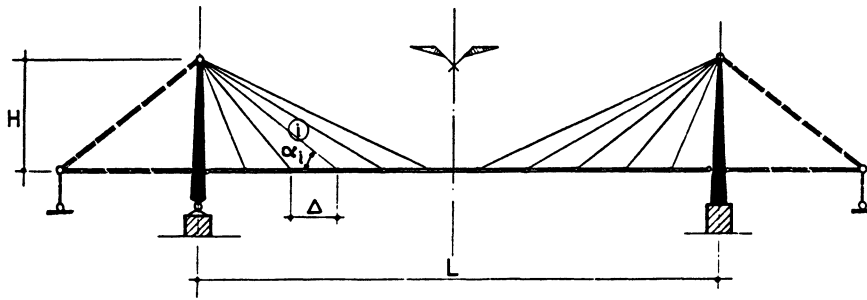


Fig.10

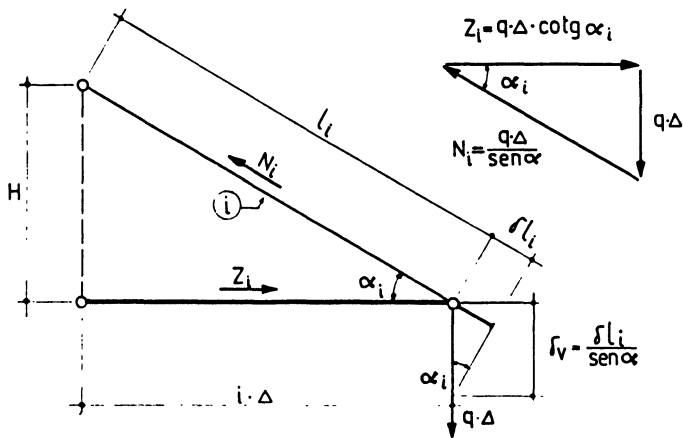


Fig.11

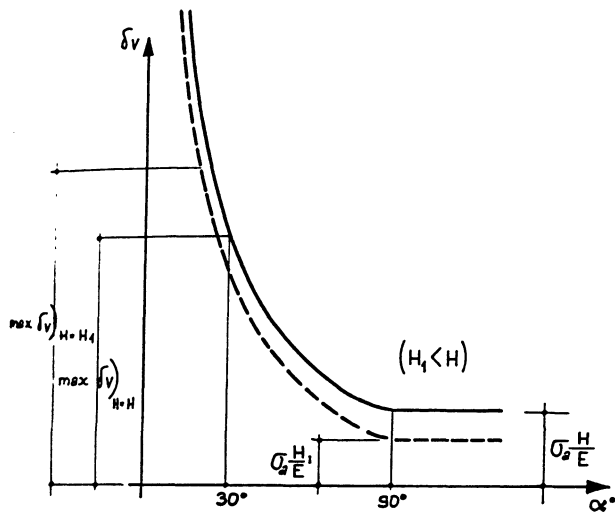


Fig.12

However, for long spans this stiffness reduces considerably in the central area of the span for a length of about $(0.3 \div 0.4) L$ across the mid-span. This is due, above all, to the reduction in the axial stiffness of the longest cables due to their dead load:

$$\frac{E \cdot A}{l} = \frac{EA}{1 + \frac{\gamma^2 l_0^2 E}{12\sigma^3}} \quad (5)$$

where:

A = cross section of cable
 l = length of cable
 l_0 = horizontal projection of l,
 σ = stress in the cable

In order to overcome this handicap, and so to introduce the cable stayed bridge with all its technical-economic advantages into the field of larger spans, certain innovations are needed in their design construction and erection. Let us consider some of these possible innovations.

A first solution to counter the Dischinger effect may be obtained by fitting a series of counter-stays AB', AB'', AB''', AB'''' , etc..., stiffly anchored in A (Fig.13); in this case, and in the hypothesis of inextensibility of the counter-stays, the function $E \cdot A / l$ becomes the straight line (shown by the dotted line in Fig.14) of equation:

$$\frac{E \cdot A}{l} = \frac{EA}{l}$$

An intermediate behaviour takes place in the real hypothesis of more or less extensible counter-stays (Fig.14 curves α , β , γ , etc...) . Such counter-stays permit to contain the Dischinger effect and to increase the cross section of the stayed-cable without changing the force N_g .

Only in this case low-resistance cables (e.g.prestressed concrete cables) could be optimally used even for spans greater than 400 m.

A second solution, proposed by the author in 1969, provides for counter-stays to be fitted as per Fig.15, i.e. so as to connect the counter-stays themselves in correspondence of

the deck points, and permits to obtain a considerable decrease of the Dischinger effect, considering also the fact that the axial rigidity of the counter-stays is very high because the values l_0 of the horizontal projections of their length are generally very low.

Generally speaking, a stiffening achieved according to the arrangement indicated in the first solution involves the use of a quantity of steel for the counter-stays greater than for the second solution.

Let us now investigate and analyze the efficiency of the counter-stays according to the scheme of Fig.15.

If a single stay rod is placed according to Fig.16 and tensioned with a force F , the increase f of the deflection of the cable mid-point is linked to force F by the relation (Fig.17).

$$\frac{4Nf}{L} = 2N\text{sen}\beta = F$$

In fact, at the 1st order, there is no increase of the axial force N in the cable because of the applied force F .

In fact we have:

$$\text{sen}\beta = \frac{f}{\frac{L}{2}},$$

and therefore:

$$f = \frac{FL}{4N}.$$

If we now go back to the scheme as per Fig.16, the point A - where the stayed-cable is connected to the truss- may be subjected to a vertical sag, as point B; on the contrary, point C, the pier head, may, as a first approximation, be considered fixed.

The vertical displacement v_A of point A then increases the axial force in the cable

$$\Delta N = \frac{E_* A}{L} \Delta L ,$$

where ΔL is the component of v_A along the cable axis; but in this case, because of the stay rod, the reduced modulus E_* is to be calculated with reference to a cable with length = $L/2$: in fact the mid-point of the stayed-cable is linked to the stay rod and therefore the free span of the cable is halved. This is true if the increase of the deflection Δf due to the force increase ΔN (Fig.18) is of the same order of magnitude as ΔL , i.e. if the stay rod has sufficient rigidity.

As regards the validity of the stay rod as the restrain of the cable mid-point, we finally have to check that the deflection increase Δf due to v_A and v_B is small, that is, in the same order of magnitude as ΔL . In fact, because of ΔL , we have an increase Δf given by:

$$\Delta f = \frac{f \Delta N}{\frac{K_t L}{4} + N} = \frac{f}{\frac{K_t L}{4} + N} \frac{E_* A}{L} \Delta L ;$$

and since:

$$f = \frac{FL}{4N} ,$$

we obtain:

$$\frac{\Delta f}{\Delta L} = \frac{F}{N} \frac{E_* A}{K_t L + N} < \frac{F}{N} \frac{E_* A}{K_t L} .$$

Therefore, if A_t and L_t are respectively the cross-sectional area and the length of the stay rod (counter-stay) , we obtain:

$$\frac{\Delta f}{\Delta L} < \frac{F}{N} \frac{E_* A}{\frac{EA_t}{L_t} L} \approx \frac{F}{N} \frac{L_t}{L} \frac{A}{A_t} \approx \frac{F}{N} \frac{1}{2} \frac{A}{A_t} .$$

If we assume $F/N \cong 0.01$, then it is also: $A_t/A \cong 0.01$, and therefore $\Delta f/\Delta L$ is in the order of the units.

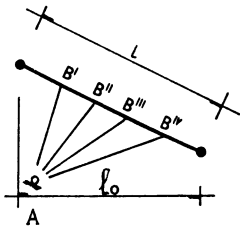


Fig. 13

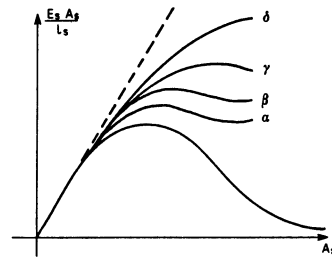


Fig. 14

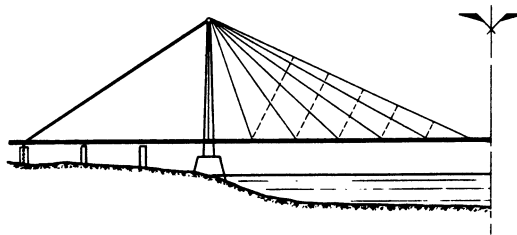


Fig. 15

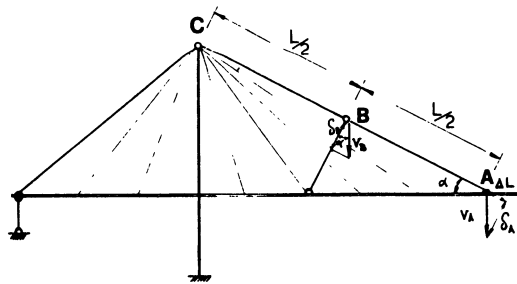


Fig. 16

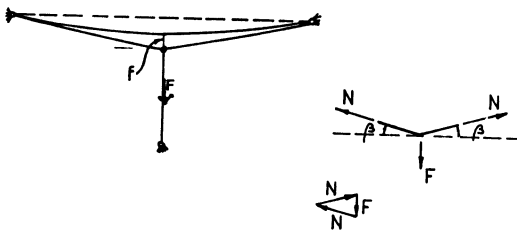


Fig. 17

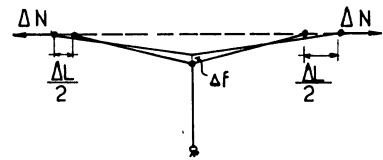


Fig. 4.16.

Fig. 18

We may conclude that the stay rods may stiffen the cables so long as the initial force F is at least in the order of $0.01N$. As a first approximation, therefore, the effect of the stay rods is to interrupt the span of the cables as regards the calculation of the Dischinger module.

However, in order to limit the possibility of deformation of the stayed-cable bridge, it is paramount that every cable has to be sized so as to offer maximum axial rigidity E^*A , where E^* is the virtual elastic modulus (Dischinger) estimated in the presence of permanent loads only, and A is the cross-sectional area of the cable.

In sizing the stayed-cable, two factors should be considered:

- a) The axial force in it, in the configuration subjected to dead loads only, is determined, and its value is (Fig.19)

$$N_g = \frac{g\Delta}{\text{sen}\alpha}$$

- b) If $\sigma_g = N_g/A$ is an "assigned stress" in the stayed-cable under permanent loads, the cross-sectional area value is:

$$A = \frac{N_g}{\sigma_g} .$$

The value of σ_g is to be established taking into account the maximum increase σ_p due to live loads and the value of the allowable fatigue stress, and also the need to guarantee sufficient axial rigidity to the cable.

The value of stress σ_g that ensures the maximum value for axial rigidity $E^* A$ is then estimated; the result is:

$$E^*A = E \frac{N_g}{\sigma_g} \frac{1}{1 + \frac{\gamma^2 l_0^2 E}{12\sigma^3}} = E N_g \varphi(\sigma_g) \quad (6)$$

The function:

$$\varphi(\sigma_g) = \left(\sigma_g \left(1 + \frac{\gamma^2 l_0^2 E}{12\sigma^3} \right) \right)^{-1}$$

runs as shown in Fig.20, where the rigidity of the cable appears, given the values N_g, γ, l_0 it shows a maximum in correspondence of a suitable value of σ_g determined by the condition:

$$\frac{d\varphi}{d\sigma_g} = 0 ,$$

that, for the optimal value $(\sigma_g)_{opt}$, provides the expression:

$$(\sigma_g)_{opt} = \sqrt[3]{\frac{\gamma^2 l_0^2 E}{6}} . \quad (7)$$

Therefore (6), through (7), gives the maximum value that may be obtained for the axial rigidity $E \cdot A$, the value of which is:

$$(E \cdot A)_{opt} = \frac{2}{3} N_g E \sqrt[3]{\frac{6}{\gamma^2 l_0^2 E}} . \quad (8)$$

The values of $(\sigma_g)_{opt}$ and $(E \cdot A)_{opt}$ are represented in Fig.21 for steel cables ($\gamma = 7,85 \text{ t/m}^2$; $E = 2.1 \times 10^7 \text{ t/m}^2$)

If in (6) we let:

$$K_o = \frac{\gamma^2 l_0^2 E}{12 N_g^3} ,$$

the same may be written as follows:

$$E_o = \frac{E}{1 + K_o A^3} .$$

This function is represented in Fig.22 for certain values of K_o as N_g varies.

If we multiply everything by A/l (with $l = \text{constant}$), we have:

$$\frac{E_o A}{l} = \frac{E}{l \left(\frac{1}{A} + K_o A^2 \right)} . \quad (9)$$

The curve $E \cdot A/l$ (Fig.23) for a certain value of K_o increases

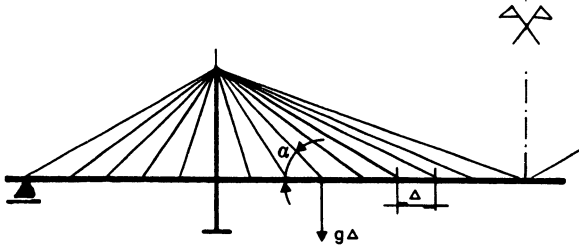


Fig.19

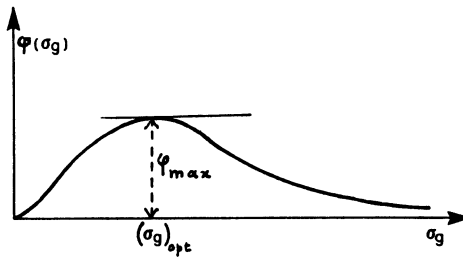


Fig.20

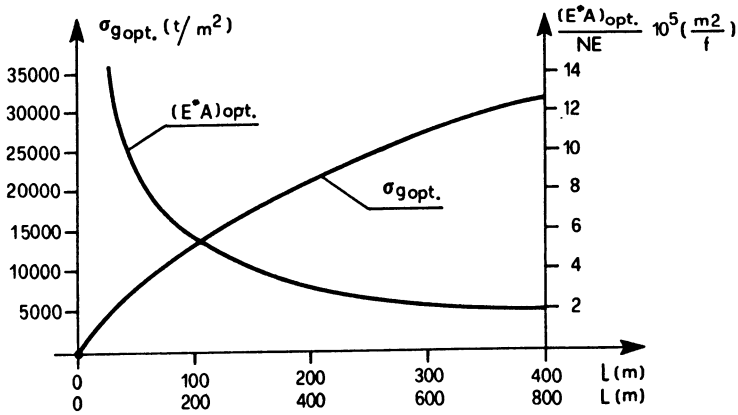


Fig.21

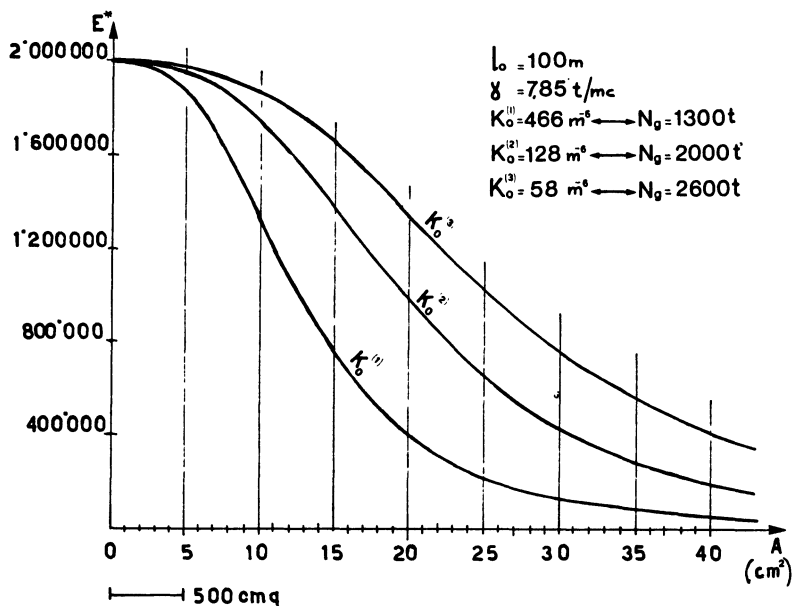


Fig.22

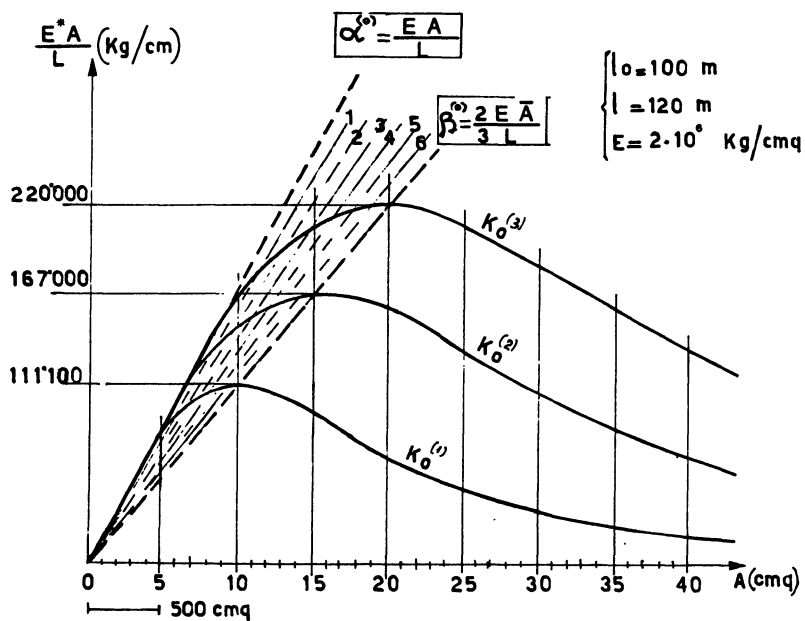


Fig.23

in an almost linear manner for very small values of A (very high tensions $\sigma_g = N_g/A$, at first exceeding any limit), reaching then a maximum for $A = \bar{A}$ obtained from the equation:

$$\frac{d}{dA} \left\{ \frac{E \cdot A}{l} \right\} = 0 ,$$

decreasing to zero for $A = \infty$ (i. e. $\sigma = 0$)

This result indicates that, generally speaking, it is possible to obtain an axial stiffening of the stayed-cables by increasing the area of the resisting cross-section up to the limit of \bar{A} .

In order to increase the flexural rigidity of the structure through an increase of the axial rigidity of the stayed-cables, we may also use a cable with a larger cross-section, obtained, starting from the original stayed-cable, by injection of mortar in the sheath, and subsequent prestressing by means of an additional cable with cross-section A_{II} (Fig.24).

If load N_g is entrusted completely to the section A_I of the main cables (cables I), we have:

$$\sigma_g^{(I)} = \frac{N_g}{A_I} (\cong \sigma_{sm}) .$$

After the injection and cure of the mortar, the secondary cables (with section A_{II}) are pre-tensioned to a value $0.9 \sigma_{amm}$, and at the same time the main cables (I) are relieved from stress, reaching a value:

$$\sigma_g^{(I)A} \cong 0,9 \sigma_{sm} ,$$

while concrete is prestressed with a stress:

$$\sigma^{(0)} = - \frac{\sigma_c A_{II}}{A_c + n A_I} (\cong 140 + 180 \text{ kg cm}^{-2}) .$$

The subsequent intervention of live overloads brings the stress in the steel cables (main and secondary) from $0.9 \sigma_{amm}$ to $\sigma_g + \sigma_p \cong \sigma_{amm}$, making the phenomenon of fatigue in the steel cables negligible, since $\Delta \sigma \cong 0,1 \sigma_{amm}$, while concrete is relieved from stress to a value: $|\min \sigma_c| \cong -0,10 \sigma_c^{(0)}$.

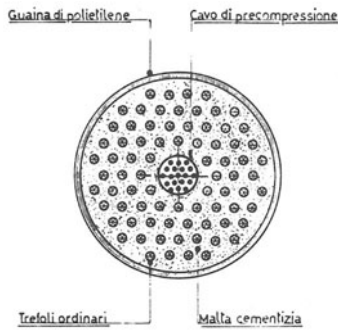


Fig.24a

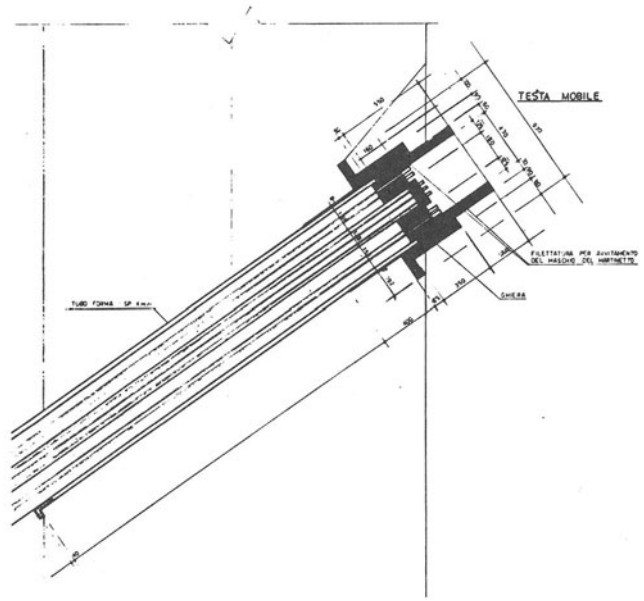


Fig.24b

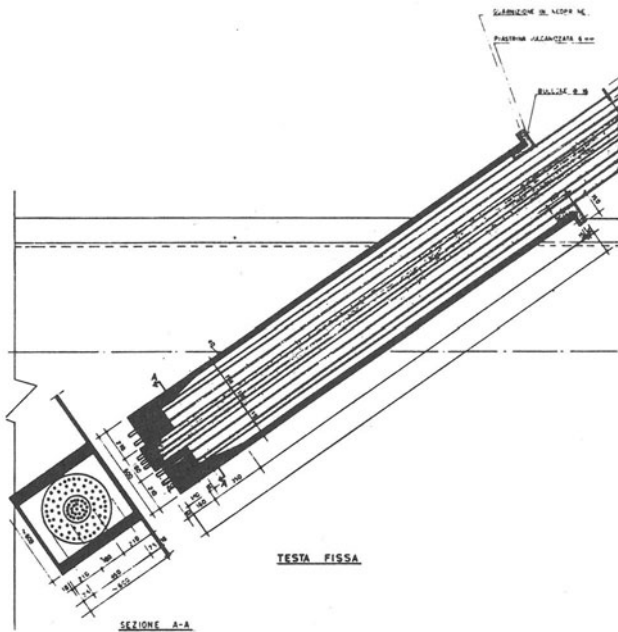


Fig.24c

The axial rigidity of the stayed-cable thus treated is therefore modified in the expression $E^* A$, for the following reasons:

- the area A of the cable has been increased, which undoubtedly is a positive fact;
- the elastic modulus E^* is instead reduced because the mortar adds weight to the cable.

In order to check the effect of the reduction of E^* modulus we should remember the original expression of this quantity. From an analysis of the behaviour of a stayed-cable with cross-section A and with weight per unit of length $g = \gamma A$ subject to an axial force N_g , we obtain the following expression for modulus E^* :

$$E_* = \frac{E}{1 + \frac{g^2 l^2 EA}{12 N_g^2}} .$$

If we assume the stayed-cable to be rigid with respect to the flexural deformability of the truss, the overall stress in the stayed-cable remains fixed after prestressing.

If we homogenize the areas of concrete in steel, the overall value of area A_t is:

$$A_t = A_I + A_{II} + \frac{A_c}{n} ; \left(n = \frac{E}{E_c} \right) .$$

The elasticity modulus of the prestressed stayed-cable, E_p^* becomes:

$$E_p^* = \frac{E}{1 + \frac{g_t^2 l^2 EA_t}{12 N_g^2}} ,$$

where g_t is the weight per unit of length of the prestressed stayed-cable:

$$g_t = \gamma (A_I + A_{II}) + \gamma_c A_c .$$

The modulus E_p^* may then be written as:

$$E_p^* = \frac{E}{1 + \frac{\gamma_t^2 l_0^2 E}{12 \bar{\sigma}_g^3}} \quad (10)$$

where:

$$\gamma_t = \frac{g_t}{A_t} \quad ; \quad \bar{\sigma}_g = \frac{N_g}{A_t} \quad .$$

The ratio between the axial rigidity of the prestressed stayed-cable and the axial rigidity of the steel stayed-cable, may be considered as an indication of the effectiveness of prestressing: its value is:

$$K = \frac{E_p^* A_t}{E_s A} = \frac{A_t}{A} \frac{1 + \frac{\gamma_t^2 l_0^2 E}{12 \bar{\sigma}_g^3}}{1 + \frac{\gamma_t^2 l_0^2 E}{12 \bar{\sigma}_g^3}} \quad .$$

This ratio may theoretically be greater than, equal to, or lower than 1.

Relation (10) supplies for rigidity $E_p^* A$ of the prestressed stayed-cable an expression similar to (6), i.e. for the prestressed stayed-cable, too, as $\bar{\sigma}_g$ varies, the axial rigidity runs according to Fig.20, and therefore a maximum value $(E^* A_t)_{opt}$

that, taking into account (8), is:

$$(E_p^* A_t)_{opt} = \frac{2}{3} N_g E \sqrt[3]{\frac{6}{\gamma_t^2 l_0^2 E}} \quad . \quad (11)$$

Relation (11) shows that the maximum axial rigidity value of a prestressed stayed-cable only depends on the average specific weight γ_t , l_0 and N_g being equal.

The value of the ratio between the maximum optimum axial rigidity of the steel stayed-cable and the maximum optimum axial rigidity of a prestressed stayed-cable, is therefore:

$$\frac{(E_s A)_{opt}}{(E_p A_t)_{opt}} = \sqrt[3]{\frac{\gamma_t}{\gamma}}$$

And since

$$\frac{\gamma_t}{\gamma} = \frac{\gamma(A_I + A_{II}) + \gamma A_c}{\gamma(A_I + A_{II} + A_c/n)} = \frac{\gamma(A_I + A_{II}) + \gamma_c A_c}{\gamma(A_I + A_{II}) \frac{\gamma}{n} A_c},$$

as γ_c is always $> \gamma/n$, therefore: $\gamma_t / \gamma > 1$.

In conclusion, the maximum optimum axial rigidity of the cables is obtained with steel-only cables.

But the simplest and most effective solution for the axial stiffening of the stayed-cables is based on a criterion that, with particular construction methods, provides for the static interaction of high-tensile steel stranded cable and the sheath when this is formed by a tubular steel sleeve:

- 1) The cables formed only by the strands support, by themselves, all the dead load of the deck, reaching a stress value σ_g , value that, added to tension σ_p induced by live loads, does not exceed the allowable static value for the type of steel used, i.e. the value apart from the fatigue strength of the strands.
- 2) The steel sheath, only after the application of all dead loads to the deck, is solidly fixed to the cable, rigidly connecting the sheath to the stay heads by means of welding.

With this process the cross-section A_s of the strands is increased by the value A_p corresponding to the cross-section of the steel sheath only for absorbing the stresses arising in the stayed-cables because of the live overloads.

The injection of mortar in the steel sheathing shall be done after the cable heads of the high-tensile steel strands have been solidly fixed to the sheathing formed by the low-

tensile steel tube. This operation is carried out, if possible, with the aid of a movable load placed on the deck in correspondence of the section in which a pair of stayed-cables are connected to the deck. This load shall be present during the injection operations and until the (quick) cure of the mortar.

In this case the tensional layers in the stayed-cables are identified by the following values.

During a first stage a stress arises in the strands:

$$\sigma_*^{(1)} = \sigma_g = \frac{N_g}{A_*}$$

due to the dead loads.

During a later stage, because of the live loads, the tension in the strands reaches the value:

$$\max \sigma_* = \sigma_g + \frac{N_p}{A_* + A_\phi}$$

During this stage the stress reaches the following value in the steel sheathing:

$$\sigma_\phi = \frac{N_p}{A_* + A_\phi}$$

The maximum stress in the strands and the maximum stress in the sheathing shall not exceed $\sigma_{x_{am}}^{(F)}$ and $\sigma_{\phi_{am}}^{(F)}$, respectively, of the fatigue strength of the strands and of the steel sheathing.

The effects on the static behaviour of the bridge are clearly positive, as it is easily possible, by fully using the strength characteristics of the materials used, to almost halve the maximum flexural sag that would occur when forming the stayed-cables by using only high-tensile steel strands.

We shall presently show an application of this interesting solution to a double-track railway bridge designed by my office for crossing a 350 m wide navigable channel (Fig.25).

The cross sectional area of cables, formed by strands and steel sheathing in combination, in line with the full utilization of the strength characteristics of the materials used, permitted to reduce of about 60% the deflections of the bridge related to those corresponding to use cables formed only by strands of high tensile steel.

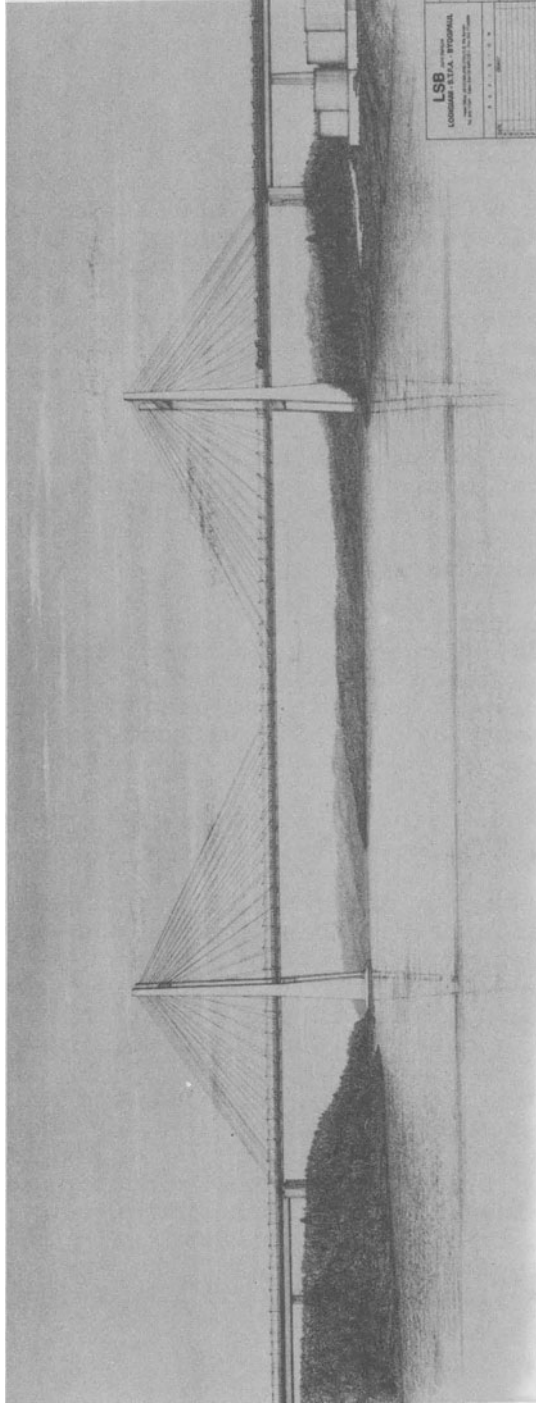


Fig. 25

In order to project the cable stayed bridges, with all its technical and economical advantages into the field of the maximum spans attainable with the suspension bridges, a high number of innovations is needed in their design and erection.

Let us consider some of these possible innovations.

To start with, notice that for cables in general and particularly for longer cables, if l_0 could be halved for the same σ ; then, with the live load acting on the central span, there would be a small percentage reduction of E^* compared to E , and so reduced deflections of the deck.

If, as a new step, the longitudinal displacement u of the top of the towers could also be reduced, then the deflections of the deck would be furtherly reduced too. In addition, if the values of H could also be reduced without at the same time reducing the lower values of α , then at the points where the cables join the deck, there would be no increase in the deflection of the deck itself.

These goals can be reached by adopting the bridge system shown in fig.26.

Note the following details:

- 1) The introduction of a special box cross-section counter-stay horn-shaped in steel plate (braced transversally), which makes it possible to halve the values of l_0 for longer cables, and also to reduce the height H of the towers by (10-15)% without reducing the values of α_{min} .
- 2) The use of reinforced concrete towers of height $H'=(0.85-0.90)H$, A-shaped in the longitudinal plane.

In order to check the efficacy of the structural system of fig.26 compared to the cable-stayed bridge system of fig.27, some comparisons were made with reference to a cable-stayed bridge of three main spans (600+1800+600)m designed by the present writer and others in the Lambertini Group for a road and rail crossing over the Strait of Messina (see fig.1).

For the same spans and loads, this new system tending to reduce the influence of parameters E^* , u and α_i for longer cables gave the results shown in fig.26 and 27 for the flexibility of the bridge. Note the reduction in the maximum values of the elastic deflections in the central area of the deck. They are about 34% lower, and with an elastic curve distinguished by smaller values of the maximum inclinations of the deck itself; values of N in the deck will be reduced too.

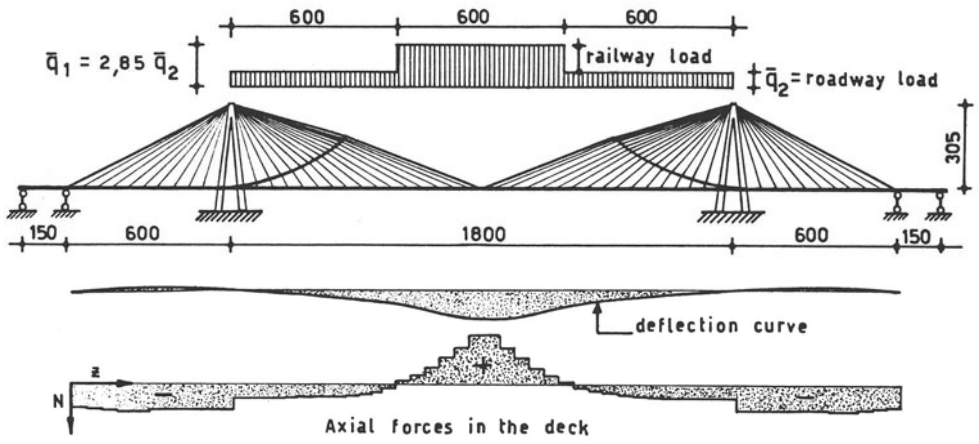


Fig.26: Cable stayed bridge system with horn-shaped counter-stay

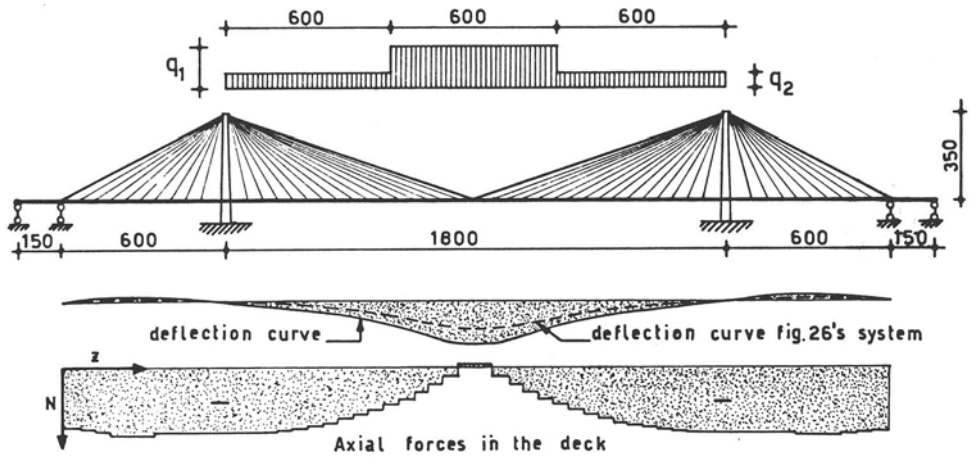


Fig.27: Typical cable stayed bridge system for long spans

The horn shaped counter-stay makes it possible to erect the structures of the central span in two stages. In the first the horn and the two upper half-stays are erected at the same time as the cables of the side span. In the second stage the erection of the central span (deck and lower half-stays) is completed.

The A-shaped tower, still in the longitudinal plane, would also reduce the L/l ratio, which for the classical cable-stayed bridge was fixed at 3.00 to ensure that the anchorage cables had an adequate safety coefficient for stability against unloading when the mobile overload is present only on the side spans.

In this way the stiff A-shaped reinforced concrete tower would make it comfortably possible to increase each side span to 700m, thus permitting the two anchorage piers to reach the land on either side of the Strait, at a distance of 3200m in the point where the sea-bed is less deep.

The planned continuity of the deck beyond anchorage piers with two small self-supporting 150m spans, and the addition of two (tensile) counter-stays connecting at the two intermediate points the anchorage cables to the lower parts of the towers, offer a further contribution to the reduction of the flexural deformations of the deck for a system with such ratios between the spans.

BIBLIOGRAPHY

- De Miranda F. , Sylos Labini F.: Condizioni di ottimalizzazione del peso strutturale del ponte strallato con schema a ventaglio - Costruzioni Metalliche, n°1/1972.
- De Miranda F., Como M., Grimaldi A., Maceri F.: Basic Problems in Long Span Cable Stayed Bridges - Dept.of Structures, University of Calabria, Report n°25, 1979.
- De Miranda F. : Ponti strallati di grande luce Ed.Sc.A.Cremonese - Roma 1980.
- Gimsing N.J. : Cable supported Bridges - Concept and Design John Wiley & Sons - 1982.
- De Miranda F. : Design - Long Span Bridges - International Symposium on Steel Bridges London 25-26 Feb.1988 - Institution of Civil Engineers.

ON THE DURABILITY OF REINFORCED AND PRESTRESSED CONCRETE STRUCTURES

M. Mele

University "La Sapienza", Rome, Italy

E. Siviero

Istituto Universitario di Architettura, Venice, Italy

«In infrastructures, which more and more need to be designed as national European systems, a uniform functionality in the territory must be sought overriding the lack of coordination in investment and maintenance activity.»

Carlo Azeglio Ciampi
Governor of the Banca d'Italia
Final comments
May 1990

1. Introduction

Vitruvio, in *Treatise on Architecture*, indicated as requisites for buildings: *firmitas*, *utilitas* and *venustas*. Safety (*firmitas*) therefore always had to accompany functionality (*utilitas*) and the rules of appearance (*venustas*). It may be assumed, in a more general acceptance, that *firmitas* also contains the concept of continuation in time. In that sense, however, a new requisite, *vetustas*, must be explicitly added. In fact, when referring to natural stones, he recommended extraction of samples from the quarry and leaving them exposed to the weather for two years, checking their condition before, and the Istituto Universitario di Architettura of Venice has adopted these so much so as to insert them in its own coat of arms (fig. 1).



Fig. 1. Vitruvio: *Firmitas, utilitas, venustas*
Istituto Universitario di Architettura of Venice.

The idea of durability, considered as an awareness of deterioration for disrepair phenomena, became very apparent from the second half of the XVIIIth century, in parallel with the advent of building technology based on the use of new materials (steel, concrete) as alternatives to the traditional materials (timber, brickwork) where the time-behavioural characteristics were better known. In fact at that time the first phenomena of embrittlement of the first iron bridges, phenomena of cracking of concrete and corrosion of steels, and later – after the first application of prestressed reinforced concrete, – phenomena of corrosion under the prestressing steel forces and unsuccessful injection in post-tension cable sheathing, became apparent.

Subsequently, as from the '50s, new materials were used without full knowledge, based on an experimentation support, owing to compelling needs for the short term reconstruction of what had been destroyed by the events of war.

In the last ten years, progress in the methods of structural analysis, together with an increased architectural creativity and an at times excessive use of prefabrication, have led to the frequent use of reduced thickness with ever smaller dimensions without adequate care in studying the construction details.

Added to this a very limited maintenance so that structures designed with a correct structural plan have deteriorated over the period of 20-25 years with serious functional difficulties and heavy repair costs. In addition, difficulties of access to the faulty parts have frequently caused further delays to inspections and performance of the appropriate action. As from the '80s the improvement in the quality of cement has led to a reduction in the quantities used while still achieving the required strengths. However this also increased the porosity of the concrete which, as is known, is one of the major causes of corrosion by external agents.

Even from the aspect of increase in mechanical properties, the at times frantic search to achieve the greatest strength in a short time, in order to satisfy technical standards, has resulted in a flattening of the time curve with an apparently reduced reserve of strength as compared with those previous years (fig. 2).

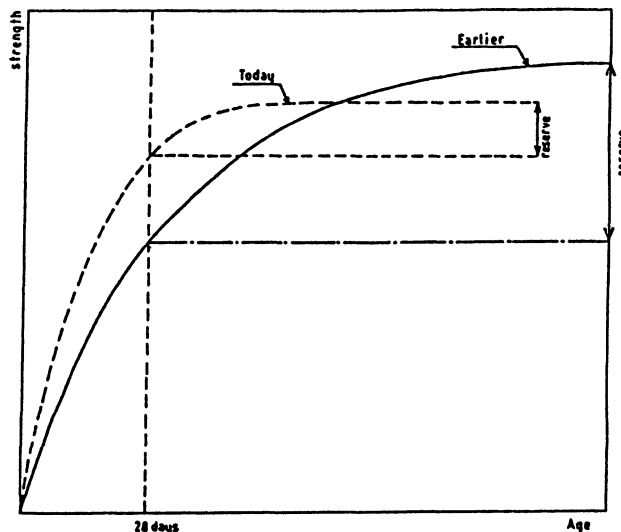


Fig. 2. Stress variation with time for concretes in the past and today.

It has therefore become necessary to develop a constructional awareness in the professional community and a sense of responsibility of the various operators in the light of sufficient time response of the structure to its original design and its intended use, particularly in view of the relative financial implications. Accordingly, the concept of durability and maintenance have now become a decisive part in the cultural-technical background of Public Administrations. In particular, a thorough analysis of these problems is contained in an ANAS document, published in 1988, on the «durability of road structures», which examines various concurrent causes including in particular:

- the design and building of ever more slender structures using a systematic and frantic search for structural lightness achieved by progress in structural analysis and the development of constructional procedures;
- less careful study of the constructional details and working details as a consequence, *inter alia*, of the post-eighties separation between the roles of the designer and the worksite manager;
- the ever wider use of prefabrication techniques, not matched by a use of reliable materials and fastenings, and careful checks particularly at the time of testing.

All this has been partially faced by the introduction of semi-probabilistic rules for approach to the limit states whereby control of the work is required not only with regard to safety against collapse but also in respect of the working conditions which represent, although incompletely, a check on certain durability problems.

In a definition given to the mixed FIP/CEB committee, durability is expressed as the suitability of a structure to withstand attacks by various corrosive agents, whilst essentially maintaining the functional features unaltered. This definition, which refers to the behaviour of the material in environmental and operating conditions, is equivalent to expressing durability as a longterm property, one which is therefore linked to the loss of performance as a function of time.

The concept of durability must therefore be extended from the intrinsic material to the structural items, on to the structures overall. More properly the term of «efficiency» should be used for structures in the sense of matching between the functional duration and the life of the structure itself.

It is therefore possible to define durability as the suitability of a structure to retain its original functioning use in normal working and maintenance conditions during the entire anticipated life period. In that way other parameters, closely linked to the definition of durability, are involved.

This trend towards allocating greater scientific strictness to the concept of durability is confirmed in the definition given by ASTM in the document «Standard practice for developing acceleration tests to aid prediction of the service life of building components and materials» of 1981: durability is the capacity to maintain the service life of a product, a component, a unit or the entire structure over an allocated time.

Service condition and therefore capability of use have been seen as the capacity of these units to perform the functions for which they have been designed and constructed. These service characteristics are affected by externals of atmospheric, ecological and degradation or deterioration. That definition of durability, as given above, is combined with the more modern definition of service life, considered as that period, following the construction of a structure, during which all the remain at the minimal acceptable values in ordinary working conditions. Therefore durability and service life are on design requirements to be satisfied for a pre-established period of time.

This relationship between durability and service life was adopted and developed from the technical aspect and also from the economic and functional aspect during a CEB-RILEM workshop held in October 1986 at Bologna relating to the durability of concrete structures, noting how service life can be identified from the technical, functional and economic aspects defined as follows:

- Technical Service Life (TSL: period of time beyond which an unacceptable service condition is reached. This aspect, within the approach to the limit conditions, is linked to the concept of safety as final limit state, to the concept of operation as limit service state and concept of external quality of the structure from the appearance aspect;
- Functional Service Life (FSL): period of time beyond which the structure becomes obsolete from the functional aspect. The functional duration is clearly influenced by any modifications over the course of time as compared with the operating requirements provided for at the outset;
- Economical Service Life (ESL): period of time beyond which a total substitution of the structure is economically more advantageous than its continuation in service with recourse to maintenance or repairs.

Economic life therefore depends on a cost-benefits balance sheet for the use of a structure with repair and maintenance costs or total rebuilding costs.

The technical service life is however linked to the maintenance of a minimum level of efficiency which must indeed be considered as relating to safety, usability and external characteristics.

In the light of the foregoing clarifications it may be asserted that the correct design of a lasting structure or, as is said, «design for durability» must materialise in a technical duration of the structure which is greater than or at least equal to the other two, therefore introducing a relationship of dependency of the life of the structures on functional or economic factors.

It is therefore possible to identify a service life which depends on the one hand on the properties of the materials and structural characteristic and, on the other hand, on the environmental conditions on functional and economic requirements and also the maintenance carried out.

In brief, the effective life of structure will consist of the minimum value between TSL, FSL and ESL, whilst the objective of the design from the aspect of durability will be achieved when it is guaranteed that the TSL is not less than the FSL or ESL.

The time factor therefore enters in the philosophy of the structural design, it being necessary to guarantee the retention of the margin of initial safety throughout the entire service life, which entails the maintenance of its integrity over the course of time. This aspect induces us to consider maintenance in a wider acceptance than usual which includes the need for checks, repairs, substitutions as activities for which the owner of the structure is responsible and which are not strictly connected to the guarantee of durability of the structure. Furthermore, whilst structural safety, considered apart from thorough knowledge of the actions and characteristics of materials, constitutive laws and structural behaviour, the same cannot be said when the valuation includes the time factor. In fact, from this aspect, knowledge is still lacking and accordingly precise standards are also lacking. Therefore at present the sole indications are limited to a statement of principles of general characteristics such as:

- use of the structure;
- performance criteria;
- the environment;

- the materials used;
- the form of the structural elements and the constructional details;
- the quality of work and control level;
- the protective measures;
- maintenance.

It is in fact necessary for durability to be considered as a fundamental prerequisite in the phases of:

- planning and design;
- realisation;
- use period.

In this context, in order to achieve the pre-established objective, strict cooperation between owner, designer, builder and user becomes absolutely necessary and each of these has to perform his own role in conjunction with the others.

The design documents therefore cannot be limited to drawings accompanied by technical specifications for realisation, but must also include the plans for control and maintenance of the structure.

According terms of reference to the following aspects, becomes of fundamental importance:

- for the design, in order to reduce the probability of the occurrence of human errors;
- for the realisation in order to identify and correct insufficient results in the productive process;
- for maintenance, as a control that the safety levels remain unchanged over time.

The consequences of failure to control may indeed become dramatic as unfortunately too many examples show.

In that sense, a useful reference may consist of what is known as the «law of the five» (De Sitter) which identifies the following four phases in the life of a structure

- A. design and realisation;
- B. ordinary maintenance;
- C. special maintenance with local damages;
- D. general repairs with structural restoration;

forming a brief evaluation criterion for the costs of action during the various phases based on the adoption of a multiplier 5 in change in between one phase and another in the instance of progression of negligence.

So considering the extra cost in the instance of good design and correct performance during phase A as being equal to 1, failure to implement this induces an extra cost:

- in phase B equal to 5;
- in phase C equal to 25;
- in phase D equal to 125.

It follows that it is necessary to act correctly both during phase A with good design, correct realisation and adequate quality control and during phase B with inspection, control, maintenance, systematic operations, thus achieving an extension of the service life of the structure from its there aspects mentioned above: technical, economic and functional.

In that sense, the design choice is therefore effected by reducing the overall cost function, defined as follows, to a minimum:

$$C_g = C_o + \sum p_i C_i$$

where:

C_g overall cost;

C_o initial cost;

C_i cost of repair action during the life of the structure;

p_i the probability that the event which requires the action of repair will be required.

In brief, from a general point of view, the durability design criteria, particularly in accordance with the CEB FIP Model Code 1990, may be identified as follows:

- a) choice of the structural shape suitable for the environment, accessibility, inspection and maintenance;
- b) good quality of the concrete mix and sufficient cover of the bars;
- c) correct design of reinforcing details;
- d) control of the nominal spacing;
- e) provision if necessary of protection of the steel and/or for the concrete surface;
- f) specific technical details for the materials to be used with recommendation for use and indications for maintenance of time of live.

However, to tackle the matter of durability from a theoretical aspect has proved to be a fairly difficult problem. In that sense, an attempt has been made by a study group of CTE coordinated by prof. Toniolo in the Italian CEB Group on the subject «durability» of CEB-FIP Model Code 1990. These concepts were then adopted by other scholars in three ANAS seminars by prof. Radogna on 30th October 1989 at Rome, by prof. Migliacci on 13th November 1989 at Milan and Mr. Macori, engineer, on February 13th 1990 at Padua.

In view of the substantial interest which they assume and the subsequent developments which have become apparent, these concepts have been adopted in their entirety in paragraph 6 of this note appearing below.

2. Deterioration and protection factors

The required life for a structure and the inspection and maintenance programme call for protection levels linked to environmental conditions and also to the chemical and physical attack mechanisms.

As indicated by Eurocode 2, environmental conditions may be classified in 5 exposure classes (table 1).

In general, chemical attack can be originated by:

- use of the structure;
- corrosive environment;
- contact with acid solutions or gases or sulphate salts;
- chlorides;
- alkaline-aggregate reactions.

Physical attack results usually from:

- abrasion;
- freezing/unfreezing action;
- penetration of water.

In any event, sufficient corrosion of the metal reinforcing is required. In normal conditions, this objective is achieved by an adequate cover consisting of good-quality concrete characterised by low permeability.

Further protective measures must be implemented in particularly corrosive environments both for the concrete surfaces and the reinforcing itself.

Tab. 1. Exposure classes related to environmental conditions (Eurocode 2).

Exposure classes		Examples of environmental conditions
1 dry environment		interior of buildings for normal habitation or offices ⁽¹⁾
2 humid environment		a without frost <ul style="list-style-type: none"> – interior of buildings where humidity is high (e.g. laundries) – exterior components – components in non-aggressive soil and/or water
		b with frost <ul style="list-style-type: none"> – exterior components exposed to frost – components in non-aggressive soil and/or water and exposed to frost – interior components when the humidity is high and exposed to frost
3 humid environment with frost and de-icing salts		interior and exterior components exposed to frost and de-icing agents
4 sea water environment	a without frost	<ul style="list-style-type: none"> – components completely or partially submerged in sea water, or in the splash zone – components in saturated salt air (coastal area)
	b with frost	<ul style="list-style-type: none"> – components partially submerged in sea water or in the splash zone and exposed to frost – components in saturated salt air and exposed to frost
The following classes may occur alone or in combination with the above classes:		
5 aggressive chemical environment ⁽²⁾	a	<ul style="list-style-type: none"> – slightly aggressive chemical environment (gas, liquid or solid) – aggressive industrial atmosphere
	b	<ul style="list-style-type: none"> – moderately aggressive chemical environment (gas, liquid or solid)
	c	<ul style="list-style-type: none"> – highly aggressive chemical environment (gas, liquid or solid)

(1) This exposure class is valid only as long as during construction the structure or some of its components is not exposed to more severe conditions over a prolonged period of time.

(2) Chemically aggressive environments are classified in ISO/DP 9690.

Tab. 2. Minimum cover requirements for normal weight concrete ⁽¹⁾ (Eurocode 2).

		Exposure classes, according to Table 1								
		1	2a	2b	3	4a	4b	5a	5b	5c ⁽³⁾
Minimum ⁽²⁾ cover (mm)	Reinforce- ment	15	20	25	40	40	40	25	30	40
	Prestressing steel	25	30	35	50	50	50	35	40	50

Notes

- (1) In order to satisfy the provisions of EC 2. These minimum values for cover should be associated with particular concrete qualities, to be determined from table 3 in ENV 206.
- (2) For slab elements, a reduction of 5 mm may be made for exposure classes 2-5. A reduction of 5 mm may be made where concrete of strength class C40/50 and above is used for reinforced concrete in exposure classes 2a-5b, and for prestressed concrete in exposure classes 1-5b. However, the minimum cover should never be less than that for Exposure Class 1.
- (3) For exposure class 5c, the use of a protective barrier, to prevent direct contact with the aggressive media, should be provided.

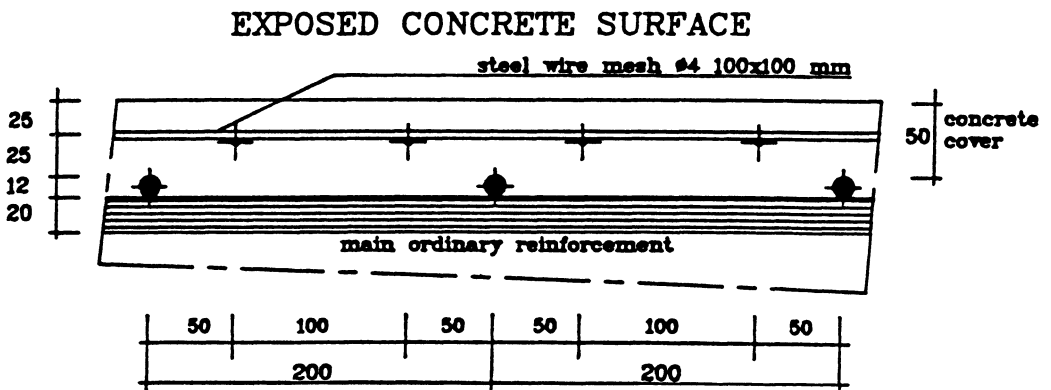


Fig. 3. Detail of surface reinforcement in aggressive environment with high concrete cover.

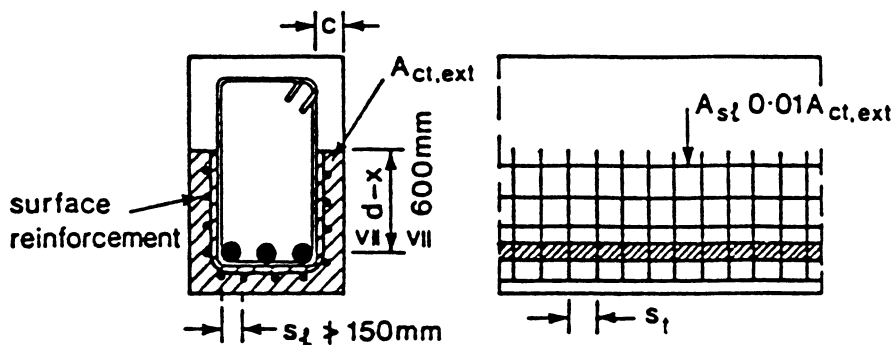


Fig. 4. Surface reinforcement as proposed by Eurocode 2.

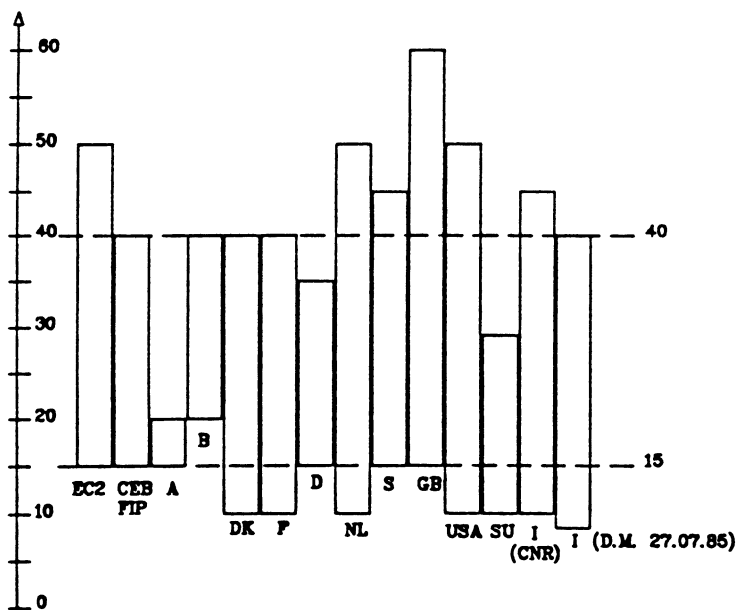


Fig. 5. Concrete cover (mm) as suggested in national and international standards.

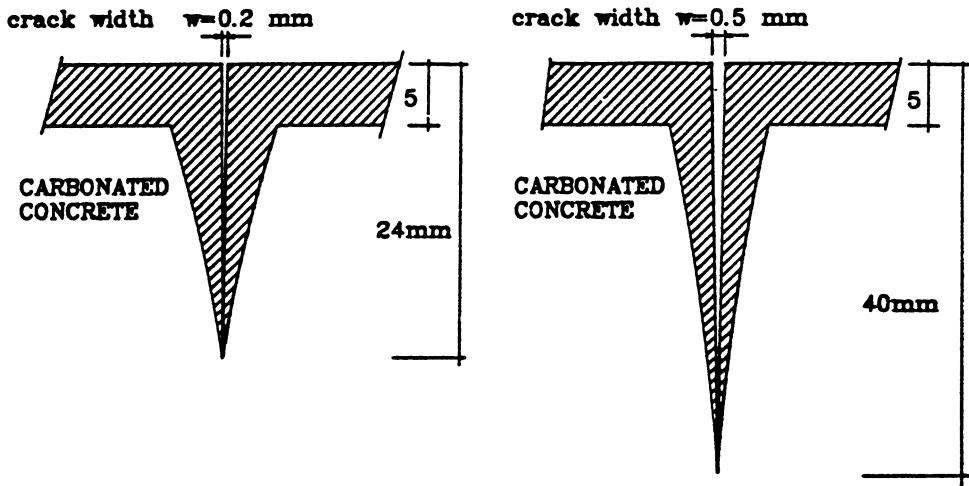


Fig. 6. Penetration of chemical attack on a concrete surface after one year for a crack width of 0,2 mm (6a) and of 0,5 mm (6b).

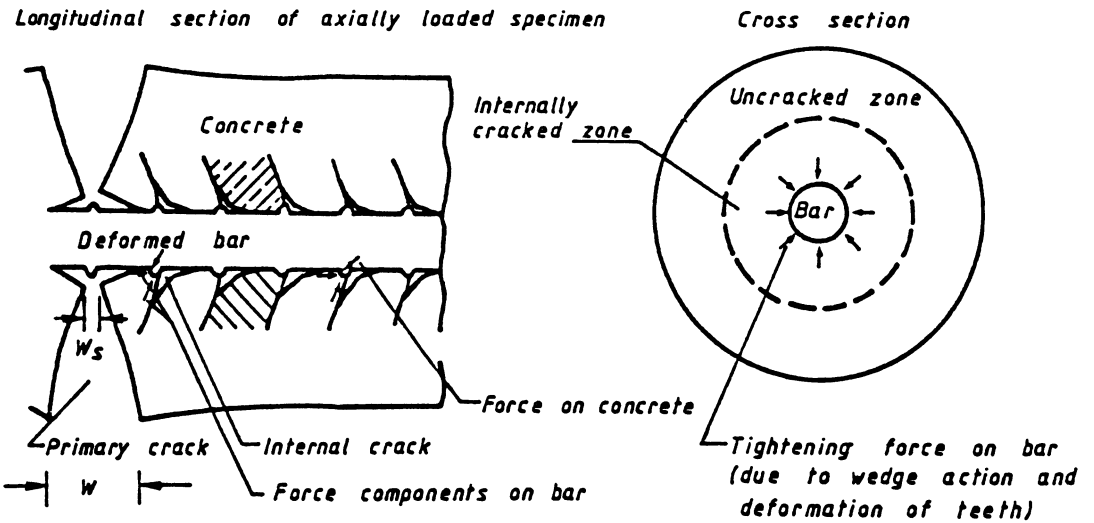


Fig. 7. Detail of crack near a reinforcing bar and local slip.

The protection of reinforcing against corrosion depends, as is known, on the continuous presence of a surrounding alkaline environment which is guaranteed by the concrete coating.

The thickness of the required coating depends both on the conditions of exposure and the quality of the concrete itself (table 2).

In certain cases, for high concrete cover, it may be necessary to provide a skin reinforcing both to control and to guarantee adequate resistance against detachment by parts of the concrete (figures 3 and 4).

In fact, by looking at the concrete covers required in the various standards (figure 5) it is clear that, with values in excess of 40-50 mm, the use of skin reinforcement is required.

This is justified by the conditions of chemical attack over the course of time in the presence of cracking, as schematically shown in figure 6 which demonstrates the extent of carbonation after a year of exposure for a crack of a size of 0,2 mm (figure 6a) and 0,5 mm (figure 6b) respectively, whilst figure 7 gives the details of the crack by the reinforcing bar together with the local slip. The danger of steel corrosion is therefore evident.

Accordingly it will be necessary to limit the size of the cracks and protect the structure from corrosive environments.

It goes without saying that a further protection of the steel is not only appropriate but at times even necessary.

This objective can be achieved by the use of bars protected by epoxy resins or galvanised or in stainless steel or with recourse to cathodic protection.

3. Materials

3.1 Concrete

Knowledge of deterioration factors and the possibility of use of materials and resources to overcome them nowadays makes it possible to design a concrete which is not only lasting but strong.

Furthermore it is necessary to modify the habit of the mind of the designer who will therefore not only use the strength characteristics of an ideal concrete to the maximum, but also act so that the desired properties are maintained unchanged for the useful life of the designed structure.

In fact, although concrete is the material which is most widely used in building, knowledge of its properties and in particular of its behaviour over the course of time is very limited. An adequate «culture» for a material, the microstructure of which should also be considered, is also lacking.

But in the field of design it can also be said that sufficient awareness in consideration of all the properties of concrete is also lacking. A structure is in fact normally described by geometrical details (section, height and dimensions in general), accompanied by efficiency indications (strength or admissible stresses), all of these completely abstract as compared with the complex reality of the material with the structure is produced. Even when, for structures of a certain size, attention is paid to the characteristics of the material, considering for example shrinkage, creep and the coefficient of thermal expansion of the concrete, at times this is carried out with formal calculations without going into the physical reality or, if necessary, the chemical reality of the material.

Indeed concrete demonstrates a substantial capacity for adaptation, generally

corresponding quite well to expectations, but when exposed to unexpected stresses or corrosion, at times it is subject to early deterioration.

The two fundamental parameters to obtain a lasting concrete are, as is known, the W/C ratio and the strength class.

There is no doubt whatsoever that concrete must contain a minimum amount of cement so much so that in the concreting regulations of the principal countries, including European ENV 206, the minimum proportion of cement is prescribed together with the maximum W/C ratio, according to the degree of corrosion of the environment and the maximum dimensions of the aggregate (table 3).

The W/C ratio and degree of hydration combination determines, for the hardened cement paste determines the degree of porosity which is linked to its strength and permeability.

At normal temperatures some of the constituents of Portland cement begin to hydrate immediately in contact with water, but when the reaction products affect the anhydrous cement granules the reactions slow down substantially. At this point suitable curing assumes fundamental importance and this consists in keeping the cement paste as saturated as possible with water at least until the space filled by it has been substituted by hydration products in other words until its capillary porosity is completely blocked. The hydration process in fact can take place only when the vapour tension in the pores is some 80% of the saturation value. In the vicinity of that value the hydration speed is at the maximum.

The suggestion of a practical nature to devote particular care to curing the poured concrete during the initial period is therefore fundamental, not only in order to obtain optimum development of strength but to avoid dangerous cracking from shrinking owing to drying and in particular to make it impermeable if it is also to be lasting. It is therefore necessary to keep the poured concrete as damp as possible until it has reached sufficient mechanical strength properties, which can be evaluated from time to time in relation to the product and its use. Of particular importance is the study of the cracking phenomenon, particularly in relation to the time of appearance of the cracks (figure 8).

Before of during setting, cracks can be:

- a) of an intrinsic nature owing to the phenomenon of cracking and plastic settlement (figure 9);
- b) of an extrinsic nature owing to frost, heat variations, the giving way of formwork (figure 10);

After setting, cracking can be:

- a) of a physical nature; porous inert, shrinking, cracking;
- b) of a chemical nature: corrosion, alkali-silicon, carbonation;
- c) of a thermal nature: thermal cycles, hydration heat, accelerated maturing;
- d) of a structural nature: external loads (figure 11), deferred phenomena (figure 12), differential settlement (figure 13), adhesion (figure 14), errors in fitting reinforcing (figure 15).

A table of cracking which shows the various aspects mentioned above appears in figure 16, whilst figure 17 shows the details of cracking possible in structures.

It is therefore necessary to stress the snare of cracking which can occur during setting. In fact, during the hardening, the concrete gradually acquires a tensile strength, although limited, whilst the presence of the reinforcing prevents it from becoming strained. Cracking commences after a few hours from the poring when the tension generated by the prevented straining overcomes the tensile strength (figure 18) with simultaneous net reduction in deformability (figure 19).

From what has been stated above it is therefore essential to design carefully the concrete mix having recourse, where necessary, to use of appropriate superplasticizing additives to reduce the W/C ratio.

Tab. 3. Durability requirements related to environmental exposure (ENV 206).

Requirement	1	2	3	4	5	6	7	8	9
	Exposure class according to table 1								
	1	2a	2b	3	4a	4b	5a	5b	5c ⁽¹⁾
max w/c ratio for ⁽²⁾ : - plain concrete - reinforced concrete - prestressed concrete	— 0.65 0.60	0.70 0.60 0.60	0.55	0.50	0.55	0.50	0.55	0.50	0.45
min. cement content ⁽²⁾ in kg/m ³ for: - plain concrete - reinforced concrete - prestressed concrete	150 260 300	200 280 300	200 280 300	300	300	300	200 280 300	300	300
min. air content of fresh concrete in % for nomi- nal max aggregate size of ⁽³⁾ : - 32 mm - 16 mm - 8 mm	— — —	— — —	(4) 4 5 6	4 5 6	— — —	4 5 6	— — —	— — —	— — —
frost resistant aggregates ⁽⁶⁾	—	—	yes	yes	—	yes	—	—	—
impermeable concrete	—	—	yes	yes	yes	yes	yes	yes	yes
types of cement for plain and reinforced concrete according to EN 197							sulphate resistant ce- ment ⁽⁵⁾ for sulphate contents: > 500 mg/kg in water > 3000 mg/kg in soil		
<p>The above values of w/c ratio and cement content are based on cement where there is long time experience in many countries. However, at the time of drafting this pre-standard experience with some of the cements standardized in EN 197 is limited to local climatic conditions in some countries. Therefore during the life of this pre-standard, particularly for exposure classes 2b, 3, 4b the choice of the type of cement and its composition should follow the regulations valid in the place of use of the concrete. Alternatively the suitability for the use of the cements may be proved by testing the concrete under the intended conditions of use. Additionally, cement CEI may be used generally for prestressed concrete. Other types of cement may be applied if experience with these types is available and the application is allowed by the regulations valid in the place of use of the concrete.</p>									
<p>(1) In addition, the concrete shall be protected against direct with the aggressive media by coatings unless for particular cases such protection is considered unnecessary. (2) Pozzolana or latent hydraulic additions may be taken into account for the minimum cement content and the maximum water-cement ratio only if permitted by requirements of the national standards and regulations valid in the place of use. (3) With a spacing factor of the entrained air void system > 0.20 mm measured on the hardened concrete. (4) In cases where the degree of saturation is high for prolonged periods of time. Other values or measures may apply if the concrete is tested and documented to have adequate frost resistance according to the regulations valid in the place of use of the concrete. (5) The sulphate resistance of the cement shall be judged on the basis of national standards and regulations in the place where the concrete is used. (6) Assessed against the regulations valid in the place of use of the concrete.</p>									

CAUSE DI FESSURAZIONE
CAUSE OF CRACKING

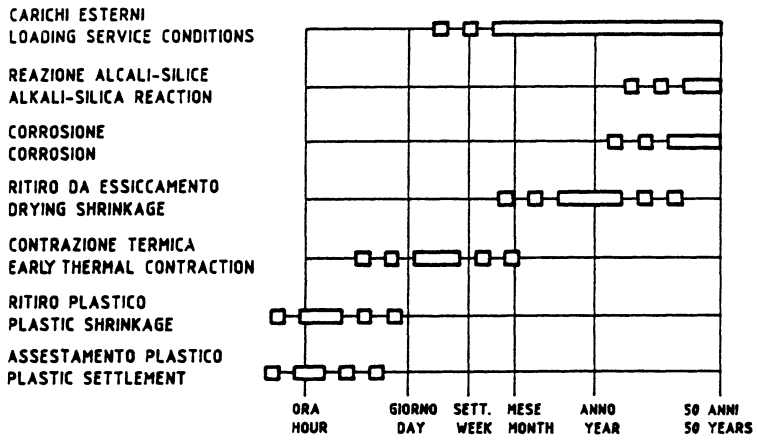


Fig. 8. Time of appearance of cracks.

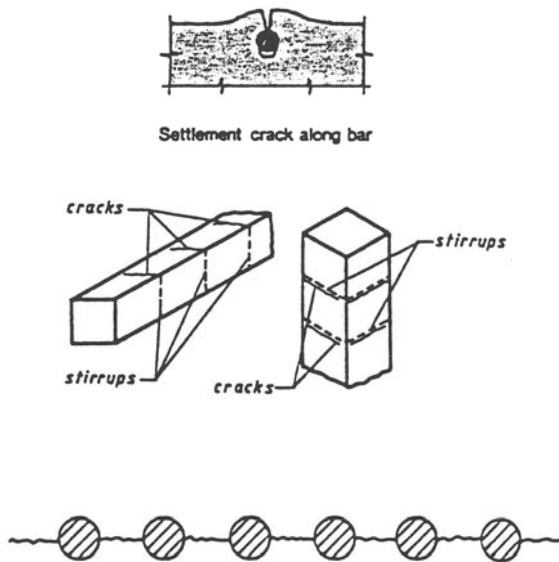


Fig. 9. Cracks due to plastic settlement.

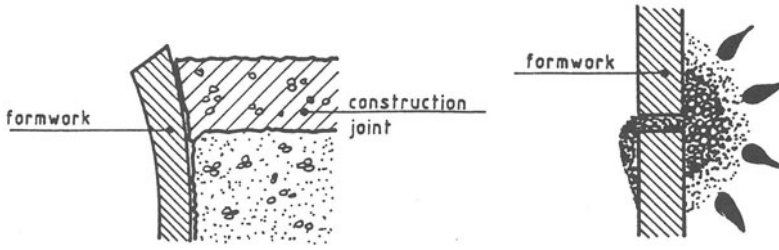


Fig. 10. Inadequate formwork.

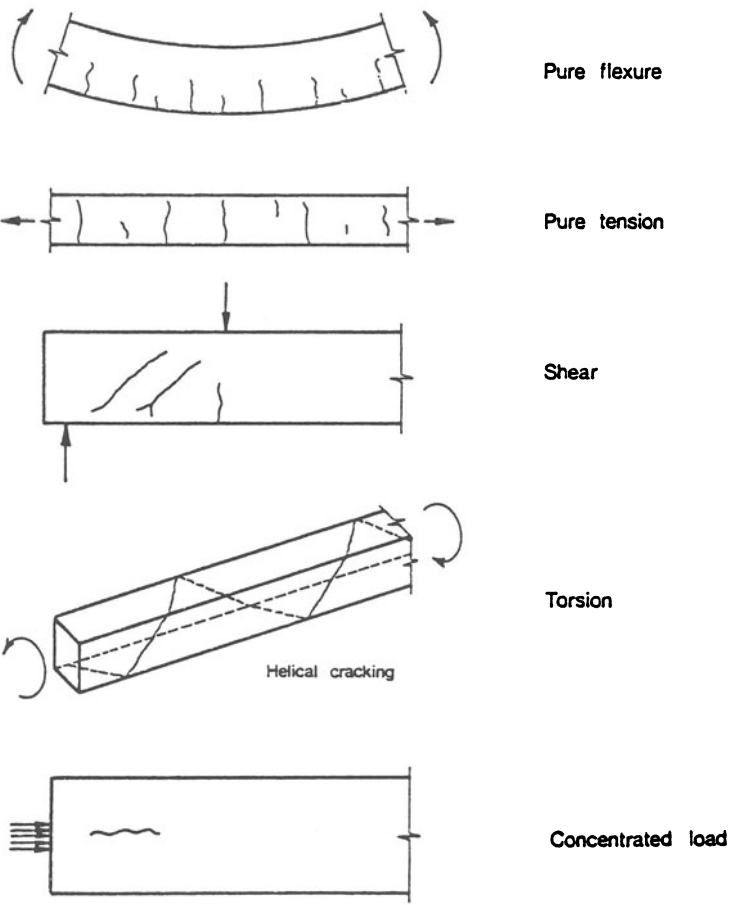


Fig. 11. Load induced cracks.

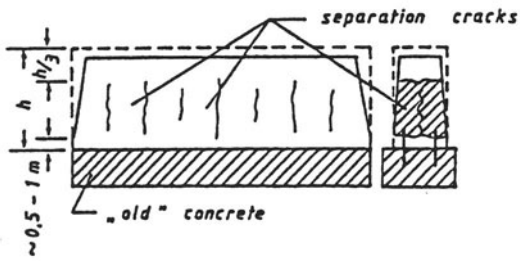


Fig. 12. Cracking due to coupling of different age concrete in a wall.

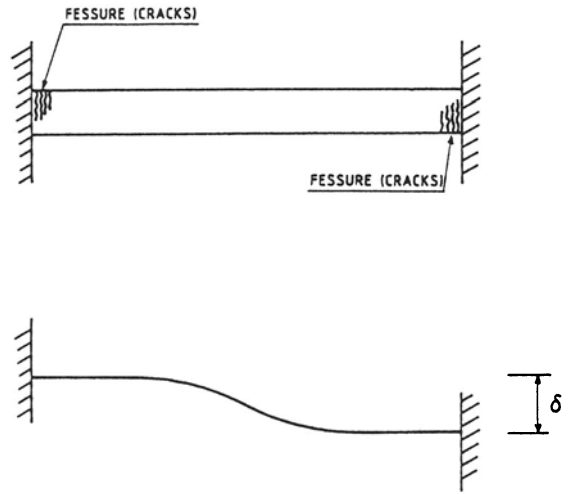


Fig. 13. Cracking due to differential settlements.

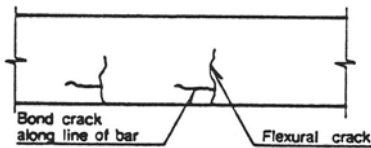


Fig. 14. Cracks due to lack of bond and anchorage of bars.

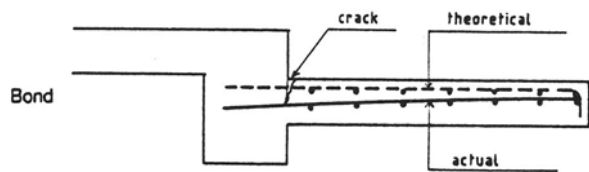


Fig. 15. Errors of placing of reinforcement in cantilever.

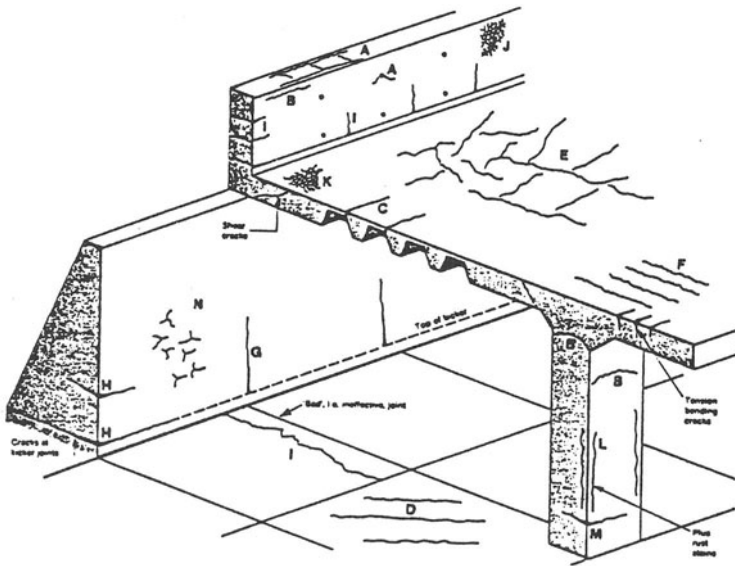


Fig. 16. Examples of cracks in hypothetical concrete structure.

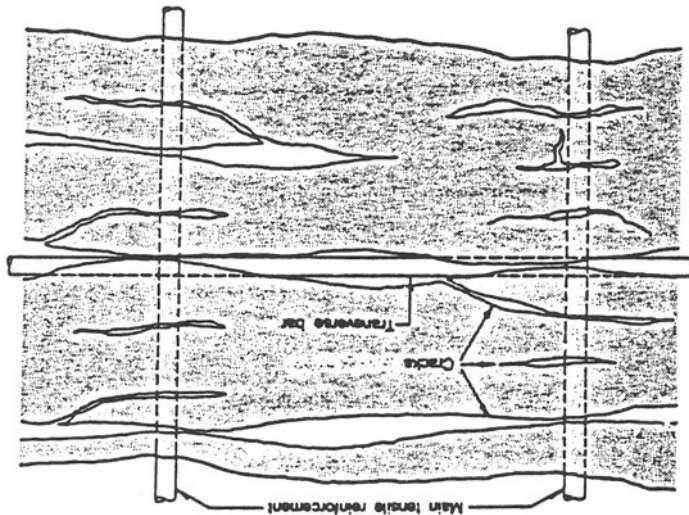


Fig. 17. Alignment of cracking pattern relative to reinforcement on top of a slab.

Classification of cracks as in figure 16.

Type of cracking	Letter (see figure)	Subdivision	Most common location	Primary, cause (excluding restraint)	Secondary causes factors	Remedy (assuming basic redesign is impossible) in all cases reduce restraint	Time of appearance
Plastic settlement	A	Over reinforcement	Deep sections	Excess bleeding	Rapid early drying conditions	Reduce bleeding (air entrainment) or revibrate	Ten minutes to three hours
	B	Arching	Top of columns				
	C	Change of depth	Trough and waffle slabs				
Plastic shrinkage	D	Diagonal	Roads and slabs	Rapid early	Low rate of bleeding	Improve early curing	Thirty minutes to six hours
	E	Random	Reinforced concrete slabs				
	F	Over reinforcement	Reinforced concrete slabs	Ditto plus steel near surface			
Early thermal contraction	G	External restraint	Thick walls	Excess heat generation	Rapid cooling	Reduce heat and/or insulate	One day to two or three weeks
	H	Internal restraint	Thick slabs	Excess temperature gradients			
Long-term drying shrinkage			Thin slabs (and walls)	Inefficient joints	Excess shrinkage inefficient curing	Reduce water content improve curing	Several weeks or months
Crazing	J	Against formwork	Fair faced concrete	Impermeable formwork	Rich mixes	Improve curing and finishing	One to seven days sometimes much later
	K	Floated concrete	Slabs	Over-trowelling	Poor curing		
Corrosion of reinforcement	L	Natural	Columns and beams	Lack of cover	Poor quality concrete	Eliminate causes listed	More than two years
	M	Calcium chloride	Precast concrete	Excess calcium chloride			
Alkali-aggregate reaction	N		(Damp locations)	Reactive aggregate plus high-alkali cement		Eliminate causes listed	More than five years

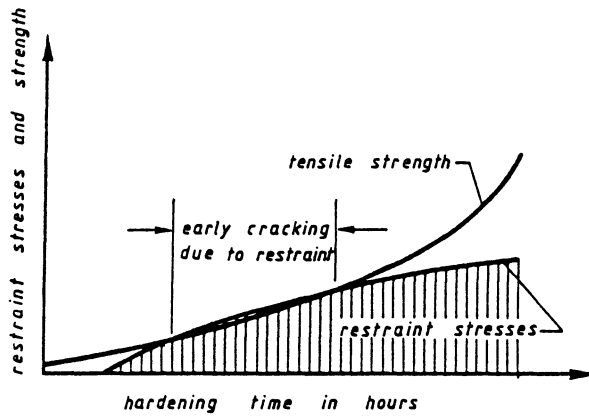


Fig. 18. Evaluation of strength and restraint stresses in young concrete (schematic).

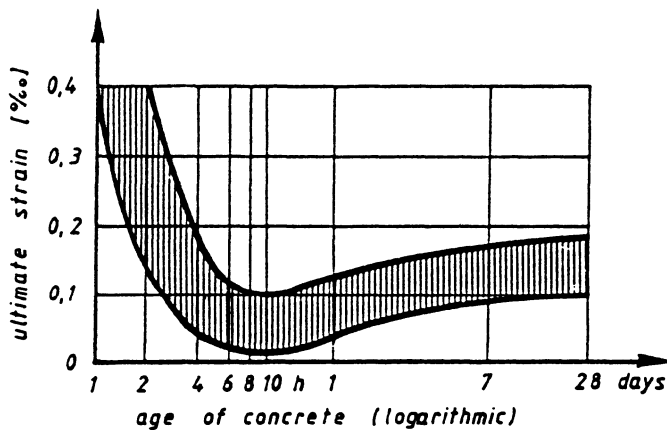


Fig. 19. Ultimate tensile strain of concrete depending on age.

Marked progress in the preparation of high-durability concretes has recently taken place with use of special additives having a pozzolan and thixotropic action which in addition to the densifying effect arising from the reduction of water owing to the presence of plasticizers, produces a further increase in the microstructural density to fill the interstitial voids between the granules of cement with particles of amorphous silicon, much smaller than the cement granules (figure 20).

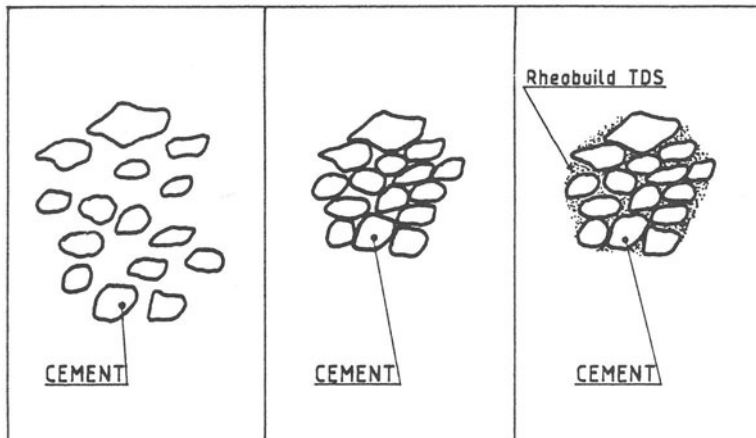


Fig. 20. Additive with high pozzolanic and tixotropic action.

In that way, an extremely dense and compact concrete is obtained, capable of physically resting the penetration of corrosive agents and also incapable of chemical attack owing to the absence of lime.

3.2 Steel

As indicated in paragraph 2, the protection of the reinforcing against corrosion depends on the continuous presence of an alkaline environment in which the metal bar is immersed.

In that case a microscopic layer of passivated ferric oxide is formed on the surface, preventing anodic dissolution.

When the pH falls below value 9 owing to carbonation of the concrete or attack of the chlorides, chemical attack, which spreads speedily to the final condition, begins.

A schematization of the process is given in figure 21.

In those conditions, it appears necessary to have recourse to protective measures for the bars to prevent deterioration.

To that it is possible to use:

- bars covered with epoxy resins;
- galvanised bars;
- stainless steel bars.

Alternatively what are known as «corrosion inhibitors» can be used.

With regard to bars protected by epoxy resins, their initial use goes back to 1973 with applications in the United States. The results obtained seem to be quite good although the risk – not to be neglected – of damage to the protective film which can take place for various reasons, particularly during the transport and use phase, persists.

This aspect calls for particular care in the protective coating quality control process. In fact, with this technology, the protection provided to the bars against corrosion consists essentially

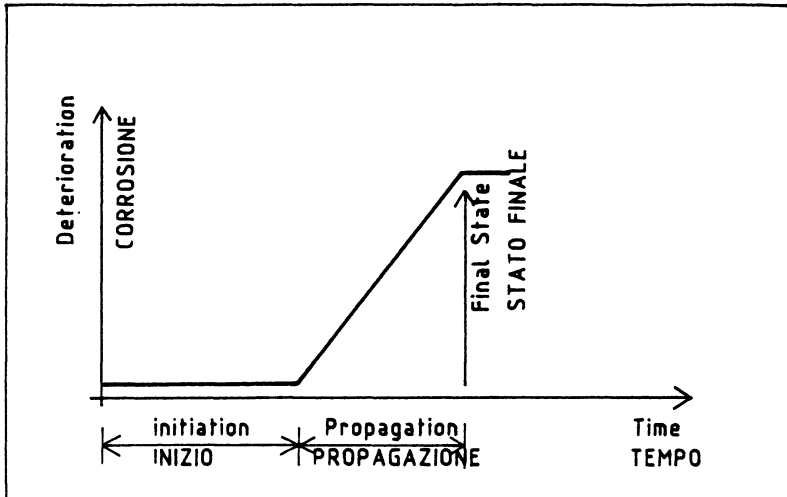


Fig. 21. Scheme of reinforcement corrosion.

of a physical barrier, with generally no chemical interaction between the protective film with its interface with the aggregate. Furthermore, one aspect which has not yet been completely solved is that of aging of the resin and its reaction of the course of time with organic substances which may be present in the concrete.

With regard to galvanised bars, these have become widely used over recent years.

With dip-galvanising at 450-460 degrees C, a zinc thickness of approximately 70-100 microns, sufficient to protect the steel from corrosive agents, is generally obtained.

This protection acts at physical level, as a true and real barrier and at galvanic level, with the zinc and steel immersed in the concrete which acts as an electrolyte where, owing to the difference in potential, the zinc behaves as an anode in relation to the steel, preventing its rusting (figure 22).

Furthermore, in current circumstances, there is no general consensus on the corrosion behaviour of galvanised reinforcing bars in time terms in relation to the level of alkalinity of cement, the use of additives, the variability of the W/C ratio, partial or total exposure to the corrosive environment.

It seems however that one can state the following:

- galvanised steel tolerates a higher concentration of chlorides than ordinary steel;
- in exposed structures in a marine atmosphere the deterioration of the steel coating is greatly delayed and even reduced when zinc bars are used;
- with highly alkaline concretes a loss of protection of galvanised bars is possible. However this phenomenon can be adequately controlled with the use of chrome additives.

In any event, using galvanised bars, it seems to be effectively possible to reduce the coating of concrete, at least in normal type environmental conditions.

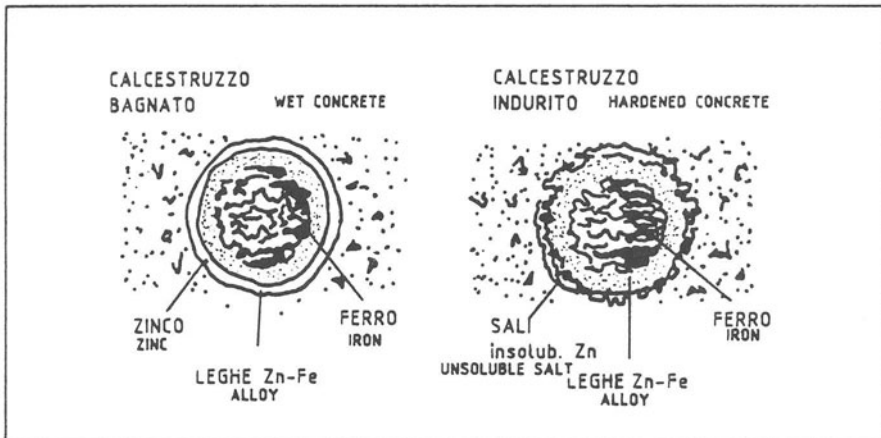


Fig. 22. Protective action of the zinc in reinforcing bars.

The use of stainless steel bars which, in current circumstances, represent the best offer on the market, but less so from the technical aspect, certainly appears to be effective.

Although the use of high bond stainless steel bars as reinforcing for concrete is quite recent, knowledge of their behaviour under chemical attack is well known and depends mainly on their chemical composition.

Its somewhat high initial cost justifies its general use in the entire structure only in very important cases in particularly corrosive environments, for example: structures subjected to freezing and unfreezing cycles, tunnels, marine structures, off-shore structures.

A reasonable compromise between the economy aspect and the technical result can be achieved by the use of stainless steel as surface skin reinforcement where high cover is required.

Finally, some notes from professor Pedeferrri on cathodic protection, recently introduced in Italy.

«Cathodic protection takes place by making the potential of the structure to be protected more negative in relation to the corrosive environment so as to eliminate the corrosion reaction or to reduce it to negligible values. The polarization effect is obtained by circulation of a weak direct current from the environment to the structure which therefore functions as a cathode, with the use of a second electrode functioning as an anode.

In practise the cathodic protection is achieved in two different ways:

- with «sacrificial anodes», that is by coupling with a reactive metal, such as zinc, aluminium or magnesium, which gives off electrons to the steel by means of a short circuit-current and, simultaneously, sends positive ions in solution, becoming corroded;
- with an «imposed current» or by means of an external electrical circuit in which an electromotive force is inserted acting as a pump which sends electrons to the earth to be protected cathodically, taking them from an inert metal immersed in the solution which functions as an insoluble anode.

The cathodic protection of the reinforcing in concrete applied in the past to prestressed piping and underground tanks, such as structures at sea, has been becoming widespread in recent years for the protection of bridge decks, in particular when these have been contaminated by antifreeze salts.

In electrochemical terms the effect of this protection is that of causing the cathodic polarization of the reinforcing and maintaining the potential of a steel at a range in which the corrosion reaction stops or proceeds at a negligible rate. The reduction in the potential entails the stoppage of corrosion even in the present of chlorides.

In the design and realisation of cathodic protection imposed current installations, the most complex aspect is that of design of the anode structure in relation to the high resistivity of the concrete and the limited volume of electrolyte (concrete) through which the current is distributed.

The first imposed current installations used individual anodes in cast iron, silicon iron or graphite, supported by the slabs and covered by a layer of conductive asphalt as secondary anode, in order to distribute the current from the primary anode to the whole of the surface to be protected and to limit acid attack at the anode/concrete interface. Installations produced in accordance with this concept operate but require maintenance of the conductive asphalt coating.

Subsequently anodic structures consisting of titanium or platinum-niobium wire with a backfill of conductive material were produced, housed in a series of parallel channels in the metal covering, section 2x2 cm approx. and length 10-12 m, spaced by approximately 30 cm. In order to achieve the channeling, avoiding an effect on the reinforcing with the resulting short circuiting between the reinforcing and the anodic structure, an adequate metal cover thickness is necessary. Currently the development of anodic structures is directed towards grid systems, possibly available in the form of plastic or metal based networks, to be located on the bridge to be protected, and to be anchored with a layer of concrete to which a waterproofing layer can eventually be applied».

4. Design aspects

The concept of durability must from the outset lie behind the design choices. As mentioned in the introduction, the immediate economic aspects which, in the more recent past, have led towards incorrect choices, can no longer constitute the sole factor for evaluation.

Systematic recourse to prefabrication as a technology considered to be in the forefront, has proved to be disappointing. Particularly in relation to the lack of attention in the realisation phase, it has created more problems than it has solved.

Work site industrialisation and part prefabrication with pouring during the completion work can certainly find ample space provided that the operating methods are carefully evaluated by carefully studying the constructional details and providing the most suitable devices to facilitate inspection and maintenance over the course of time.

The design and its realisation, must therefore be closely integrated, particularly in the case of important structures.

Realisation in several phases enormously conditions the state of stress, not only in the transitory phases but also in the final utilisation states.

The structure has a memory of the phases passed through and the structural calculation must take due account of this.

In general terms, the predominant line is now, in primis, the elimination where possible of transversal joints which have to be designed with perfect impermeability. It will therefore be appropriate to have recourse to hyperstatic schemes of the continuous type or, if they are isostatic, those which at least make the slab continuous.

Gerber hinges must be eliminated or, where they appear, designed with ample space for inspection and maintenance (figure 23).

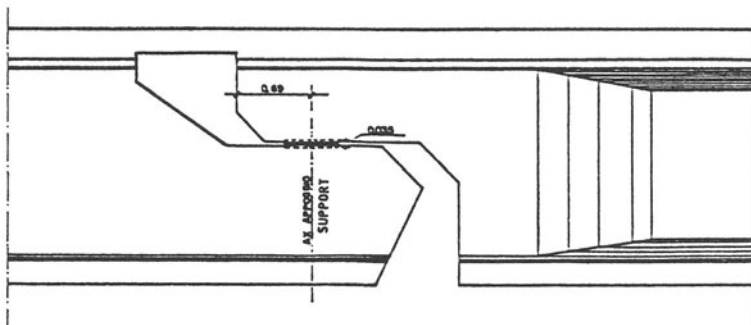


Fig. 23. Detail of a Gerber hinge.

A suitable and robust transition slab between the upset and the shoulder must be provided to eliminate the «step» generated by the settlement of the upset and thus avoid early damages to the structure. Slenderness of structural parts must be limited both globally in the height/span ratio of beams, and locally in the thickness of slabs, webs, spans of cantilevers etc. In that way strains and stresses are contained. The greater thickness available also allow for a safer and more easy positioning of the reinforcing and possibility of guaranteeing more reliable concrete pouring (figure 24).

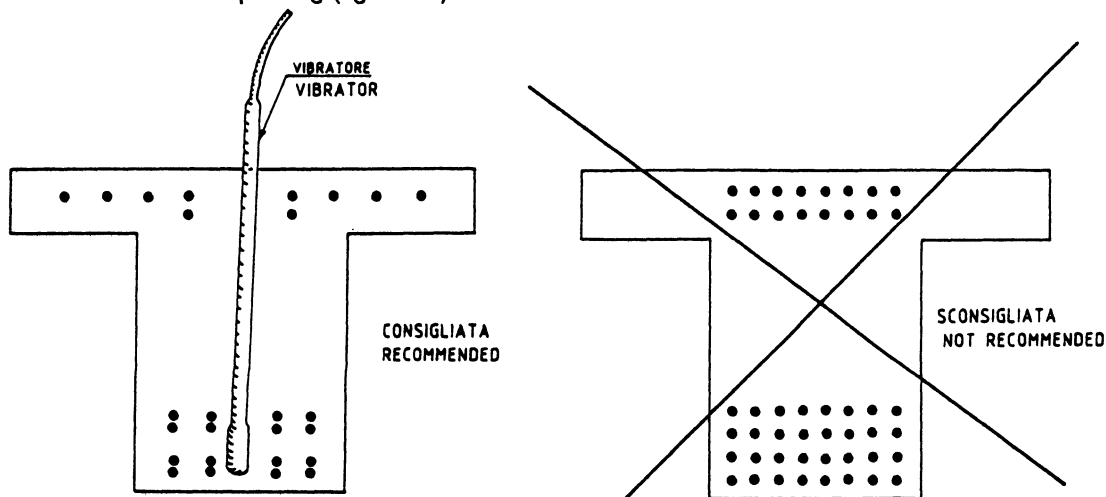


Fig. 24. Bar arrangement in cross sections.

In that sense a limitation of the minimum thickness of slabs and webs appears to be opportune in particular, assuming:

- for slabs a lower limit of 20 cm;
- for webs a lower limit of 14 cm, never going beyond 1/10th of the height in the case of T or double T beams or below 1/12th of the greatest dimension in the case of the walls of box beams.

Particular attention should be paid to the maximum stresses on the materials, bearing in mind the fact that the values admitted by the Standards are frequently found to be excessive in relation to the phenomena of cracking and fatigue which have become apparent after a few years of service.

Another important aspect is the geometry of the transversal section of the structure. This must be of compact form, reducing the surface-volume ratio to minimum (figure 25).

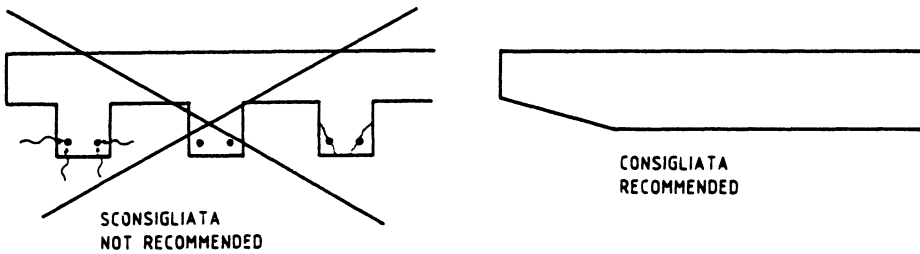


Fig. 25. Geometry of cross sections.

In such a way, in addition to a reduction of exposure to corrosive agents, the advantage – not to be neglected – of the convenient placing of the reinforcing is achieved, avoiding dangerous congestions and thus facilitate the concrete pouring.

With regard to the reinforcing, the correct design should be aimed at reducing cracks and ensuring good anchorage in the concrete. Anchorages should be offset, avoiding the simultaneous ending of a group of bars. Insufficient anchorage may in fact induce dangerous cracking, local chipping as far as loss of the balance of the beam (figure 26, 27, 28).

Off-load thrusts which are caused by the need to balance the system of transversal forces originating from the anchorage should also be avoided. Adequate coverings and suitable bracing should therefore be provide (figure 29, 30).

In any event, it should be recalled that the layout of the reinforcing should be directed, where possible, in the direction of the isostatic tensile lines (figure 31, 32).

But there are further aspects to be considered with the utmost attention in the design phase. For example, the elimination of water/concrete contact is of fundamental importance for the life of the structure.

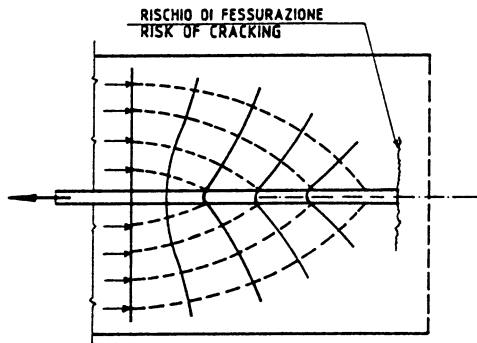


Fig. 26. Anchorage of a bar: stresses in concrete.

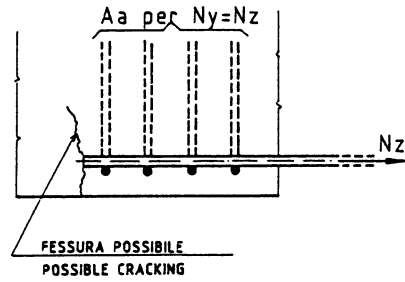


Fig. 27. Anchorage of a bar: necessity of transverse reinforcement.

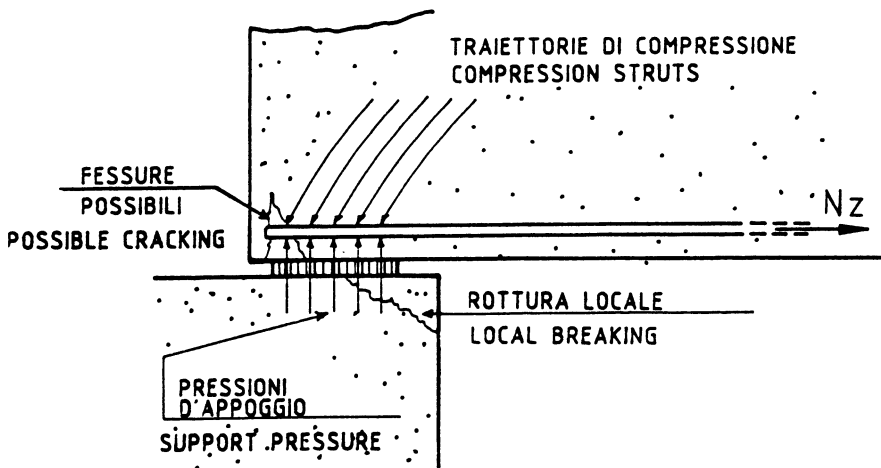


Fig. 28. Detail in the support.

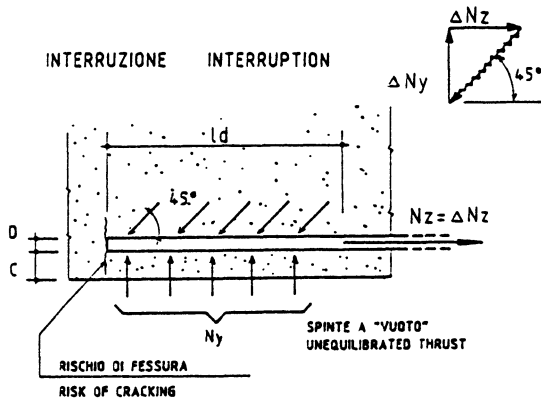


Fig. 29. Unequibrated thrust due to anchorage of a bar.

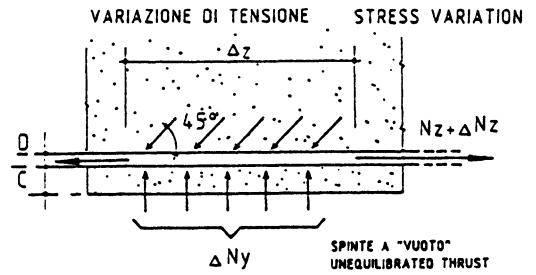


Fig. 30. Unequibrated thrust due to stress variation.

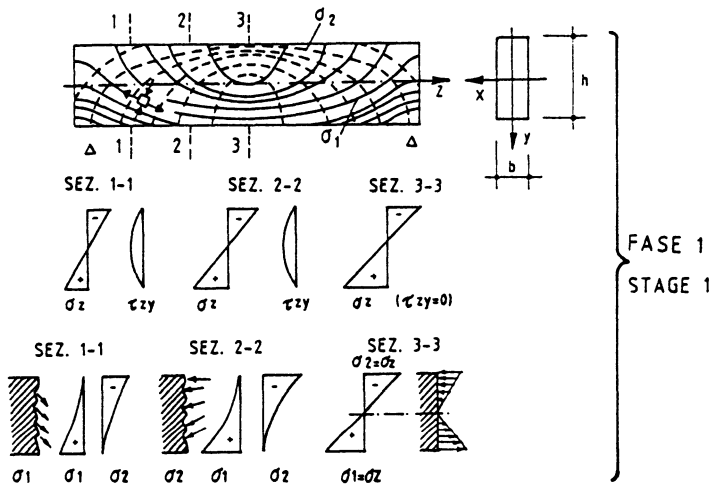


Fig. 31. Stress distribution in a simply supported beam uniformly loaded (stage I).

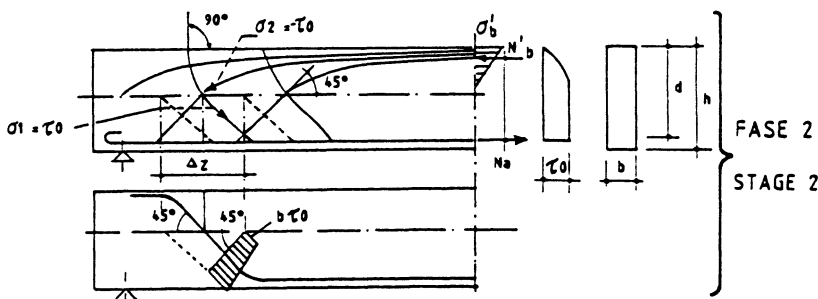


Fig. 32. Stress distribution in a simply supported beam uniformly loaded (stage II).

Washing (figure 33) and dripping (figures 34, 35) should therefore be avoided by an adequate design of water run-off (figures 36, 37, 38, 39) and of the water-seal joints (figure 40), with the possible replacement of deteriorating items (figures 41, 42) and, as mentioned, providing the possibility of inspecting the various non-visible parts.

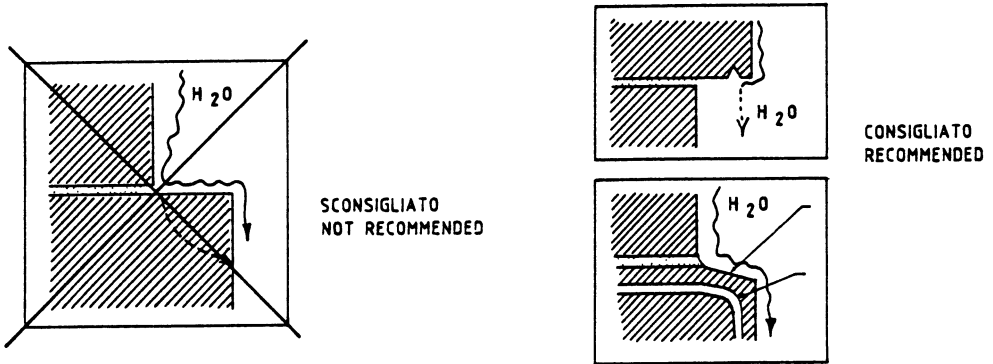


Fig. 33. Washing.

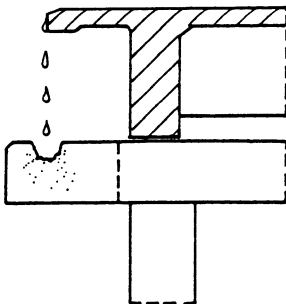


Fig. 34. Dripping.

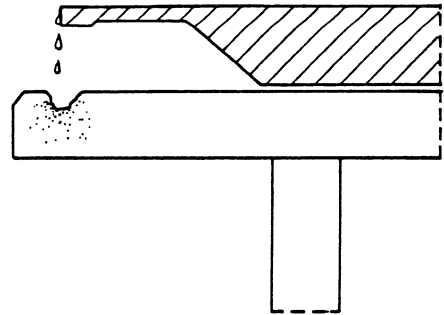


Fig. 35. Dripping.

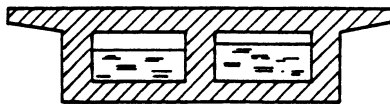


Fig. 36. Lack of water discharge.

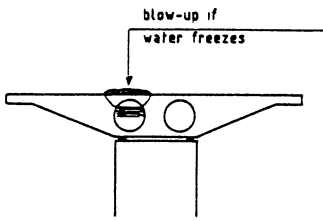


Fig. 37. Lack of water discharge.

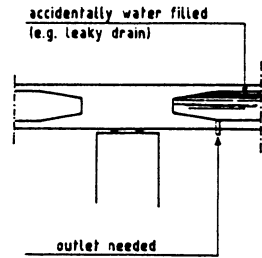


Fig. 38. Lack of water discharge.

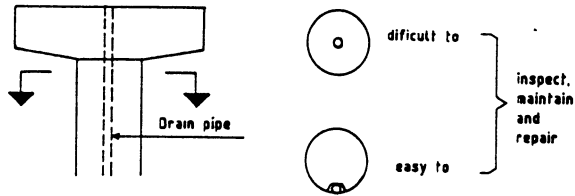


Fig. 39. Water discharge in a pile.

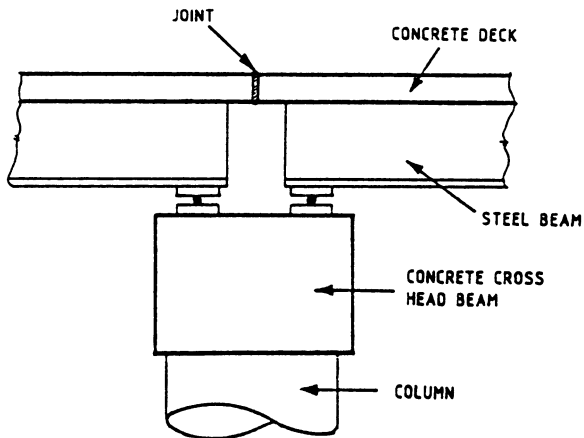


Fig. 40. Impermeable joint.

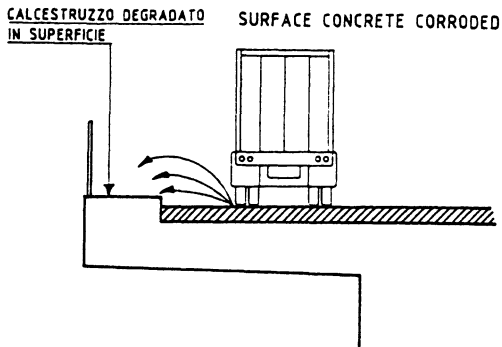


Fig. 41. Surfaces subject to corrosion.

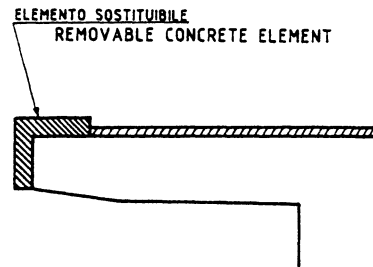


Fig. 42. Replaceability.

Finally one comment on construction techniques. The «disappointment» at the poor results obtained with integral prefabrication, particularly in view of the limited care devoted to the design and realisation of the joints, nowadays recommends that prefabrication should be limited to the longitudinal beams and that the slab should be cast in situ.

In case of prestressed reinforced concrete, the need to ensure reliable adhesion between the prestressed reinforcing and the concrete should be stressed, not only for static reasons but also in order to protect the cables.

In many instances the tendency to use pretensioning bars rather than post-tensioning cables can be seen. The more obvious reason is that since there is no absolute guarantee of perfect success of the injection, any corrosion of the cable is decidedly less dangerous in terms of safety.

Although this is certainly true, it nevertheless is likewise true that in order to avoid unnecessary penalties, the problem should be solved upstream with the necessary controls in order to guarantee quality.

An a priori disapproval of post-tensioning cable beams does not appear to be justifiable both in view of their greater rationality from the static aspect and efficiency of reinforcing, and because the problem of injection does not present particularly important difficulties when appropriate materials and techniques are used.

When, however, the technique of prestressing with external cables is adopted, this being particularly frequent in restoration work, it is preferable for the protection of the cables to be ensured by adopting reinforcing of the bonded type (bars pre-coated with resin or strands lubricated and coated with PVC) rather than recourse to a sprayed concrete coating (which tends to crack easily) or galvanisation (which brings in problems of fatigue strength and life). In addition the cables have to be fixed to the beams by suitable devices capable of taking up the offload thrusts exerted by the reinforcing where the reinforcing changes direction; finally it is appropriate for these devices to be provided with rather limited spacing (not more than ten metres) both in order to attenuate cable vibration and to constrain the cables to follow the deformation of the beams as much as possible.

Finally, again from the point of view of constructional realisation, it should be pointed out that progress in concrete technology currently makes it possible to carry out in situ and in any environmental condition, concrete pouring which is just as reliable as when effected in the prefabrication works, at the same time accelerating production cycles. This explains the

current widespread tendency towards structural solutions which are cast in situ which, no longer penalised by the quality of the concretes and construction times, present all the advantages of monolithic structures and uniformity in the rheological properties of the concrete.

These results are achieved by designing the concrete with the use of plasticizing, super plasticizing and hyperplasticizing additives by means of which it is possible to increase the mechanical strength even at low temperature, the impermeability, the dimensional stability and durability in the presence of high thermal variations.

The use of super-plasticizing additives furthermore may constitute a valid alternative to the heat treatment of concrete (steam curing). It is possible in fact to substitute a complete cycle (14 to 22 hours at 70°) with:

- simple addition of superplasticizer in non-winter months;
- addition of a superplasticizer integrated with a light thermal cycle (2-3 hours of steam) in the winter months, achieving in each case after 18-20 hours, the same mechanical strengths as can be achieved with a complete steam cycle.

Furthermore, the elimination of this latter treatment makes it possible to achieve further advantages such as:

- the elimination or reduced use of equipment necessary from the application of heat cycles;
- the increase in mechanical strength on long curing;
- the reduction of the time dependent phenomena (shrinkage and creep) and therefore better behaviour of the structures in service.

It is therefore possible to obtain reliably, in any climatic condition, concretes which have after 18-20 hours of curing, a strength equal to some 70% of the required characteristic, this latter characteristic being reached after three days of curing. It is obvious that this cannot fail to limit interest in the prefabricated structural solutions and should indeed direct the attention of the designer and builder towards solutions which are overall more correct provided that the rationality and constructive economy are based on industrialisation of the worksite and reliability of the materials used there, rather than on simple saving of time obtained by reducing work in situ to pure and simple assembly operations.

5. The quality assurance

In accordance the quality of concrete structures is currently entrusted, partly to the designer who has the responsibility for the design of the structures and partly to the site manager who will comply with the provisions of Law, checking compliance between the work and the design and also observance of the regulations relating to the implementation of the design and the quality of the materials used. In general, all this takes place with the supervision of the work and the carrying out of some tests on the concrete and on the steel and, furthermore, a static test in accordance with procedures largely laid down by Law.

Load testing is frequently carried out on completed structures. Obviously a control procedure of this type finished up by being somewhat reductive. Much more significant is the result obtained when the test is carried out during the course of the work. The concept of testing during the course of the work is adopted with ever greater frequency in order to give better guarantee for the Administrations, giving wide terms of reference to the technician who has to express himself with an official report and operate with real possibilities of action.

Control must therefore relate to the designing, realisation of the work but also the activity of the site Manager on behalf of the customer.

What is known as the final acceptance must provide for complete description and a geometrical survey of the work with an indication of any discrepancies from the design, errors in subverticality of the piles, cracks existing at the time of construction for reasons of various types, checking the state of deformation of the structural elements owing to the effect of permanent loads. In addition to the tests on the material, the test certificate must contain details relating to the tightening of the cables, the recorded loss, the injected operations.

This document is intended to assume the function of a real «record of birth» of the structure to which constant reference may be made in the inspection of the structure for further comparison with the initial situation when an anomalous fact is found during the life of the structure.

All this procedure appears to be somewhat limitative and, in fact, nowadays the concept of a quality of construction obtained by means of organised procedures which involve all persons participating in the realisation of the work.

According to that concept, quality is not considered as an abstract concept but a group of measurable parameters and not from a deterministic point of view but rather a probabilistic aspect. Quality assurance is a methodology which, according to systematic and planned actions, is capable of supplying an adequate degree of reliability that a structure and its parts will provide the required performance in the envisaged operating conditions. This is, as already mentioned, in relation to the following aspects:

- for the design, in order to reduce the probability of occurrence of human errors;
- in the realisation, in order to identify and correct insufficient results in the productive process;
- in maintenance, as a control that the safety measures remain unchanged over the course of time.

That methodology, which must involve the entire constructional process (promotion design, materials, realisation and use) is described in various manuals, e.g. «Quality Assurance Systems for Concrete Construction, published by the American Concrete Institute» (ACI, Journal 7/85) and also with regard to structures in reinforced concrete and prestressed reinforced concrete, in the more recent Eurocode 2, 1989 and CEB-FIP Model Code 1990.

A first aspect relates to the measures for the prevention of human errors which must be implemented.

In all the technical procedures of the construction process, e.g. adequate structural analysis; drawings, complete and easily readable lists and documents; application of systems not very sensitive to errors; procedure for construction of a simple type; structure easily accessible for inspection and maintenance etc.

In the organisation and constructional process management sector, for example: clear definition of the task and responsibilities of the employees and their co-operation.

In the field which influence human behaviour, e.g.: measures aimed at increasing the capacity and motivation of the employees and reducing the influence of intentional or unintentional disturbance factors; continuous construction and training etc.

According to the CEB-FIP Model Code 1990, a plan generated for quality assurance must concern the following aspects at least:

1. Organisation of the personnel at the various action levels (responsibility authority, inter-relationships) etc;
2. The way to achieve the required objectives;

3. Project control including procedures for variations during the course of the work;
4. Control of documents both in view of their reliability and the capability of tracing them at the appropriate places and within the required times;
5. Supplies relating to services, products acquired, sub-supplies;
6. Production and construction;
7. Data recording.

It should be pointed out that this latter aspect is of extreme importance for the purposes of future inspections for the programme relating to maintenance over the course of time. Measures to identify and correct insufficient results are implemented by quality control which is one of the aspects of quality guarantee.

The quality control consists of:

- acquiring information;
- formation of opinions based on information;
- decisions based on opinions.

This is explained by the following phases:

- individual checks;
- internal control;
- external control;
- compliance control.

The control is effected for various phases of the constructional process:

- the design;
- the materials and the components, the production and the construction;
- the complete structure;
- the realisation.

With regard to the design it is necessary to carry out:

- check of compliance between the specifications laid down and those effectively adopted;
- verification that the calculation models and the numerical models are correct;
- verification that the drawings and other design documents are in accordance with the calculations carried out and the required specification.

The calculation controls can be effected using various techniques:

- direct verification following the design step by step;
- parallel verification carrying out the calculations independently of the original design;
- cross verification when the results of the intermediate and final calculations are used at input data to demonstrate validity.

The design controls must check that:

- the calculation results have been correctly transferred;
- the documents are consistent one with the other;
- the drawings are clearly interpretable without ambiguity.

The control materials and the components provide for two phases:

- production control (production process);
- conformity control (identification, testing, compliance).

The production and construction control relate not only to the materials and components but also to:

- connections and assemblies;
- construction and erection procedures;
- structure geometry.

Table 4 summarizes the various aspects dealt with.

Control during the operation of the structure must provide for the following checks:

- condition of any protective systems;
- modifications in materials the originating and/or progression of faults;
- the local and general deformative condition.
- the deterioration of the materials and/or components which may reduce structural safety.

From this aspect, the responsibility for control is clearly that of the owner who must therefore acquired and record all information suitable for defining the programme for the necessary maintenance and servicing.

Tab. 4. Objects of material and component production and construction control (Eurocode 2).

Object	Control of materials and production	Control of construction and workmanship
Concrete	Constituent materials Composition, production fresh concrete hardened concrete	Transport, placing, compacting Curing Surface finish
Formwork and falsework	Materials	Robustness, erection, removal, cambering, deflections, ground supports, tightness, internal surface
Reinforcement	Specified material properties Surface conditions	Handling and storage, cutting, assembling, fixing, laps and joints, welding, placing Cover to reinforcement
Prestressing steel and devices	Specified material properties Surface condition Prestressing devices Straightness of tendons Grout	Handling and storage Cutting Placing Prestressing devices Tensioning Grouting
Structural members; Precast Units		Dimensional deviations Camber, deflection Compliance with the order

6. Theoretical measurement of durability

According to the proposals of the above mentioned working group of CTE for the MODEL CODE 1990, durability of a structure is verified when the required service life T_s does not exceed the conventional design life T_c . This is defined by means of a standard formula representing the various indexes as partial factors in multiplication terms:

$$T_s = T_c \prod_i \alpha_i$$

where:

- T_c the conventional limit of life assumes for example equal to 100 years;
 α_i partial factors which take account of the various aspects involved as follows:
 α_1 depending on the W/C ratio (table 5);
 α_2 depending on the workability of the mix (slump value) and the technique for the production of the concrete (table 6);
 α_3 depending on the class strength of the concrete (table 7);
 α_4 depending on the curing and environmental conditions (table 8);
 α_5 depending on the condition and type of surface finish (table 9);
 α_6 depending on the cover thickness (table 10);
 α_7 depending on the class of exposure of the environment not taken account elsewhere (table 11);
 α_8 depending on special situations relating to the structural typology (table 12).

Tab. 5. Water content factor α_1 , referred to water/cement ratio of concrete mix.

W/C	≤ 0.45	0.46-0.50	0.51-0.55	0.56-0.60	≥ 0.61
α_1	1.00	0.95	0.90	0.80	0.70

Tab. 6. Workability factor α_2 , related to the consistence of fresh concrete (slump test in cm) and to special techniques of production.

slump	humid ≤ 5	plastic 6+10	semifl. 11+15	fluid ≥ 16	extruded —
α_2	0.80	0.90	0.95	1.00	1.00

Tab. 7. Resistance factor α_3 , related to the strength class of concrete.

class	16	20	25	30	≥ 35
α_3	0.75	0.85	0.90	0.95	1.00

Tab. 8. Curing factor α_4 , related to the curing provisions and to the ambient conditions.

treatment	sheltered	ambient medium	severe
open	0.95	0.85	0.70
protected	1.00	0.95	0.85
heated	0.95	0.95	0.95

Tab. 9. Structure factor α_5 , referring to the service state of reinforced concrete elements and to their surface finishing.

service state	free-face	surface finishing current	special
Exposure classes 1 and 2a (covered construction)			
cracked	0.85	0.95	1.00
uncracked	0.95	1.00	1.00
compressed	1.00	1.00	1.00
Exposure classes 2a (uncovered) and 2b (covered)			
cracked	0.70	0.85	0.95
uncracked	0.35	0.95	1.00
compressed	0.95	1.00	1.00
Exposure classes 2b (uncovered), 3, 4 and 5			
cracked	0.55	0.75	0.90
uncracked	0.75	0.90	1.00
compressed	0.90	1.00	1.00

Tab. 10. Cover factor α_6 , referred to the increased design value c over the minimum concrete cover c adopted for reinforcement detailing.

$c - \bar{c}$ (mm)	0	5	≥ 10	plain concrete
α_6	0.90	0.95	1.00	1,00

Tab. 11. Exposure factor α_7 , due to environmental conditions effects not included in the other factors.

class	1	2	3	4	5a	5b	5c
α_7	1.00	0.95	0.90	0.85	0.80	0.70	0.60

Tab. 12. Special factor α_g , due to particular cases of structures:

- A – «any other case»;
- B – prestressed concrete elements with unbonded post-tensioned internal tendons with grease protection;
- C – prestressed concrete elements with bonded post-tensioned tendons in grouted internal ducts;
- D – prestressed concrete with bonded tendons having sheathed unbonded parts;
- E – elements with enclosed metallic devices protected by simple surface grouting.

situation	exposure classes		
	1, 2a (covered)	2a (uncovered), 2b (covered)	2b (uncovered), 3 - 4 - 5
A	1.00	1.00	1.00
B	0.90	0.85	0.75
C	0.95	0.90	0.80
D	0.95	0.90	0.80
E	1.00	0.95	0.85

A further step in this direction can be taken by considering two additional partial factors in relation to the quality assurance process and control activity during the lifetime:

α_9 depending on the quality control during the design and realisation;

α_{10} depending on the inspection and maintenance programme.

This is a first attempt at tackling this matter in an organised manner. Furthermore, beyond the numerical indications contained in the tables and which should in any event encounter adequate experimental reflection, a fundamental merit of the proposed method is the indication of a possible path to be followed.

7. Conclusion

To conclude we would like to cite several comments which Christian Menn elaborated at the XI congress of the FIP held at Hamburg in June 1990 on the topic «The place of durability in Bridge design concepts»: «In the construction of bridges it is not particularly difficult to increase the durability – Bridges, like every other structure are designed, in questions of detail too, according to certain basic fundamentals and such must be executed with care using the ideal materials. The damages that have considerably reduced the lifespan of the structure are in great part consequence of errors in construction, inappropriate use of materials, and lack of maintenance. These errors are now well known and it is the task of engineers to avoid them. Durability factors cannot be attained by employing new untried technologies that absolve the designer and the owner of their responsibility of a quality project control. Old errors must not be repeated for the sake of a reduction of construction costs and completion time». Also to mention is that «the engineers must also realise that an effective strategy to increase the durability must be based on analysis of detail and a rational application of material technology. We must finally free ourselves from exhaustive «exact» analysis that takes up a lot of energy and distracts us from the real problems. Durability can be guarantee with a minimum of calculation».

To confirm the above we can, without going back too far in time, observe the well thought out bridges of Robert Maillart, jobs well carried out, and for the main part in a decent state of repair almost fifty years on. When the project is well conceived and execution is correct, suffice a few protective measures combined with satisfactory checking procedure, consideration of the climate, effective inspection and maintenance to guarantee a lifespan respecting the expectations of those concerned.

References

1. Vitruvio: Trattato dell'Architettura.
2. Comportement en service, entretien et réparation, CEB Bulletin d'information n. 138 Août 1980.
3. Durability of concrete structures, State-of-the art report, CEB Bulletin d'information n. 148 Février 1982.
4. CEB-RILEM International workshop "Durability of concrete structures" Copenhagen, May 1983, Workshop Report, CEB Bulletin d'information n. 152, April 1984.
5. Comportement en service entretien et réparation, CEB Bulletin d'information n. 163, Mars 1984.
6. Draft to CEB-GUIDE to Durable concrete structures, CEB Bulletin d'information n. 166, May 1985.
7. Collegio degli Ingegneri di Milano: Le opere in calcestruzzo, Durabilità Protezione Ripristino, CLUP Milano 1986.
8. Giampiero Del Piero (a cura di): Manutenzione, Riparazione e Durabilità delle strutture in cemento armato, CISM Udine 1987, Collana di Ingegneria Strutturale n. 5.
9. Pietro Pedeferr (a cura di): Corrosione e Protezione delle strutture metalliche e in cemento armato negli ambienti naturali, CLUP Milano 1987.
10. M. Macori, G. Scaramuzzi, V. Alunno Rossetti, M. Mele, G. Fontanieri: Durabilità delle opere d'arte stradali, ANAS, Roma febbraio 1988.
11. Filippo Navarra, Le problematiche sul ripristino delle costruzioni monumentali, civili e industriali, Padova 4 marzo 1988.
12. Franco Massazza: Durabilità delle strutture in cemento armato, Il materiale, Padova 27 maggio 1988.
13. Enzo Siviero: Durabilità delle strutture in cemento armato - Il progetto, Padova 27 maggio 1988.
14. Peter Schiessl (a cura di): Corrosion of steel in concrete, Report of the Technical Committe 60 CSC RILEM, Chapman and Hall 1988.
15. Giampiero Tognon: Indirizzi tecnologici per la realizzazione di calcestruzzi e strutture durevoli, Cluva Editrice, Venezia 1989.
16. Elio Giangreco, Edoardo Cosenza: Durabilità dei materiali e delle strutture. Corso sul consolidamento statico delle strutture in c.a. e c.a.p., Treviso 6-10 marzo 1989.
17. Durable Concrete Structures, CEB Design Guide, CEB Bulletin d'information, n. 182 June 1989.
18. Giandomenico Toniolo (a cura di): Proposta del Gruppo di Lavoro CTE al Gruppo Italiano CEB sulla durabilità delle strutture in c.a. nell'ambito del CEB-FIP Model Code 1990, Milano 1989.

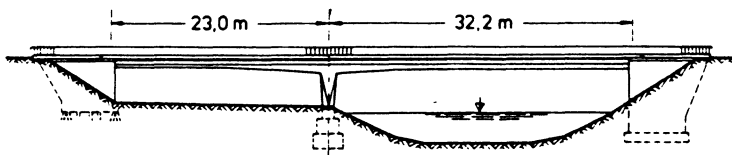
19. Commission of the European Communities: Industrial Processes Building and Civil Engineering. Eurocode n. 2, Design of Concrete Structures. Part. 1: General Rules and Rules for Buildings, October 1989.
20. Emanuele Filiberto Radogna: Seminario ANAS, Calcestruzzi e malte ad alta durabilità, Roma 30 ottobre 1989.
21. Antonio Migliacci: Seminario ANAS, Milano 13 novembre 1989.
22. Medardo Macori, Durabilità delle opere d'arte stradali: aspetti teorici, Padova 13 febbraio 1990.
23. CEB-FIP Model Code 1990, First Draft. CEB Bulletin d'information, n. 195-196, March 1990.
24. AA.VV.: Corrosione delle armature del calcestruzzo, INARCOS Ingegneri Architetti Costruttori, Bologna n. 508, aprile 1990.
25. G. Menditto, R. Capozucca, N.N. Cerri, L. Marini: Protective treatment of steel bars in reinforced concrete structures. Methods and experimental results. Steel '90, Advanced Technology Protective Treatment and Aesthetics, Genova 7-11 maggio 1990.
26. Luca Sanpaolesi: Protection of concrete reinforcements, the state of the art - Steel '90 Advanced Technology Protective Treatment and Aesthetics, Genova 7-11 maggio 1990.
27. Enzo Siviero: Durability of reinforced concrete structures and use of stainless steel, Steel '90 Advanced Technology Protective Treatment and Aesthetics, Genova 7-11 maggio 1990.
28. Federation Internationale de la Précontrainte. Proceedings XI Congress, FIP '90, Hamburg, June 4-9 1990.
29. De Luisa A., Cimolino M.: Analisi tecnico-economica delle opere d'arte stradali, esame di una direttrice tipo. Tesi di laurea IUAV, luglio 1990.

CRACKING DUE TO THERMAL EFFECTS ON BRIDGES

H. Falkner

Technical University of Braunschweig, Braunschweig, Germany

The thermal effects on bridges, with regard to the crack development and imposed deformations can, if not treated carefully by either computational and/or constructional means, result in considerable damage to the structure. Some bridges constructed in the last two or three decades show examples of this undesired effect, but nevertheless the few cases published are only the peak of an iceberg of numerous cases of damage, sometimes in connection with other effects, which can be linked to the thermal influence on bridges. See Fig. 1, which shows the damaged web of the Jagst Bridge in Germany.



Elevation of the Jagst Bridge

Crack pattern on the damaged web

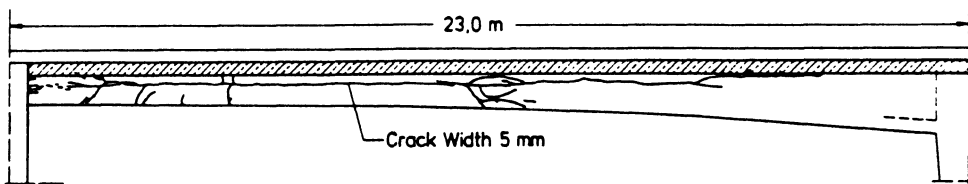


Fig. 1: Crack pattern of the damaged Jagst Bridge

A typical example for the crack development in prestressed concrete bridges is the cracking in the internal span(s) of three or more span bridge, or the crack development near the internal support of a two span bridge. In transverse direction the cracking in a box girder bridge due to thermal effects normally takes place in the web or the deck, especially when thin members are monolithically connected with thick construction members, see Fig. 2.

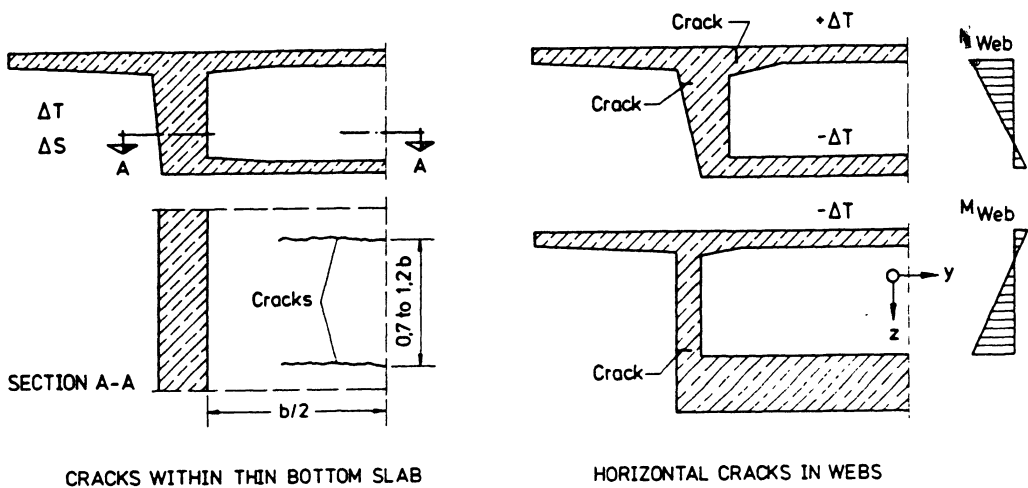
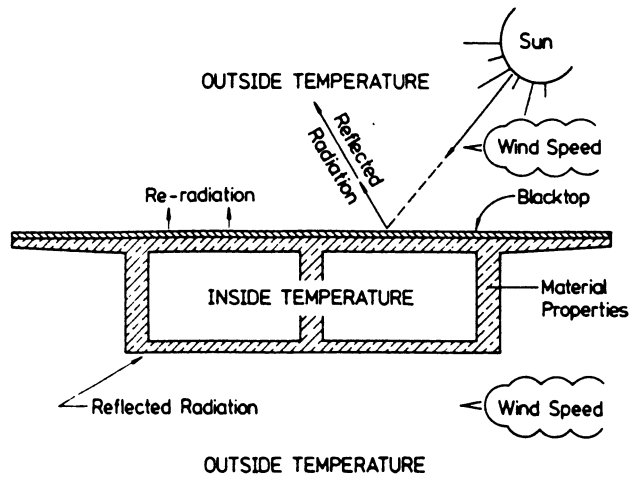


Fig. 2: Typical crack development in a box-girder bridge

Not only the temperature effects on the internal stresses of the whole structure have to be regarded. The total elongation of the structure caused by a constant temperature rise can cause the same damaging effects, e. g. roller bearings rolling from their base plates or additional imposed deformations by insufficiently dimensioned expansion joints.

In order to study the thermal effects on bridges, one has to define the many parameters affecting the temperature distribution within the cross section, such as:

- air temperature
- solar radiation
- re-radiation
- convection
- density
- conductivity
- specific heat
- time
- wind speed.



From this enumeration it becomes clear, that it is hardly possible to take all these factors specifically into account in a bridge design. The wind speed or the daily cycle of shade/air temperatures changes the temperature distribution within the cross-section, but for a bridge design it is essential to find a description for the maximum expected temperature gradient and the change of the average temperature with respect to the bridge temperature at the time of erection.

Different countries have developed more or less sophisticated approaches to this problem. These vary from a simple temperature gradient over the depth of the cross-section and a fixed value of the average temperature increase or decrease to a more sophisticated assessment of the temperature differential taking the depth of the cross-section and the thickness of the bridge deck, the blacktop-cover and even the colour of the bridge into account. The form of this temperature differential is either described by some form of a parabola or by polygonal lines. In some countries even the increase and decrease of the average temperature to be applied in the design can depend on the actual location of the structure. A comparison between different temperature differentials according to various sources is given in Fig. 3.

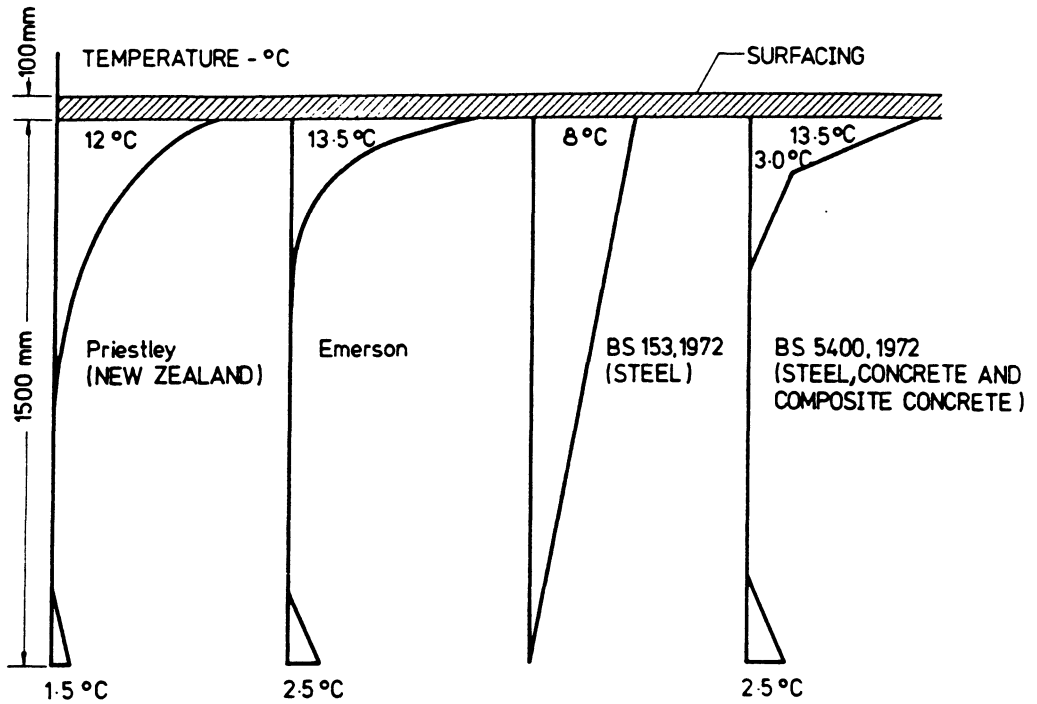


Fig. 3: Comparison of different temperature differentials for a 1500 mm depth of section according to various sources

These non-linear temperature differentials have been developed on the basis of extensive temperature measurements in different countries, and, if compared with each other, show more or less the same shape and temperature values. But one has to bear in mind, that the application of these non-linear temperature differentials are in contrast with the normal design assumption that the section remains plane after deformation. On account of this then only a part of the temperature field can be responsible for the sections deformation and it must be linear (see Fig. 4). The difference between the strains which could be caused by neglecting the influence of the sections fibres upon one another and the strains of a plane section due to temperature would have to be taken up by self-equilibrating stresses (see Fig. 4.). Therefore it is customary to determine a plane temperature field from these temperatur differentials for the computation of the restraining forces, whereas the self-equilibrating stresses will not produce any forces and moments within the cross-section.

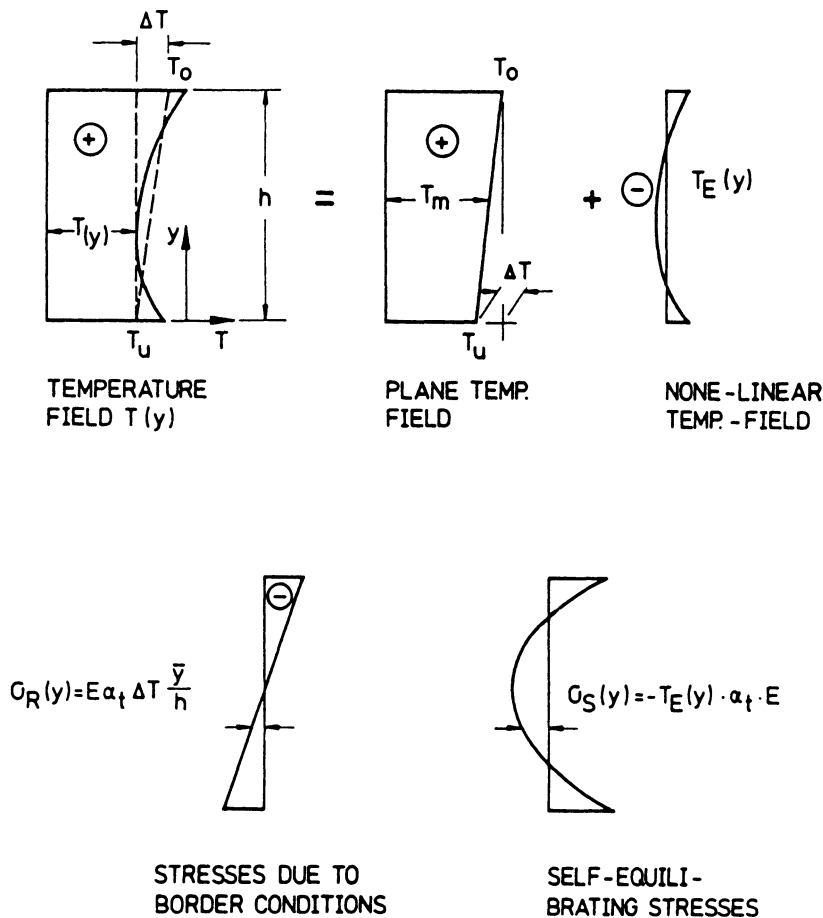


Fig. 4: Sectional stresses due to temperature; section remains plane

In this context the influence of the heat of hydration has to be mentioned. If during the hydration process the warm concrete is cooled down at the surface, it can lead to tensile stresses which in most cases exceed the tensile strength of the young concrete. In order to avoid these effects the control of the heat of hydration by choosing a low heat cement, proper detailing of the construction members and a curing concept is essential. If these precautions are taken, it is normally possible to reach a balance between the tensile stresses in the building member and the development of the tensile strength of the concrete in order to avoid this cause of damage (see Fig. 5).

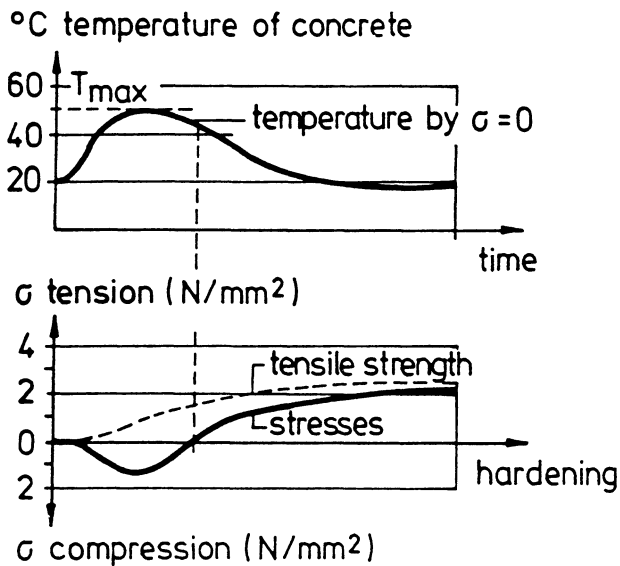


Fig. 5: Temperature and stress development in a cross-section during the hydration process

The result of a structural analysis will be as close to reality as one succeeds in taking the actual structural behaviour into account. If a simple linear analysis of the structural behaviour is carried out, an additional increase of the temperature differential will result in a proportional increase of the structural response. If the effect of creep is taken into account, one can already assume a slight decrease of the structural response, but some investigations show that the assumption of a reduction of approximately 10 % seems to be realistic. The most realistic results will be obtained if the non-linear behaviour of a reinforced or prestressed concrete structure is taken into account. Here, especially if the ultimate limit state of the structure is approached, an increase in the temperature differential will result only in a minor increase of the structural response, see Fig. 6.

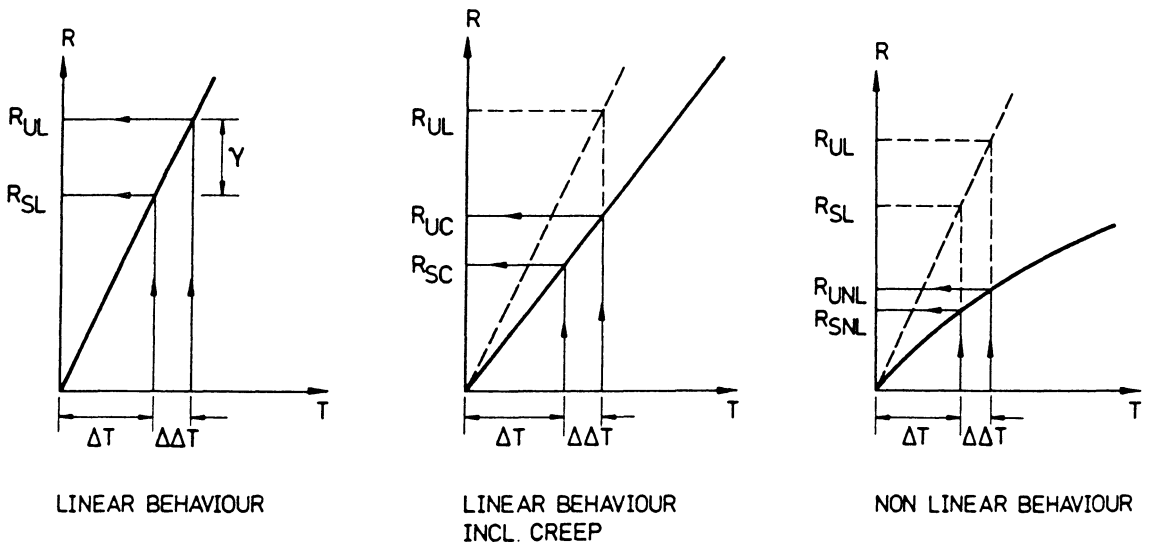


Fig. 6: Safety considerations for an additional temperature rise ΔT with regard to the structural response

This non-linear behaviour has to be considered within the scope of the structural safety considerations. Therefore the superposition of restraint- and load effects for the service limit and ultimate limit state is normally carried out with different partial safety factors, which, for the service limit state take account of the mostly still linear behaviour of the structure and the normally non-linear behaviour under ultimate load conditions, where, as mentioned already, an additional temperature gradient results only in a disproportional increase of the total structural response, as can be seen in Fig. 7.

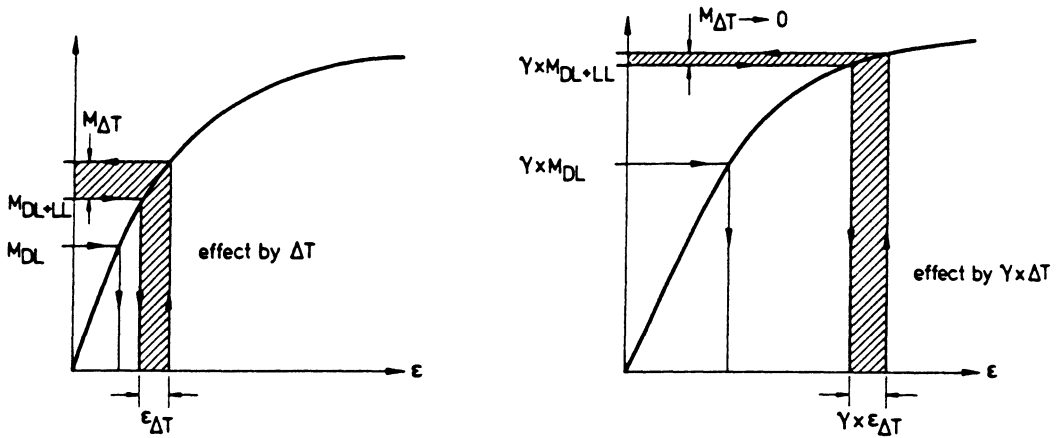


Fig. 7: Decrease of $M_{\Delta T}$ under load effects above service conditions for a ductile structure

This loss of stiffness, in a concrete structure due to the development of cracks until a stabilized crack pattern is reached (see Fig. 8), on one hand reduces the restraint forces on the other hand appears visible on the surface of the structure. Therefore the crack development, especially with regard to the allowable crack width and distance has to be carefully

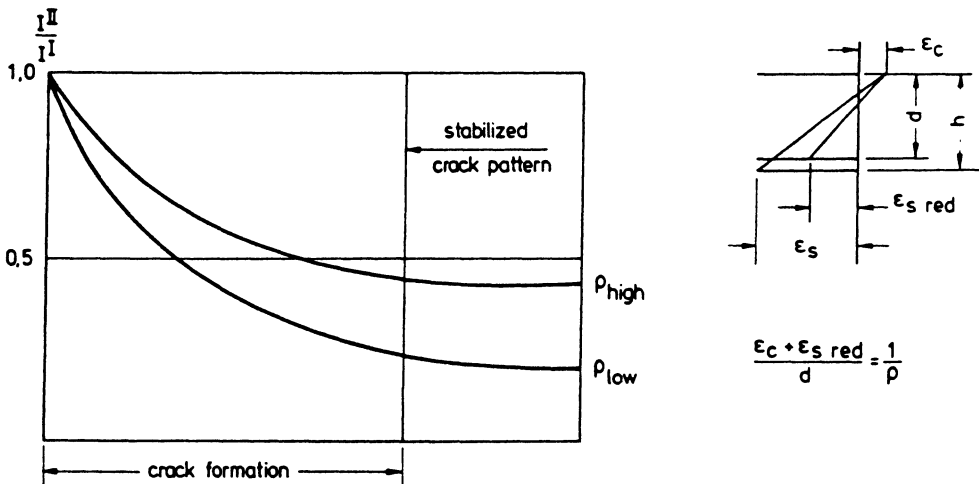


Fig. 8: Loss of stiffness due to cracking

controlled by the amount, placement and spacing of reinforcement in the endangered zones of the structure. This is especially important for reinforced and partially prestressed structures, where the development of cracks is already an explicit part of the design assumption. Moreover, it is not advisable to try to control the crack development in a fully prestressed structure by increasing the prestressing force, but it has proved to be more effective to control the crack development in the endangered zones by the placement of carefully designed constructive reinforcement. This is mainly due to the poor bond characteristics of grouted prestressing cables and the low ductility of the prestressing steel. Therefore a structure with a certain amount of reinforcement steel behaves, as far as the ductility and the crack development is concerned, far better than a fully prestressed structure, where the rupture of one prestressing cable may lead to a progressive failure of the other prestressing cables and can endanger the whole structure.

The horizontal displacements of the superstructure, due to a constant temperature rise, are normally defined by the distance from a resting point or the fixing point of a bridge (see Fig. 9). All these displacements have

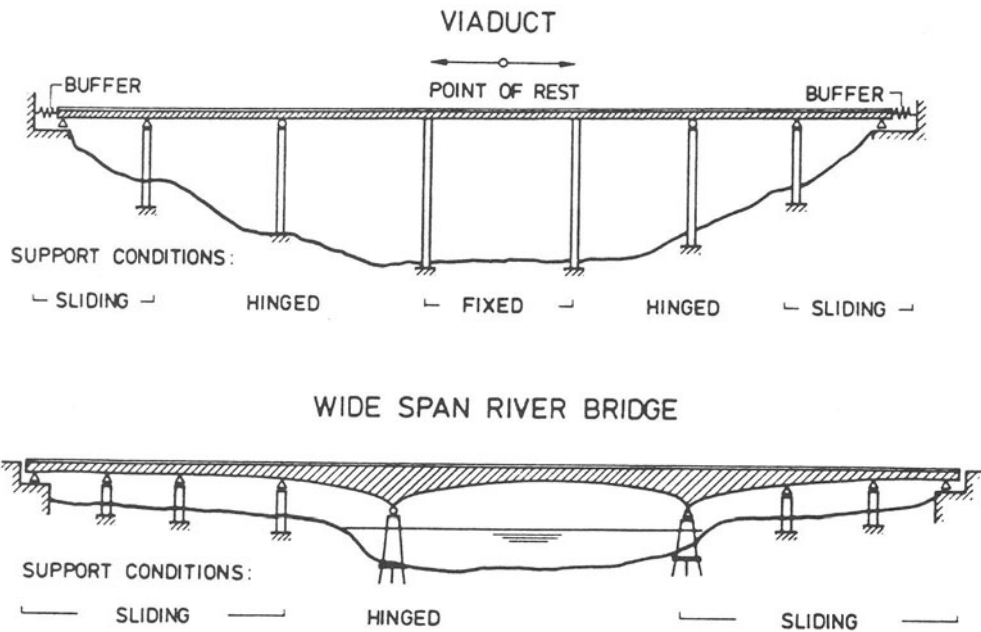


Fig. 9: Possible static systems for different types of bridges

normally to be absorbed at the end of the structure by appropriately dimensioned expansion joints, and therefore the arrangement of the bearings and the fixing point has to be carefully considered in order to minimize these movements. Sometimes, depending on the slenderness of the supporting columns, slide bearings can be omitted in the middle of a bridge near the resting point, if the restraint actions due to imposed deformations on the columns remain sufficiently small, which is normally not the case for systems with short, compact piers (see Fig. 9). Even the orientation of a bridge, i. e. the heating of only one webs depending on the height of the sun can induce horizontal deflections which have to be accounted for. For smaller bridge systems these deformations are normally negligible, but should at least be considered by constructional means for wide-span bridge systems.

An example for extensive temperature measurements carried out on a newly erected bridge is the Rhine Bridge Cologne-Deutz (see Fig. 10). Here, over a period of 2 1/2 years the bridge temperatures, deflections (vertical and horizontal) and movements of the bearings were measured. Examples of these measurements are given in Fig. 11 and 12.



Fig. 10: View of the Rhine Bridge Cologne-Deutz

MEASURING PROFILE 1 - ABUTEMENT "DEUTZ"

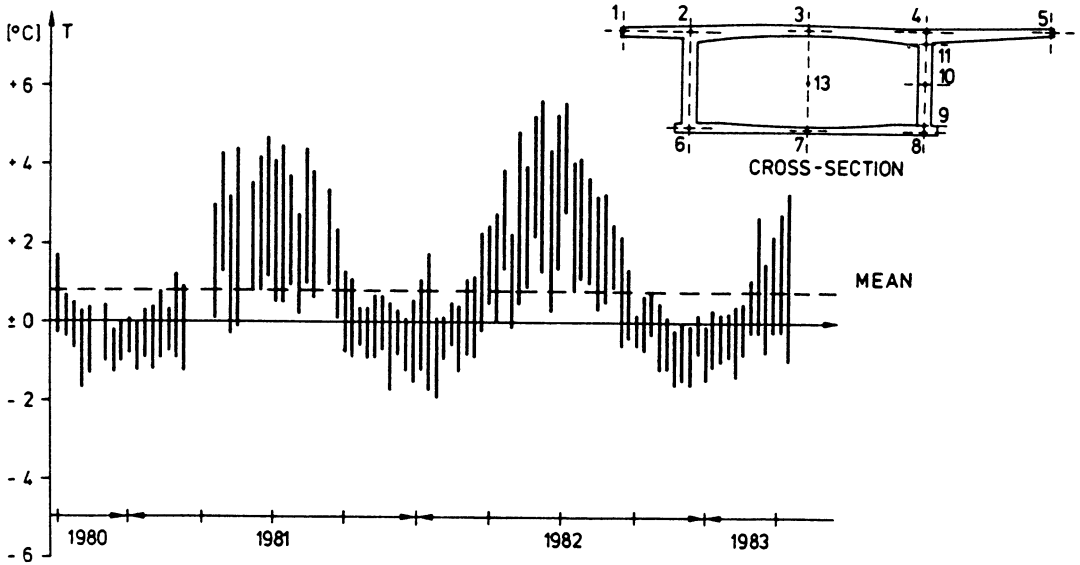


Fig. 11: Rhine Bridge Cologne-Deutz: Temperature difference between deck and bottom plate

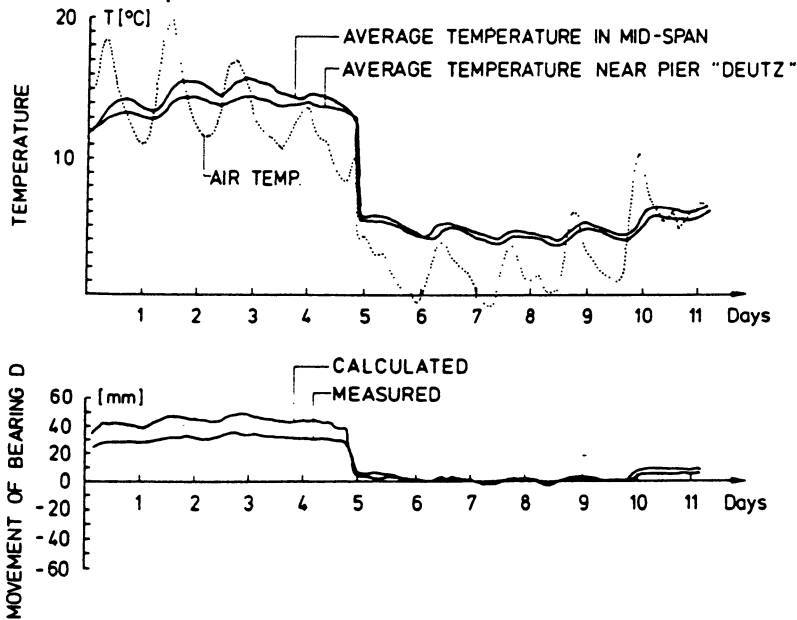


Fig. 12: Rhine Bridge Cologne-Deutz: Daily cycle of air temperature, average bridge temperature and movements of the bearing on abutement "Deutz"

Another example for a bridge, where, due to the actual shape of the bridge, the influence of the temperature had to be taken very explicitly into account is the Ganter Bridge on the Simplon Pass (see Fig. 13).



Fig. 13: The Ganter Bridge on the Simplon Pass road against the sunlight

Furthermore it has to be mentioned, that for very long multiple span bridge systems the arrangement of expansion joints at both ends, but with fairly large movements, or the arrangement of additional expansion joints over the intermediate supports with lower movements, i. e. for prefabricated bridge systems, can be considered. But as these additional expansion joints always provide weak points within the structural system, a policy of minimizing the possible expansion joints should be followed.

The development and introduction of structures with external prestress, either for new bridges or for the repair of insufficiently designed or dimensioned older structures, leads to one final point which should be mentioned. So far the temperature for the prestressing cables can be assumed to be the same than the temperature of the surrounding concrete. But with the arrangement of the prestressing cables on the outside of the webs, between the webs of a T-beam or inside a box-girder cross-section, temperature differences between the prestressing cables and the cross-

section can occur (see Fig. 14). For these cases one has to consider if these differences can lead to significant restraint actions and how they have to be taken into account in the actual design.

ADDITIONAL CONSIDERATIONS FOR EXTERNAL (OR INTERNAL) PRESTRESSING CABLES

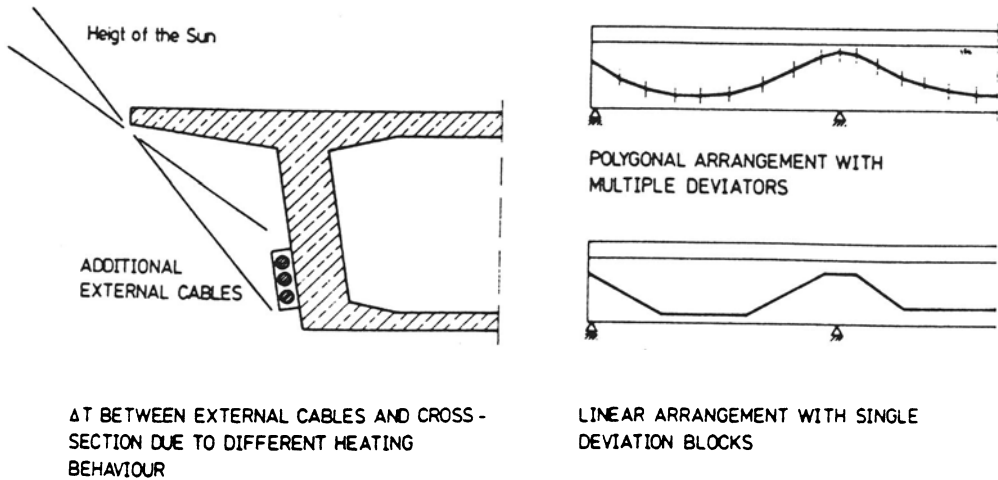


Fig. 14: Temperature considerations for bridges with external prestressing cables

STRUCTURAL EFFECTS OF TIME DEPENDENT BEHAVIOUR OF CONCRETE

F. Mola

Politechnic of Milan, Milan, Italy

ABSTRACT

The procedures for the linear viscoelastic analysis of R.C. and P.C. structures with particular emphasis to bridge-structures are presented. After a brief discussion of the fundamental properties of the constitutive linear viscoelastic law, based on the superposition integral, the two simplified models, namely the classical model and the Dischinger model are presented and widely discussed, stating their stress-strain laws of differential type. The numerical algorithms and the approximate techniques allowing to express in a convenient way for the applications the integral constitutive law are then introduced and a particular discussion is devoted to the algebraic approximate procedures. The homogeneous structures are then examined and the basic theorems of linear viscoelasticity are deduced, showing the results deriving from an exact analysis when loads or imposed deformations or additional restraints are applied to the structure. As regards the non homogeneous structures the very important class related to the homogeneous viscoelastic structures with elastic restraints is studied. With reference to bridge structures this class is very important as it includes the cable-stayed bridges or the bridge beams with P.C. or steel-concrete transverse sections. The problem of the evaluation the state of stress in cable stayed bridges or in P.C. or steel concrete sections is approached by means of the unified procedure, stated by the author and called Reduced Relaxation Function Method, which is here applied in its direct or inverse form.

The method is explained in its fundamental aspects and approximate solutions of particular simplicity are suggested, defining the upper and lower bounds for the exact solution. In a wide number of actual cases these bounds are very close so that the approximate solutions can be recommended for practical purposes. Three numerical examples, related to cable stayed bridges and to a steel-concrete section are then discussed showing the marked effects of creep on the long term state of stress of this kind of bridge structures.

1. INTRODUCTION

Concrete exhibits time dependent deformations of two kinds: the first referred as shrinkage deformation is independent from the state of stress and the second called creep deformation is produced by the applied sustained stresses. These deformations have generally a not negligible influence on the behaviour of R.C. and P.C. structures and in many cases their effects can be very marked so that they have interested in a large extent structural engineers, researchers and builders, as it is pointed out by the very high number of theoretical and experimental works published in the last three decades.

The shrinkage deformation, more exactly called drying shrinkage, produces a time-developing volumetric shrinking of the hardened concrete and is essentially a consequence of the loss of water from the concrete pores. As it is independent from the applied stress it can be considered as an imposed isotropic deformation having a prescribed time-law and can be easily taken into account in the structural analysis.

As regards R.C. and P.C. statically determinate structures composed by unidimensional elements as beams and columns, shrinkage produces self-equilibrated stresses in the transverse sections as it is elastically restrained by the reinforcement, while in redundant structures further stresses arise as a consequence of the reactions of the redundant restraints. In order to proceed to a correct structural analysis a reliable description of the shrinkage deformation, based on experimental data has to be performed. The results of several experimental works, [1], [2], [3], [4], show that the final values reached by the shrinkage deformation are quite large, approximately similar to the elastic ones produced by the service loads, so that internal or external restraints can generate high tensile stresses in the concrete and in R.C. structures the development of cracks which can cause an advanced structural degrading. In P.C. structures shrinkage reduces the prestressing force and the structural safety as regards the cracking limit state. When the reinforcement is not symmetrically disposed in the transverse sections or the shrinkage deformation depends in a non linear way from the geometrical coordinates, the restraining stresses produce flexural deformations which can generate not negligible transverse displacement as in the case of composite steel-concrete sections or P.C. beams

connected to R.C. slabs. The delayed deformations produced by applied sustained stresses, referred as creep, have structural effects quite different from those related to shrinkage as they modify the constitutive strain-stress law of the material. A reliable evaluation of the creep deformations can be made only by means of a wide experimental research from which one can define theoretical models able to correctly predict the structural behaviour and its evolution in time. Referring to the structural service phase, where the state of stress is not too high, about $\sigma_c \leq 0,4 f_c$, the experimental results, [5], [6], [7], [8], can be fitted by means of the theory of linear viscoelasticity, based on the principle of superposition and show that the final values of the creep deformations are of about (2+5) times larger than the elastic ones. According to linear theory of viscoelasticity the general formulation of the uniaxial strain-stress law of concrete drives to an integral form which is very complex from the computational point of view, so that simplified models or approximate formulations of the integral form are of great interest, in order to obtain approximate results sufficiently refined for practical purposes without performing cumbersome calculations. The creep structural effects are more important when the structure exhibits marked inhomogeneity or the sequence of the applied stresses or imposed deformations is complex. Generally creep produces variations of the state of stress in non homogeneous redundant structures, stress redistributions in the transverse sections of R.C. or P.C. members, reduction of the state of stress produced by imposed deformations, particularly the prestressing force, the arising of reactions in the restraints imposed after the application of the sustained actions. From these facts we can conclude that the creep effects are particularly important in the structures built in several phases, subjected to actions applied at different times and to the imposition of additional restraints during the construction process.

These aspects are typical of the present bridge structures for which the building procedure is of great importance in order to obtain efficient and economical constructions. The building procedures of modern bridge structures require the presence of parts made of concretes of different rheological properties, as it takes place in the P.C. beams connected to R.C. slabs or the presence of homogeneous parts subjected to loads and restraints applied at different times as in the segmental bridges or the presence of homogeneous viscoelastic parts and elastic parts as in the cable-stayed bridges.

At the present time a reliable analysis of a bridge structure requires the evaluation of the effects of the time dependent deformations of concrete, so that the Codes [9], [10], [11], [12] give the basic clauses for the time-dependent structural analysis, however, a comprehensive formulation of the problem and the explanation of the most convenient algorithms, either exact or approximate is not easily available in the technical literature, so that in the present chapter, after a brief introduction to the theory of linear viscoelasticity, the basic methods for the creep structural analysis will be discussed and a particular algorithm for the structural analysis of cable-stayed bridges

and P.C. or steel-concrete composite sections, called the Reduced Relaxation Function Method will be presented with some numerical applications.

2. FUNDAMENTALS OF THE THEORY OF LINEAR VISCOELASTICITY

Under a uniaxial stress $\sigma(t)$, applied from t_0 and in presence of an imposed deformation $\bar{\epsilon}(t)$, the concrete strain-stress law, according to the linear theory of viscoelasticity can be written in the subsequent form

$$\epsilon(t) = \int_0^t d\sigma(t') J(t, t') + \bar{\epsilon}(t) \tag{1}$$

where $J(t, t')$ is the creep function given by the expression

$$J(t, t') = \frac{1}{E(t')} (1 + \varphi(t, t')) \tag{2}$$

The creep function represents the strain produced by a unit stress applied from t' where $E(t')$, $\varphi(t, t')$ are respectively the elastic modulus and the creep coefficient. The time-development of the creep function is reported in fig. 1 and the following mathematical conditions hold:

$$J(t', t') = \frac{1}{E(t')} \quad , \quad \varphi(t', t') = 0$$

$$\frac{\partial J(t, t')}{\partial t} \geq 0 \tag{3}$$

$$\frac{\partial J(t, t')}{\partial t'} \leq 0$$

The integral in eq. (1) is the mathematical formulation of Mc Henry

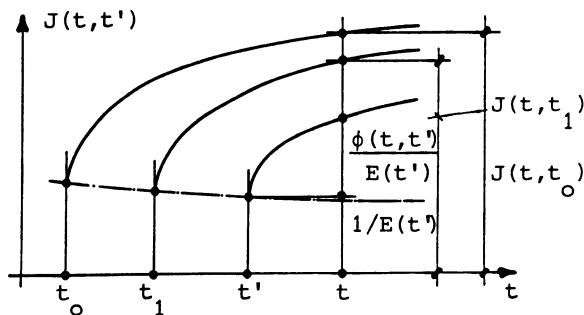


Fig.1 Creep function

Principle of Superposition, [13], [14], [15], and has to be considered as Stieltjes integral.

Denoting by $\Delta\sigma_i(t_i)$ the instantaneous stress increments arising at the times t_i , eq. (1), in its explicit form becomes

$$e(t) = \sigma(t_0) J(t, t_0) + \sum_i \Delta\sigma_i(t_i) J(t, t_i) + \int_{t_0}^t d\sigma(t') J(t, t') + \bar{e}(t) \quad (4)$$

represented in the particular case of step varying stress and $\bar{e}(t) = 0$ in fig. 2.

Eq. (1) allows to calculate the strain when the stress is known, while if the strain is known, it becomes a Volterra integral equation in the unknown stress $\sigma(t)$. In order to solve this equation, denoting by $R(t, t')$ the solving kernel of eq.(1), given by the solution of the

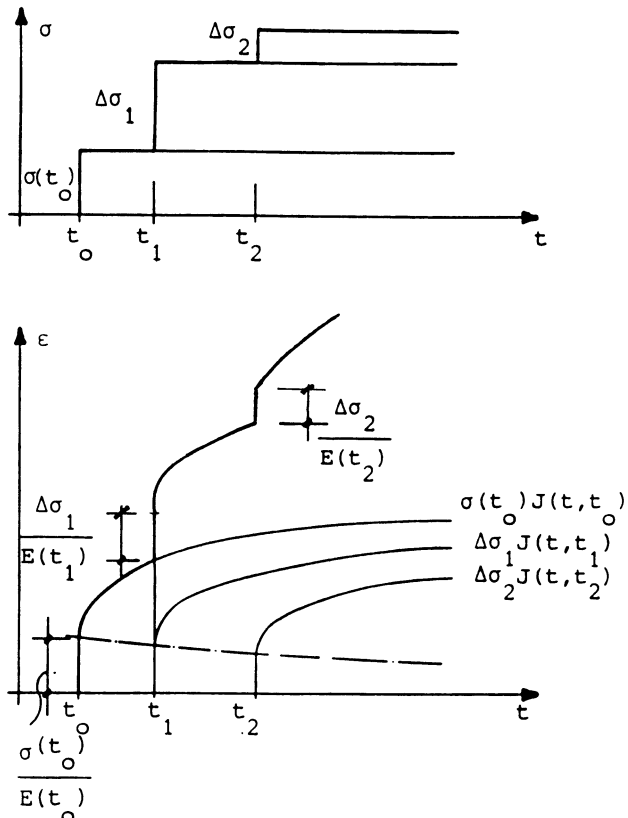


Fig.2 Application of the Superposition Principle for a step stress path

integral equation:

$$\int_0^t \frac{\partial R(\tilde{t}, t')}{\partial \tilde{t}} J(t, \tilde{t}) d\tilde{t} = 1 \quad (5)$$

the application of the Principle of superposition to eq. (1) gives:

$$\sigma(t) = \int_0^t d(e(t') - \bar{e}(t')) R(t, t') \quad (6)$$

The function $R(t, t')$ is called relaxation function and it satisfies to the conditions

$$R(t', t') = \frac{1}{J(t', t')} = E(t')$$

$$\frac{\partial R(t, t')}{\partial t} \leq 0 \quad (7)$$

$$\frac{\partial R(t, t')}{\partial t'} \geq 0$$

The time-development of the relaxation function is shown in fig. 3 and in fig. 4 is graphically represented the integral operation expressed by eq. (5).

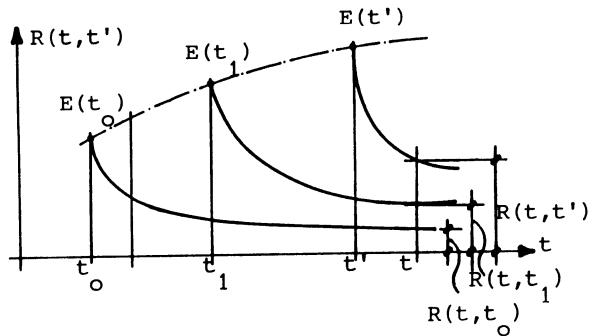


Fig.3 Relaxation function

The experimental data show that the analytical expression of the creep function $J(t, t')$ can be put in the form of sum or product of two functions depending only on the variable t' or on the argument $(t-t')$. According to the product form, adopted in [16], we have:

$$J(t, t') = \frac{1}{E(t')} [1 + f(t') g(t-t')] \quad (8)$$

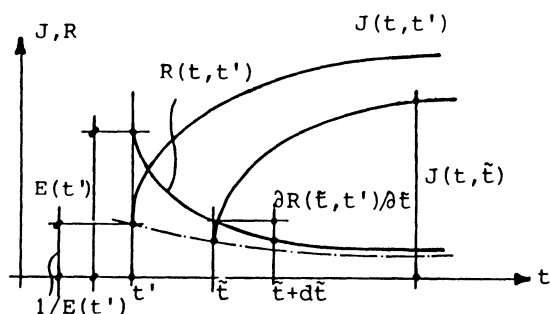


Fig. 4 Geometrical representation
of integral equation (5)

while the sum form, adopted in [17] gives

$$J(t, t') = \frac{1}{E(t')} + f_1(t-t') + [g(t) - g(t')] \quad (9)$$

Expressions (8), (9) assume that the creep deformation can be obtained combining the creep behaviour of two limiting models, namely the classical viscoelastic model and the rate of creep or Dischinger model. In the classical viscoelastic model we have $J(t, t') = J(t - t')$ while the Dischinger model assumes $J(t, t') = 1 / E(t') + [\varphi(t) - \varphi(t')] / \bar{E}_0$.

These two models allow to highly simplify the analysis of viscoelastic structures as they reduce the integral law (1) to differential laws which are much more simple and do not require significant computational efforts.

3. THE CLASSICAL VISCOELASTIC MODEL

From the rheological point of view this model derives from the assembly of elementary models, [18], [19], [20]. These models, sketched in fig. 5 are the elastic model, also called Hooke model and the viscous fluid model, named Newton model. The uniaxial constitutive law for the Hooke model is

$$\epsilon(t) = \frac{\sigma(t)}{E} \quad (10)$$

while for the Newton model we have

$$\dot{\epsilon}(t) = \frac{\sigma(t)}{\eta} \quad (11)$$

The elastic modulus E and the viscosity coefficient η are kept constant

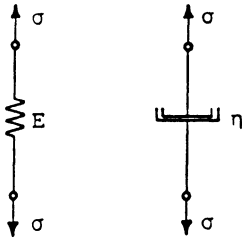


Fig.5 Hooke elastic model
and Newton viscous model

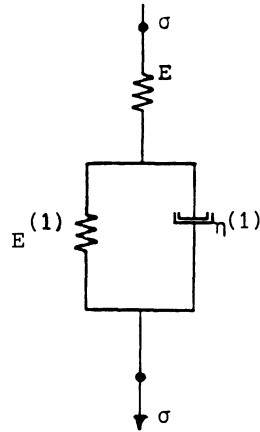


Fig.6 Classical viscoelastic standard model

in time and the dot represents the derivative with respect the time t (e.g. $\dot{\epsilon} = d\epsilon(t) / dt$).

Assembling these two elementary models we can build the composite model of fig. 6 named standard creep model, which is governed by the subsequent equilibrium and compatibility equations

$$\begin{aligned}\sigma_H &= \sigma \\ \sigma_H^{(1)} + \sigma_N^{(1)} &= \sigma \\ \epsilon_H + \epsilon_N^{(1)} + \bar{\epsilon} &= \epsilon\end{aligned}\tag{12}$$

The constitutive laws of the elementary models allow to write

$$\begin{aligned}\epsilon_H &= \frac{\sigma_H}{E} \\ \epsilon_H^{(1)} &= \frac{\sigma_H^{(1)}}{E^{(1)}} \\ \dot{\epsilon}_N^{(1)} &= \frac{\sigma_N^{(1)}}{\eta^{(1)}}\end{aligned}\tag{13}$$

so that combining eqs. (12) and (13) we obtain the following strain-stress law for the composite model

$$\dot{\epsilon} - \frac{\dot{\bar{\epsilon}}}{\tau^*} + \frac{(\epsilon - \bar{\epsilon})}{\tau^*} = \frac{\dot{\sigma}}{E} + \frac{\sigma}{E} (1 + \varphi_{\infty}) / \tau^*\tag{14}$$

where for the parameters τ^* , E , φ_{∞} the subsequent expressions hold

$$\tau^* = \frac{\eta^{(1)}}{E^{(1)}} = \text{retardation time} \quad (15)$$

Eq. (14) is a first order differential equation with constant

$$\varphi_{\infty} = \frac{\left(\frac{1}{E^{(1)}}\right)}{\left(\frac{1}{E}\right)} = \text{final value of the creep coefficient} \quad (16)$$

Eq. (14) is a first order differential equation with constant coefficients and it is equivalent to the integral law (1). As a particular case for $\bar{\epsilon} = 0$, $\sigma = 1$ applied in t' from eq. (14) we obtain the deformation $\epsilon(t)$ representing the creep function $J^{(c)}(t, t')$, which is the solution of the differential equation

$$\dot{\epsilon} + \frac{\epsilon}{\tau^*} = \frac{1}{E} (1 + \varphi_{\infty}) / \tau^* \quad (17)$$

with the initial condition

$$\epsilon(t') = \frac{1}{E} \quad (18)$$

From eqs. (17), (18) we easily obtain

$$\epsilon(t) = J^{(c)}(t, t') = \frac{1}{E} \left[1 + \varphi_{\infty} \left(1 - e^{-\frac{(t-t')}{\tau^*}} \right) \right] \quad (19)$$

In an analogous way for $\bar{\epsilon} = 0$, $\epsilon = 1$ applied in t' the stress $\sigma(t)$ coinciding with the relaxation function is obtained from eq. (14) solving the differential equation

$$\frac{1}{\tau^*} = \frac{\dot{\sigma}}{E} + \frac{\sigma}{E} (1 + \varphi_{\infty}) / \tau^* \quad (20)$$

with the initial condition

$$E = \sigma(t') \quad (21)$$

From eqs. (20) and (21) we have:

$$\sigma(t) = R^{(c)}(t, t') = \frac{E}{1 + \varphi_{\infty}} \left[1 + \varphi_{\infty} \cdot e^{-\frac{(1 + \varphi_{\infty})}{\tau^*} (t - t')} \right] \quad (22)$$

The expressions (19), (22) show that the creep function $J^{(c)}(t, t')$ and the relaxation function $R^{(c)}(t, t')$ depend from the argument $(t-t')$, so that, as it is pointed out in fig. 7, the $J^{(c)}$ and $R^{(c)}$ curves do not modify their configuration when t' varies, as they are simply rigidly translated along the t axis.

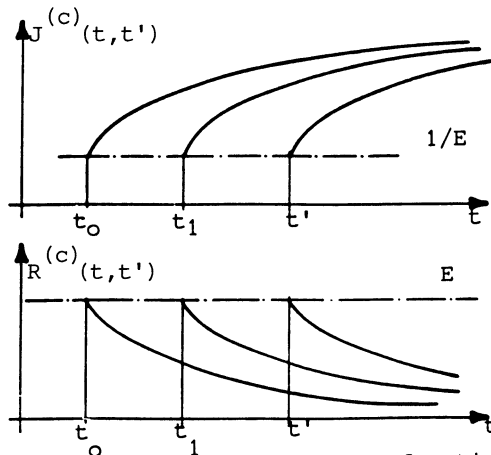


Fig.7 Creep and relaxation functions of the Classical standard model

From eq. (19), for the creep coefficient $\varphi^{(c)}(t, t')$ we derive the expression:

$$\varphi^{(c)}(t, t') = \varphi_{\infty} \left(1 - e^{-\frac{(t-t')}{\tau}} \right) \quad (23)$$

and eliminating the exponential in eqs. (23) and (22) we derive:

$$R^{(c)}(t, t') = \frac{E}{1 + \varphi_{\infty}} \left[1 + \varphi_{\infty} \left(1 - \frac{\varphi^{(c)}(t, t')}{\varphi_{\infty}} \right)^{(1 + \varphi_{\infty})} \right] \quad (24)$$

so that we can state that the relaxation function $R^{(c)}$ and the creep coefficient $\varphi^{(c)}$ are connected by a functional relation expressed in a finite form.

From eqs. (19), (23), (24) we derive the following asymptotic values for $J^{(c)}$, $\varphi^{(c)}$, $R^{(c)}$

$$\begin{aligned} \lim_{t \rightarrow \infty} J^{(c)}(t, t') &= \frac{(1 + \varphi_{\infty})}{E} \quad , \quad \forall t' \\ \lim_{t \rightarrow \infty} \varphi^{(c)}(t, t') &= \varphi_{\infty} \quad , \quad \forall t' \\ \lim_{t \rightarrow \infty} R^{(c)}(t, t') &= \frac{E}{(1 + \varphi_{\infty})} \quad , \quad \forall t' \end{aligned} \quad (25)$$

Eqs. (25) allow to proof a basic property of the classical model. Let us suppose that the model is subjected to a generic stress path, only satisfying the asymptotic condition

$$\lim_{t \rightarrow \infty} \sigma(t) = \sigma(\infty) < \infty \quad (26)$$

In this case, evaluating the limit for $t \rightarrow \infty$ of eq. (1) and remembering the first of eqs. (25) we obtain

$$e(\infty) = \sigma(t_0) \frac{(1+\varphi_\infty)}{E} + \frac{(1+\varphi_\infty)}{E} \int_{t_0}^t d\sigma(t') = \sigma(\infty) \frac{(1+\varphi_\infty)}{E} + \bar{e}(\infty) \quad (27)$$

From eq. (27) we can observe that for $t \rightarrow \infty$ the constitutive law of the classical model coincides with that of an elastic model with a modified elastic modulus E' given by the expression

$$E' = \frac{E}{(1+\varphi_\infty)} \quad (28)$$

so that inserting eq. (28) in eq. (27) we obtain the following strain-stress elastic law

$$e(\infty) = \frac{\sigma(\infty)}{E'} + \bar{e}(\infty) \quad (29)$$

4. THE DISCHINGER MODEL

This model also derives from the assembly of elementary models for which the parameters are supposed varying in time. For the Dischinger model, sketched in fig. 8 and discussed in [21], [22], [23] the equilibrium and compatibility equations become

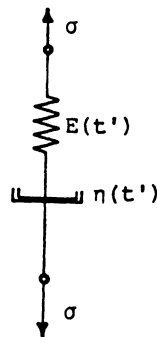


Fig.8 Dischinger model

$$\begin{aligned}
 \sigma_H &= \sigma \\
 \sigma_N &= \sigma \\
 e_H + e_N + \bar{e} &= e
 \end{aligned}
 \tag{30}$$

and the constitutive laws for the elementary models give

$$\begin{aligned}
 \dot{e}_H &= \frac{\dot{\sigma}_H}{E(t)} \\
 \dot{e}_N &= \frac{\sigma_N}{\eta(t)}
 \end{aligned}
 \tag{31}$$

Combining eqs. (30) and (31) we obtain the following constitutive law for the Dischinger model

$$\dot{e} - \frac{\dot{e}}{\bar{e}} = \frac{\dot{\sigma}}{E(t)} + \frac{\sigma}{\eta(t)}
 \tag{32}$$

From eq. (32) for $\bar{e} = 0$, $\sigma = 1$ applied in t' we can reach the creep function $J^{(D)}(t, t')$ by solving the differential equation

$$\dot{e} = \frac{1}{\eta(t)}
 \tag{33}$$

with the initial condition

$$e(t') = \frac{1}{E(t')}
 \tag{34}$$

Integrating eq. (33) we have

$$e(t) = J^{(D)}(t, t') = \frac{1}{E(t')} + \frac{\varphi^{(D)}(t) - \varphi^{(D)}(t')}{E_{28}}
 \tag{35}$$

where

$$\varphi^{(D)}(t) = \int \frac{1}{\eta(t')} dt' \cdot E_{28}
 \tag{36}$$

and E_{28} is the elastic modulus calculated for $t' = 28$ days. The choice of E_{28} is merely conventional, as we can refer the creep coefficient expressed by eq. (36) to the actual modulus $E(t')$ or to any other value of the elastic modulus. However the modulus E_{28} is universally accepted as it was for the first time adopted by Dischinger.

From eq. (32), putting $\bar{e} = 0$, $\sigma = 1$ applied in t' we obtain the relaxation function $R^{(D)}(t, t')$ by solving the differential equation

$$\frac{\dot{\sigma}(t)}{E(t)} + \frac{\sigma(t)}{\eta(t)} = 0
 \tag{37}$$

with the initial condition

$$\sigma(t') = E(t') \tag{38}$$

From eq. (37), (38) we obtain

$$R(t) = R^{(D)}(t, t') = E(t') e^{-\int_{t'}^t \frac{E(\xi)}{\eta(\xi)} d\xi} \tag{39}$$

As a particular case, if we assume a constant elastic modulus $E(t') = E_{28}$, from eq. (39), remembering eqs. (36), (35) we derive

$$R^{(D)}(t, t') = E_{28} e^{-\Phi^{(D)}(t, t')} \tag{40}$$

so that, as for the classical viscoelastic model we can state a finite functional relation between the relaxation function and the creep coefficient. The analysis of the curves $J^{(D)}(t, t')$ and $R^{(D)}(t, t')$, reported in fig. 9 and fig. 10 shows that the creep function curves are parallel

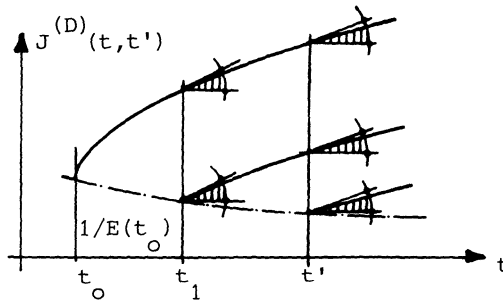


Fig.9 Creep function of the Dischinger model

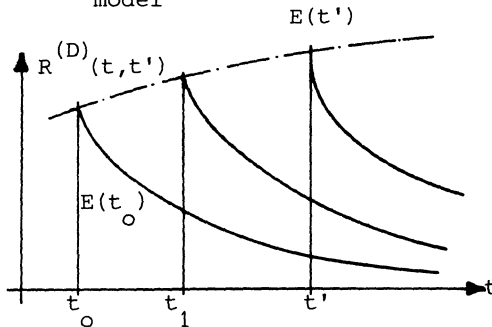


Fig.10 Relaxation function of the Dischinger model

when t' varies as the derivative $\frac{\partial J^{(D)}(t, t')}{\partial t}$ does not depend from t' while this property is no longer valid for the relaxation curves as it can be easily argued considering eq. (39).

5. ACTUAL VISCOELASTIC MODELS

The experimental results show that the creep behaviour of concrete lies at the interior of the two limiting behaviours related to the classic viscoelastic model and the Dischinger model. This fact is clearly pointed out by the results that we obtain by applying the stress path reported in fig. 11, coinciding, according to the principle of superposition, with the two superimposed stress paths of fig. 12. Applying eqs. (19) and (35), assuming that for the two limiting models

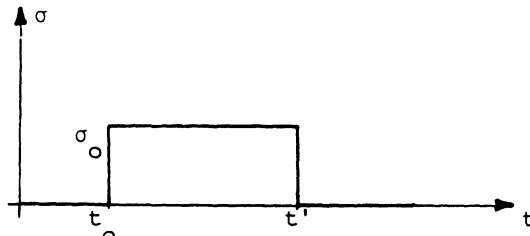


Fig.11 Loading-unloading process

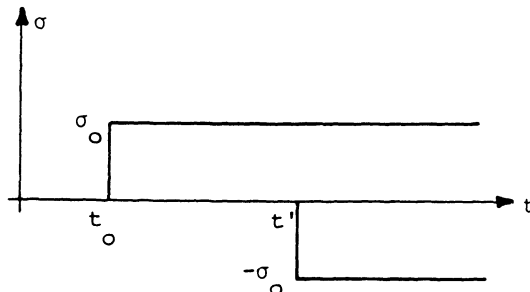


Fig.12 Application of Superposition Principle

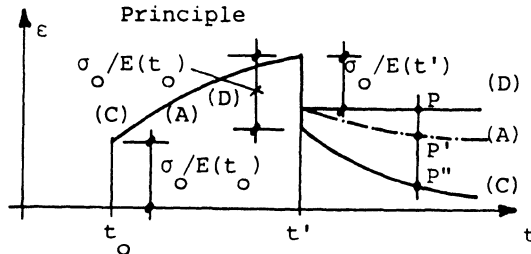


Fig.13 Deformations according to Classical Model(C), Actual Model(A) and Dischinger Model(D)

the final values of the creep coefficient are the same and the elastic modulus of the classical model coincides with the initial elastic modulus $E(t_0)$ of the Dischinger model, we obtain the strain paths indicated respectively by (C) and (D).

As reported in fig. 13, these paths are the same for $t_0 < t \leq t'$ but are quite different when the stress is removed.

According to eq. (35) for the Dischinger model the creep deformation developed for $t < t'$ is kept constant while the classical model releases this deformation and returns to its initial state, when $t \rightarrow \infty$, as stated by eq. (19).

The actual behaviour is intermediate, so that, as indicated by line (A) the creep deformation is only partially released. Defining delayed elasticity the released part of the creep deformation, represented in fig. 13 by the segments PP' or PP'' we can state that for the classical model the final value of the delayed elasticity coincides with the creep deformation stored in the interval $t_0 \leq t \leq t'$ so that the model can be defined as totally reversible. For the Dischinger model the delayed elasticity is zero and consequently this model is totally irreversible, while in the actual model the delayed elasticity is present but is smaller than that of the classical model so that it can be defined as partially reversible.

It is important to observe that if we as a first approximation assume an elastic modulus constant in time, comparing eqs. (24) and (40) it is easy to state that when the creep coefficient and the elastic modulus are the same, the subsequent inequality holds

$$R^{(D)}(t, t') \leq R^{(C)}(t, t') \quad (41)$$

where the equality is valid only for $t = t'$.

According to eqs. (19) (23) (35) and to fig. 13 we derive

$$J^{(D)}(t, t') < J^{(A)}(t, t') < J^{(C)}(t, t') \quad (42)$$

so that, from eq. (5), remembering the second of eqs. (3) and (7) we can prove that

$$R^{(D)}(t, t') < R^{(A)}(t, t') < R^{(C)}(t, t') \quad (43)$$

Eqs. (42) and (43) represent two basic properties of the linear viscoelastic theory as they allow, when the difference between the results derived from the two limiting models is sufficiently small, to assume these results as the solution of the viscoelastic problem avoiding the use of the complex integral constitutive law (1) which is substituted by the simpler differential formulations given by eqs. (14) or (32).

6. THE MODELS CEB MC78 AND ACI COMMITTEE 209

The Models CEB MC78, [9], [24], [25] and ACI [16], derive from the fitting of experimental data, adopting analytical formulations similar to those expressed by eqs. (8), (9). The CEB MC78 Model assumes for the creep function the sum form:

$$J(t, t') = \frac{1}{E(t')} + \frac{1}{E_{28}} [\beta_a(t') + \varphi_d \beta_d(t-t') + \varphi_f(\beta_f(t) - \beta_f(t'))] \quad (44)$$

with

$$\begin{aligned} E(t') &= 11875 \sqrt[3]{f_{cm}(t')} \quad (\text{MPa}) \\ f_{cm}(t') &= f_{cm}(\infty) \left[\frac{t'}{t' + 47} \right]^{\frac{1}{2,45}} \\ \beta_a(t') &= 0,8 \left[1 - \left(\frac{t'}{t' + 47} \right)^{\frac{1}{2,45}} \right] \\ \beta_d(t-t') &= \left[\frac{t-t'}{t-t'+328} \right]^{\frac{1}{4,2}} \\ \beta_f(t) &= \left[\frac{t}{t + K_1(h_o)} \right]^{K_2(h_o)} \quad (45) \\ K_1(h_o) &= \exp \left[\frac{5,02}{h_o} + \ln(6,95 \cdot h_o^{1,25}) \right] \\ K_2(h_o) &= \exp \left[0,00144 h_o - \frac{1,1}{h_o} - \ln(1,005 h_o^{0,2954}) \right] \\ \varphi_d &= 0,4 \\ \varphi_f &= (4,45 - 0,035\xi) \cdot \exp \left[4,4 \cdot 10^{-5} \cdot h_o - \frac{0,357}{h_o} - \ln \left(\frac{h_o^{0,1667}}{2,6} \right) \right] \end{aligned}$$

In the previous relationships $f_{cm}(t')$ is the cylindrical compressive strength at time t' , $h_o = \frac{2A}{P}$ (cm) is the notional thickness of the

member measured by the ratio between the area of the transverse section and one half of the perimeter directly exposed to the exterior where the relative humidity is $\xi\%$ and times t, t' are expressed in days.

For the shrinkage deformation $\epsilon_{sh}(t)$ the following expression are assumed

$$\epsilon_{sh}(t) = \epsilon_{s1} \cdot \epsilon_{s2} \cdot \beta_s(t) \quad (46)$$

with

$$\beta_s(t) = \left[\frac{t}{t + K_3(h_o)} \right]^{K_4(h_o)}$$

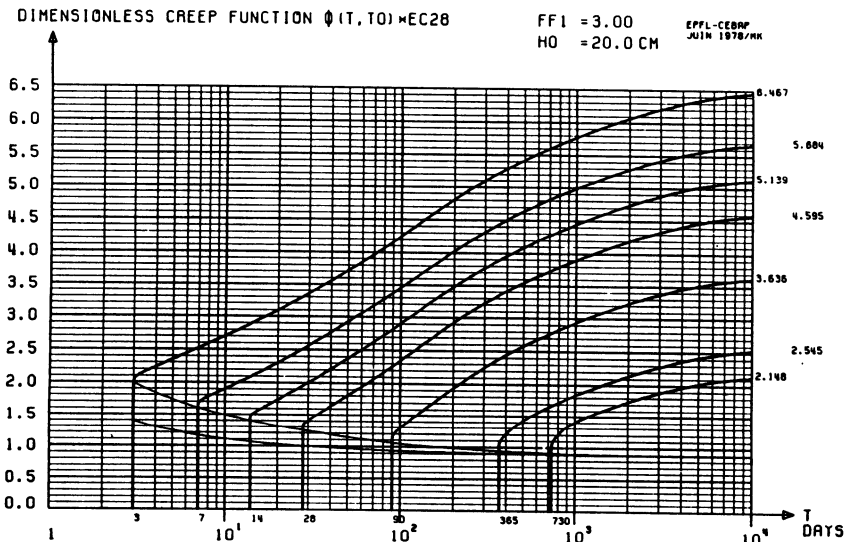
$$K_3(h_o) = 11,8 \cdot h_o + 16$$

$$K_4(h_o) = \exp \left[-0,00257 h_o + \frac{0,32}{h_o} + \ln(0,22 \cdot h_o^{0,4}) \right] \quad (47)$$

$$\epsilon_{s1} = (0,000775 \xi^3 - 0,1565 \xi^2 + 11,0325 \xi - 303,25) \cdot 10^{-5}$$

$$\epsilon_{s2} = \exp \left[0,00174 h_o - \frac{0,32}{h_o} - \ln \left(\frac{h_o^{0,25}}{1,9} \right) \right]$$

In fig. 14, and in fig. 15, taken from Ref. [24], are reported for various t' the creep function J and the relaxation function R obtained solving by means of the algorithm exposed in the next section the



integral equation (5). In fig. 16 is reported, from Ref. [24] the time development function $\beta_s(t)$ and in fig. 17 the function $\epsilon_{s2}(h_o)$ related to the shrinkage deformation.

The ACI Model adopts the product form assuming

$$J(t-t') = \frac{1}{E(t')} \left[1 + 1,25 \varphi(\infty, 7) t'^{-0,118} \frac{(t-t')^{0,6}}{10 + (t-t')^{0,6}} \right] \quad (48)$$

$$E(t') = E_{28} \left(\frac{t'}{4 + 0,85 t'} \right)^{\frac{1}{2}} \quad (49)$$

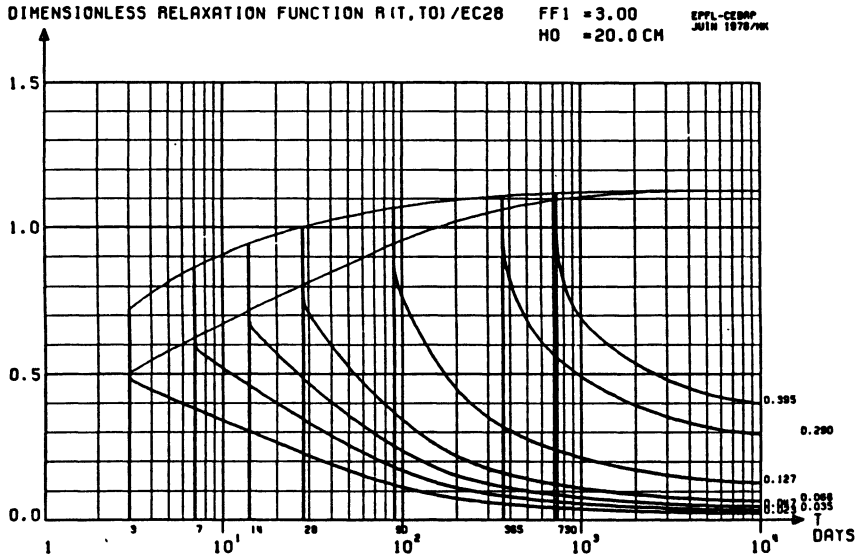


Fig.15 Relaxation function of CEBMC78 Model (from Ref.24)

where the coefficient $\varphi(\infty, 7)$ represents the final value of the creep coefficient for $t' = 7$ days dependent from the environmental conditions and from the notional thickness h_0 , as explained in detail in [26]. For the shrinkage deformation the following expression is proposed:

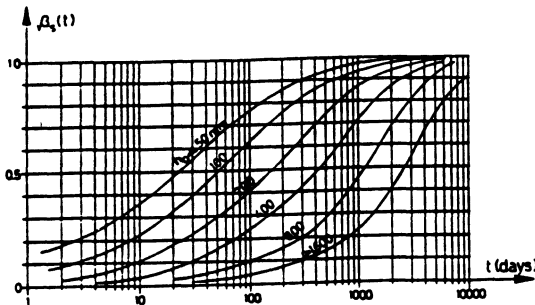


Fig.16 Time-development of shrinkage according CEBMC78 (from Ref.24)

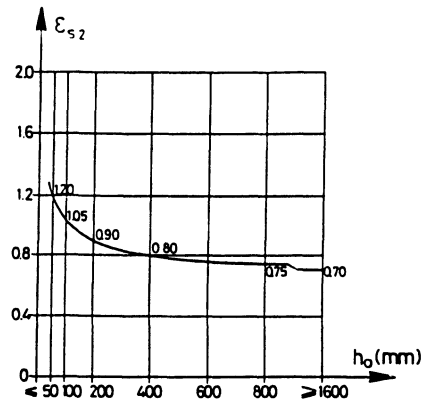


Fig.17 Influence of notional thickness on shrinkage (from Ref.24)

$$e_{sh}(t) = \frac{t}{35+t} e_{sh}(\infty) \tag{50}$$

Expression (50) is valid for $t \geq 7$ days and the procedures to calculate the final value $e_{sh}(\infty)$, depending from the relative humidity and from the notional thickness are widely discussed in [26].

In Table 1 some values of the nondimensional creep function $E_{28}J(t,t')$ and

t-t' (days)	t'=7 days		t'=28 days		t'=90 days	
	$E_{28}J(t,t')$	$\frac{e_{sh}(t) - e_{sh}(t')}{e_{sh}(\infty)}$	$E_{28}J(t,t')$	$\frac{e_{sh}(t) - e_{sh}(t')}{e_{sh}(\infty)}$	$E_{28}J(t,t')$	$\frac{e_{sh}(t) - e_{sh}(t')}{e_{sh}(\infty)}$
10	2.627	0.160	1.721	0.076	1.456	0.021
10 ²	4.019	0.587	2.552	0.341	2.104	0.124
10 ³	5.078	0.800	3.185	0.523	2.598	0.249
10 ⁴	5.496	0.830	3.434	0.552	2.791	0.276
∞	5.686	0.833	3.531	0.556	2.842	0.280

Table 1. Creep function and shrinkage function according to ACI Model.

of the shrinkage function $(e_{sh}(t) - e_{sh}(t'))/e_{sh}(\infty)$ are reported for various initial times t' .

7. METHODS OF STRUCTURAL ANALYSIS

The constitutive general laws (1), (6) are the basic relationships for the analysis of redundant viscoelastic structures.

The structural analysis can be performed using the Forces Method or the Displacements Method and in both cases it drives to the solution of systems of Volterra integral equations. For this reason it is of great importance to state analytical procedures for the solution of the Volterra integral equations in order to express the constitutive law (1) in a form directly applicable to the structural analysis.

When general viscoelastic models like the CEB MC78 model or the ACI model are adopted, eq. (1) has to be solved only by means of numerical algorithms or, in an approximate way, following feasible simplifying hypotheses while if we assume the classical or the Dischinger model we can transform eq. (1) into the differential equations (14) or (32) which can be integrated without great difficulties.

In order to proceed to the solution of eq. (1) in the unknown stress $\sigma(t)$, we observe that in the integral appearing in eq. (1) both σ and J are depending from t' and it is possible, as indicated in fig.18. to express $J(t, t')$ as a function of $\sigma(t')$, so that the deformation $\epsilon(t_k)$ -

$\bar{\epsilon}(t_k)$, comparing in eq. (1) and calculated at time $t = t_k$, is measured by the area of the zone (O ABC) limited by the curve $J(t,\sigma)$. Subdividing

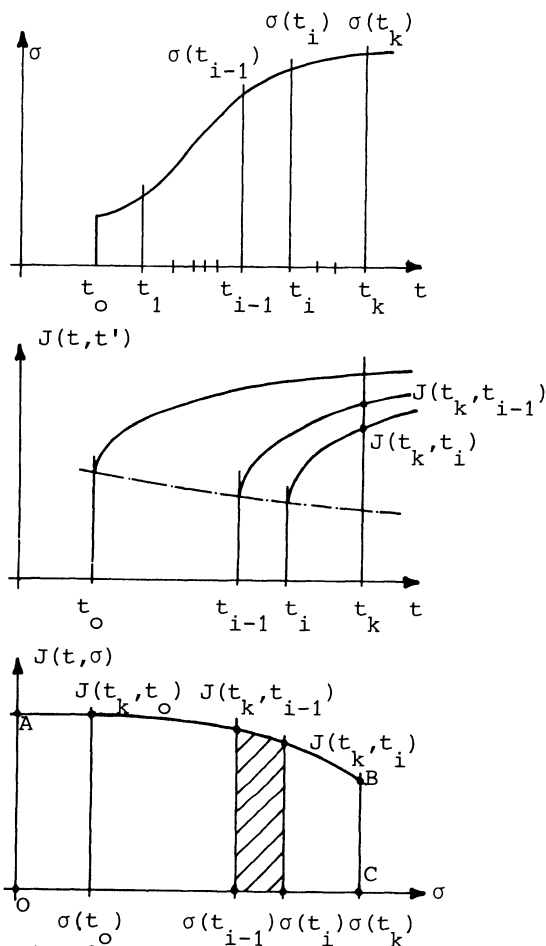


Fig.18 Iterative procedure for the solution of the Volterra integral equation

the interval $(t_k - t_0)$ in an adequate number of sub-intervals $(t_i - t_{i-1})$, $i = 1, 2, \dots, k$, the application of the rule of trapezia to the integral comparing in eq. (1) gives the subsequent expression for the evaluation of the area (O ABC)

$$e(t_k) - \bar{e}(t_k) = \frac{1}{2} \sum_{i=1}^k (\sigma(t_i) - \sigma(t_{i-1})) [J(t_k, t_i) + J(t_k, t_{i-1}) + \sigma(t_0) J(t_k, t_0)] \quad (51)$$

Introducing the quantities

$$E'(t_k) = \left[\frac{1}{2} [J(t_k, t_k) + J(t_k, t_{k-1})] \right]^{-1}$$

$$e^o(t_k) = \frac{1}{2} \sum_{i=1}^k [\beta_i \sigma(t_i) - \sigma(t_{i-1})] \cdot [J(t_k, t_i) + J(t_k, t_{i-1}) + \sigma(t_0) J(t_k, t_0)]$$

with

$$\begin{aligned}\beta_i &= 1 & i < k \\ \beta_i &= 0 & i = k\end{aligned}$$

eq. (51) becomes

$$\epsilon(t_k) = \frac{\sigma(t_k)}{E'(t_k)} + \bar{\epsilon}(t_k) + \epsilon^o(t_k) \quad (53)$$

Eq. (53) is an algebraic form relating the stress $\sigma(t_k)$, the corresponding total deformation $\epsilon(t_k)$, and the deformation $\epsilon^o(t_k)$ depending from the stress path from time t_0 to time t_{k-1} , so that this algorithm has to be applied in an iterative way implementing it on an efficient computer program which allows to calculate for each step time $(t_k - t_{k-1})$, the related stress $\sigma(t_k)$.

The results obtained from eq. (53) are very good if the width of the sub-interval $(t_i - t_{i-1})$ is conveniently chosen. As the creep function is rapidly increasing when t_i is near to t_0 a feasible subdivision of the interval $(t_k - t_0)$ can be obtained using the following formula, proposed in [24]

$$\begin{aligned}\frac{t_k - t_0}{t_{k-1} - t_0} &= 1,15 \quad , \quad k \geq 2 \\ t_k - t_0 &= 0,05 \text{ days} \quad , \quad k = 1\end{aligned} \quad (54)$$

According to eq. (54), the accuracy of the results is very high but it is necessary to perform about 90 steps in order to cover a maximum time - interval of about 10^4 days, so that this method, when the structure is quite complex becomes very expensive from the computational point of view.

A remarkable simplification of the problem is achieved expressing the area (O ABC) in the subsequent way

$$\epsilon(t) - \bar{\epsilon}(t) = \frac{\sigma(t_0)}{E(t_0)} (1 + \varphi(t, t_0)) + \frac{\sigma(t) - \sigma(t_0)}{E(t_0)} (1 + \chi(t, t_0) \varphi(t, t_0)) \quad (55)$$

substituting to the area (O' A' B C) the equivalent rectangle (O' A'' B'' C), having height $O'A'' = \frac{1 + \chi \varphi}{E(t_0)}$ and making the dashed areas of fig. 19

equal.

Eq. (55) can be used only if the function $\chi(t, t_0)$ is known and at this scope in [27] [28] this function is calculated in an approximate way

supposing that the deformation $\epsilon(t) - \bar{\epsilon}(t)$ can be expressed in the following way:

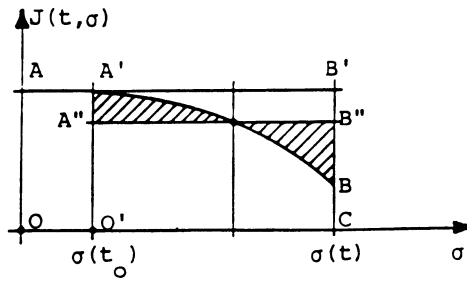


Fig.19 Solution of the Volterra integral equation, algebraic method

$$\epsilon(t) - \bar{\epsilon}(t) = a + b\varphi \quad (56)$$

with a, b arbitrary constants.

In this particular case, from eqs. (1), (6) we immediately obtain

$$\sigma(t) = a R(t, t_0) + b E(t_0) \left(1 - \frac{R(t, t_0)}{E(t_0)} \right) \quad (57)$$

$$\sigma(t_0) = a E(t_0)$$

and substituting eqs. (56), (57) in eq. (55) we derive

$$\chi(t, t_0) = \frac{1}{1 - \frac{R(t, t_0)}{E(t_0)}} - \frac{1}{\varphi(t, t_0)} \quad (58)$$

Eqs. (56), (57) allows to exactly solve the integral equation (1) in a wide number of cases, as the related χ function is independent from the values assumed by the two constants a and b . From a general point of view, the deformations or the stresses existing in the actual structures cannot be expressed by eqs. (56), (57), but their development in time as regards the most important practical situations, is not quite different from that presented in eqs. (56), (57), so the algebraic form (55) can be adopted in order to achieve a sufficiently approximate solution of the Volterra integral equation (1). For practical applications eq. (55) can be put in the following compact form

$$\epsilon(t) = \frac{\sigma(t)}{E'(t)} + \bar{\epsilon}(t) + \epsilon^0(t) \quad (59)$$

with

$$E'(t) = \frac{E(t_0)}{1 + \chi \phi} \tag{60}$$

$$\epsilon^o(t) = \frac{\sigma(t_0)}{E(t_0)} \frac{\phi(1-\chi)}{1 + \chi \phi}$$

so that we obtain an algebraic form which can be directly applied at time t without performing intermediate steps. The method based on eq. (59) is called Age Adjusted Effective Modulus Method (AAEMM) and can be further on simplified, remembering the following inequality, which has been proven in [29]

$$\frac{1}{2} \left[1 + \frac{\partial E(t)}{\partial t} \Big|_{t=t_0} / \frac{\partial R(t, t_0)}{\partial t} \Big|_{t=t_0} \right] \leq \chi \leq 1 \tag{61}$$

If we take the maximum value of χ , namely $\chi = 1$, eq. (59) becomes

$$\epsilon(t) = \frac{\sigma(t)}{E^*(t)} + \bar{\epsilon}(t) \tag{62}$$

$$E^*(t) = \frac{E(t_0)}{1 + \phi}$$

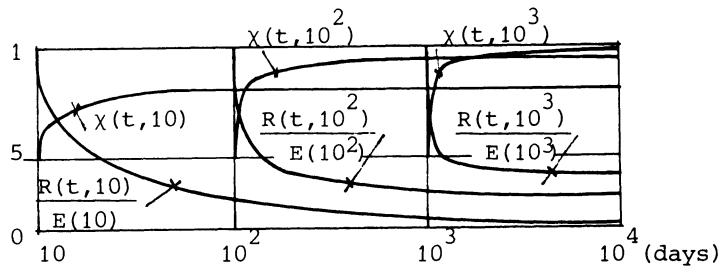


Fig.20a $\chi(t, t')$ and relaxation function according to ACI Model

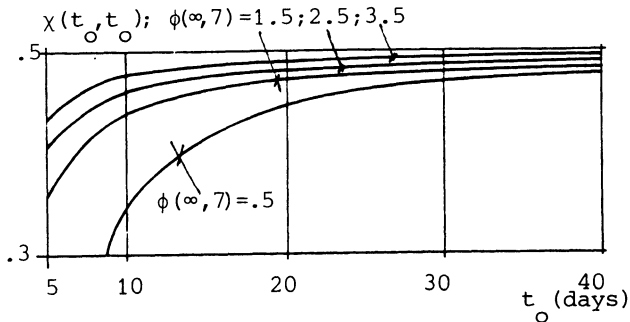


Fig.20b Variation of χ with the initial time t_0 , according to ACI model for mass concrete

and we obtain in this particular case the so called Effective Modulus Method, by which, as pointed out in fig. 19 the area (O'A'BC) is approximated by means of the external rectangle (O'A'B'C). A better approximation can be achieved observing the diagrams of fig. 20a, where, if we consider times t sufficiently greater than t_0 and times t' not too much elevated, the constant value $\chi = 0,8$ can be conveniently chosen, avoiding the evaluation of the relaxation function and consequently the solution of the Volterra integral equation (5). It is interesting to observe that in fig. 20a the initial value of χ for $t = t_0$ is always 0,5. This is a consequence of a property of the ACI Model for which

$$\frac{\partial R(t, t_0)}{\partial t} \Big|_{t=t_0} = -\infty, \text{ as we can see from fig. 20a. For this the second}$$

term in the brackets of eq. (61) vanishes and the minimum value of χ becomes 0,5 independently from t_0 . If we assume a creep model for which

$$\frac{\partial R(t, t_0)}{\partial t} \Big|_{t=t_0} \text{ is finite, as it is the case of the ACI Model for massive}$$

concrete, [16], the minimum value of χ is lesser than 0,5 as indicated in fig. 20b. Values of $\chi(t_0, t_0)$ near to 0,5 require times of application of the loads greater than 40+50 days.

8. LINEAR CREEP STRUCTURAL ANALYSIS OF R.C. AND P.C. STRUCTURES

Strictly speaking, R.C. and P.C. structures cannot be considered rheologically homogeneous as they are made of a viscoelastic material and of an elastic material. However, when we evaluate the internal actions in redundant structures, the determination of the reactions of the hyperstatic restraints is quite independent from the presence of the reinforcement as its amount is very small compared to the volume of concrete. For this reason, as a first approximation, we can formulate the hypothesis that as regards the structural analysis the R.C. or P.C. structures can be considered as homogeneous.

This hypothesis is no longer valid in evaluating the state of stress in the transverse sections as in this case the reinforcement has a marked influence in reducing the creep deformations of concrete, so that the sectional analysis of R.C. and P.C. structures has to be performed taking into account their non homogeneity. In the same way the structural non homogeneity has to be considered when the structure consists of viscoelastic homogeneous parts and elastic parts as it is the case of the modern cable-stayed bridges.

From the structural analysis point of view the transverse sections of R.C. or P.C. structures and the cable-stayed bridges can be considered as homogeneous structures with elastic restraints, represented in the first case by the reinforcing bars and in the second by the stays.

According to these considerations from a general point of view we can individualize two basic types of structures, namely the homogeneous structures and the homogeneous structures with elastic restraints. For

the homogeneous structures it is possible to state fundamental theorems which allow to perform the structural analysis by using the results obtained from the elastic analysis at the initial time while for the homogeneous structures with elastic restraints it is convenient to proceed on the basis of a general analytical algorithm, named Reduced Relaxation Function Method [30], [31] [32], in its direct or inverse form, allowing to study complex structures by means of a set of independent integral equations which can be solved adopting one of the methods previously explained.

8.1 Homogeneous Structures

Let us consider a homogeneous structure, subjected to loads and imposed deformations. Denoting respectively by $\sigma_e^{(p)}$, $e_e^{(p)}$, $\sigma_e^{(g)}$, $e_e^{(g)}$ the stresses and the deformations produced by the loads (p) and the imposed deformations (g), calculated considering a pure elastic structural behaviour with a reference modulus E_0 , let us assume that in the viscoelastic structure the stresses σ and the deformations e can be expressed as following

$$\sigma = \sigma_e^{(p)} + \sigma_e^{(g)} \frac{R(t, t_0)}{E_0} \quad (63)$$

$$e - \bar{e} = e_e^{(p)} (1 + \varphi(t, t_0)) + e_e^{(g)}$$

The stresses expressed by the first of eqs. (63) are equilibrated and the strains deriving from the second of eqs. (63) satisfy the compatibility conditions as they are linear combinations of elastic solutions and furthermore, introducing the first of eqs. (63) in eq. (1) and remembering eq. (5) we obtain the second of eqs. (63) so that these equations satisfy the constitutive law of the material. As a consequence of the uniqueness of the solution of the linear viscoelastic problem, eqs. (63) represent the required solution and clearly show that the knowledge of the elastic solutions is sufficient for the calculation of the strain and stresses in the homogeneous viscoelastic structure. Eqs. (63) express in a compact form the two fundamental theorems of linear viscoelasticity.

Let now consider a homogeneous structure subjected to constant loads applied in t_0 and impose to it an additional restraint at time $t_0^* \geq t_0$.

Denoting by $u_e^{(p)}$ the elastic deformation evaluated in the direction of the redundant action X_1 in the additional restraint, produced by the external loads and assuming elastic modulus $E(t_0)$, according to second of eqs. (63) with $e_e^{(p)} = \bar{e} = 0$, the restrained displacement for $t \geq t_0^*$ is

$$\Delta u^{(p)} = u_e^{(p)} (1 + \varphi(t, t_0)) - u_e^{(p)} (1 + \varphi(t_0^*, t_0)) \quad (64)$$

and indicating by u_{1_0} the elastic displacement produced by $X_1 = 1$, for the unknown reaction $\Delta X_1(t)$ in the additional restraint we can write the subsequent integral equation expressing that the state of displacement is compatible with the additional restraint

$$\int_{t_0^*}^t d(\Delta X_1(t')) u_{1_0} E(t_0) J(t, t') = -\Delta u^{(p)} = -u_e^{(p)} (\varphi(t, t_0) - \varphi(t_0^*, t_0)) \quad (65)$$

remembering that

$$\Delta X_{1_0} = -\frac{u_e^{(p)}}{u_{1_0}} \quad (66)$$

represents the elastic reaction in the additional restraint if the restraint were present before the application of loads, from eq. (65), applying the Superposition principle we have:

$$\Delta X_1(t) = \Delta X_{1_0} \int_{t_0^*}^t \frac{\partial \varphi(t', t_0)}{\partial t'} \frac{R(t, t')}{E(t_0)} dt' \quad (67)$$

as a particular case, if we have $t_0^* = t_0^+$, as it is the case when the additional restraint is applied immediately after the loads, and suppose that

$$\Delta X_1(t) = \Delta X_{1_0} \left(1 - \frac{R(t, t_0)}{E(t_0)} \right) \quad (68)$$

introducing eq. (68) in eq. (65) and remembering eq. (1) we obtain

$$\Delta u^{(p)} = -u_e^{(p)} \varphi(t, t_0) \quad (69)$$

coinciding with eq. (65) when $t_0^* = t_0^+$.

Eq. (68) is the solution of the problem, so that, indicating by $\sigma_e^{(p)}$ the elastic stresses produced by loads in the structure without the additional restraint and by σ_{e1} the elastic stress produced by $X_1 = 1$, we can write:

$$\begin{aligned} \sigma^{(p)}(t) &= \sigma_e^{(p)} & t_0 \leq t \leq t_0^* \\ \sigma^{(p)}(t) &= \sigma_e^{(p)} + \Delta X_1(t) \sigma_{e1} & t_0^* \leq t \leq \infty \end{aligned} \quad (70)$$

Eqs. (67), (68), (69), (70) are very important as they represent the basic solutions of the problem related to the variation of the structural scheme after the application of loads. In this case also the solution of the elastic problem calculated assuming that the additional restraint is applied before the application of loads is sufficient in order to

evaluate the state of stress and deformation of the structure at any time.

8.2 Homogeneous elastic structures with elastic restraints, cable stayed bridges

With reference to fig. 21 let us indicate by $\underline{X}(t)$ the vector of the cable forces of a cable stayed bridge subjected to sustained loads (g) and to geometrical actions produced by the prestressing of the cables, (P).

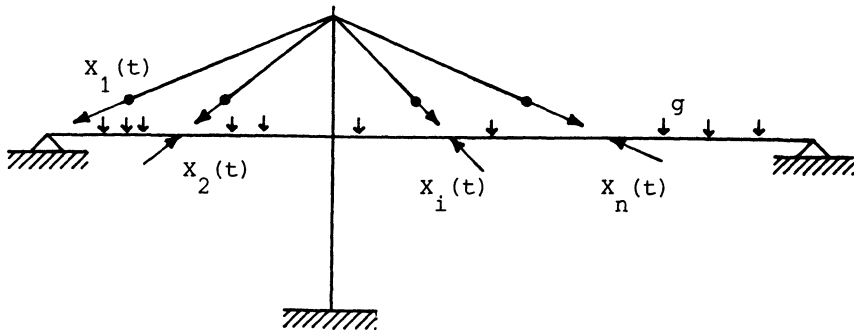


Fig.21 Cable-stayed bridge

Indicating by $\underline{F}^{(c)}(t_0)$, $\underline{F}^{(s)}$ the deformability matrices of the viscoelastic and of the elastic part and by $\underline{\delta}_0^{(c)}$ the vector of the elastic displacements of the connection points between the cables and the structures having the direction of the redundants, the compatibility equations according to eqs. (63) and the superposition principle become,

$$\int_0^t (\underline{F}^{(c)}(t_0) \underline{E}^{(c)}(t_0) J(t, t') + \underline{F}^{(s)}) d\underline{X}(t') = - \underline{\delta}_0^{(c)} \underline{E}^{(c)}(t_0) J(t, t_0) + (\underline{F}^{(c)}(t_0) + \underline{F}^{(s)}) \underline{X}_0^{(P)} \tag{71}$$

at the initial time t_0 we have

$$\underline{X}(t_0) = - (\underline{F}^{(c)}(t_0) + \underline{F}^{(s)})^{-1} \underline{\delta}_0^{(c)} + \underline{X}_0^{(P)} \tag{72}$$

so that, indicating by

$$\underline{X}_0^{(g)} = - (\underline{F}^{(c)}(t_0) + \underline{F}^{(s)})^{-1} \underline{\delta}_0^{(c)} \tag{73}$$

the initial elastic solution connected to external loads, eq. (72) gives

$$\underline{X}(t_0) = \underline{X}_o^{(g)} + \underline{X}_o^{(p)} \quad (74)$$

Introducing the coupling matrix

$$\underline{D} = (\underline{F}^{(c)}(t_0) + \underline{F}^{(g)})^{-1} \cdot \underline{F}^{(c)}(t_0) \quad (75)$$

from eq. (71) we have

$$\int_0^t (\underline{D}^* + \underline{D} E^{(c)}(t_0) J(t, t')) d\underline{X}(t') = \underline{X}_o^{(g)} E^{(c)}(t_0) J(t, t_0) + \underline{X}_o^{(p)} \quad (76)$$

where \underline{D}^* is the complementary matrix of \underline{D} .

Eq. (76) represents a system of Volterra integral equations which can be conveniently solved in the subsequent way.

Indicating by $\underline{\Omega}$ the diagonal spectral matrix (or eigenvalues matrix) of \underline{D} and by \underline{K} the corresponding modal matrix (or eigenvectors matrix), where the eigenvalues ω_i and the eigenvectors \underline{K}_i are given by the expressions

$$\begin{aligned} \det |\omega \underline{I} - \underline{D}| &= 0 \\ |\omega_i \underline{I} - \underline{D}| \underline{K}_i &= 0 \end{aligned} \quad (77)$$

with \underline{I} unit matrix, as it is well known from the algebra of linear transformations, the fundamental relationship between matrices $\underline{\Omega}$, \underline{K} , \underline{D} holds:

$$\underline{\Omega} = \underline{K}^{-1} \underline{D} \underline{K} \quad (78)$$

Introducing the new unknown vector \underline{Y} given by the equation:

$$\underline{X} = \underline{K} \underline{Y} \quad (79)$$

the inserting of eq. (79) in eq. (76), remembering eq. (78) drives to the subsequent set of independent Volterra integral equations

$$\int_0^t [(1 - \omega_i) + \omega_i E^{(c)}(t_0) J(t, t')] dY_i(t') = Y_{oi}^{(g)} E^{(c)}(t_0) J(t, t_0) + Y_{oi}^{(p)} \quad (80)$$

so that, defining the varied creep functions $J_i^*(t, t')$ by the equalities:

$$J_i^*(t, t') = \frac{1}{E^{(c)}(t_0)} [(1 - \omega_i) + \omega_i E^{(c)}(t_0) J(t, t')] \quad (81)$$

eq. (80) takes its final form

$$\int_0^t dY_1(t') J_1^*(t, t') = Y_{01}^{(g)} J(t, t_0) + \frac{Y_{01}^{(p)}}{E^{(c)}(t_0)} \quad (82)$$

Introducing the reduced relaxation functions $R_1^*(t, t')$, as the resolvent kernels of the Volterra integral equations (82), satisfying the integral equations

$$\int_0^t \frac{\partial R_1^*(\tilde{t}, t')}{\partial \tilde{t}} \cdot J_1^*(t, \tilde{t}) d\tilde{t} = 1 \quad (83)$$

the solution of eqs. (82), remembering eq. (81) becomes

$$Y_1 = \frac{Y_{01}^{(g)}}{\omega_1} \left[1 + (\omega_1 - 1) \frac{R_1^*(t, t_0)}{E^{(c)}(t_0)} \right] + Y_{01}^{(p)} \frac{R_1^*(t, t_0)}{E^{(c)}(t_0)} \quad (84)$$

and remembering eq. (79), for the unknown vector \underline{X} we obtain the matrix form:

$$\underline{X} = \underline{K} \underline{\Omega}^{-1} \left[\underline{I} + (\underline{\Omega} - \underline{I}) \frac{\underline{R}^*(t, t_0)}{E^{(c)}(t_0)} \right] \underline{K}^{-1} \underline{X}_0^{(g)} + \underline{K} \frac{\underline{R}^*(t, t_0)}{E_0} \underline{K}^{-1} \underline{X}_0^{(p)} \quad (85)$$

where $\underline{R}^*(t, t_0)$ is the diagonal matrix of the reduced relaxation functions $R_1^*(t, t_0)$.

Eq. (85) can be put in a different form introducing the vector $\underline{X}_{0,rig}^{(g)}$ which takes place when the elastic restraints are perfectly rigid i.e. for $\underline{F}^{(s)} = 0$. In this case from eq. (73) we derive:

$$\underline{X}_{0,rig}^{(g)} = - \left[\underline{F}^{(c)}(t_0) \right]^{-1} \cdot \underline{\delta}_0^{(c)} \quad (86)$$

and comparing eqs. (86) and (73) we obtain

$$\underline{X}_{0,rig}^{(g)} = \underline{D}^{-1} \underline{X}_0^{(g)} \quad (87)$$

Introducing eq. (87) in eq. (85), remembering eq. (78) we finally obtain

$$\underline{X} = \left[\underline{I} - \underline{K} \frac{\underline{R}^*(t, t_0)}{E^{(c)}(t_0)} \underline{K}^{-1} + \underline{K} \frac{\underline{R}^*(t, t_0)}{E^{(c)}(t_0)} \underline{\Omega} \underline{K}^{-1} \right] \underline{X}_{0,rig}^{(g)} + \underline{K} \frac{\underline{R}^*(t, t_0)}{E^{(c)}(t_0)} \underline{K}^{-1} \underline{X}_0^{(p)} \quad (88)$$

Eqs. (75) and (88) allow to state two basic properties affecting the eigenvalues ω_i and the vector \underline{X} . As regards the eigenvalues, let us consider the elastic energy $U^{(e)}$ stored in the viscoelastic part, and the energy $U^{(s)}$ stored in the elastic part when we apply to the structure the vector of forces $\underline{\tilde{X}}_i$ in the cables coinciding with the i -th eigenvector \underline{K}_i .

From the fundamental clauses of elastic structural analysis we have:

$$\begin{aligned} U^{(e)} &= \frac{1}{2} \underline{K}_i^T \underline{F}^{(e)} \underline{K}_i \\ U^{(s)} &= \frac{1}{2} \underline{K}_i^T \underline{F}^{(s)} \underline{K}_i \end{aligned} \quad (89)$$

so that for the whole structure derives

$$U^{(st)} = U^{(e)} + U^{(s)} = \frac{1}{2} \underline{K}_i^T (\underline{F}^{(e)} + \underline{F}^{(s)}) \underline{K}_i \quad (90)$$

From the second of eqs. (77) and remembering eq. (75) we obtain:

$$\omega_i \underline{K}_i = \underline{D} \underline{K}_i = (\underline{F}^{(e)} + \underline{F}^{(s)})^{-1} \cdot \underline{F}^{(e)} \cdot \underline{K}_i \quad (91)$$

and consequently

$$\underline{F}^{(e)} \underline{K}_i = (\underline{F}^{(e)} + \underline{F}^{(s)}) \underline{K}_i \cdot \omega_i \quad (92)$$

Comparing eqs. (92) (90) (89) we derive:

$$\omega_i = \frac{U^{(e)}}{(U^{(e)} + U^{(s)})} \quad (93)$$

so that all the eigenvalues ω_i , representing the ratio between the elastic energy stored in the viscoelastic part and that of the whole structure, are real and satisfy the inequality:

$$0 \leq \omega_i \leq 1 \quad (94)$$

The particular case $\omega_i = 0$ takes place when the elastic part is infinitely deformable, or in other words when the elastic restraints are practically negligible, while the upper value $\omega_i = 1$ corresponds to elastic restraints highly stiff, practically rigid, for which $\underline{F}^{(s)} = 0$. The inequality (94) allows to calculate in advance the reduced relaxation functions and to prepare tables considering ω_i as a parameter, so that an easy evaluation of the terms of matrix \underline{R}^* can be made. In fig. 22 it has been reported one of those tables, calculated using the numerical algorithm of eq. (53) and adopting the CEB MC78 model.

In order to proof the property related to vector \underline{X} let us suppose to

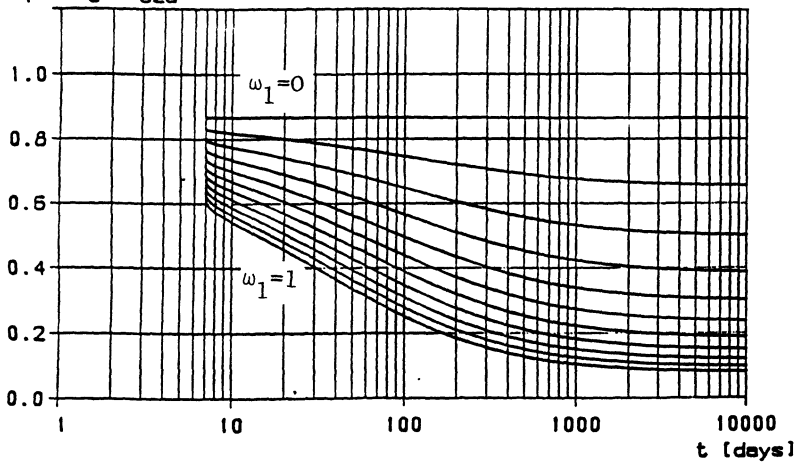
prestress the cables in such a way that the total force existing in them, sum of that produced by external loads ($\underline{X}_o^{(g)}$) and that due to prestressing ($\underline{X}_o^{(p)}$) is made equal to the force $\underline{X}_{o,rig}^{(g)}$ connected to the external loads if the cables were rigid.

In this case we have

$$\underline{X}_o^{(g)} + \underline{X}_o^{(p)} = \underline{X}_{o,rig}^{(g)} \tag{95}$$

$h_o=20\text{cm}$; R.H.=70% ; $t_o=7\text{days}$

$R_i(t, t_o)/E_c28$ $\omega_1=0+0.1n$ ($n=1,2,3,\dots,10$)



$t-t_o$ [days]	0	7	15	30	60	120	365	1095	3300	10000
$\omega_1=0.001$.86562	.86533	.86521	.86503	.86480	.86453	.86407	.86373	.86356	.86349
$\omega_1=0.050$.84832	.83669	.83012	.82166	.81080	.79809	.77745	.76267	.75321	.75225
$\omega_1=0.100$.83331	.80918	.79671	.78075	.76042	.73691	.69949	.67333	.66033	.65520
$\omega_1=0.150$.81786	.78328	.76532	.74288	.71429	.68163	.63067	.59585	.57883	.57215
$\omega_1=0.200$.80302	.75886	.73634	.70776	.67198	.63157	.56977	.52851	.50864	.50089
$\omega_1=0.250$.78869	.73380	.70900	.67514	.63309	.58616	.51577	.46882	.44805	.43960
$\omega_1=0.300$.77487	.71401	.68335	.64479	.59728	.54488	.46779	.41858	.39561	.38674
$\omega_1=0.350$.76152	.69337	.65924	.61650	.56426	.50729	.42507	.37373	.35012	.34106
$\omega_1=0.400$.74862	.67381	.63636	.59009	.53375	.47300	.38696	.33440	.31058	.30148
$\omega_1=0.450$.73615	.65524	.61518	.56541	.50351	.44166	.35290	.29983	.27612	.26711
$\omega_1=0.500$.72409	.63761	.59501	.54230	.47935	.41298	.32240	.26938	.24603	.23720
$\omega_1=0.550$.71241	.62083	.57595	.52064	.45506	.38668	.29504	.24251	.21970	.21111
$\omega_1=0.600$.70111	.60486	.55793	.50030	.43249	.36252	.27046	.21876	.19660	.18830
$\omega_1=0.650$.69017	.58963	.54006	.48118	.41147	.34031	.24832	.19771	.17631	.16832
$\omega_1=0.700$.67955	.57511	.52468	.46320	.39188	.31986	.22837	.17904	.15844	.15078
$\omega_1=0.750$.66926	.56124	.50932	.44625	.37360	.30099	.21035	.16243	.14267	.13535
$\omega_1=0.800$.65928	.54798	.49473	.43026	.35652	.28357	.19405	.14764	.12873	.12176
$\omega_1=0.850$.64959	.53530	.48085	.41517	.34053	.26745	.17929	.13443	.11639	.10975
$\omega_1=0.900$.64018	.52316	.46764	.40090	.32556	.25253	.16589	.12263	.10543	.09913
$\omega_1=0.950$.63104	.51152	.45506	.38739	.31152	.23870	.15372	.11207	.09569	.08971
$\omega_1=1.000$.62216	.50036	.44306	.37460	.29833	.22585	.14264	.10259	.08702	.08135

Fig.22 Reduced relaxation functions according to CEBMC78

So that the forces imposed by prestress, according to eq. (87) are:

$$\underline{X}_o^{(P)} = (\underline{I} - \underline{D}) \underline{X}_{o,rig}^{(g)} \quad (96)$$

Introducing eq. (96) in eq. (88) and remembering eq. (78) we obtain

$$\underline{X}(t) = \underline{X}_{o,rig}^{(g)} \quad (97)$$

Eq. (97) has a great importance in practical design of cable-stayed bridges, as it states that if by means of an initial prestressing of the cable we introduce the forces corresponding to the case of rigid restraints, these forces cannot vary in time and the state of stress of the structure is not influenced by creep.

8.3 P.C., R.C. AND COMPOSITE STEEL-CONCRETE SECTIONS

When performing the sectional analysis it is possible to proceed in the same way followed for the structural analysis, applying the Reduced Relaxation Function Method in its inverse form. Referring to the section of fig. 23, indicating by $\underline{\Psi}$ the vector of the sectional deformabilities

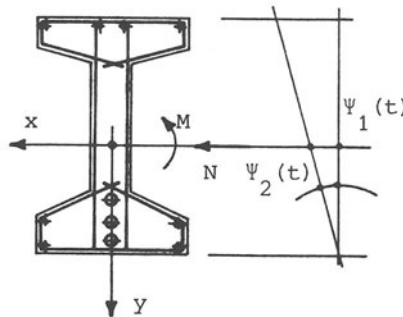


Fig.23 P.C. section and strain diagram

and by $\underline{\rho}^T = |1 - y|$ the vector of the generalized coordinates, assuming the Bernoulli-Navier hypothesis we have:

$$\begin{aligned} \underline{e}^{(c)} &= \underline{\rho}^T \cdot \underline{\Psi} \\ \underline{e}^{(s)} &= \underline{\rho}^T \cdot \underline{\Psi} \\ \underline{e}^{(sp)} &= \underline{\rho}^T \cdot \underline{\Psi} + \underline{e}_o^{(sp)} \end{aligned} \quad (98)$$

where $\underline{e}_o^{(sp)}$ is the imposed elastic deformation due to the prestressing of

steel. From eq. (6) and considering that the steel is supposed elastic, we have:

$$\begin{aligned}\sigma^{(c)} &= \int_0^t d[\underline{\rho}^T \underline{\Psi}(t') - \underline{e}_{sh}(t')] R(t, t') \\ \sigma^{(s)} &= E^{(s)} \underline{\rho}^T \underline{\Psi} \\ \sigma^{(sp)} &= E^{(sp)} \underline{\rho}^T \underline{\Psi} + E^{(sp)} \underline{e}_o^{(sp)}\end{aligned}\quad (99)$$

The sectional equilibrium requires that

$$\int_{A^{(c)}} \underline{\rho} \sigma^{(c)} dA^{(c)} + \sum_I \underline{\rho} \sigma_I^{(s)} A_I^{(s)} + \sum_J \underline{\rho} \sigma_J^{(sp)} A_J^{(sp)} = \underline{Q} \quad (100)$$

where $\underline{Q}^T = |N \ M|$ is the vector of the internal actions.

Combining eqs. (99) and (100) and introducing the stiffness matrices $\underline{B}^{(c)}$ and $\underline{B}^{*(s)}$ of the creeping part and of the reinforcement, according to the expressions

$$\begin{aligned}\underline{B}^{(c)} &= E^{(c)}(t_o) \int_{A^{(c)}} \underline{\rho} \underline{\rho}^T dA_c \\ \underline{B}^{*(s)} &= E^{(s)} \sum_I \underline{\rho} \underline{\rho}^T A_I^{(s)} + E^{(sp)} \sum_J \underline{\rho} \underline{\rho}^T A_J^{(sp)}\end{aligned}\quad (101)$$

and the vector \underline{Q}_{sh} , $\underline{Q}^{(P)}$ of the internal actions equivalent to shrinkage and prestressing

$$\underline{Q}_{sh} = \int_0^t \int_{A^{(c)}} \underline{\rho} \frac{\partial \underline{e}_{sh}(t')}{\partial t'} R(t, t') dA^{(c)} dt' \quad (102)$$

$$\underline{Q}^{(P)} = -E^{(sp)} \sum_J \underline{\rho} \underline{e}_{oJ}^{(sp)} A_J^{(sp)} \quad (103)$$

eq. (100) becomes:

$$\int_0^t (\underline{B}^{(c)} \frac{R(t, t')}{E^{(c)}(t_o)} + \underline{B}^{*(s)}) d\underline{\Psi}(t') = \underline{Q} + \underline{Q}_{sh} + \underline{Q}^{(P)} \quad (104)$$

At the initial time we have:

$$(\underline{B}^{(c)} + \underline{B}^{*(s)}) \underline{\Psi}(t_o) = \underline{Q} + \underline{Q}^{(P)} \quad (105)$$

so that, introducing the interaction matrix

$$\underline{\underline{A}} = \left(\underline{\underline{B}}^{(c)} + \underline{\underline{B}}^{*(a)} \right)^{-1} \underline{\underline{B}}^{(c)} \quad (106)$$

eq. (104) can be written in the subsequent form

$$\int_0^t \left(\underline{\underline{A}} \frac{R(t, t')}{E^{(c)}(t_0)} + \underline{\underline{I}} - \underline{\underline{A}} \right) d\underline{\underline{\Psi}}(t') = \underline{\underline{\Psi}}(t_0) + \underline{\underline{\Psi}}_{esh}(t) \quad (107)$$

where

$$\underline{\underline{\Psi}}_{esh}(t) = \left(\underline{\underline{B}}^{(c)} + \underline{\underline{B}}^{*(s)} \right)^{-1} \underline{\underline{Q}}_{esh}(t) \quad (108)$$

is the solution of the problem in the elastic domain connected to the shrinkage deformation. In order to solve the system of Volterra integral equations (107) we can proceed by means of the Reduced Relaxation Function Method in its inverse form, by means of the linear transformation

$$\underline{\underline{\Psi}} = \underline{\underline{K}}^* \underline{\underline{\Phi}} \quad (109)$$

$$\underline{\underline{K}}^{*-1} \underline{\underline{A}} \underline{\underline{K}}^* = \underline{\underline{\Omega}}^* \quad (110)$$

where $\underline{\underline{K}}^*$, $\underline{\underline{\Omega}}^*$ are the modal and spectral matrices of $\underline{\underline{A}}$. Introducing the varied relaxation functions

$$\bar{R}_i(t, t') = \left[\omega_i^* \frac{R(t, t')}{E^{(c)}(t_0)} + 1 - \omega_i^* \right] \cdot E^{(c)}(t_0) \quad (111)$$

and their resolvents $\bar{J}_i(t, t')$ solutions of the independent Volterra integral equations

$$\int_0^t \frac{\partial \bar{J}_i(\tilde{t}, t')}{\partial \tilde{t}} \bar{R}_i(t, \tilde{t}) d\tilde{t} = 1 \quad (112)$$

the solution of eq. (107), applying the principle of superposition and introducing the diagonal matrix $\bar{J}(t, t')$ immediately becomes

$$\underline{\underline{\Psi}} = \underline{\underline{K}}^* \bar{J}(t, t_0) E^{(c)}(t_0) \underline{\underline{K}}^{-1*} \underline{\underline{\Psi}}(t_0) + \underline{\underline{K}}^* E^{(c)}(t_0) \int_0^t \bar{J}^*(t, t') \underline{\underline{K}}^{*-1} d\underline{\underline{\Psi}}_{esh}(t') \quad (113)$$

A particular simplification of eq. (113) is obtained if one supposes that the shrinkage and creep are affine in time. In this case we have

$$\underline{\epsilon}_{sh}(t) = \frac{\underline{\epsilon}_{sh}(\infty)}{\underline{\varphi}_\infty} \varphi(t, t_0) \quad (114)$$

so that, remembering eq. (102), we obtain

$$\underline{Q}_{sh} = \int_0^t \int_{A^{(c)}} \underline{\rho} \frac{\underline{\epsilon}_{sh}(\infty)}{\underline{\varphi}_\infty} \frac{\partial \varphi(t', t_0)}{\partial t'} R(t, t') dA^{(c)} dt' \quad (115)$$

and from eq. (108)

$$\underline{\Psi}_{esh}(t) = \underline{\Psi}_{esh}(\infty) \left(1 - \frac{R(t, t_0)}{E^{(c)}(t_0)} \right) \quad (116)$$

where

$$\underline{\Psi}_{esh}(\infty) = \left(\underline{B}^{(c)} + \underline{B}^{*(s)} \right)^{-1} E^{(c)}(t_0) \int_{A^{(c)}} \underline{\rho} dA^{(c)} \cdot \underline{\epsilon}_{sh}(\infty) / \underline{\varphi}(\infty) \quad (117)$$

From eq. (113), remembering eq. (116) and (112), we reach finally the expression

$$\underline{\Psi} = \underline{K}^* \underline{J} E^{(c)}(t_0) \underline{K}^{-1} \underline{\Psi}(t_0) + \underline{K}^* \underline{\Omega}^{*-1} \left[\underline{J}^*(t, t_0) E^{(c)}(t_0) - \underline{I} \right] \underline{K}^{-1} \underline{\Psi}_{esh}(\infty) \quad (118)$$

which is formally similar to eq. (85).

Eqs. (113) or (118) give the sectional deformability vector, so that the second and third of eqs. (99) allow to calculate the stresses in the steel, while in order to obtain the concrete stresses, indicating by $\Delta \underline{\Psi}$ the variation of the deformation vector, the sectional equilibrium gives:

$$\Delta \underline{Q}^{(c)} + \Delta \underline{Q}^{(s)} + \Delta \underline{Q}^{(sp)} = 0 \quad (119)$$

so that from eq. (101)

$$\Delta \underline{Q}_c = - \underline{B}^{*(s)} \Delta \underline{\Psi} \quad (120)$$

In the viscoelastic homogeneous part, according to the fundamental theorem expressed by eqs. (63) we have:

$$\Delta \underline{Q}^{(c)} = \underline{B}^{(c)} \Delta \underline{\Psi}_e \quad (121)$$

$$\Delta \underline{\sigma}^{(c)} = E^{(c)}(t_0) \underline{\rho}^T \Delta \underline{\Psi}_e \quad (122)$$

Combining eqs. (122), (120) remembering eq. (121) we finally obtain

$$\Delta \underline{\sigma}^{(c)} = - E^{(c)}(t_0) \underline{\rho}^T \underline{B}^{(c)-1} \underline{B}^{*(s)} \Delta \underline{\Psi} \quad (123)$$

9. CALCULATION of $R_i^*(t, t_0)$, $\bar{J}_i(t, t_0)$

The reduced relaxation functions R_i^* or the functions $\bar{J}_i(t, t_0)$ are the basic elements to calculate the solutions of the preceding problems, deriving from the application of the Reduced Relaxation Function Method in its direct or indirect form. The calculation of these two functions, which are the solutions of the Volterra integral equations (83), (112) can be made using the methods illustrated in 7. From a general point of view the functions R_i^* , \bar{J}_i have to be calculated in a numerical way from the Volterra integral equations (83) and (112), or, in an approximated form, using expression (58). This expression, defines a finite exact functional relationship between χ , R and J which, as a first approximation can be considered valid also when the functions R_i^* , J_i^* are introduced.

According to this hypothesis, remembering eq. (58) we can write

$$\chi = \frac{1}{1 - \frac{R_i^*}{E^{(c)}(t_0)}} - \frac{1}{\omega_i \Phi} \quad (124)$$

Solving eq. (124) for R_i^* we obtain

$$\frac{R_i^*}{E^{(c)}(t_0)} = 1 - \frac{\omega_i \Phi}{1 + \chi \omega_i \Phi} \quad (125)$$

In the same way putting in eq. (58) \bar{R}_i and \bar{J}_i , we have:

$$\chi = \frac{1}{1 - \frac{\bar{R}_i}{E^{(c)}(t_0)}} - \frac{1}{E^{(c)}\bar{J}_i - 1} \quad (126)$$

Remembering eq. (111) and eq. (58) we can write

$$1 - \frac{\bar{R}_i}{E^{(c)}(t_0)} = \omega_i^* \left(1 - \frac{R}{E^{(c)}(t_0)} \right) \quad (127)$$

$$\frac{1}{1 - R / E^{(c)}(t_0)} = \frac{1 + \chi \Phi}{\Phi} \quad (128)$$

Introducing eq. (128) in (127) and comparing with eq. (126) we obtain

$$\bar{J}_i = \frac{1}{E^{(c)}(t_0)} \left[1 + \frac{\omega_i^* \Phi}{1 + \chi \Phi (1 - \omega_i^*)} \right] \quad (129)$$

Eqs. (125), (129) give approximate values for the functions R_i^* and \bar{J}_i .

They are very simple to use and their accuracy is generally satisfactory so that for practical purposes these equations can be conveniently recommended for the analysis of non homogeneous structures.

In an alternate way as explained in [30], we can derive these functions adopting the classical viscoelastic model or the Dishinger model in order to describe the creep behaviour of concrete.

At this scope, for the classical model, inserting $\omega_i \varphi_m$ in eq. (24) we have

$$R_i^{*(c)} = \frac{E}{1 + \omega_i \varphi_m} \left[1 + \omega_i \varphi_m \left(1 - \frac{\varphi^{(c)}}{\varphi_m} \right)^{(1 + \omega_i \varphi_m)} \right] \quad (130)$$

and remembering eqs. (111) and (22), eq. (112) can be put in the differential form

$$\frac{\partial \bar{J}_i^{(c)}}{\partial t} + \bar{J}_i^{(c)} \frac{E}{\tau^*} [1 + \varphi_m (1 - \omega_i^*)] = (1 + \varphi_m) / \tau^* \quad (131)$$

with the initial condition

$$\bar{J}_i^{(c)} (t = t_0) = E.$$

Integrating eq. (131) and remembering eq. (23) we obtain

$$\bar{J}_i^{(c)} = \frac{1}{1 + (1 - \omega_i^*) \varphi_m} \frac{1}{E} \left[1 + \varphi_m (1 - \omega_i^*) \left(\frac{\varphi_m - \varphi}{\varphi_m} \right)^{(1 + (1 - \omega_i^*) \varphi_m)} \right] \quad (132)$$

As regards Dishinger model, from eq. (40) we have:

$$R_i^{*(D)} = E_{28} e^{-\omega_i \varphi^{(D)}} \quad (133)$$

and from eq. (112) remembering eqs. (111) (40) we obtain the differential form

$$\frac{\partial \bar{J}_i^{(D)}}{\partial \varphi^{(D)}} + (1 - \omega_i^*) \bar{J}_i^{(D)} = 1 \quad (134)$$

$$\bar{J}_i^{(D)} (t = t_0) = E_{28}$$

having the solution

$$\bar{J}_i^{(D)} = \frac{1}{E_{28} (1 - \omega_i^*)} \left[1 - \omega_i^* e^{-(1 - \omega_i^*) \varphi^{(D)}} \right] \quad (135)$$

Eqs. (125), (130), (133) and eqs. (129), (132), (135) according to the

properties of the classical and the Dischinger models satisfy the inequalities:

$$R_i^{(D)} < R_i^* < R_i^{(c)} \quad (136)$$

$$\bar{J}_i^{(c)} < \bar{J}_i < \bar{J}_i^{(D)} \quad (137)$$

10. NUMERICAL EXAMPLES

As a first example let us consider the cable-stayed bridge of fig. 24, taken from [31]. The permanent load, applied at $t_0 = 28$ days gives the subsequent initial values, elastically evaluated, for the forces in the cables

cable	n.	1	2	3	4	5	6	7
force	(ton)	45,20	67,20	73,10	70,20	57,7	33,8	339,4

The behaviour of concrete has been described by means of the CEB MC78 Model obtaining the time diagrams of the cable forces, related to their initial value, reported in fig. 25 and fig. 26. These values are obtained

from eq. (88) with $\underline{x}_0^{(P)} = 0$ as the prestressing is not considered in this calculation. We can see that the variations in the cable forces are quite large as the structural non homogeneity is marked.

The increments of the axial force in the cables 1 to 6 and in the cable 7 produce a reduction of the bending moments in the beam which as it can be argued from eq. (88) tends to assume a distribution similar to that corresponding to rigid cables. It is finally important to observe the high accuracy connected to the analysis performed on the basis of the algebraic creep law which gives the results represented by the small circles in fig. 25 and 26.

In fig. 27, taken from [32], an analogous problem is studied for load applied at $t_0 = 112$ days, using the CEB MC78 Model or the ACI Model to describe the creep behaviour of concrete.

In fig. 28 the time increments of the cable forces, are reported and a not negligible difference between the results deriving from the two models arriving to a maximum value of about 6,5% is observed. In fig. 29 the bending moment diagrams are reported, showing the drastic reduction of the maximum values produced by creep which, increasing the forces in the cables, makes the moment distribution to tend toward that corresponding to rigid cables. This distribution, as indicated by eq.

(88) cannot be achieved, as for $t \rightarrow \infty$ we have $\underline{X}(\infty) \neq \underline{X}_{o,rig}^{(g)}$. This is possible only applying the prestressing forces given by eq. (96) and in this case the structure behaves as a structure with rigid restraint,

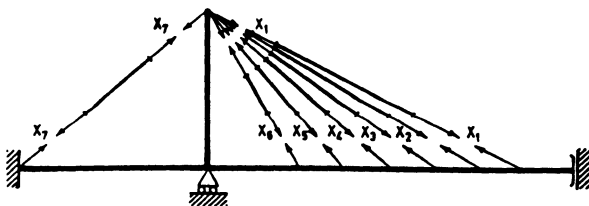
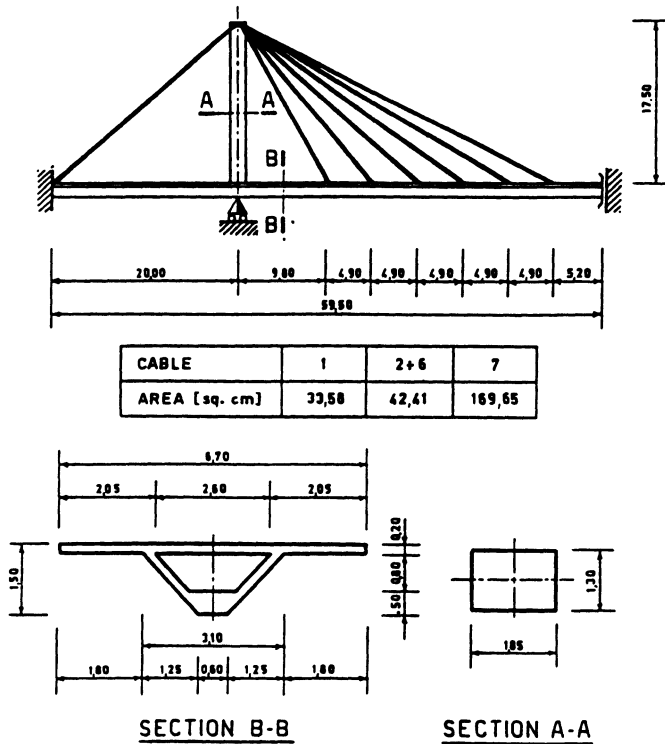


Fig.24 Cable stayed bridge (from Ref.31)

which, according to the fundamental theorem of eq. (63) maintains constant in time the state of stress, increasing in an affine way the elastic initial deformation.

As a final example let us consider the composite steel concrete section of a bridge beam illustrated in fig. 30, subjected to the constant bending moment $M_0 = 2531 \text{ tm}$ and referred to a system of coordinates having its origin in the centroid of the homogenized section. For this section, as reported in [33], the two eigenvalues are respectively $\omega_1^* = 0,90672$; $\omega_2^* = 0,00246$, and according to the ACI Model the two reduced creep functions $\bar{J}_i (i=1,2)$ have been calculated by means of the

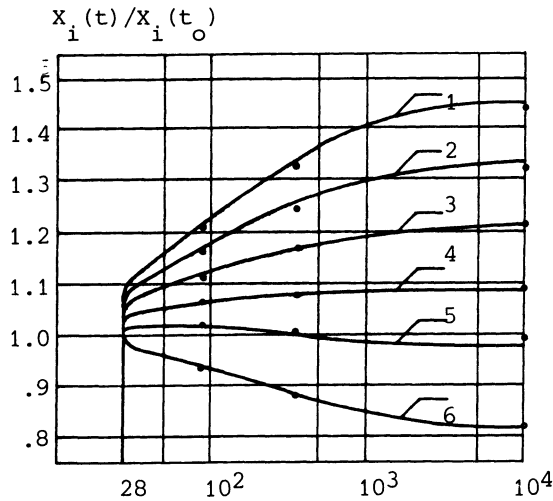


Fig.25 Relative time-variations of the forces in cables 1 to 6 (from Ref.31)

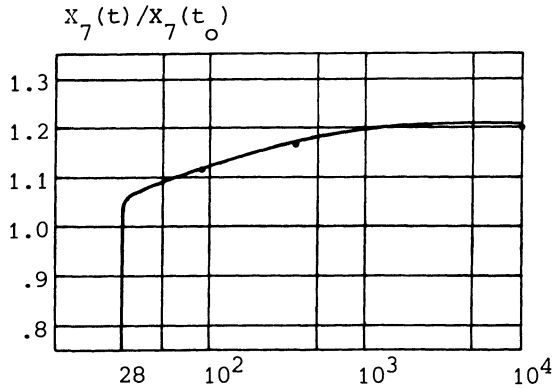


Fig.26 Relative time-variation of the force in cable 7 (from Ref.31)

iterative numerical procedure of eq. (53). The same functions have been determined also adopting the two limit models according to eq. (132) and (135) and by means of the algebraic creep law of eq. (129) with the approximate constant value $\chi = 0,8$. The results reported in Table 2 show that the bounds of the inequality (137) are very close so that the sectional analysis performed following the simplified models is of good accuracy and can be adopted for practical calculations. It is important

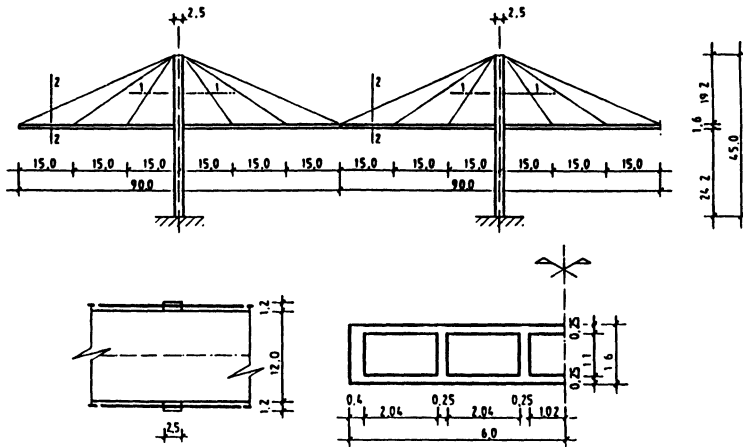


Fig.27 Cable-stayed bridge (from Ref.32)

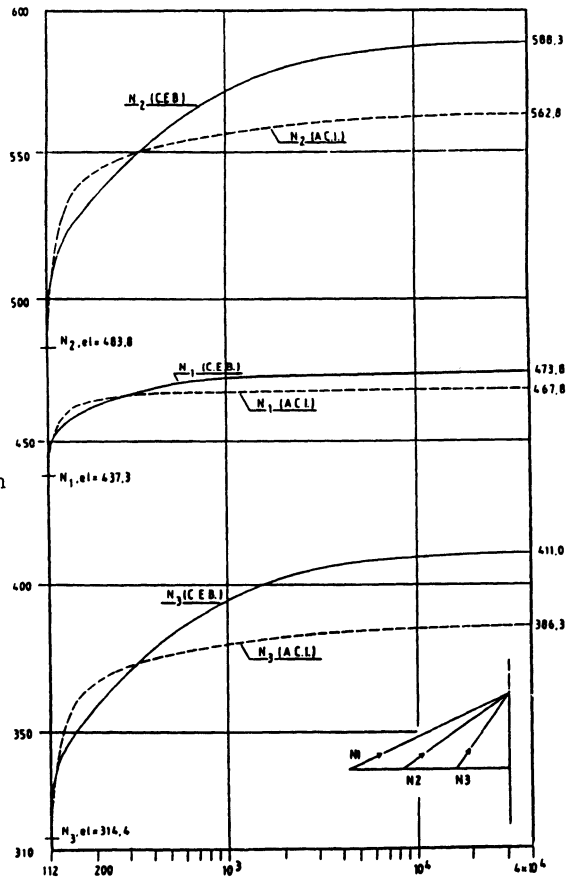


Fig.28 Relative time-increments in cable forces according to CEB and ACI models (from Ref.32)

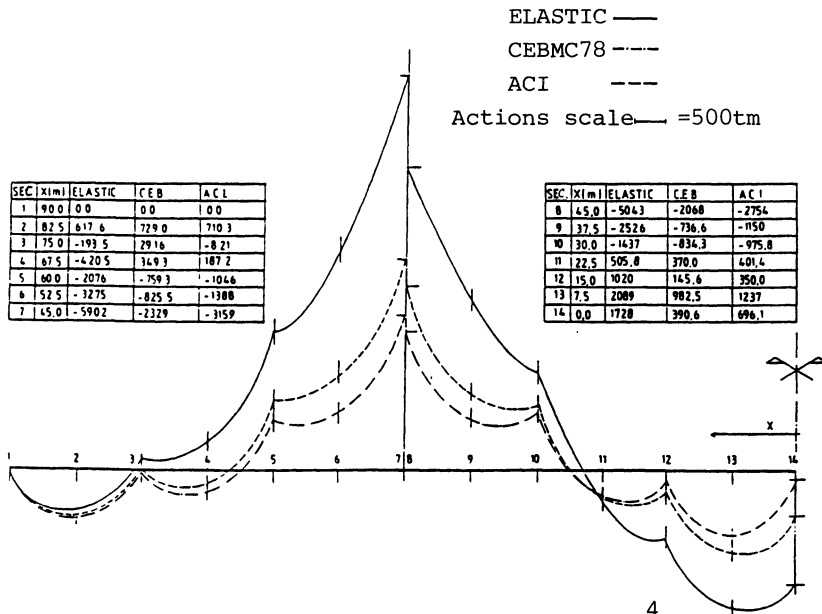


Fig.29 Bending moment diagram at $t=t_0$ and $t=10$ days (from Ref.32)

to note that the inequality (137) is always satisfied by the results of the general algorithm, for which the accuracy is very high while adopting the approximate algebraic creep law of eq. (129) the inequality may be in some cases violated. In the present example this happens for $(t-t') = 10^2$ days but also in this case the difference with respect to the numerical algorithm is very small, so that the algebraic creep law, owing to its simplicity and accuracy can be conveniently recommended for

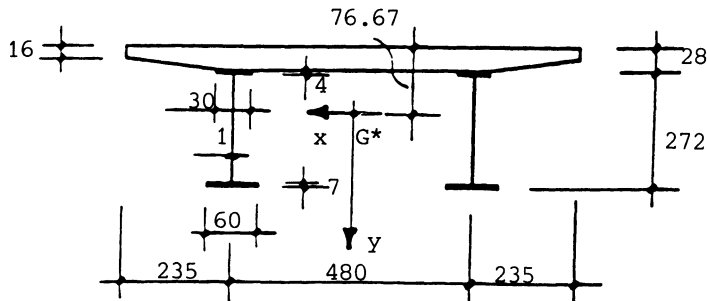


Fig.30 Composite steel-concrete section (from Ref.33)

t-t'	Numerical Method eq. (53)		Dischinger Model eq. (139)		Classical Model eq. (132)		Algebraic Model eq. (129)	
	$E_{28} \bar{J}_1$	$E_{28} \bar{J}_2$	$E_{28} \bar{J}_1$	$E_{28} \bar{J}_2$	$E_{28} \bar{J}_1$	$E_{28} \bar{J}_2$	$E_{28} \bar{J}_1$	$E_{28} \bar{J}_2$
10^2	2.29	1.00175	2.31	1.00200	2.28	1.00170	2.26	1.00120
10^3	2.76	1.00185	2.79	1.00220	2.70	1.00180	2.70	1.00190
10^4	2.93	1.00185	2.97	1.00220	2.82	1.00180	2.86	1.00190

Table 2. Reduced Creep Functions, (t-t') in days.

practical purposes. In fig. 31 the stresses in the beam and in the slab are reported, showing the marked redistribution which takes place due to creep. The relative increment of the curvature, measured by the slope of the stress diagram in the elastic beam is about 45% and, as the beam

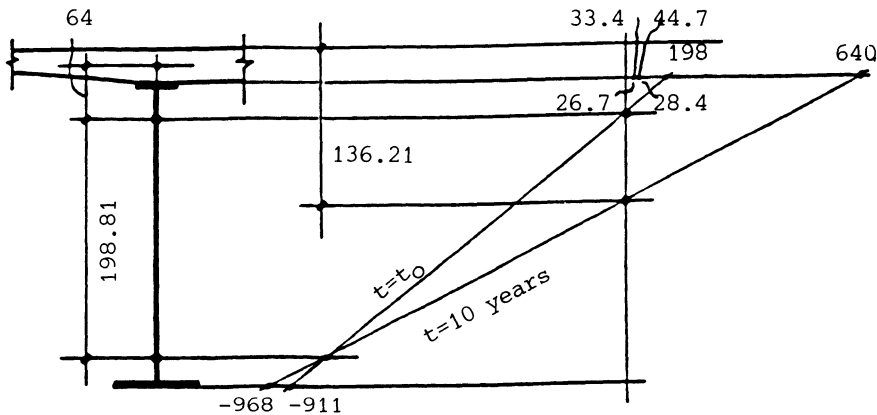


Fig.31 Stress diagrams at time t_0 and time $t=10$ years (kgf/cm^2)

section is constant along the longitudinal axis, this increment is the same for the transverse displacements. It is important to observe that the increase of the transverse displacements is quite small, as the elastic part is large compared to the concrete slab.

11. CONCLUDING REMARKS

The creep structural analysis of R.C. and P.C. structures requires different computational efforts connected to the level of non homogeneity of the structure and to the peculiarity of the mathematical algorithms adopted for the solution of the system of integral equations which governs the problem. If we follow the hypothesis of structural

homogeneity, as it is possible for R.C. and P.C. structures, affected by a very small amount of reinforcement, the knowledge of the creep and of the relaxation function is sufficient in order to predict the structural behaviour under imposed loads and deformations. As the creep models suggested by the Codes are expressed only in terms of creep function, the analysis of homogeneous structures requires the solution of the Volterra integral equation relating the functions J and R in order to obtain the relaxation function R. This function is obtained by inverting the creep constitutive law, or in other words, by determining the resolvent kernel of the Volterra integral equation expressing the creep law, when the deformation due to the applied stress has a constant unit value.

The analysis of non homogeneous structures, in particular the viscoelastic structures elastically restrained, requires more complex algorithms, which, however, can be reduced to only one general procedure named the Reduced Relaxation Function Method. This procedure can be applied in its direct form when the forces method is followed or in its inverse form when the displacements method is adopted. In both cases two particular sets of functions, namely the reduced relaxation functions or the reduced creep functions have to be determined by solving a sequence of independent Volterra integral equations. The algorithms for the solutions of these equations can be conveniently chosen in the range of the approximate algorithms related to simplified creep models or to simplified algebraic creep law, as in many practical cases the accuracy of the results is quite satisfactory.

Only when the results obtained following the simplified creep models are too much different, more refined algorithms as the one based on the iterative application of the superposition principle are required in the evaluation of the reduced relaxation or creep functions.

In every case, however, the Reduced Relaxation Function Method stands as the most efficient tool for the analysis of homogeneous viscoelastic structures elastically restrained, particularly for the analysis of P.C. or composite steel-concrete sections subjected to axial load and bending moment. In this case the problem involves only two unknowns, so that the calculation of the eigenvalues of the interaction matrix is immediate and the evaluation of the reduced creep functions which can be performed by means of the simplified procedures shows in general good accuracy and can be easily applied by the practitioners.

REFERENCES

1. Troxell, G.E., Raphael, J.M., Davis, R.W.: Long Time Creep and Shrinkage tests of Plain and Reinforced Concrete, ASTM Proceedings, 58(1958), 1-20.
2. Reichart, T.W.: Creep and Drying Shrinkage of Lightweight and Normal Weight Concretes, National Bureau of Standards, U.S.A. NBS Monograph 74 (1964), 1-30.

3. Hansen, T.C., Mattock, A.H.: Influence of Size and Shape of Member on Shrinkage and Creep of Concrete: ACI Journal 63 (1966) 267-289.
4. L'Hermite, R., Mamillan, M.: Retrait et Fluage des Betons, Annales ITBTP, Supplement 21, 1968.
5. L'Hermite, R., Mamillan M., Lefèvre, C.: Nouveaux Résultats de Recherches sur la Deformation et la Rupture du Béton, Annales ITBTP 18 (1965) 325-360.
6. Wei-Wen Yu, Winter, G.: Instantaneous and Long-Time Deflections of Reinforced Concrete Beams Under Working Loads, ACI Journal 57 (1960) 29-50.
7. Mamillan, M., Savin, V.: Étude Expérimentale sur le Fluage du Béton. Verification du Principe de Superposition, Materiaux et Constructions, RILEM, Vol. 14, 81 (1981) 177-189.
8. Hanson, J.A., : A 10-year Study of Creep Properties of Concrete, Concrete Laboratory Report N. Sp-38, U.S. Department of the Interior, Bureau of Reclamation, Denver, Colorado, 1953.
9. FIP (Federation Interantional de la Precontrainte) - CEB (Comité Eurointernational du Béton): Code Modèle pour les Structures en Béton. CEB Bulletin d'Information N. 124, 1978.
10. AASHTO, Standard Specifications for Highways Bridges, 11th Edn. 1-467, AASHTO, Washington, D.C. 1973.
11. Italian Ministry of Public Works: Italian Building Code for R.C. and P.C. Structures, 1985, (in italian).
12. EH-82 Instruccion para el Proyecto y la Ejecución de Obras de Hormigon en Masa o Armado, Comision Permanente del Hormigon, Madrid, 1986.
13. Mc Henry, D.: A new Aspect of Creep in Concrete and its Applciation to Design, Proceedings ASTM, 43 (1943) 1069-1086.
14. Ross, A.D.: Creep of Concrete under variable Stress, ACI Journal, Vol. 54 (1958) 739-758.
15. Maslov, G.N., Thermal Stresses in Concrete Masses with Account of Concrete Creep (in Russian), Gosenergoizdat, 28(1940) 175-188.
16. ACI (American Concrete Institute) Committee 209: Prediction of Creep, Shrinkage and Temperature Effects in Concrete Structures, in : Designing for Effects of Creep, Shrinkage and Temperature in

Concrete Structures. ACI Publication SP27-3 (1971) 41-93.

17. Rüsç, H., Jungwirth, D., Hilsdorf, H., : Kritische Sichtung der Verfahren zur Berücksichtigung der Einflüsse von Kriechen und Schwinden des Betons, Beton und Stahlbetonbau, H. 68 (1973) 49-60; 76-86; 152-158.
18. Nowacki, W.: Theorie du Fluage, Eyrolles, Paris, 1965.
19. Persoz, B.: Introduction à l'Étude de la Rheologie, Dunod, Paris, 1960.
20. Bland, D.R.: Theory of Linear Viscoelasticity, Pergamon Press, Oxford, 1960.
21. Dischinger, F.: Untersuchungen über die Knicksicherheit, die Elastische Verformung und das Kriechen des Betons bei Bogenbrücken, Der Bauingenieur H. 18 (1937) 487-520; 539-552; 595-621. H. 20 (1939) 53-63; 286-294; 426-437; 563-572.
22. Whitney, C.S.: Plain and Reinforced Concrete Arches, ACI Journal Vol. 28 (1932) 479-519.
23. Glanville, W.H.: The Creep or Flow of Concrete under Load, Studies in Reinforced Concrete, part III, Dept. Scientific and Industrial Research, Building Research Technical Paper N. 12, London (1930).
24. FIP-CEB Manual on Structural Effects of Time-dependent Behaviour of Concrete, CEB Bulletin d'Information N. 142-142bis, Georgi Publishing Co. Saint-Saphorin, CH 1984.
25. Rüsç, H., Jungwirth, D: Stahlbeton Spannbeton, Band 2, Werner Verlag, Düsseldorf 1976.
26. Branson, D.E.: Deformation of Concrete Structures, Mc Graw-Hill, New York, 1977.
27. Trost, H.: Auswirkungen des Superposition Prinzips auf Kriech und Relaxation Probleme bei Beton und Spannbeton, Beton und Stahlbetonbau H. 62 (1967) 230-238.
28. Bazant, Z.P.: Prediction of Concrete Creep Effects Using Age-Adjusted Effective-Modulus method, ACI Journal, Vol. 69 (1972) 212-217.
29. Mola, F.: Methods for the analysis of linear viscoelastic structures, Studi e Ricerche Vol. 3 Italcementi Bergamo (Italy) (in italian) (1981).

-
30. Mola, F.: Linear viscoelastic analysis of non homogeneous structures, Studi e Ricerche vol. 8 Italcementi Bergamo (Italy) (in italian) (1986) 119-196.
 31. Mola, F., Malerba, P.G., Pisani, M.A. Creep and Shrinkage Effects on the Cable-Stayed Bridges Behaviour, Proceedings of the International Conference on Cable-Stayed Bridges, Vol. 1, Bangkok, Thailand, (1986) 657-667.
 32. Mola, F., Malerba, P.G., Pisani, M.A.: Structural non homogeneity and additional restraints effects on the long term behaviour of precast R.C. or P.C. Bridges, Proceedings of the Symposium of the Italian R.C. and P.C. Association, Vol. 2, Stresa Italy (1987) 505-519 (in italian).
 33. Mola, F.: Applications of the Reduced Relaxation Function Method to the Analysis of homogeneous viscoelastic structures, Studi e Ricerche Vol. 4 Italcementi Bergamo (Italy) (in italian) (1982) 211-235.

TECHNOLOGICAL FACTORS IN THE DESIGN OF FOUNDATION PILES

C. Viggiani

University of Naples, Naples, Italy

ABSTRACT

It is well known that the behaviour of foundation piles is markedly affected by technological factors, particularly for cast in situ piles. Some examples are presented to substantiate this statement, concerning recent experiences with large diameter bored piles and continuous flight auger piles in the pyroclastic soils of eastern Naples area.

A pre-loading cell, aimed at improving the load-settlement behaviour of the base of large diameter bored piles, is then described.

Finally, some data and comments are presented about loading tests on instrumented piles and non destructive integrity test methods, such as sonic logging and mechanical admittance tests.

1. INTRODUCTION

Piles are often adopted in the foundations of bridges, and indeed they represent by far the most frequent solution. There are many reasons for this: the high values of loads, the frequent occurrence of weak soils, the need of founding deep enough to be safe against scouring effects.

A complete discussion of all the problems of pile foundations is clearly out of the scope of this paper; only some aspects, that are believed to be particularly interesting or topical, will be touched.

As it is well known, the behaviour of the foundation piles is markedly affected by technological factors. The influence is particularly significant for cast in situ bored piles that are the large majority in Italy and are particularly suited for bridges, due to the ease of reaching diameters up to 2 m and lengths up to many tens of meters. This paper will be devoted to a discussion of some of these factors.

Most of the experiences reported, though being of general relevance, have been collected in the pyroclastic soils of eastern Naples area. The essential features of the subsoil in this area are therefore presented in par. 2.

Some striking examples of the influence of technological factors on the behaviour of large diameter bored piles (par. 3) and continuous flight auger piles (par. 4) are reported.

A particular type of pre-loading cell, aimed at improving the load settlement behaviour of the base of large diameter bored piles, is described in par. 5. The results of a full scale investigation on instrumented piles are reported and discussed, pointing out the features connected with the use of the pre-loading cell.

The marked and somewhat random influence of technological factors makes the theme of controls particularly significant. Some aspects of loading tests on instrumented piles are discussed in par. 6, while non destructive integrity test methods, such as cross hole sonic logging and mechanical admittance tests, are described in par. 7.

2. THE SUBSOIL OF EASTERN NAPLES AREA

The plain lying east of the city of Naples is being interested by an intense construction activity, in connection with enterprises like the new Directional Centre with its high rise buildings, the new Law Court, roads and hydraulic infrastructures. Most of these structures are founded on piles; a large amount of experience on their behaviour became therefore available.

The subsoil of the area had been thoroughly investigated by a number of Authors (CROCE, PELLEGRINO, 1967; RIPPA, VINALE, 1982; VINALE, 1988), and appears rather uniform in its essential features (fig. 1).

Starting from the surface and going downward, the fol-

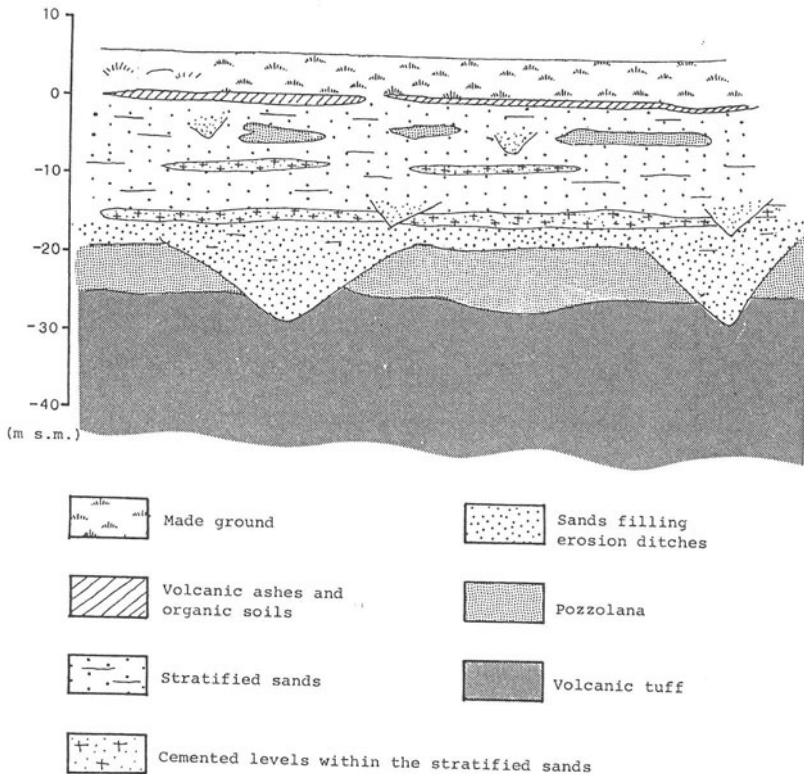


Fig. 1. Schematic constitution of the subsoil in eastern Naples area

lowing soils are typically found:

- made ground;
- volcanic ashes and organic soils;
- stratified sands;
- pozzolana, loose or weakly indurated;
- volcanic tuff.

The made ground has a thickness of 3 - 4 m and consists essentially of masonry remains and tuff fragments embedded in a silty brown matrix of pyroclastic nature.

The ashes and organic soils represent the bottom of the marsh that occupied this part of the plain until less than a century ago. The ashes have a silty texture and exhibit a slight plasticity; the organic soils are generally pyroclastic sediments with diffused organic matter, but sometimes peat layers are found.

The stratified sands are alluvial soils of volcanic origin (sand, pumices, lapilli and ashes) washed out from the surrounding hills and deposited under lagoonal or marsh environment. The thickness of each layer ranges between some tens of centimeters and some meters.

The sands are underlain by a pyroclastic formation consisting of pozzolana (cohesionless or slightly indurated) and tuff; they belong to the same geological formation, and differ only by the degree of diagenesis.

The upper part of the formation, starting at a depth of 25 - 30 m, consists generally of cohesionless pozzolana; then indurated pozzolana and tuff are found.

The tuff is a soft rock, with a compressive strength ranging from 20 to 100 kg/cm²; the thickness of the layer is usually of some tens of meters.

At some places, depending on the conditions prevailing at the time of deposition, the tuff is missing and the pyroclastic formation consists entirely of cohesionless and slightly indurated pozzolana.

The ground water table is found at a depth of about 2 m below the ground surface, that has an average elevation of 5 m above mean sea level.

3. LARGE DIAMETER BORED PILES

Where the tuff is found within 30 - 35 m from the surface, the majority of high rise buildings have been founded on large diameter bored piles penetrating the tuff for a length of 2 - 3 times their diameter.

Fig. 2 reports some CPT results referring to two different sites; it may be seen that the characteristics of the soils overlying the tuff at the two sites are practically identical, except for the depth of the tuff that is 28 m at a site and 33 m at the other one.

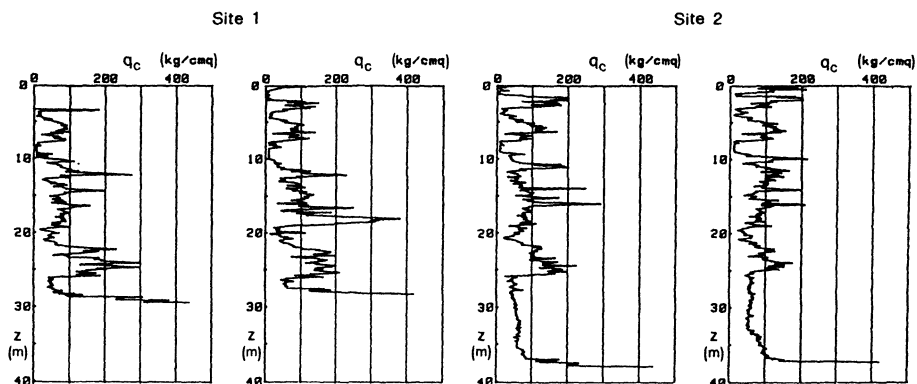


Fig. 2. Profiles of the point resistance of CPT in sites 1 (tests a in fig. 3) and 2 (tests b, c and d in fig. 3)

In both sites bored piles socketed into the tuff, with a diameter of 0,8 m, have been adopted; the results of some loading tests are reported in fig. 3.

At the site 2, piles have been drilled with bentonite mud. The results of 7 proof loading tests are included in the narrow band a in fig. 3; it may be seen that the scatter of results is rather low. The displacements of piles head are smaller than the elastic shortening of the shaft of the piles, thus indicating the occurrence of a significant side resistance.

At the site 1, in order to avoid the practical problems connected with the management of drilling mud, piles were drilled within a thin metallic casing that was left in the soil. Proof loading tests (curves d in fig.3) gave very unsatisfactory results. The retrieval of the casing after

concreting the pile improved the behaviour (curves c). Finally a vibrator was adopted to install a metallic casing for the whole pile length; the soil within the tube was then removed and the socket in the tuff drilled by an auger; after concreting, the casing was retrieved, always by vibration. This technique gave results (band b in fig. 3) comparable to those obtained in the site 2.

The data reported in fig. 3 appear very effective in exemplifying the influence of the construction techniques on the behaviour of the foundation piles, even in a case (piles bearing on a rock base) where such an influence was not expected to be significant.

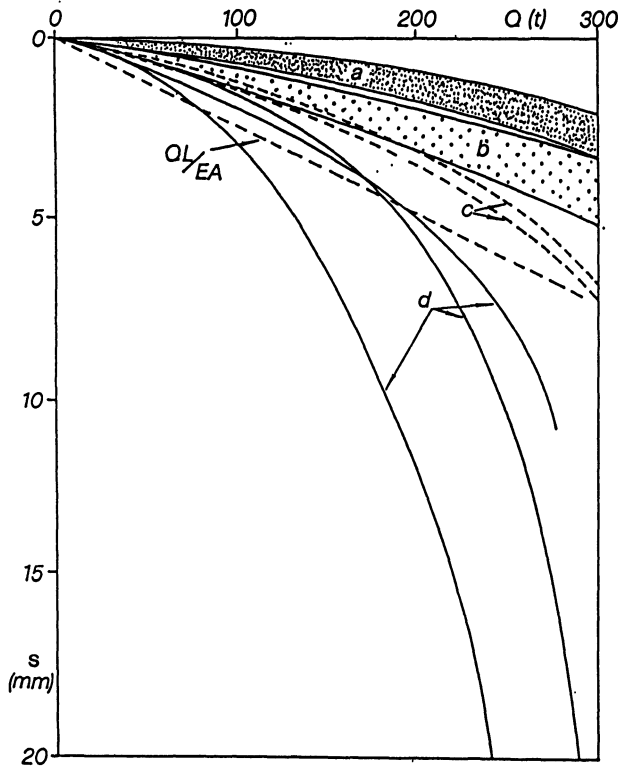


Fig. 3. Results of loading tests on bored piles with a diameter of 0,8 m, end bearing on the tuff. a) n. 7 tests on piles with $L = 35 - 40$ m bored with bentonitic mud; b) n. 4 tests on piles with $L = 30$ m, bored within a casing introduced in advance by vibration; c) piles with $L = 30$ m bored with a casing; d) piles drilled with a casing left in the soil

4. CONTINUOUS FLIGHT AUGER PILES

Continuous flight auger piles (VAN IMPE, 1984, 1988; MASCARDI, 1985; VAN WEELE, 1988) are increasingly used in many circumstances; contractors claim that they offer the advantages of both driven and bored piles without the related disadvantages; in particular, they are claimed to be relatively insensitive to construction procedures.

Auger piles are installed by means of a hollow stem with an inner diameter of 10 - 15 cm, provided with a screw on its outer surface. The auger is inserted into the soil by the combined action of an axial thrust and a torque; the ratio between the vertical travel and the revolutions, however, is always less than the pitch of the screw. Accordingly, the penetration implies a lateral compression of the soil and also the removal of some soil.

After the auger has reached the desired depth (fig. 4), the temporary closure plate below the central stem is pushed away by pumping concrete or mortar through the stem and the auger is lifted, removing from the ground the soil within the screw. Being generally the volume of the removed soil less than the volume of the pile, the net resulting effect is a compression of the soil surrounding the pile; the resulting situation is intermediate between that of a bored and that of a driven pile.

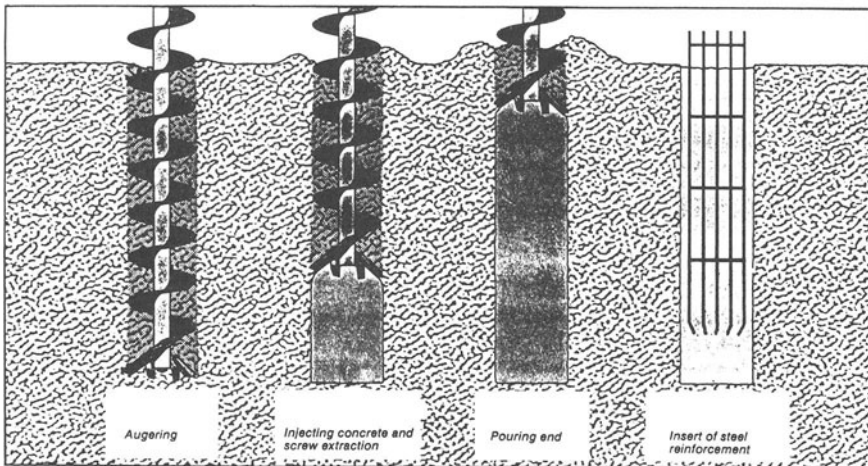


Fig. 4. Stages in the installation of a continuous flight auger pile (TREVI)

The procedure allows a safe and rapid installation of piles with a diameter ranging from 40 cm up to 1 m and a length up to 30 - 35 m. It is suited to weak soils, produces an effective horizontal compression of the soil, acts without the vibration and noise of driven piles.

A major shortcoming of auger piles is the difficulty of placing a reinforcement cage. This must be lowered into the shaft immediately upon completion of concreting, and usually it must be of a short length.

In order to improve this aspect, the diameter of the central stem has to be substantially increased and the width of the spiral welded at the outside decreased.

The pile known with the trade name of "Presso-Drill", for instance, is characterized by a ratio between the diameter of the stem d_0 and the overall diameter d ranging between 0,7 and 0,9.⁰

The scheme is reported in fig. 5. After the auger has

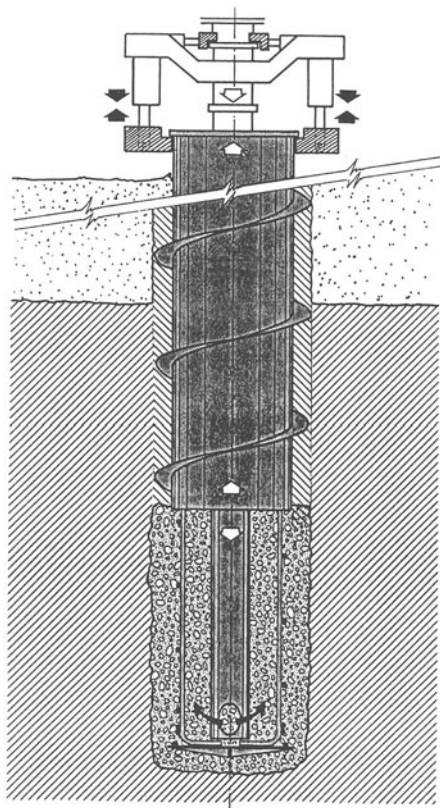


Fig. 5. Procedure of installation of a pile type Presso-Drill, developed by Icels Pali (MASCARDI, 1985)

reached the desired depth under the combined action of an axial thrust and a torque, a reinforcing cage and a concreting tube are lowered into the stem. While concreting, the auger is lifted by jacks contrasting upon the concreting tube, that stops the cage hindering its lifting and compresses the soil below the temporary bottom closure plate.

Piles of the latter type have been extensively adopted in eastern Naples area. In many applications, for instance, piles with $d_0 = 0,5$ m, $d = 0,6$ m, $L = 16$ m have been adopted; loading tests gave values of the bearing capacity around 250 t.

At a site where the subsoil was characterized by the CPT results reported in fig. 6, piles with $d_0 = 0,71$ m, $d = 0,96$ m, $L = 21,5$ m exhibited a bearing capacity exceeding 700 t (CAPUTO, VIGGIANI, 1988).

This kind of results is within the range obtained, in the same soils, with driven piles.

A number of CPT have been performed, before and after the construction of some piles, at a distance of about 1 m from the pile axis; in fig. 7 (CAPUTO, VIGGIANI, 1988) the ratio of the mean values of q_c measured after (q_c) over the values measured before construction (q_{c0}) is plotted against depth. As in driven piles, a general improvement of the soil properties is obtained.

For another site, located around 500 m apart, the soil profile and some CPT and SPT results are reported in fig. 8. A large multi-storey garage has been founded in this site on Presso-Drill piles with $d_0 = 0,66$ m, $d = 0,8$ m, $L = 12,5$ m. In this case proof loading tests have shown that the

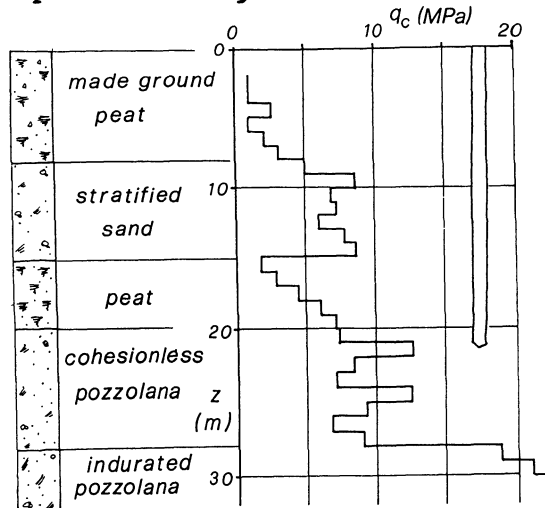
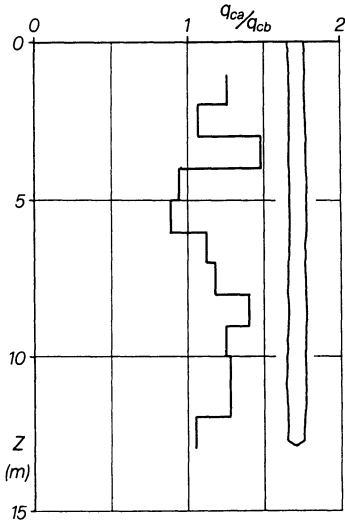


Fig. 6. Constitution of the subsoil and average CPT results at a site in the eastern Naples area



Ratio between the values of q_c measured after (q_{ca}) and before (q_{cb}) the installation of the piles of the Presso-Drill type

Fig. 7. Site of fig. 6

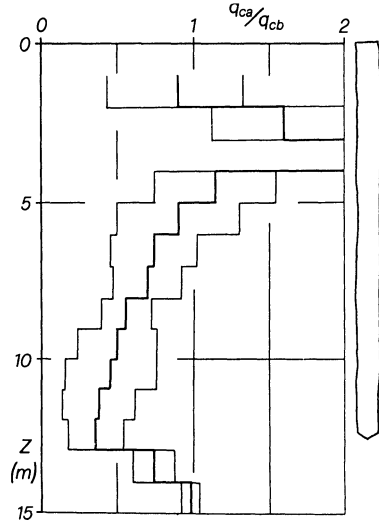


Fig. 9. Site of fig. 8

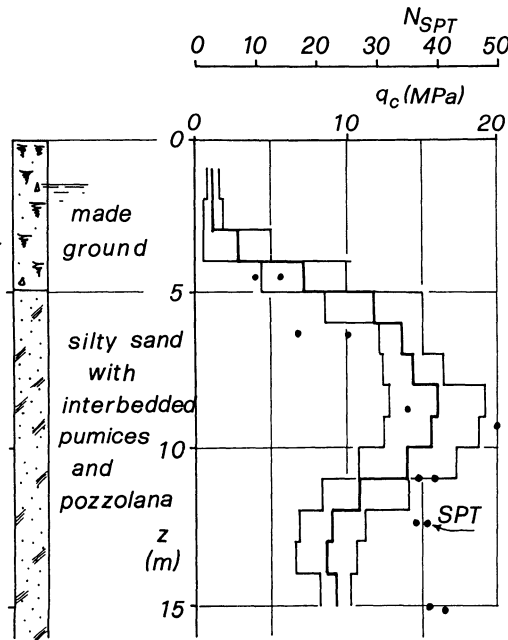


Fig. 8. Constitution of the subsoil and results of CPT and SPT at a site close to that of fig. 6

behaviour of piles was less satisfactory, and very similar to that of bored piles.

The results of CPT performed before and after the installation of the pile in the vicinity of some piles have been processed as in fig 7 and are reported in fig. 9. An overall decrease of the penetration resistance in the vicinity of the piles is evident.

It can be concluded that constructional factors affect also the behaviour of auger piles.

In order to understand the reasons of this influence, let us attempt an analysis of the penetration of the auger into the soil.

From a kinematical viewpoint (fig.10), if v is the rate of penetration and n that of revolution, in a time interval Δt we have:

- volume of displaced soil:

$$V_d = \frac{\pi d_0^2}{4} v \Delta t$$

- volume of soil removed by the screw:

$$V_s = \frac{\pi}{4} (d^2 - d_0^2) (nl - v) \Delta t$$

where l is the pitch of the screw.

If $v = nl$, $V = 0$; the screw penetrates into the soil without removing any material. If $v = 0$ the auger acts as an

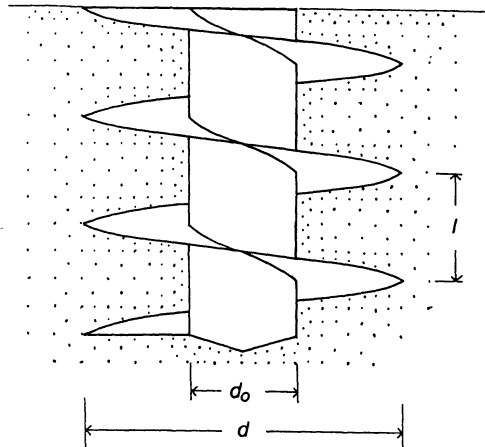


Fig. 10. Geometrical properties of the continuous flight auger

Archimedean screw, removing a volume of soil:

$$v_{a \max} = \frac{\pi}{4} n l \Delta t (d^2 - d_0^2)$$

In order to have a net compression effect, the displaced volume must exceed the removed one. From the condition:

$$v_d \geq v_a$$

it follows that:

$$v \geq n l \left(1 - \frac{d_0^2}{d^2} \right) \quad (1)$$

Is this ratio between the rates of penetration and revolution feasible? To answer this question, let us analyze the mechanics of the penetration.

During the penetration (fig. 11) the screw is acted upon by: an axial thrust Q , deriving from the weight of the equipment plus the reaction of anchors, if any; a resistance P of the soil on the temporary bottom plate closing the central stem; an axial force N produced by the torque M .

The latter can be expressed:

$$N = \frac{2M}{d + d_0} \frac{\pi d - l \operatorname{tg} \phi}{\pi d \operatorname{tg} \phi - l} \quad (2)$$

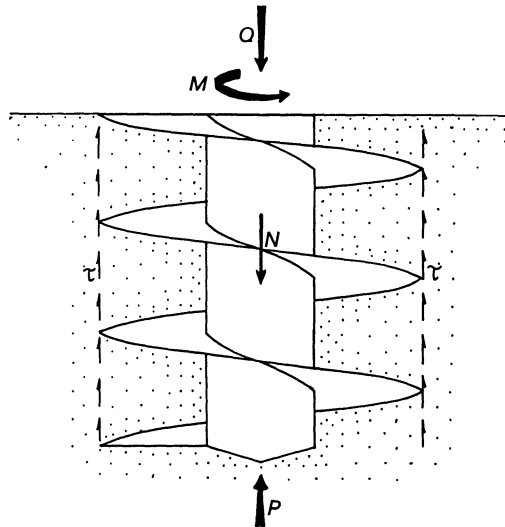


Fig. 11. Forces acting upon the auger during the penetration

having assumed that the coefficient of friction between the soil and the screw equals $\text{tg}\phi$.

To have penetration, the sum of Q plus M must exceed P ; hence:

$$M \geq (P - Q) \frac{d + d_0}{2} \frac{\pi d \text{tg}\phi + 1}{\pi d - l \text{tg}\phi} \quad (3)$$

The force N is transferred to the soil as a tangential stress on the cylindrical surface of the screw; in order not to have a shear failure, the shearing strength τ_{lim} of the soil should not be exceeded.

$$\tau = \frac{N}{\pi dz} \leq \tau_{\text{lim}} \quad (4)$$

Assuming $\tau_{\text{lim}} = k \text{tg}\phi \gamma z / 2$, where k is an earth pressure coefficient, it follows from (2) and (4):

$$M \leq \frac{d + d_0}{4} \frac{\pi d \text{tg}\phi + 1}{\pi d - l \text{tg}\phi} \pi dz^2 \gamma k \text{tg}\phi \quad (5)$$

Assuming the equality in (3) and (5), combining them and expressing P as $\pi d_0^2 N_q \gamma z / 4$, the following expression of Q is obtained:

$$\frac{Q}{\gamma d^3} = \frac{\pi}{4} \frac{z}{d} \left(N_q \frac{d_0^2}{d^2} - 2k \text{tg}\phi \frac{z}{d} \right) \quad (6)$$

The axial thrust Q (eq. 6) needed for penetration vanishes when:

$$\frac{z}{d} = 0 \quad \text{or} \quad \frac{z}{d} = \frac{N_q}{2k \text{tg}\phi} \frac{d_0^2}{d^2}$$

The value of Q reaches a maximum at:

$$\frac{z}{d} = \frac{N_q}{4k \text{tg}\phi} \frac{d_0^2}{d^2}$$

The maximum value is:

$$\frac{Q_{\max}}{\gamma d^3} = \frac{\pi}{32} N_q^2 \frac{d_0^4}{d^4}$$

The trend of $Q/\gamma d^3$ as a function of z/d is plotted in fig 12 for typical values of k , N_q and d_0/d . It may be seen that, when a torque M expressed by eq. (3) is available, in order to get a penetration without soil removal an axial thrust Q is needed; its value increases with increasing penetration depth, reaches a maximum and then decreases and eventually vanishes.

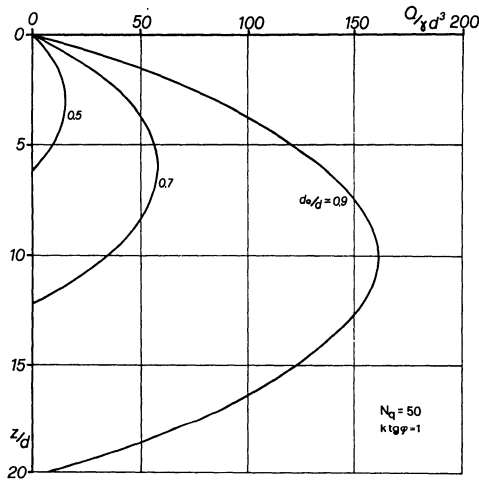


Fig. 12. Axial thrust Q needed for penetration as a function of the depth of penetration z

These findings agree with the common experience that everyone has done when screwing a screw into the wood. At the beginning a substantial thrust on the screwdriver is needed, otherwise the wood is stripped; but once the screw has penetrated a sufficient depth, only a torque is needed to continue the penetration.

The maximum value of the axial thrust needed for penetration without soil removal (fig. 13) increases with increasing the ratio d_0/d .

Coming back to the auger piles, it may be concluded that, in order to obtain a "good" pile, i.e. a pile where soil displacement exceeds soil removal:

- at the beginning of the penetration, a large axial thrust is needed;
- after reaching a sufficient depth, only a large torque is needed;

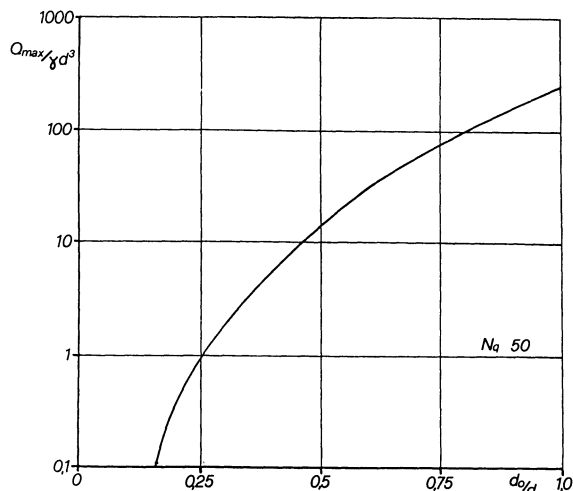


Fig. 13. Maximum value of the axial thrust needed for penetration as a function of the ratio d_0/d

— both Q and M , and hence the power required to the equipment, increase with increasing d_0/d .

For the existing equipment (MASCARDI, 1985) Q ranges from 2 to 10 t and M from 2 to 16 tm. It may be easily realized that, in the majority of practical cases, the available equipment have not a power sufficient to penetrate the soil without removal. The penetration rate v , as already stated, is then always lower than n_1 , and some soil removal during their penetration can not be avoided. As a consequence, the soil surrounding the pile loosens, and the penetration becomes possible; the bearing capacity of the pile, however, decreases.

If the condition (1) is satisfied, the net effect of the penetration is a compression of the soil, and the resulting behaviour of the auger pile approaches that of a driven pile. If the eq. (1) is not satisfied, because the equipment is not powerful enough for the conditions (soil properties, dimensions of the pile) prevailing, the behaviour of the resulting auger pile tends to that of a bored pile.

The evidence reported above is in overall agreement with these conclusions. The "good" auger piles of the first site (fig. 7) had a ratio l/d in the range from 20 to 30 and a ratio $d_0/d = 0,75$; these values are compatible with an installation without an excessive removal of soil.

On the contrary, the piles of the second site (figs. 8 and 9), that behaved as bored piles, were characterized by more unfavourable values of the ratios l/d (15) and d_0/d (0,87).

5. PRE-LOADING CELL

As it is well known (see, for instance, Whitaker, 1976) the base resistance of the large diameter bored piles is mobilized after substantial vertical displacements, its ultimate value being attained at a displacement in the range of 15% - 25% of the pile diameter d .

As a consequence, the design of foundations with large diameter bored piles is controlled by settlement rather than bearing capacity considerations; in the usual design practice (WRIGHT, REESE, 1979) the working load is essentially resisted by the side friction and only a small fraction of the available base resistance can be mobilized.

In this situation, the use of pre-loading cells at the base offers considerable potential as a means of improving the load-settlement behaviour of the pile base in order to attain a better mobilization of the base resistance at working loads and, finally, a more economical design.

Early attempts of this kind had been based on mere cement grouting below the pile base, through one or more outlets at the pile bottom (SIMONS, 1961); various provisions to obtain a uniform grout distribution have been tried (DIAMANTI, 1973). These systems proved unsatisfactory in some instances, especially in fine grained soils where a uniform grouting is not possible and the grout mixture comes in an irregular pattern of breakthroughs ("claquages").

Such experiences have led to the concept that, rather than trying to grout the soil below the pile base, it is convenient to reconsolidate it by means of a displacement grout acting essentially as a flat jack.

The pre-loading cell developed by Lizzi (1976) is based on this concept. As indicated in fig. 14, it is formed by two circular perforated steel plates having about the same diameter of the pile, spaced 20 - 30 mm apart and completely independent from each other. The two plates are wrapped together by an outer impermeable PVC membrane and an inner canvas envelope, forming a closed cell; two or more injection tubes extend from the cell to the surface.

The cell is dipped at the bottom of the drilled hole, together with the reinforcement cage, if any; the pile shaft is then concreted.

Once the shaft concrete has hardened, grouting of the cell is started through one of the injection pipes; the

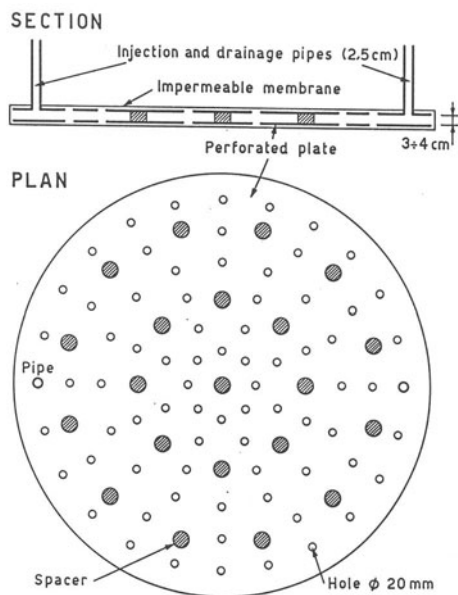


Fig. 14. Pre-loading cell developed by Lizzi (1976)

second pipe acts initially as a vent and it is closed when an outflow of grout is recognized.

After filling the cell, under increasing pressure the grout makes the two plates separate and move apart; under further increasing pressure, the PVC wrapping bursts leaving free access to the grout into the soil and allowing free movement of the plates. With this technique, a sort of flat jack with unlimited travel is formed, compressing uniformly the soil and pushing the pile upward; since no valves or other kind of obstacles prevent the free flow of the grout, the pressure measured at the surface allows a very reliable estimate of the upward force exerted upon the pile bottom.

The injection is stopped when.

- either the pile top begins to undergo some upward displacements (side resistance of the pile shaft approaching its ultimate value),
- or the volume of injected grout increases without increasing the pressure (a sort of bearing capacity failure of the soil below the pile base is being approached).

If needed, the injection can be carried out in more than one stage.

Of course, besides the flat jack action, some improvement of the soil around the pile base by grout impregnation is likely to occur, especially in coarse grained soils.

Lizzi (1976) suggests to obtain a preliminary estimate of the ultimate bearing capacity Q_{ult} of the pile from the maximum pressure that can be applied to the pre-loading cell during the pre-loading stage. He argues that, if the maximum grouting pressure p_i produces an upward displacement of the pile top, then it may be stated that:

$$p_i A = S; \quad p_i A \leq P \quad (7)$$

where A is the area of the pile base, S the ultimate side resistance and P the ultimate base resistance. Alternatively, if the maximum grouting pressure produces a steady increase of the injected volume without displacing the pile, it may be stated that:

$$p_i A \leq S \quad p_i A = P \quad (8)$$

In both cases:

$$Q_{ult} = P + S \geq 2p_i A \quad (9)$$

Eq. (9) represents an estimate of a lower bound of the bearing capacity. It is based on the assumption that: (i) the pre-loading cell actually acts as a flat jack; (ii) the values of S and P for upward and downward loading of the pile are equal. Both assumptions appear to be conservative.

Some full scale observations have been carried out by Viggiani and Vinale (1983), who performed load tests on four piles with a length of 42 m and a diameter of 1,5 m (piles A and C) or 2 m (piles B and D). The test area is located, as usual, in the eastern Naples area, in a site where the tuff is missing; the piles bear in the slightly indurated pozzolana and were drilled under bentonite mud.

All the piles were instrumented in 8 sections by strain gages extensometers, allowing the determination of the distribution of the axial load along the pile shafts. Piles C and D were provided with a pre-loading cell of the type described above.

Fig. 15 reports the volume V_i of grout injected into the cells during the pre loading stage, as a function of the injection pressure p_i .

The maximum pressure attained was equal to 4,0 MPa for pile C and to 4,4 MPa for pile D; the corresponding volumes of pumped grout have been of 2,5 and 4,1 m³ respectively. On the basis of previous experiences in similar soils, the final volumes of indurated displacement grout should be of the order of 1,2 and 2,0 m³ respectively.

It may be noted that the ratio between these volumes and the area of the pile base is equal to about 0,65 m for

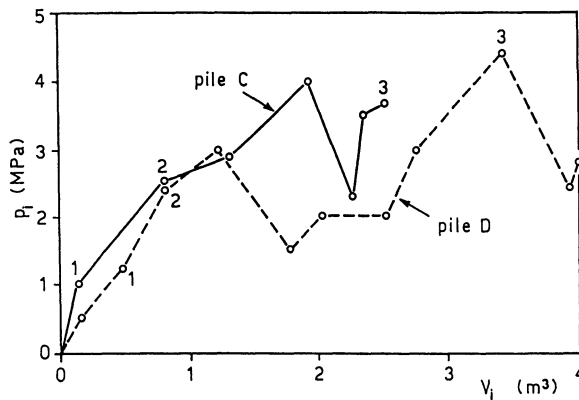


Fig. 15. Volume V_i of grout injected during the pre-loading stage of the piles C and D as a function of the injection pressure p_i

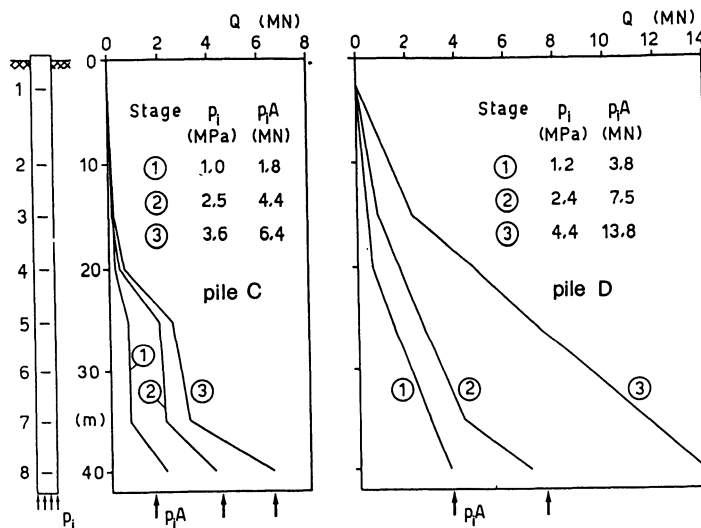


Fig. 16. Distribution of the axial load Q along the shaft of the piles C and D during the pre-loading stage

both piles; this length corresponds to the travel of an ideal flat jack expanding with a constant section equal to the cross section of the pile. The actual travel is likely to be much smaller, due to lateral expansion of the grout bulbs.

During the grouting operations, the distribution of the axial load along the shaft of the piles was measured; some of the results obtained are reported in fig. 16.

These findings substantiate the idea that the pre-loading cell acts essentially as a flat jack; as a matter of fact, the axial load measured near the pile base is very nearly equal to the grout pressure multiplied by the cross section of the pile. This upward force is resisted by side friction and, accordingly, it decreases moving upward along the shaft of the pile, vanishing near the pile top.

30 days after injecting the cells, the four piles were load tested to failure, except pile D for which the capacity of the reaction frame was exceeded before attaining failure the scope of this paper; in fig. 17, anyhow, the load-settlement curves of the four piles are reported. Besides the curve total load Q - top settlement s , also the curves side resistance S -settlement at mid length and base resistance P -settlement at the base are reported.

A marked improvement of the performances of piles equipped with the pre-loading cell may be observed. The total bearing capacity increases by 30% - 40%, the increase being mostly accounted for by a corresponding increase of the base resistance P . Still more evident is the improvement of the load-settlement behaviour, due to an earlier mobilization of both the base and side resistances.

In fig. 18 the distributions of the axial load along

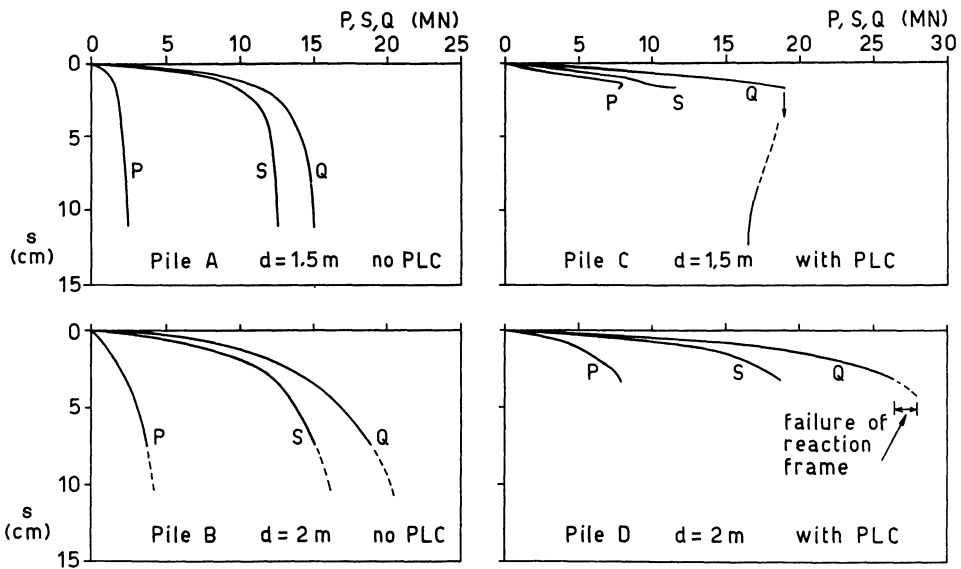


Fig. 17. Load - settlement curves for the four piles during the loading tests. Total load Q , side resistance S and point load P are plotted respectively against the settlement of the top, the mid point of the shaft and the base of the pile.

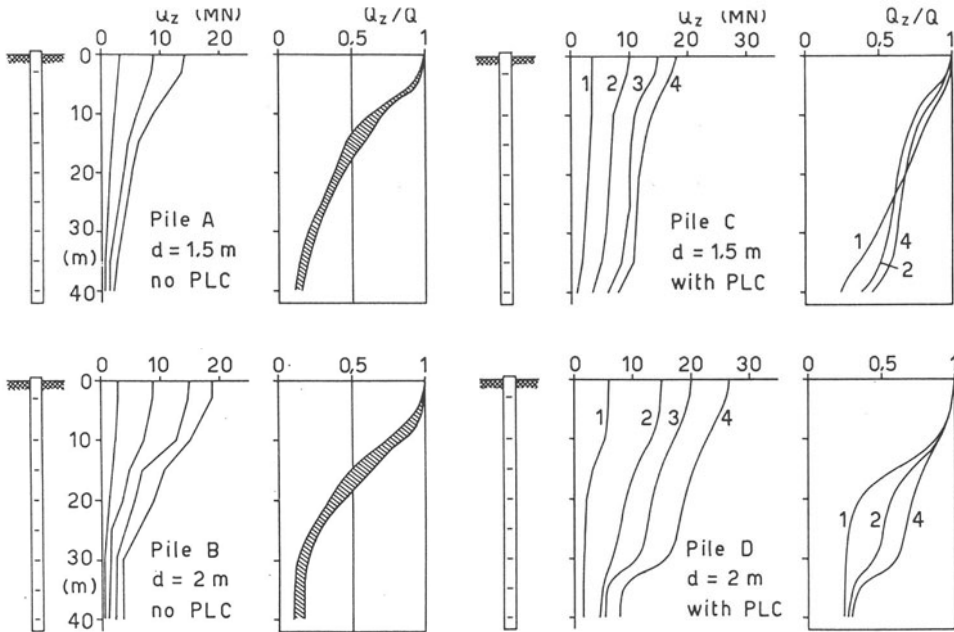


Fig. 18. Distribution of the axial load Q_z along the shaft of the four piles during the loading tests

the shaft of the piles at various load levels are reported.

In piles A and B, not equipped with the pre-loading cell, the mobilization of P and S has been very nearly proportional, and P accounts for 10% - 15% of the total applied load over the whole range of loads.

In piles C and D, with the pre-loading cell, the percentage of load taken by the pile base increases with increasing load level, reaching 30% - 45% of the total load in the failure range.

The data collected allow a check of the procedure to evaluate a lower bound of the bearing capacity presented before (eq. 7 to 9). The relevant data are listed in the following table.

pile	d(m)	p_i (MPa)	$2p_i A$ (MN)	S(MN)	P(MN)	Q_{ult} (MN)
C	1,5	4,0	14,2	11,5	8	19
D	2,0	4,4	27,6	19,0	8	28

Eq. (9) appears to be satisfied in both cases, thus substantiating the proposed procedure; it must be said, however, that this result may be somewhat fortuitous since eq. (8) is not satisfied by the results obtained on the pile D.

6. LOADING TESTS ON INSTRUMENTED PILES

Loading tests of foundation piles are rather common in the construction practice, and are indeed the most satisfactory procedure to check the successful construction of a pile (proof tests) or to measure its bearing capacity (tests to failure). The test set up and procedures are well known (MARCHETTI, 1975; AGI, 1984).

For small and medium diameter piles the maximum test load is in the range of some tens to a few hundreds of tons. In these cases, a number of piles between 2% and 4% of the total is usually proof tested in Italy.

In the case of large diameter piles, the test load attains many hundreds and even thousands of tons; the test is therefore extremely expensive. For this reason, the number of tests that are performed in practice is very small, just for those piles that need a careful control because of the very high service loads.

The attempt of getting a maximum of data from such expensive tests appears therefore justified. This can be done by instrumenting the shaft of the pile to determine the distribution of the axial load and the transfer curves across the base and along the lateral surface.

Besides providing valuable informations for the foundation design in the particular case under investigation, these findings allow the development of semiempirical design criteria (VIGGIANI, 1973; MEYERHOF, 1976; GHIONNA et al., 1979). And indeed the availability of a wealth of data referring to relatively uniform soil types and to well defined construction techniques is believed to be a prerequisite for a substantial improvement of our capacity of predicting the behaviour of piles.

Accordingly, some informations on the instrumentation of piles are given below, with the aim of promoting a diffusion of these techniques, that are relatively simple and whose cost is not high in comparison to the total cost of a loading test.

Further details can be found in a number of papers (MARCHETTI, 1975; WRIGHT, REESE, 1979; CAPUTO et al., 1989; ROCCHI et al., 1989).

The load is applied to the test pile by a hydraulic jack, and it is normally determined by measuring the oil pressure in the jack. It has been found that this measurement is very unreliable, because of the random occurrence of

significant friction between the ram and the cylinder; therefore the provision of a load cell interposed between the jack and the reaction frame is mandatory.

Rugged load cells, suited for use under the adverse conditions prevailing on a construction site but yet very accurate and reliable are now currently available; their full scale capacity reaches even 1000 tons (fig. 19).

The distribution of the axial load along the shaft of the pile may be determined in the following ways.

- Direct measurement of the load by means of load cells interrupting the continuity of the shafts at various depths (PRICE, WARDLE, 1983).
- Measurements of the vertical displacements of a number of points at various depths by means of tell-tales (SNOW, 1965) or amovable extensometers (BAGUE-LIN, JEZEQUEL, 1975).
- Measurements of the axial strain in some sections by means of suitable strain gages (REESE, O'NEILL, 1988; CAPUTO et al., 1989).

The direct measurement is the most satisfactory technique, since it is unaffected by factors such as the effective area of the pile and the compression modulus of the concrete. Unfortunately, it is very expensive and may be adopted only in special cases.

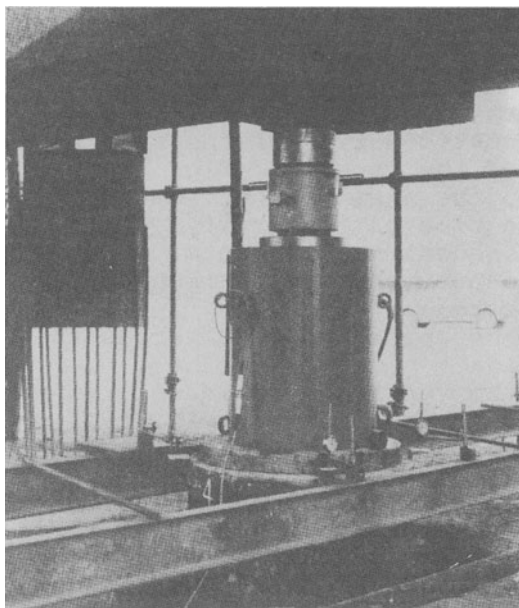


Fig. 19. Hydraulic jack and strain gages load cell; full scale : 1000 t

The writer has systematically adopted the strain measurement technique, with strain gages bonded to steel bars with square cross section $0,8 \times 0,8 \text{ cm}^2$ and a length of 40 cm. The strain gages are covered by a watertight resin protection.

These "strain bars" are fixed to the reinforcement cage (fig. 20) in a number of at least 3 (better 4) in each measuring section. The number of sections varies between 3 and 8, depending on the length of the pile, the subsoil conditions and the liberality of the sponsor.

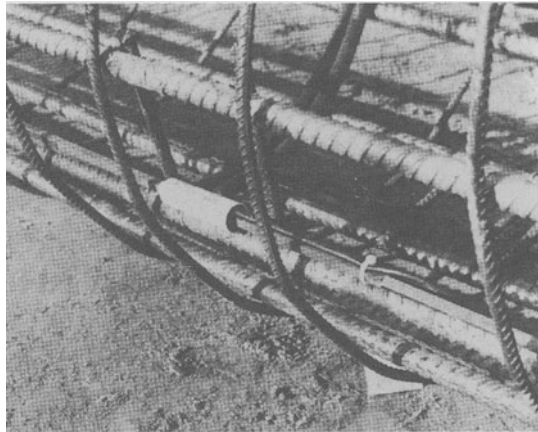


Fig. 20. Strain bar fixed to the reinforcement cage

Soon after concreting the shaft, the strain bars are checked and a systematic survey of the strain is carried out during the curing of the concrete (fig. 21). The increment of strain due to the shrinkage of the concrete must be negligible at the time of load test, otherwise it could affect all the subsequent measurements.

During a load test on an instrumented pile the following data are collected:

- the curve of the applied load Q versus the settlement s of the pile head;
- the values of the vertical strain ϵ_z in the instrumented sections at the various load levels.

To calculate the values of the axial load N from the values of the axial strain ϵ_z the axial rigidity EA of the pile should be known (E = Young modulus of the concrete; A = area of the cross section of the pile, taking into account the reinforcement).

For a pile cast in situ the area A can be determined only as an average value over a certain pile length, by monitoring the volumes of concrete and the levels of the

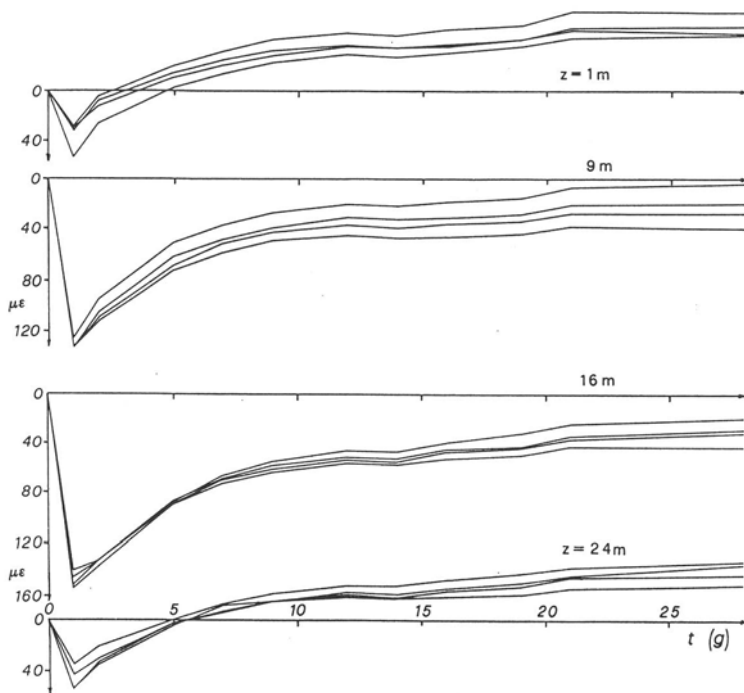


Fig. 21. Strain measurements at various depths in the shaft of a pile during the curing of the concrete

surface of the concrete in the pile shaft during concreting. The values of E depend on the curing condition prevailing in the different instrumented sections, such as overburden pressure and occurrence of ground water, as well as on the composition of the concrete and the procedure of casting.

For a given pile it is usually assumed that the rigidity EA is constant over the shaft; with this assumption, the distribution of N along the shaft is proportional to that of the axial strain ϵ_z and may be obtained from it once the value of N in any section is known.

The value of N in the upper first instrumented section may be taken as known, because this section is purposely located near the pile head and the fraction of load taken by side friction is negligible at that level.

A better approximation may be easily obtained, if needed, by assuming a realistic distribution of the side resistance between the head of the pile and the first instrumented section.

From the measurements of the settlement of the head of the pile and of the axial strain in the instrumented sections, the displacement of all the points of the pile may be

determined; it should be always directed downward. Sometimes apparent upward displacements result from the data; should this be the case, the assumption that EA is constant would be no more acceptable and more sophisticated elaborations would be needed accounting for the observed variations of A , if any, for the non linearity of the concrete (variations of E with the load level), for informations on the quality of the concrete obtained by sonic logging, if any.

The final result of the elaboration is a diagram of the axial load N along the shaft of the pile for each applied load Q . Transfer curves of side shear may also be developed; an example is reported in fig. 22.

An example of the kind of results that can be obtained by loading tests on instrumented piles has been reported in the previous par. 5.

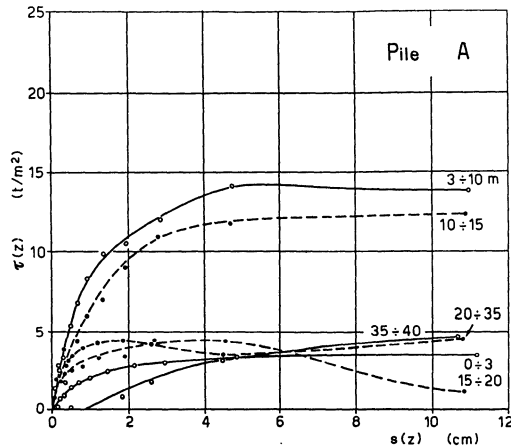


Fig. 22. Transfer curves of side resistance at various depths. Pile A of fig. 17

7. INTEGRITY TESTING

The expensiveness of the loading tests on large diameter piles makes the non destructive integrity testing methods very interesting. They allow a rapid and cheap check of the quality of the pile and make it possible to test a large proportion of the piles (or even all the piles).

The test methods most widespread in Italy are the sonic logging and the mechanical admittance (CARABELLI, LIBERATI, 1985).

As it is well known, the former requires 2 or 3 access tubes for sondes to be cast in the pile. This implies a pre-selection of the pile to be tested, with the possibility of greater care being taken in the construction of these particular piles. Of course, if all the piles are tested this disadvantage becomes an advantage.

Sonic logging is conducted from hole to hole by horizontal scanning, dipping a transmitter probe in one hole and a receiver in another; the logging is based on recording the velocity of sound waves in the concrete between the transmitter and the receiver. The results give continuous and detailed informations about the quality of the concrete and the occurrence of defects such as voids, porous concrete or soil inclusions.

The cost is in the range of 200.000 - 400.000 lit per pile, in addition to the cost of the access tubes. If these are made by steel, as it is desirable, they can be computed in the reinforcement area.

In the mechanical admittance method a steady pulsating force or an impact force is applied to the pile head by a small vibrator or by a light hammer. The induced velocity of the pile head as well as the applied force are then simultaneously monitored; from these data it is possible to retrieve informations regarding the integrity and stiffness of the pile, its length and the occurrence of major changes in its cross section.

The cost is in the range of 50.000 - 250.000 lit per pile, and no previous preparation of the pile is needed.

The sonic logging, at present, is believed to be more exhaustive and reliable; however, it gives only informations on the quality and integrity of the concrete in the pile shaft.

The mechanical admittance method is much more uncertain, since expert interpretation of the results is needed;

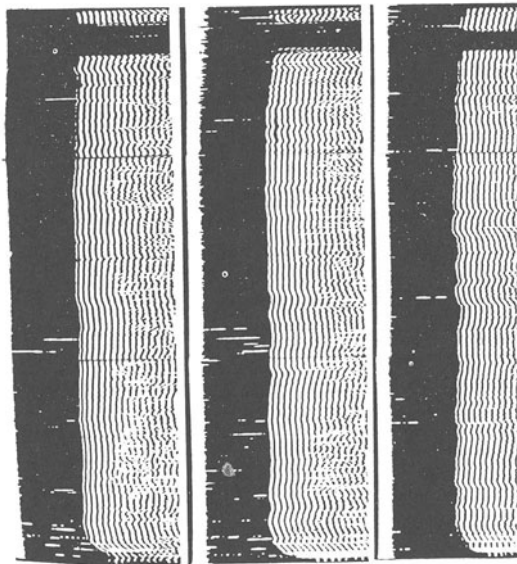


Fig. 23. Results of sonic logging of a bored pile with $d=2\text{m}$ and $L=42\text{m}$

nevertheless, it offers some potential of estimating the bearing capacity of the pile and the pile-soil stiffness at low strain. Recently, this method is evolving towards a dynamic load test, in which a substantial force is applied to the head of the pile (e.g., by the drop of a pile hammer) (HERITIER, 1989).

In fig. 23 (VIGGIANI, VINALE, 1983) the results of sonic logging on a large diameter bored pile are reported. A striking defect is evident on a stretch of 2,5 m near the head of the pile.

A large inclusion of soil and drilling mud was actually detected by excavating around the head of the pile (fig. 24); it probably occurred during the withdrawal of the guide casing.

In other cases the results obtained are less clear. At a site in the eastern Naples area many hundreds of bored piles, part end bearing on the tuff and part floating, were installed with diameters ranging from 0,8 m to 1,5 m and lengths from 32m to 43 m. Twenty proof loading tests are available, in addition to sonic logging of all the piles.

Some defects have been detected on four of the twenty test piles; an example is reported in fig. 25. Nevertheless (fig. 26) the results of the loading tests on the "defective" piles can not be distinguished from those on "intact" piles.

From this and many similar evidences it may be concluded that the integrity test methods, at their present

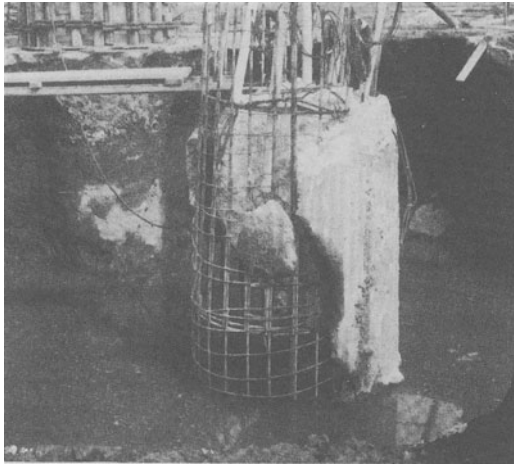


Fig. 24. The upper section of the pile of fig. 23, after excavation

development stage, have an essentially semiquantitative character

If the results of the test are satisfactory, the good quality of the concrete of the pile shaft is warranted; though being very useful, this information is far from being exhaustive.

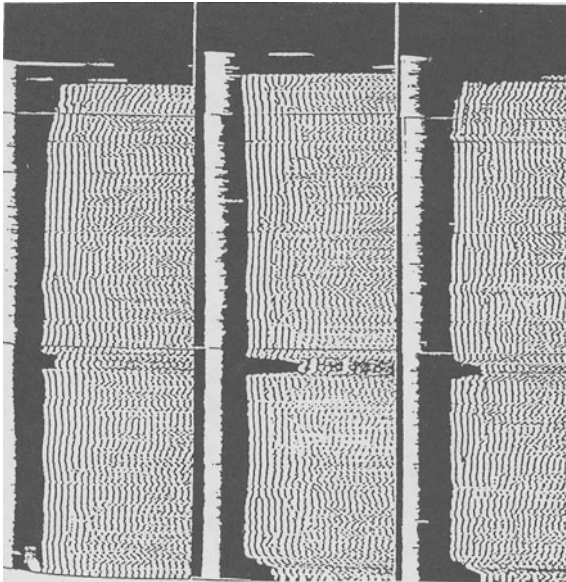


Fig. 25. Sonic logging of a bored pile with $d = 0,8$ m, $L = 34$ m

If the test evidentiates some defects, the assessment of their gravity is not straightforward.

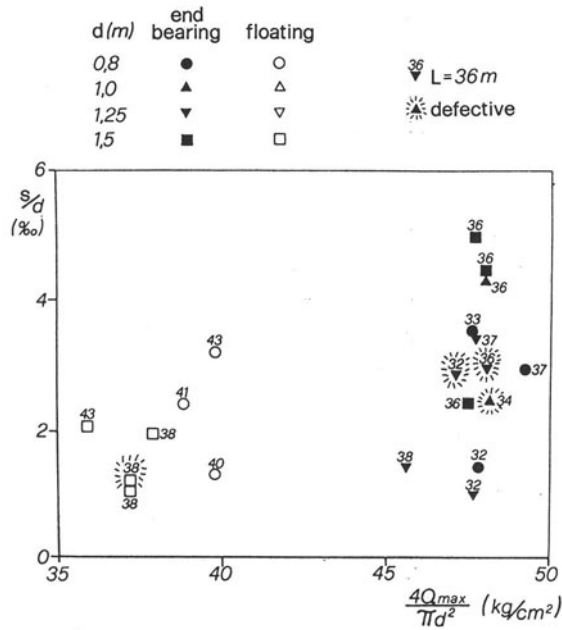


Fig. 26. Settlement at the maximum test load measured on "intact" and "defective" piles

8. CONCLUDING REMARKS

In this paper some data and comments concerning the influence of technological factors on the behaviour of foundation piles have been presented, without even attempting a systematic and exhaustive state-of-the-art.

Due to the somewhat random influence of technological factors and to the scatter of the properties of natural soil deposits, even within the same foundation significant differences occur in the behaviour of supposedly identical piles.

Some data on the variability of the load-settlement behaviour, as observed in loading tests on a substantial number of piles, are listed in the following table (CAPUTO, VIGGIANI, 1989).

SITE	FOUND.	PILES				Q_e (t)	RESULTS OF PROOF LOADING TESTS								
		Type *	L (m)	d (m)	n. of tests		at $Q = Q_e$			at $Q = 1,5Q_e$			at $s = s_{Q_e}$		at $s = s_{1,5Q_e}$
							\bar{s} (mm)	\tilde{s} (mm)	v_s	\bar{s} (mm)	\tilde{s} (mm)	v_s	v_Q	v_Q	
A	1	D	8,0	0,40	12	60	1,89	0,78	0,41	4,36	2,31	0,53	0,23	0,25	
	2	D	18,0	0,52	17	120	3,35	1,02	0,30	11,68	8,14	0,70	0,16	0,19	
B	3	D	15,0	0,50	16	80	1,43	0,51	0,36	2,76	1,07	0,39	0,22	0,20	
C	4	B	14,5	0,45	16	60	1,10	0,21	0,19	2,40	0,68	0,28	0,11	0,12	
D	5	B	20,0	0,80	22	110	0,92	0,20	0,21	2,03	0,69	0,34	0,13	0,13	
E	6	B	15,0	0,60	9	115	1,26	0,50	0,40	5,05	2,29	0,59	0,21	0,27	
	7	B	15,0	0,60	14	115	1,10	0,51	0,46	4,49	2,87	0,64	0,20	0,22	
F	8	B	20,0	0,40	19	40	0,96	0,46	0,48	1,99	0,82	0,41	0,25	0,17	
	9	B	18,0	0,60	14	75	0,88	0,42	0,48	1,78	0,82	0,46	0,29	0,23	
	10	B	18,0	0,80	6	150	2,10	0,63	0,30	5,56	1,91	0,34	0,17	0,12	
	11	B	22,0	0,50	9	58	1,64	0,87	0,53	3,61	1,98	0,55	0,37	0,28	
	12	B	22,0	0,80	19	150	2,83	0,99	0,35	8,24	4,45	0,54	0,16	0,16	
G	13	D	21,5	0,35	18	50	2,34	0,42	0,18	4,03	0,86	0,21	0,19	0,24	
H	14	B	9,0	0,50	22	30	0,25	0,04	0,17	0,46	0,07	0,15	0,10	0,08	
	15	B	9,0	0,50	10	60	0,85	0,14	0,17	1,44	0,16	0,11	0,11	0,08	
	16	B	11,0	0,50	11	60	0,92	0,13	0,14	1,61	0,27	0,17	0,12	0,13	
I	17	A	15,5	0,60	6	110	2,77	0,91	0,33	6,05	2,17	0,36	0,25	0,25	
L	18	A	12,6	0,80	10	140	5,40	2,34	0,43	12,71	5,03	0,40	0,21	0,13	

* D = driven pile; B = bored pile; A = auger pile; Q_e = service load; \bar{s} = mean value; \tilde{s} = standard deviation; v_s = coefficient of variation of the settlement; v_Q = coefficient of variation of the load

From the viewpoint of the design, this kind of results could engender a serious lack of confidence. The design of pile foundation is indeed based essentially on an empirical or semiempirical approach. Any rational analysis is necessarily based on oversimplified models and allows but an evaluation of the relative weight of the different factors.

The main role of the theory is actually to provide a logical framework to arrange the results of the experience, in order to generalize them and make them available in other cases.

Isn't this exactly the scheme of "...rational principles that the mind imposes to the sensible data so that they can be part of the experience...", that characterizes the Kantian rationalism?

Even with his feet in the mud of a pile yard, the geotechnical engineer remains holder of a rational culture!

9. REFERENCES

- AGI (1984) Raccomandazioni sui pali di fondazione. Roma.
- BAGUELIN F., JEZEQUEL J.F. (1975) Mesure des élongations dans les pieux et tirants à l'aide de extensomètres amovibles. Travaux.
- CAPUTO V., VIGGIANI C. (1988) Some experiences with bored and auger piles in Naples area. Symp. on deep foundations on bored and auger piles, Ghent. Balke-
ma, Rotterdam.
- CAPUTO V., GAMBACORTA F., VIGGIANI C. (1989) Pali trivellati di grande diametro nei terreni piroclastici del Napoletano. XVII Convegno Italiano di Geotecnica, Taormina.
- CAPUTO V., VIGGIANI C. (1989) Intervento alla discussione, Sessione n.2, XVII Convegno Italiano di Geotecnica, Taormina.
- CARABELLI E., LIBERATI G. (1985) Controlli non distruttivi dei pali di fondazione. Conf. di Geotecnica di Torino, XII Ciclo.
- CROCE A., PELLEGRINO A. (1967) Il sottosuolo della città di Napoli. Caratterizzazione geotecnica del territorio. VIII Convegno Italiano di Geotecnica, Cagliari.
- DIAMANTI R. (1973) Intervento alla discussione, Sessione 1, XI Convegno Italiano di Geotecnica, Milano.
- GHIONNA V., JAMIOLKOWSKI M., LANCELOTTA R. (1979) Valutazione della capacità portante di un palo di fondazione. Conf. di Geotecnica di Torino, IX Ciclo.
- HERITIER B: (1989) Capacité portante des pieux par chargement dynamique. La methode CEBTP. XII Int. Conf. Soil Mech. Found. Eng., Rio de Janeiro.
- LIZZI F. (1976) Pieux de fondation Fondedile à cellule de precharge. Construction, n. 6, Paris.
- LIZZI F., VIGGIANI C., VINALE F. (1983) Some experiences with pre-loading cells at the base of large diameter bored piles. VII Asian Reg. Conf. Soil Mech. Found. Eng., Haifa.
- MARCHETTI S. (1975) Prove di carico verticale statico su pali con o senza strumentazione. Conf. di Geotecnica di Torino, VII Ciclo.
- MASCARDI C. (1985) Esecuzione e cenni sul dimensionamento dei pali trivellati con elica continua. Conf. di

Geotecnica di Torino, XII Ciclo

- MEYERHOF G.G. (1976) Bearing capacity and settlement of pile foundations. Journ. Geot. Eng. Div., Proc. ASCE, n. GT3.
- PRICE G., WARDLE I.F. (1983) Recent developments in pile-soil instrumentation systems. Field Meas. in Geomechanics, Zurich.
- REESE L.C., O'NEILL M.W. (1988) Field load tests on drilled shafts. Symp. on deep foundations on bored and auger piles, Ghent. Balkema, Rotterdam.
- RIPPA F., VINALE F. (1982) Experiences with CPT in eastern Naples area. 2nd ESOPT, Amsterdam.
- ROCCHI G., ALBERT L.F., VACCA O., NARDOCCI A., SALVI M., MONTINARO N. (1989) Prove di carico strumentate a rottura su pali di grande diametro trivellati in sabbia. XVII Convegno Italiano di Geotecnica, Taormina.
- SIMONS M., H. (1961) Discussion, Session 3b, V Int. Conf. Soil Mech. Found. Eng., Paris, vol. 3.
- SNOW R. (1965) Tellaies. Foundations facts, Raymond International.
- VAN IMPE W. (1984) Pile loading test results on an Atlas screwpile. 6th Budapest Conf. Soil. Mech. Found. Eng.
- VAN IMPE W. (1988) Consideration on the auger piles design. Symp. on deep foundations on bored and auger piles, Ghent. Balkema, Rotterdam.
- VAN WEELE A.F. (1988) Cast in situ piles. Installation methods, soil disturbance and resulting pile behaviour. Symp. on deep foundations on bored and auger piles, Ghent. Balkema, Rotterdam.
- VIGGIANI C. (1973) Significato e limiti delle teorie e dei procedimenti di calcolo per la progettazione dei pali di fondazione. Studi e rendiconti, Corso di Perfezionamento nelle costruzioni in c.a., Politecnico di Milano.
- VIGGIANI C., VINALE F. (1983) Comportamento di pali trivellati di grande diametro in terreni piroclastici. Rivista Italiana di Geotecnica, vol. XVII, n. 2.
- VINALE F. (1988) Caratterizzazione del sottosuolo di un' area campione di Napoli ai fini di una microzonazione sismica. Rivista Italiana di Geotecnica, vol. XXII, n. 2.
- WHITAKER T. (1976) The design of pile foundations. Pergamon Press, Oxford.
- WRIGHT S.J., REESE L.C. (1979) Construction of drilled shafts and design for axial loading. U.S. Dpt. of Transportation: Drilled Shafts Manual, vol I. Washington.

COMPUTER BASED STRUCTURAL ANALYSIS OF BRIDGES

S. Odorizzi

University of Padua, Padua, Italy

SUMMARY

Some applications are presented for the computer based structural analysis of bridges. The possibility of employing general purpose computer programs is also discussed, with specific reference to finite element programs, to get an effective solution of a variety of problems typical of such structures. The methods here proposed are not at all exhaustive of the subject; they are aimed to characterize the attitude with which the user of any actual computer program should face a particular category of structures.

1. INTRODUCTION.

Most of the general methods for the computer based modelling and analysis of structures and continuous bodies are well established as far as their theoretical assumptions and analytical developments are concerned, as well as the features more strictly pertaining to the practice of their being coded into computer programs.

The applications to particular structures - that is structures entering categories with respect to the problems brought up and to the methods of solution - induce two typical attitudes, reflecting two classes of problems partially complementary.

Any structure can be handled by general purpose programs. At the most the performances of such programs can be improved by writing a procedure chaining the logical sequence of the operations and reworking the results, to comply also with the requirements of given standards. For instance a finite element fully three-dimensional model is commonly applicable.

On the other hand, and more frequently under condition of recurrence of a specific problem, a particular program should be implemented. This is normally quite far from the general procedures for the structural modelling, as tends to reproduce the hand calculations, the assumptions and the approximations of which are accepted with the aim of speeding up the solution, obtaining everyday professional results.

Fearing to have enough time to study a problem thoroughly, both the approaches should co-exist, entrusting the designer with the decision of employing a numerical model when the complexity of the matter or some conditions laying within the problem spoil the application of an approximated fixed-schema program.

In this paper the methods and their applications are roughly classified into three groups.

The first group includes the applications which are not implementing numerical procedures established within the methods of computer based structural analysis, such as those programs - directly written by the user or committed to specialized software houses - which are reproducing a hand calculation for a given practical purpose. For instance the problem of drawing from the stress resultants the stress distribution over a section of a structural member falls into this category. As these applications do not give rise to any general subject of discussion, they are not mentioned in what follows.

The second category covers the so-called semi-numerical or semi-analytical methods. These formulations are quite general, but the applications are suitable for particular structures, including most of the bridges. Here the solution for slab bridges as a series of continuous plates connected to beams having rotatory and flexural inertia is presented, as well as the finite prism method.

The third category concerns the numerical methods and, in particular, the finite element method. A general discussion is proposed and some details are given on the implementation of a variable thickness thick plate element and on the geometrically non-linear analysis of combined beam and cable structures.

2. ANALYSIS OF SLAB BRIDGES AS A SERIES OF CONTINUOUS PLATES CONNECTED TO BEAMS HAVING ROTATORY AND FLEXURAL INERTIA.

The application is fully described in references [1] and [2]. Here the discussion is proposed as a useful implementation of the finite strip method, an extension of which is presented in the next paragraph.

The method is introduced referring to the following figure 1, showing a rectangular simply supported bridge deck, with ledgers only at the ends.

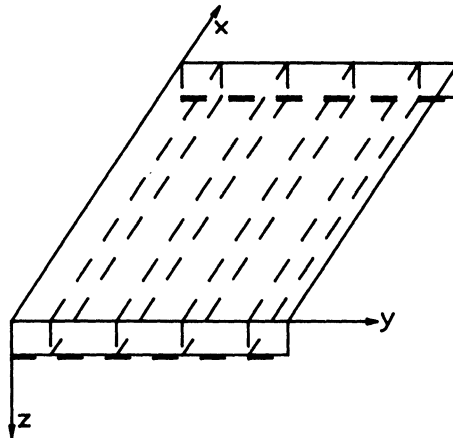


Fig. 1 Schema of the bridge deck.

The slab is divided into strips of constant or linearly variable thickness according to geometric conditions or position and arrangement of loads. In the longitudinal direction the stiffness coefficients of beams and slabs are expressed in Fourier's series, imposing the continuity and the equilibrium equations to each term of the expansion. The loads are also described in terms of Fourier's series. Transversally to the deck the integration is carried out in exact form. Hence the problem is reduced to a one-dimensional one, and from an operative point of view any harmonic contribution is similar to the analysis of a continuous beam on elastic supports. The precision depends only on the number of harmonic terms employed.

Developing the stiffness matrices and the equivalent nodal loads of the problem the authors start from further assumptions. These are

- that the deck plate is a flat plate, connected to simply supported, constant cross-section beams, having rotatory and flexural inertia and rigidly bounded to the end ledgers;

- that the ledgers are perfectly rigid in their own plane and without torsional stiffness;
- that bending stresses and in-plane stresses of the plate are independent of each other;
- that the loads are transversally constant over any strip;
- that concentrated loads are only in correspondence of subdivision lines.

Therefore the position of the longitudinal beams and the hypotheses on the loads give the conditions for the strip subdivision of the deck.

In the above references the Levy's solution is adopted for the plate. The corresponding stiffness matrices can be obtained by formally expressing each term, and hence imposing to any harmonic a vertical displacement (fig. 2)

$$w_n = \gamma_{on} \sin\left(\frac{n\pi x}{l}\right) ; \quad \varphi_n = 0 \quad (1)$$

and a rotation (fig. 3)

$$\varphi_n = \Phi_{on} \sin\left(\frac{n\pi x}{l}\right) ; \quad w_n = 0 \quad (2)$$

Such displacement and rotation are on the edge i of the strip, while the opposite edge j is fully clamped.

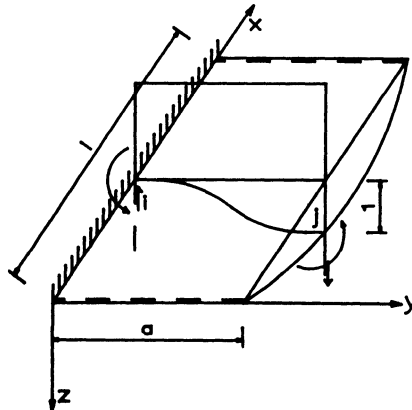


Fig. 2 Reference schema for the imposed displacement.

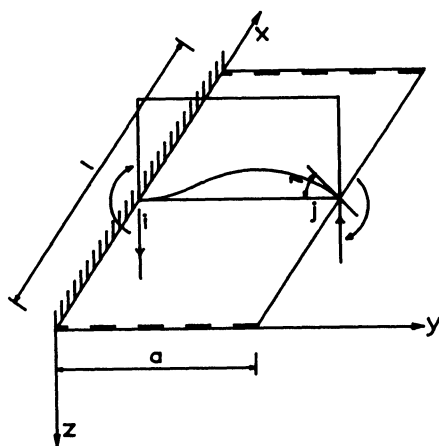


Fig. 3 Reference schema for the imposed rotation. The corresponding stress parameters are obtained

$$\left(M_{wn} \right)_i = \frac{n^2 \pi^2}{l^2} B \frac{\sinh^2 \alpha_n + \alpha_n^2}{\sinh^2 \alpha_n - \alpha_n^2} \gamma_{on} \sin \left(\frac{n\pi x}{l} \right) \quad (3)$$

$$\left(T_{wn} \right)_i = \frac{2n^3 \pi^3}{l^3} B \frac{\sinh \alpha_n \cosh \alpha_n + \alpha_n}{\sinh^2 \alpha_n - \alpha_n^2} \gamma_{on} \sin \left(\frac{n\pi x}{l} \right)$$

$$\left(M_{\varphi n} \right)_i = \frac{2n\pi}{l} B \frac{\sinh \alpha_n \cosh \alpha_n - \alpha_n}{\sinh \alpha_n - \alpha_n}$$

$$\left(T_{\varphi n} \right)_i = \frac{n^2 \pi^2}{l} B \frac{\sinh^2 \alpha_n + \alpha_n^2}{\sinh^2 \alpha_n - \alpha_n^2}$$

$$\left(M_{wn} \right)_j = \frac{2n^2 \pi^2}{l^2} B \frac{\alpha_n \sinh \alpha_n}{\sinh^2 \alpha_n - \alpha_n^2} \gamma_{on} \sin \left(\frac{n\pi x}{l} \right)$$

$$(T_{wn})_j = \frac{2n^3 \pi^3}{l^3} B \frac{\sinh \alpha_n + \alpha_n \cosh \alpha_n}{\sinh^2 \alpha_n - \alpha_n^2} \gamma_{on} \sin\left(\frac{n\pi x}{l}\right)$$

$$(M_{\varphi_n})_j = \frac{2n\pi}{l} B \frac{\sinh \alpha_n - \alpha_n \cosh \alpha_n}{\sinh^2 \alpha_n - \alpha_n^2}$$

$$(T_{\varphi_n})_j = \frac{2n^2 \pi^2}{l^2} B \frac{\alpha_n \sinh \alpha_n}{\sinh^2 \alpha_n - \alpha_n^2}$$

where

- M is the bending moment distribution,
- T is the shear force distribution,
- w refers to the vertical displacement,
- φ refers to the rotation,
- i refers to the edge i,
- j refers to the edge j,
- n is the harmonic number,

and

$$B = \frac{Es^3}{12(1-\nu^2)} \quad (4)$$

$$\alpha_n = \frac{n\pi a}{l} \quad (5)$$

Hence the stiffness coefficients are determined employing the virtual work equation.

The equivalent nodal loads are drawn referring to a strip which is simply supported at the ends and fully constrained along the longitudinal edges. To this strip the following load is applied

$$q(x, y) = q_0 \sin \frac{n\pi x}{l} \quad (6)$$

obtaining after some algebra the equivalent nodal forces.

Then the overall stress state is determined imposing the equilibrium conditions along each subdivision line. This yields for any harmonic contribution to a linear system of equations of the form

$$K_n w_n = F_n \quad (7)$$

Once the displacements are obtained, the stress parameters can also be drawn by proportion. Eventually all the harmonic contributions are summed up.

3. THE FINITE PRISM METHOD.

The finite strip method, an application of which has just been described combining strips and beams for the analysis of bridge decks, roots back to references [3] and [4].

The idea is extended to three-dimensional problems as a combination of finite elements and Fourier's series. Approaches of this type are well established and have been worked out in quite a remote past of informatics [5],[6],[7],[8]. Reference [9] deals with simply supported bridge boxes; reference [10] gives an almost complete review of the method.

The main advantage of the method has been pointed out in the past as the possibility of substantially reducing the computational efforts and the computer core memory requirements, as a consequence of dealing with a three-dimensional problem through a series of two-dimensional ones. Nowadays the practical use of the method depends probably more on the possibility of having a 'natural' description of problems and loads.

The method applies to structures as those in figure 4.

To focus the leading idea of such approach, the deflection of a simply supported beam (fig. 5) is firstly introduced.

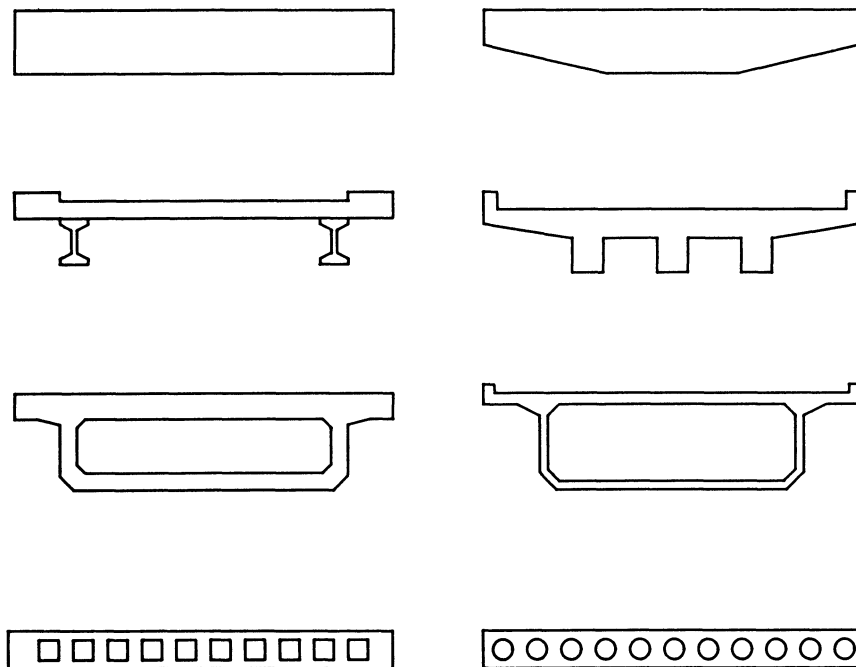


Fig. 4 Typical structures to which the finite prism method applies.

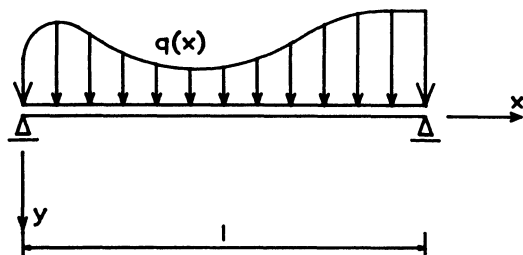


Fig. 5 Simply supported beam under distributed loading.

The differential equation for a beam in bending is

$$q(x) = EJ \frac{d^4 y}{dx^4} \quad (8)$$

in which y must satisfy the boundary conditions

$$y = 0 \quad \text{at } x = 0 \quad \text{and } x = 1 \quad (9)$$

$$\frac{d^2y}{dx^2} = 0 \quad \text{at } x = 0 \quad \text{and } x = 1$$

The deflection y can be expanded in Fourier's series as :

$$y = \sum_{m=2}^{\infty} a_m \sin\left(\frac{m\pi x}{1}\right) \quad (10)$$

where m refers to the harmonic term, and a_m is the unknown amplitude of the m^{th} harmonic.

The loading $q(x)$ is defined by the Fourier's series

$$q(x) = \sum_{m=1}^{\infty} b_m \sin\left(\frac{m\pi x}{1}\right) \quad (11)$$

where b_m is the amplitude for the harmonic m , and can be obtained using the Euler's formula

$$b_m = \frac{2}{1} \int_0^1 q(x) \sin\left(\frac{m\pi x}{1}\right) \quad (12)$$

Therefore, for a given harmonic of load the problem is one of finding the unknown amplitude a_m which uniquely describes the deflected profile for that harmonic. Substituting equations (10) and (11) into equation (8) leads to

$$a_m = \frac{1^4 b_m}{m^4 \pi^4 EJ} \quad (13)$$

The final deflected profile can be obtained carrying out the summation (10) over an adequate number of terms.

This series converges rapidly. For instance the mid-span deflection corresponding to a triangular distributed load is determined

with precision of three digits using only three terms of the series, and with precision of two digits using only the first term of the series.

To generalize, reference is made to the prismatic solid of figure 6, which can be also generated by sweeping the section through a circular arc. According to the displacement approach, the displacements are described in terms of harmonic functions along the longitudinal direction, while maintaining the shape functions typical of the finite element formulation in the cross-section. Therefore the convergence depends on the number of harmonic terms as well as on the finite element subdivision.

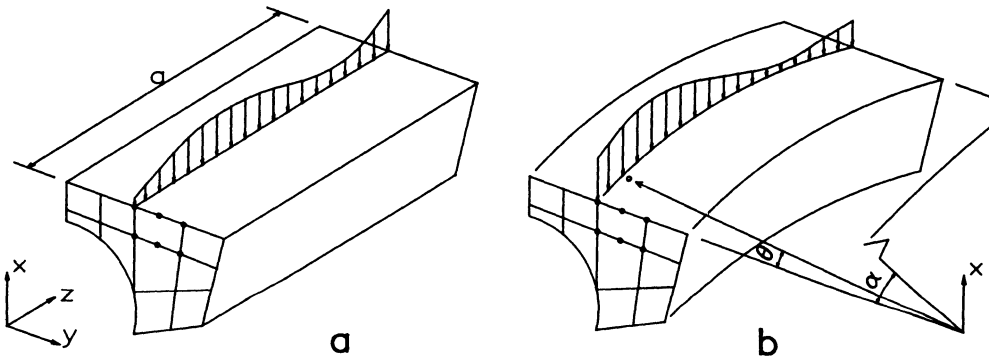


Fig. 6 Typical prismatic situation: a-straight prism, b-curved prism.

In what follows, to give some details of the method, an isoparametric finite element formulation is proposed, based on parabolic shape functions, and simple basic functions in the longitudinal direction.

The displacements for a prismatic body can be expressed as

$$\tilde{\mathbf{a}}^T = [u, v, w] \quad (14)$$

where

$$u = \sum_{l=1}^{\infty} \sum_{i=1}^n N_i u_i^l \sin\left(\frac{l\pi z}{a}\right) \quad (15)$$

$$v = \sum_{l=1}^{\infty} \sum_{i=1}^n N_i v_i^l \sin\left(\frac{l\pi z}{a}\right)$$

$$w = \sum_{l=1}^{\infty} \sum_{i=1}^n N_i w_i^l \sin\left(\frac{l\pi z}{a}\right)$$

N_i are the shape functions, expressed in terms of curvilinear local coordinates ξ and η , n denotes the number of nodes per element and l refers to the harmonic number.

Due to the nature of the basic functions, the following boundary conditions must always apply

$$u = v = \frac{dw}{dz} = 0 \quad \text{at } z = 0 \quad \text{and } z = a \quad (16)$$

These describe a simple support condition such that at the ends of the prism the in-plane displacements and the axial strains are both zero.

The stiffness matrix of the prism gives

$$\tilde{F} = K\tilde{\delta} \quad (17)$$

where

$$\tilde{F}^T = \left[\tilde{F}^1 \dots \tilde{F}^1 \quad \tilde{F}^m \quad \tilde{F}^n \right] \quad (18)$$

$$\tilde{\delta}^T = \left[\tilde{\delta}^1 \dots \tilde{\delta}^1 \quad \tilde{\delta}^m \quad \tilde{\delta}^n \right]$$

F and δ represent respectively the vector of the equivalent nodal forces and the vector of the unknown displacements for the l^{th} harmonic.

A typical submatrix of K can be written as

$$K_{\tilde{i},j}^{l,m} = \int_v [B_{\tilde{i}}^l]^T D_{\tilde{j}} B_{\tilde{j}}^m dv \quad (19)$$

where the range of integration is taken over the whole solid volume of the prism and can be performed numerically.

The strain matrix $B_{\tilde{i}}$, by introducing the displacement components (15) becomes

$$B_{\tilde{i}}^l = \bar{B}_{\tilde{i}}^l \sin\left(\frac{l\pi z}{a}\right) + \bar{B}_{\tilde{i}}^l \cos\left(\frac{l\pi z}{a}\right) \quad (20)$$

where

$$\bar{B}_{\tilde{i}}^l = \begin{bmatrix} \frac{\partial N_1}{\partial x} & 0 & 0 \\ 0 & \frac{\partial N_1}{\partial y} & 0 \\ 0 & 0 & -N_1 \frac{l\pi}{a} \\ \frac{\partial N_1}{\partial y} & \frac{\partial N_1}{\partial x} & 0 \\ 0 & 0 & 0 \\ 0 & 0 & 0 \end{bmatrix} \quad (21)$$

$$\tilde{B}_1^1 = \begin{bmatrix} 0 & 0 & 0 \\ 0 & 0 & 0 \\ 0 & 0 & 0 \\ 0 & 0 & 0 \\ N_1 \frac{1\pi}{a} & 0 & \frac{\partial N_1}{\partial x} \\ 0 & N_1 \frac{1\pi}{a} & \frac{\partial N_1}{\partial y} \end{bmatrix} \quad (22)$$

A transformation is needed to relate the strain in curvilinear coordinates ξ and η to strain in global coordinates x, y . Such transformation may be written as

$$\begin{bmatrix} \frac{\partial u^1}{\partial x} & \frac{\partial v^1}{\partial x} & \frac{\partial w^1}{\partial x} \\ \frac{\partial u^1}{\partial y} & \frac{\partial v^1}{\partial y} & \frac{\partial w^1}{\partial y} \end{bmatrix} = \tilde{J}^{-1} \begin{bmatrix} \frac{\partial u^1}{\partial \xi} & \frac{\partial v^1}{\partial \xi} & \frac{\partial w^1}{\partial \xi} \\ \frac{\partial u^1}{\partial \eta} & \frac{\partial v^1}{\partial \eta} & \frac{\partial w^1}{\partial \eta} \end{bmatrix} \quad (23)$$

where \tilde{J} is the jacobian matrix

$$\tilde{J} = \begin{bmatrix} \frac{\partial x}{\partial \xi} & \frac{\partial y}{\partial \xi} \\ \frac{\partial x}{\partial \eta} & \frac{\partial y}{\partial \eta} \end{bmatrix} \quad (24)$$

and

$$x = \sum_{i=1}^n N_i(\xi, \eta) x_i \quad (25)$$

$$y = \sum_{i=1}^n N_i(\xi, \eta) y_i$$

The \tilde{D} -matrix, giving the stress-strain relationship, for a three-dimensional isotropic material can be written as

$$\tilde{D} = \begin{bmatrix} D_{\sim 11} & 0 \\ 0 & D_{\sim 22} \end{bmatrix} \quad (26)$$

where

$$D_{\sim 11} = \frac{E}{(1+\nu)(1-2\nu)} \begin{bmatrix} (1-\nu) & \nu & \nu & 0 \\ \nu & (1-\nu) & \nu & 0 \\ \nu & \nu & (1-\nu) & 0 \\ 0 & 0 & 0 & (1-\nu) \end{bmatrix} \quad (27)$$

$$D_{\sim 22} = \frac{E}{(1+\nu)(1-2\nu)} \begin{bmatrix} (1/2-\nu) & 0 \\ 0 & (1/2-\nu) \end{bmatrix}$$

assuming the stresses are given the following sequence

$$\tilde{\sigma}^T = \begin{bmatrix} \sigma_x & \sigma_y & \sigma_z & \tau_{xy} & \tau_{xz} & \tau_{yz} \end{bmatrix} \quad (28)$$

Hence equation (19) becomes explicitly

$$\left[K_{\sim 1, j}^{1, m} \right]^e = \int_v \left[\left[\bar{B}_{\sim 1}^1 \right]^T \sin\left(\frac{l\pi z}{a}\right), \left[\bar{B}_{\sim 1}^1 \right]^T \cos\left(\frac{l\pi z}{a}\right) \right] \begin{bmatrix} D_{\sim 11} & 0 \\ 0 & D_{\sim 22} \end{bmatrix} \begin{bmatrix} \bar{B}_{\sim j}^m \sin\left(\frac{m\pi z}{a}\right) \\ \bar{B}_{\sim j}^m \cos\left(\frac{m\pi z}{a}\right) \end{bmatrix} \quad (29)$$

Since the off-diagonal submatrices of D are zero, the products of sine and cosine terms vanish, and the above equation (29) becomes

$$\left[K_{\sim 1, j}^{1, m} \right]^e = \int_v \left[\bar{B}_{\sim 1}^1 \right]^T D_{\sim 11} \bar{B}_{\sim j}^m \sin\left(\frac{l\pi z}{a}\right) \sin\left(\frac{m\pi z}{a}\right) dV + \int_v \left[\bar{B}_{\sim 1}^1 \right]^T D_{\sim 22} \bar{B}_{\sim j}^m \cos\left(\frac{l\pi z}{a}\right) \cos\left(\frac{m\pi z}{a}\right) dV \quad (30)$$

Due to the orthogonal nature of the basic functions, there are further simplifications

$$\int_0^a \sin\left(\frac{l\pi z}{a}\right) \sin\left(\frac{m\pi z}{a}\right) dz = \begin{cases} 0 & \text{if } l \neq m \\ \frac{a}{2} & \text{if } l = m \end{cases} \quad (31)$$

$$\int_0^a \cos\left(\frac{l\pi z}{a}\right) \cos\left(\frac{m\pi z}{a}\right) dz = \begin{cases} 0 & \text{if } l \neq m \\ \frac{a}{2} & \text{if } l = m \end{cases}$$

and hence

$$K_{\sim 1, j}^{1, m} = 0 \quad \text{for } l \neq m \quad (32)$$

Therefore the overall stiffness matrix becomes diagonal and each harmonic term decouples from the others

$$\tilde{K}^1 = \left[\tilde{K}^{11} \quad \tilde{K}^{22} \quad \dots \quad \tilde{K}^{11} \quad \dots \right] \quad (33)$$

A typical submatrix becomes

$$K_{\sim 1, j}^{11} = \frac{a}{2} \int_A \left(\left[\begin{array}{c} \bar{B}_1^1 \\ \sim 1 \end{array} \right]^T D_{\sim 11} \bar{B}_j^1 + \left[\begin{array}{c} \bar{B}_1^1 \\ \sim 1 \end{array} \right]^T D_{\sim 22} \bar{B}_j^1 \right) dA \quad (34)$$

where A represents the cross-sectional area of the prism.

The loads are also resolved into Fourier's series functions, obtaining for each harmonic a vector of equivalent nodal forces. To make an example, the case of a patch load is considered, starting from the following expansion

$$p = \begin{bmatrix} p_x \\ p_y \\ p_z \end{bmatrix} = \begin{bmatrix} \sum p_x^1 \sin\left(\frac{1\pi z}{a}\right) \\ \sum p_y^1 \sin\left(\frac{1\pi z}{a}\right) \\ \sum p_z^1 \sin\left(\frac{1\pi z}{a}\right) \end{bmatrix} \quad (35)$$

where p_x and p_y and p_z represent the Fourier coefficients of the load for the 1th harmonic.

The equivalent nodal forces are

$$F_{\sim 1}^1 = \int \int_A \begin{bmatrix} p_x^1 N_1 \sin^2\left(\frac{1\pi z}{a}\right) \\ p_y^1 N_1 \sin^2\left(\frac{1\pi z}{a}\right) \\ p_z^1 N_1 \cos^2\left(\frac{1\pi z}{a}\right) \end{bmatrix} dz dS \quad (36)$$

Performing the inner integration and simplifying this reduces to

$$\vec{F}_1^1 = \frac{1}{2l} \begin{bmatrix} p_x^1 \\ p_y^1 \\ p_z^1 \end{bmatrix} \int_S N_1 dS \quad (37)$$

This integration can be performed numerically over the surface length of the element on which the load is applied. If the load is limited by z_1 and z_2 , its amplitude reduces to the form

$$p_x^1 = \frac{2q_x}{l\pi} \left[\cos\left(\frac{l\pi z_1}{a}\right) - \cos\left(\frac{l\pi z_2}{a}\right) \right] \quad (38)$$

Similar procedures can be employed for different loading patterns.

Once the the system of equilibrium equations has been solved for each harmonic, the overall displacements are obtained by summing all the contributions.

To extend the procedure to a circular prism, it is sufficient to interpret the displacements with respect to a cylindrical coordinate system, replacing the coordinate z by the angle ϑ and the span of the prism by the angle α . The displacements become

$$u = \sum_{l=1}^{\infty} \sum_{i=1}^n N_i u_i^1 \sin\left(\frac{l\pi\vartheta}{\alpha}\right) \quad (39)$$

$$v = \sum_{l=1}^{\infty} \sum_{i=1}^n N_i v_i^1 \sin\left(\frac{l\pi\vartheta}{\alpha}\right)$$

$$w = \sum_{l=1}^{\infty} \sum_{i=1}^n N_i w_i^1 \sin\left(\frac{l\pi\vartheta}{\alpha}\right)$$

and the strain components become

$$\vec{\epsilon}^T = \left[\frac{\partial u}{\partial x}, \frac{\partial v}{\partial r}, \frac{1}{r} \frac{\partial w}{\partial \vartheta} + \frac{v}{r}, \frac{\partial u}{\partial r} + \frac{\partial v}{\partial x}, \right] \quad (40)$$

$$\left[\frac{1}{r} \frac{\partial u}{\partial \theta} + \frac{\partial w}{\partial x}, \frac{1}{r} \frac{\partial v}{\partial \theta} + \frac{\partial w}{\partial r} - \frac{w}{r} \right]$$

An application of the method is shown in figure 7, where a curved composite box girder bridge is analysed.

In figure 8 the transverse load distribution is discussed for a prestressed concrete bridge.

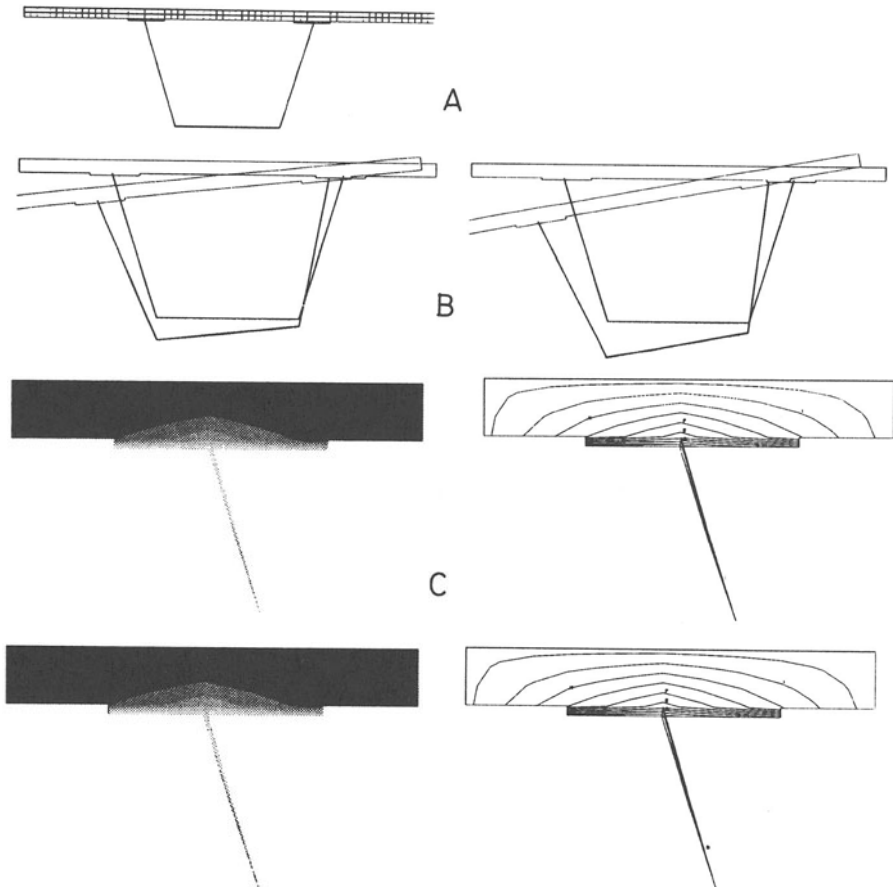


Fig. 7 Application of the finite prism method to the analysis of a curved composite box girder bridge.

A - Finite prism discretisation (span of the bridge = 70 m, radius = 450 m).

B - Deformed configurations at 1/3 of the span and at the mid-span.

C - Detail of the longitudinal stress field at 1/3 of the span and at the mid-span.

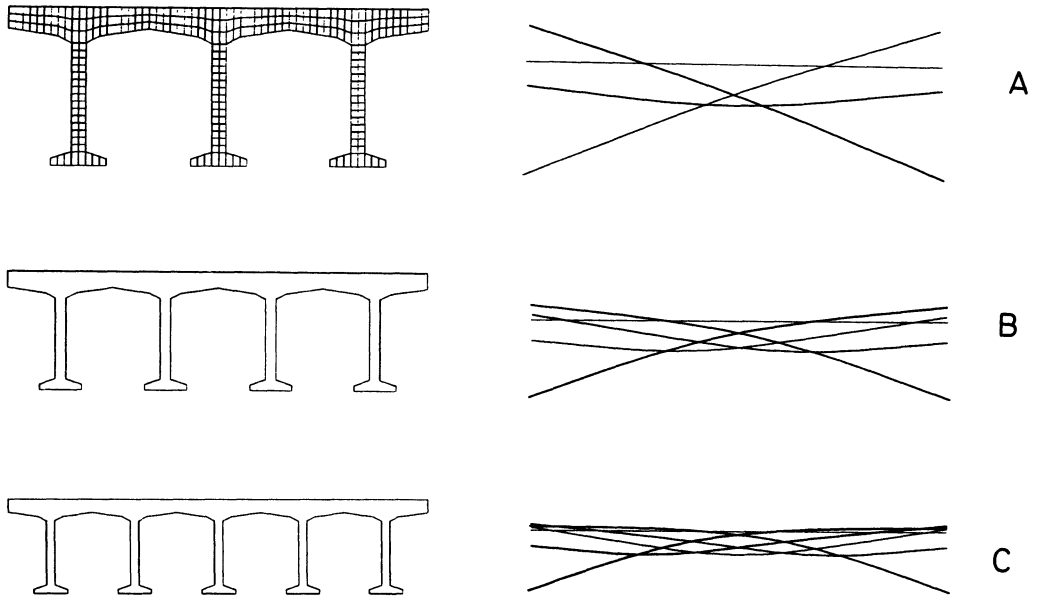


Fig. 8 Parametric study of the transverse load distribution for a prestressed concrete bridge.

A - 3 beams assembly. Influence coefficients of the midspan deflection, corresponding to loads applied with unit intensity in turn over each beam.

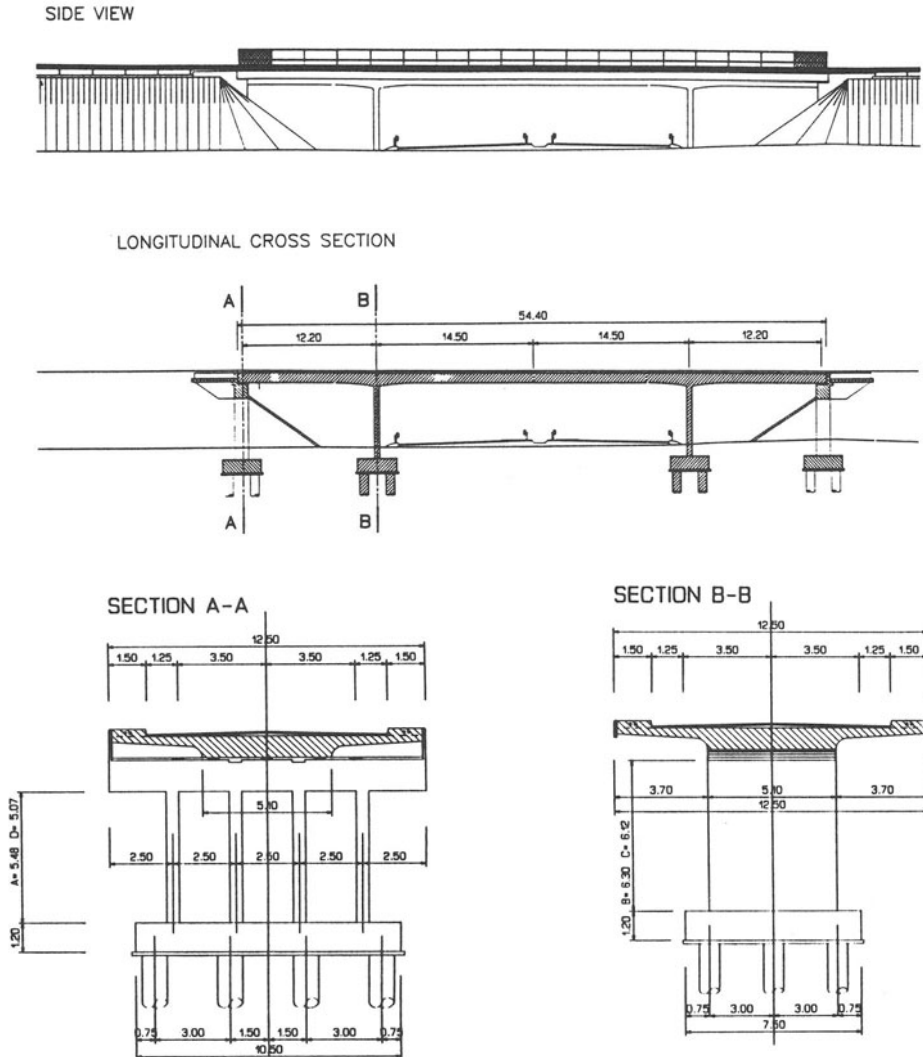
B - Same for a 4 beams assembly.

C - Same for a 5 beams assembly.

The finite prism method, as just presented in its essential form, and the previous application to the analysis of slab bridges as a series of continuous plates connected to beams having rotatory and flexural inertia, are formally restricted by the particular boundary conditions due to the basic functions which are employed. As a matter of fact, studying a continuous multi-span bridge or a bridge slab with intermediate ledgers, leads only to formal complications, as such problems can be solved by a former computation of the influence coefficients of the reaction forces on the corresponding displacements (or points of the intermediate ledgers) and by imposing subsequently the continuity. On the basis of the superposition criterion, this leads only to the introduction of some further loading conditions, whose effects - affected by coefficients drawn by a system of compatibility equations, and hence different for each external loading condition - have to be added to the external loading condition which is in turn under consideration.

4. FINITE ELEMENT MODELS. AN APPLICATION OF VARIABLE THICKNESS THICK PLATES.

Applying generalized finite element model, the behaviour of a class of structures, having the characteristics of the one shown in figure 9, can be effectively investigated taking advantage of particular thick plate elements of variable thickness.



In fact such models are advantageous with respect to fully three-dimensional models not only depending on the reduction of one dimensional degree but above all on the possibility of obtaining the results in a straightforward way for engineering applications.

Plate bending problems had a number of formulations within the finite element method. To give a reference to some early approaches, non conforming elements are worked out in [11] and [12], proving convergent under most practical conditions and today still used for the design and analysis of slabs.

Here is shortly outlined the formulation of a thick plate element, based on the assumptions adopted by Mindlin [13]. The element is derived in details in reference [14], and extended to variable thickness thick plates in [15] and [16]. The assumptions are : that the deflections (w) of the plate are small; that the normals to the midsurface before deformation remain straight but not necessarily normal to the midsurface after deformation; that the stresses normal to the midsurface are negligible irrespective of the loading. Therefore the displacement field can be uniquely specified by an independent variation of the lateral displacement w and of two angles ϑ_x and ϑ_y defining the direction of the line originally normal to the midsurface (fig. 10). In particular ϑ_x and ϑ_y represent average rotations, including angles Φ_x and Φ_y , denoting the average shear deformations, yielding to:

$$\underset{\sim}{\delta} = \begin{bmatrix} w \\ \vartheta_x \\ \vartheta_y \end{bmatrix} = \begin{bmatrix} w \\ \frac{\partial w}{\partial x} + \Phi_x \\ \frac{\partial w}{\partial y} + \Phi_y \end{bmatrix} \quad (41)$$

and

$$\underset{\sim}{\Phi} = \begin{bmatrix} -\phi_x \\ -\Phi_y \end{bmatrix} \quad (42)$$

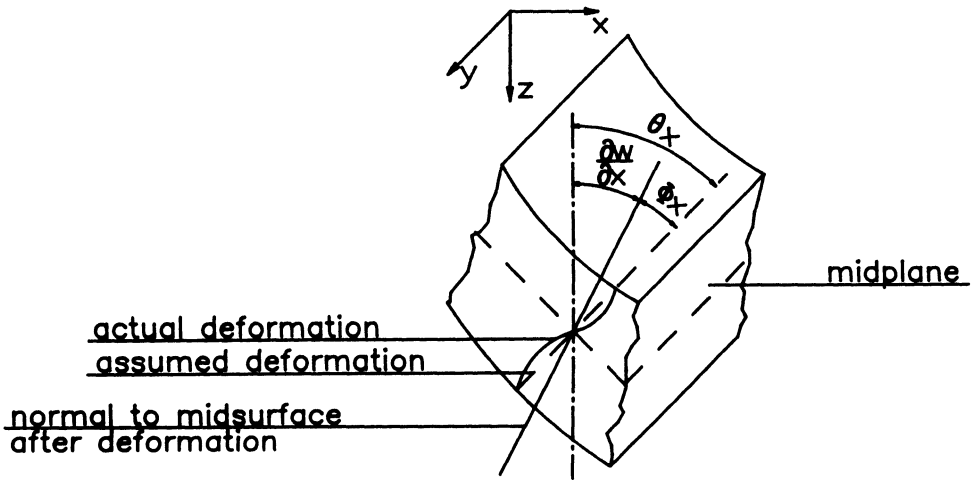


Fig. 10 Deformation of the cross-section of a thick plate of homogeneous material.

Referring to bending moments and shear forces taken as in figure 11, where the x-y plane is taken to coincide with the midsurface of the plate, the stress resultants are defined by the expression

$$\tilde{M} = \begin{bmatrix} M_x \\ M_y \\ M_{xy} \end{bmatrix} = \begin{bmatrix} \int \sigma_x z dz \\ \int \sigma_y z dz \\ \int \tau_{xy} z dz \end{bmatrix} \quad (43)$$

and

$$\tilde{Q} = \begin{bmatrix} Q_x \\ Q_y \end{bmatrix} = \begin{bmatrix} \int \tau_{xz} dz \\ \int \tau_{yz} dz \end{bmatrix} \quad (44)$$

where the integrals are calculated over the range $z=-t/2$ to $z=+t/2$, if t is the plate thickness.

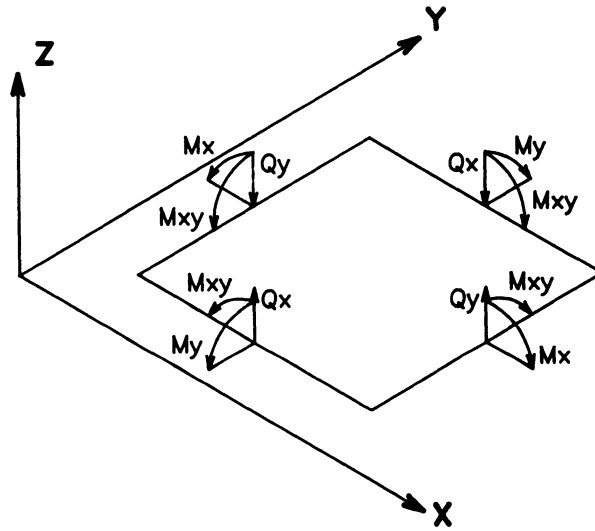


Fig. 11 Sign convention for bending moments and shear forces.

The total potential energy of the plate may be written as

$$\pi = \frac{1}{2} \int_A (\underline{M})^T \underline{\chi} + [\underline{Q}]^T \underline{\phi} \, dA - \int_A q_w \, dA \tag{45}$$

where

$$\underline{\chi} = \begin{bmatrix} \chi_x \\ \chi_y \\ \chi_{xy} \end{bmatrix} = \begin{bmatrix} - \frac{\partial \phi}{\partial x} \\ - \frac{\partial \phi}{\partial y} \\ - \left[\frac{\partial \phi}{\partial y} \frac{\partial \phi}{\partial x} \right] \end{bmatrix} \tag{46}$$

$\chi_x, \chi_y, \chi_{xy}$ are measures of bending deformation, and q is the distributed load per unit area.

The stress-strain relationships may be written in the following form

$$\tilde{M} = \tilde{D}_f \tilde{\chi} \quad (47)$$

and

$$\tilde{Q} = \tilde{D}_s \tilde{\Phi} \quad (48)$$

where for an isotropic homogeneous material

$$\tilde{D}_f = \frac{Et^3}{12(1-\nu^2)} \begin{bmatrix} 1 & \nu & 0 \\ \nu & 1 & 0 \\ 0 & 0 & (1-\nu)/2 \end{bmatrix} \quad (49)$$

and

$$\tilde{D}_s = \frac{Et}{2(1-\nu)\alpha} \begin{bmatrix} 1 & 0 \\ 0 & 1 \end{bmatrix} \quad (50)$$

where $\alpha=6/5$ allows for warping of the cross-section. For cellular plates or sandwich plates, the matrices D can be readily modified for instance as discussed in [17].

Substituting into (45) one obtains

$$\tilde{\pi} = \frac{1}{2} \int_A ([\tilde{\chi}]^T \tilde{D}_f \tilde{\chi} + [\tilde{\Phi}]^T \tilde{D}_s \tilde{\Phi}) dA - \int_A q w dA \quad (51)$$

Following standard procedures for isoparametric finite elements, a typical submatrix of K , linking nodes p and q may be written as

$$K_{\tilde{p}q} = K_{\tilde{p}qf} + K_{\tilde{p}qs} \quad (52)$$

where

$$K_{\tilde{p}qf} = \iint [B_{\tilde{p}f}]^T \tilde{D}_f B_{\tilde{q}f} dx dy \quad (53)$$

and

$$K_{\sim pqs} = \iint [B_{\sim ps}]^T D_{\sim s} B_{\sim qs} dx dy \tag{54}$$

where

$$B_{\sim 1} = \begin{bmatrix} B_{\sim f1} \\ B_{\sim s1} \end{bmatrix} = \begin{bmatrix} 0 & -\frac{\partial N_1}{\partial x} & 0 \\ 0 & 0 & -\frac{\partial N_1}{\partial y} \\ 0 & -\frac{\partial N_1}{\partial y} & -\frac{\partial N_1}{\partial x} \\ \hline \frac{\partial N_1}{\partial x} & -N_1 & 0 \\ \frac{\partial N_1}{\partial y} & 0 & -N_1 \end{bmatrix} \tag{55}$$

N are the shape functions, and the B -matrix is splitted into the part associated with bending deformations and the part associated with shear deformation.

A straightforward extension of the above element can be obtained coupling the plate with a membrane element.

The main advantages of the above formulation are:

- the reliability of the finite element, particularly if this is based on parabolic shape functions;
- the plain description of the loads;
- the interpretation of the results directly in terms of stress resultant parameters and boundary reactions;
- minimum hardware requirements;
- practically negligible numerical instability.

On the contrary there are obvious restrictions to the possible applications, in particular if the element is not coupled with a membrane one.

An application is shown for the slab bridge of figure 9. The finite element mesh adopted and some results are given in figure 12.

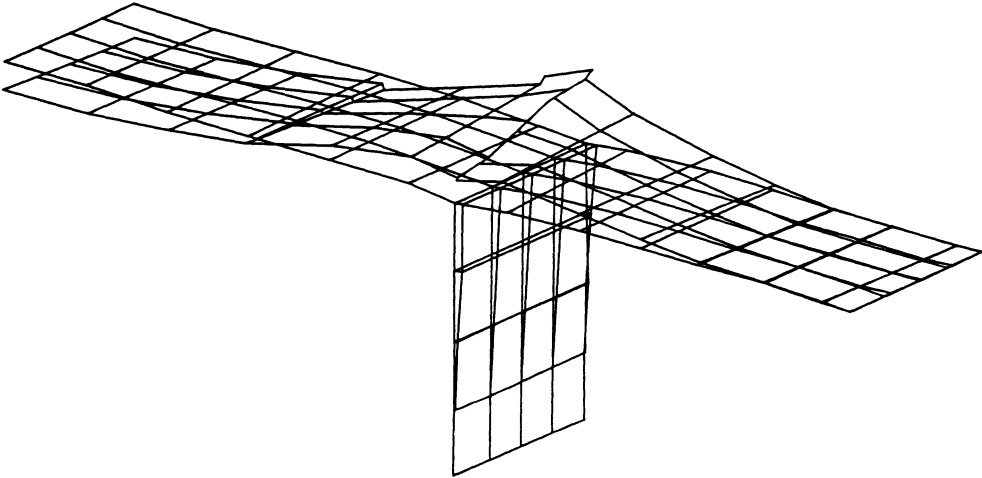


Fig. 12 Highway overpass.- Discretization with variable thickness thick elements of half structure - Bending distribution corresponding to a given loading.

5. GENERAL APPLICATIONS OF THE FINITE ELEMENT METHOD.

The previous applications have been discussed to point out that tailoring a general approach to a given category of problems leads to a more direct solution or at least to a solution which is easier to be used in practice.

However today performances of hardware and software systems address to the use of non specific tools in a number of fields, including the structural analysis. A general purpose finite element program for the analysis of the static and dynamic answer of structures and continuous bodies - characterised by linear or geometrically or material non-linear behaviour - can be effectively employed for the

majority of problems. Preference is given to the reliability of programs coming from high credit technical staffs, widely tested and well established so as to comply with the requirements of the most sophisticated modelling, giving also the opportunity to practically work in an homogeneous computational environment. In fact the time needed to input the problem data as well as the time needed to read the results is normally much longer than the time needed to run the analysis : that phases of the work have then to be favoured, trying also to keep the possibility of errors to a minimum.

Nevertheless there are some areas where general purpose programs co-exist with specific applications. This happens for instance when a procedure within a general purpose program is difficult to be controlled, like in the case of geometrically non-linear analysis of cable structures. A hypostatic problem arises, where a starting configuration has to be chosen satisfying the equilibrium and compatibility conditions, while being achievable in practice. Such type of formulation is discussed in [18], from which the example of a continuous suspension bridge is taken (fig. 13), as well as the stability analysis of a bow-string girder (fig. 14).

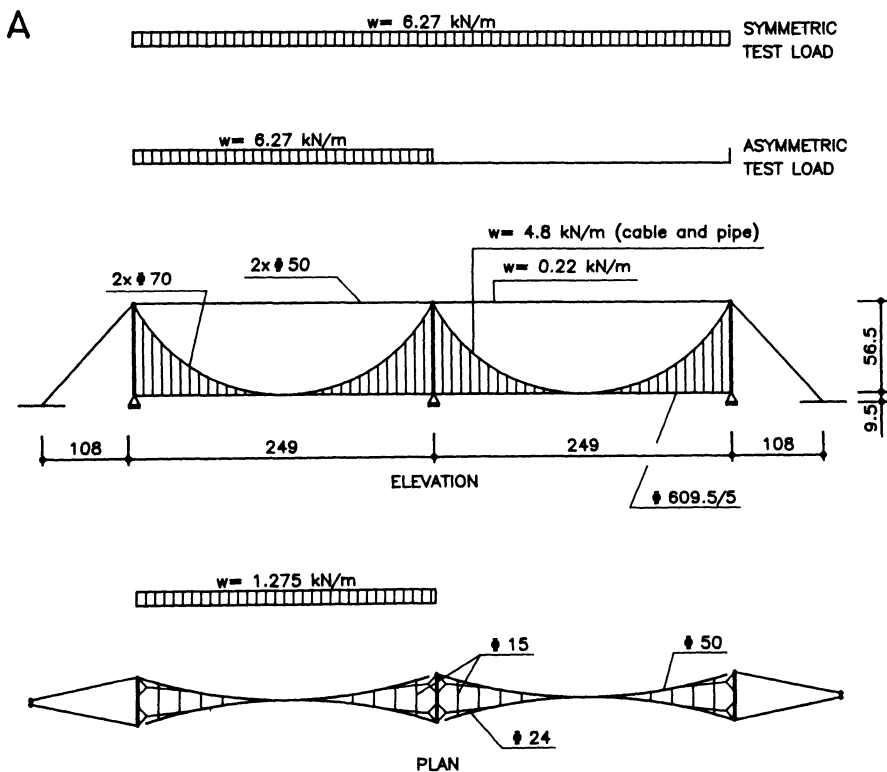


Fig. 13

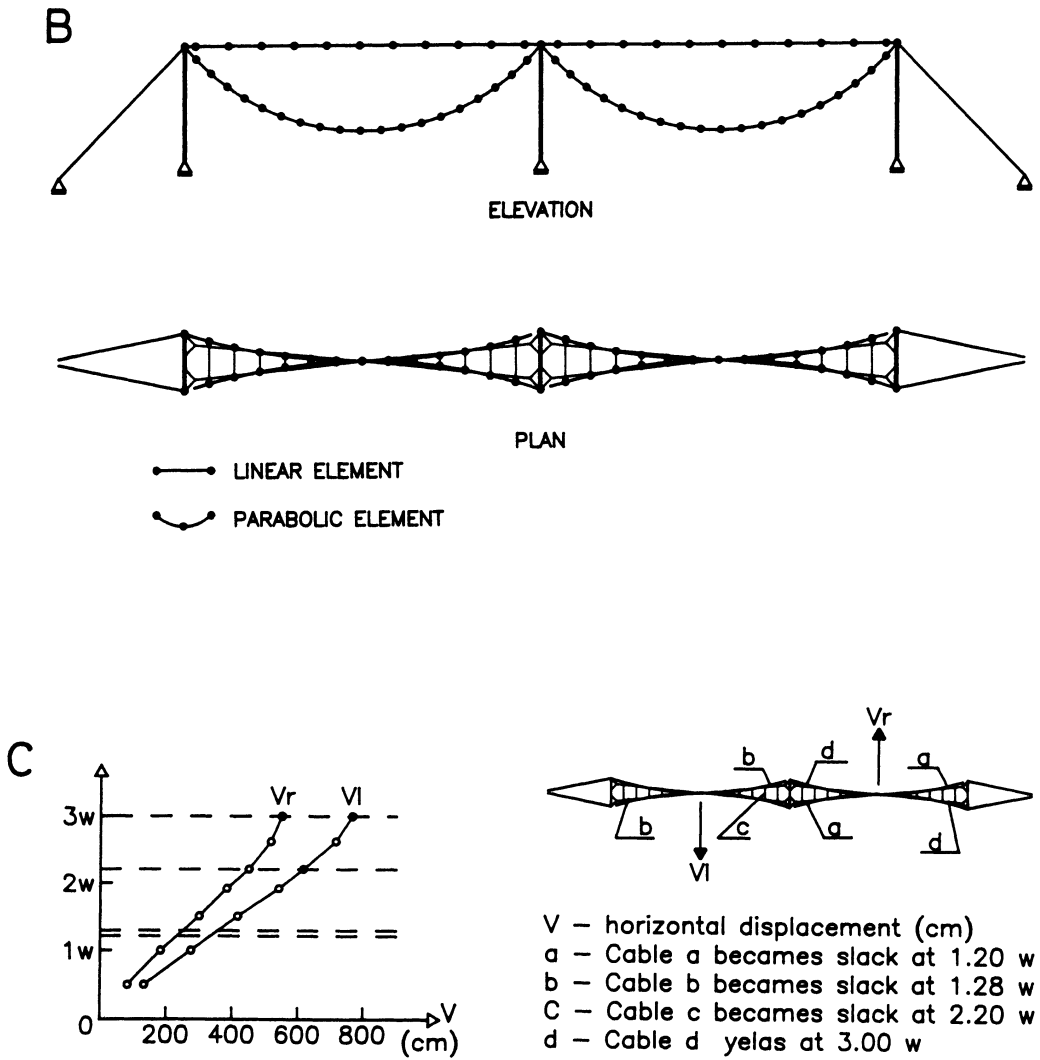


Fig. 13 Continuous suspension bridge carrying a gas pipeline.
 A - Layout and loading.
 B - Finite element model.
 C - Load/deflection behaviour (asymmetric wind loading).

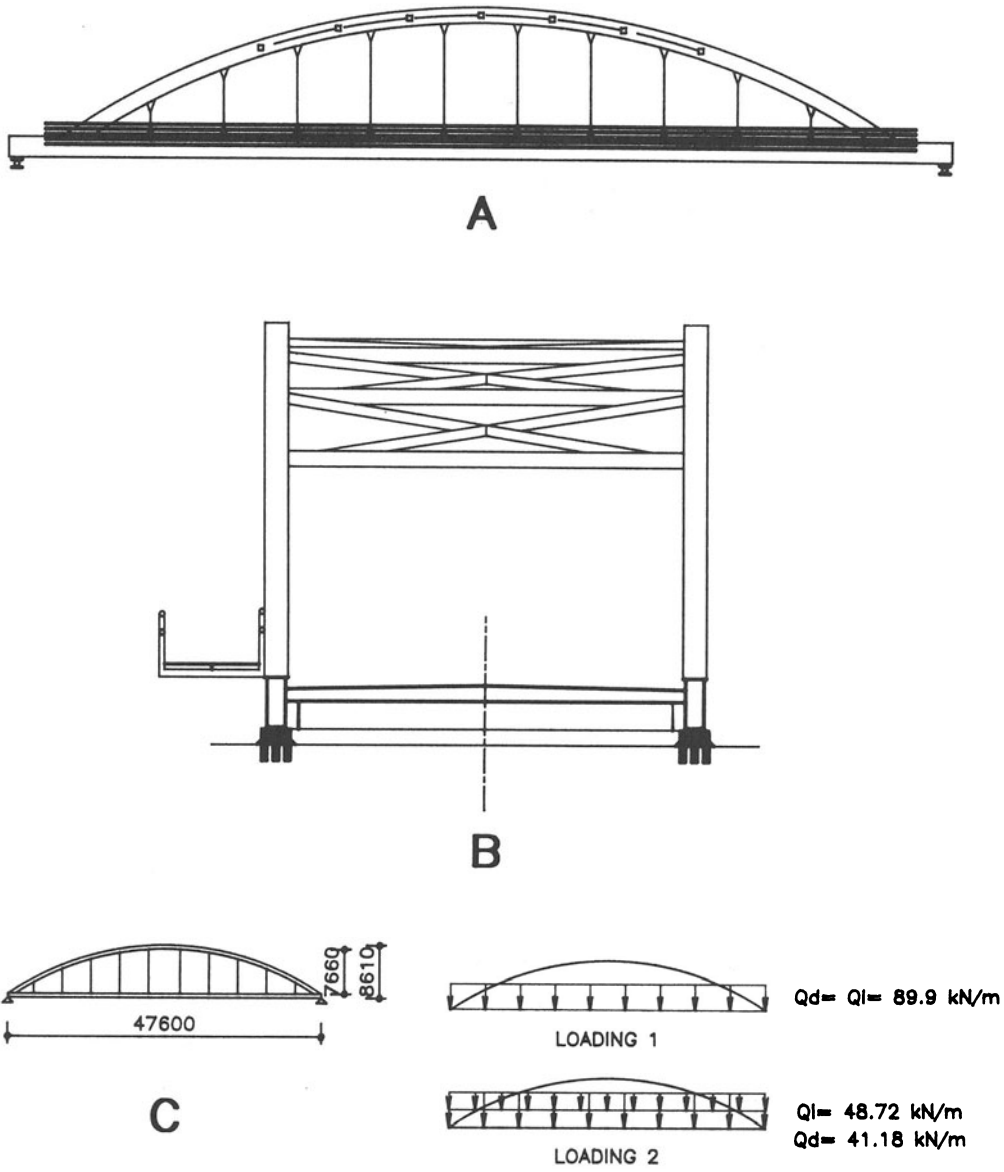


Fig. 14 Buckling analysis of a bow-string girder.
A - Elevation.
B - Front view.
C - Finite element discretisation.

A general purpose finite element program gives also overall information on the structure, pertaining to particular features of the specific problem. For instance one can limit himself to obtaining the load subdivision in a complex situation. To explain this method the example of figure 15 is considered. It is a three-span continuous reinforced concrete bridge, with four variable section longitudinal T-beams. To find the loading configurations giving any maximum stress resultant at any section of a given beam a fully three-dimensional finite element model is employed, drawing the influence coefficients of the loads on the deflections, for instance for the schemas 1 to 6 applied with unit intensity in turn over an external beam and over an intermediate one. Combining then with the cross schemas A and B, the conditions for the maximum stresses are obtained. Some results of the analysis are listed in the following table.

Loading cond.	Tot. trans. load (t/m)	Deflection				Rel. load				Absolute load			
		T 1	T 2	T 3	T 4	T 1	T 2	T 3	T 4	T 1	T 2	T 3	T 4
C.C.1	12,554	2,248	2,169	1,629	0,973	0,320	0,309	0,232	0,139	4,021	3,879	2,914	1,740
C.C.2	9,829	1,316	1,323	1,046	0,687	0,301	0,303	0,239	0,157	2,959	2,974	2,352	1,544
		0,604	0,654	0,498	0,316	0,292	0,316	0,240	0,153	2,865	3,102	2,362	1,499
C.C.3	14,503	1,689	1,689	1,270	0,787	0,311	0,311	0,234	0,145	4,507	4,507	3,389	2,100
C.C.4	8,6	0,707	0,704	0,704	0,707	0,251	0,249	0,249	0,251	2,155	2,141	2,141	2,155
		0,497	0,490	0,490	0,497	0,252	0,248	0,248	0,252	2,167	2,133	2,133	2,167
C.C.5	9,010	2,269	1,875	0,966	0,065	0,438	0,362	0,187	0,013	3,950	3,264	1,682	0,113
C.C.6	6,462	1,343	1,112	0,548	0,008	0,446	0,369	0,182	0,003	2,882	2,386	1,176	0,017
		0,617	0,560	0,251	-0,010	0,435	0,395	0,177	-0,007	2,812	2,552	1,144	-0,046

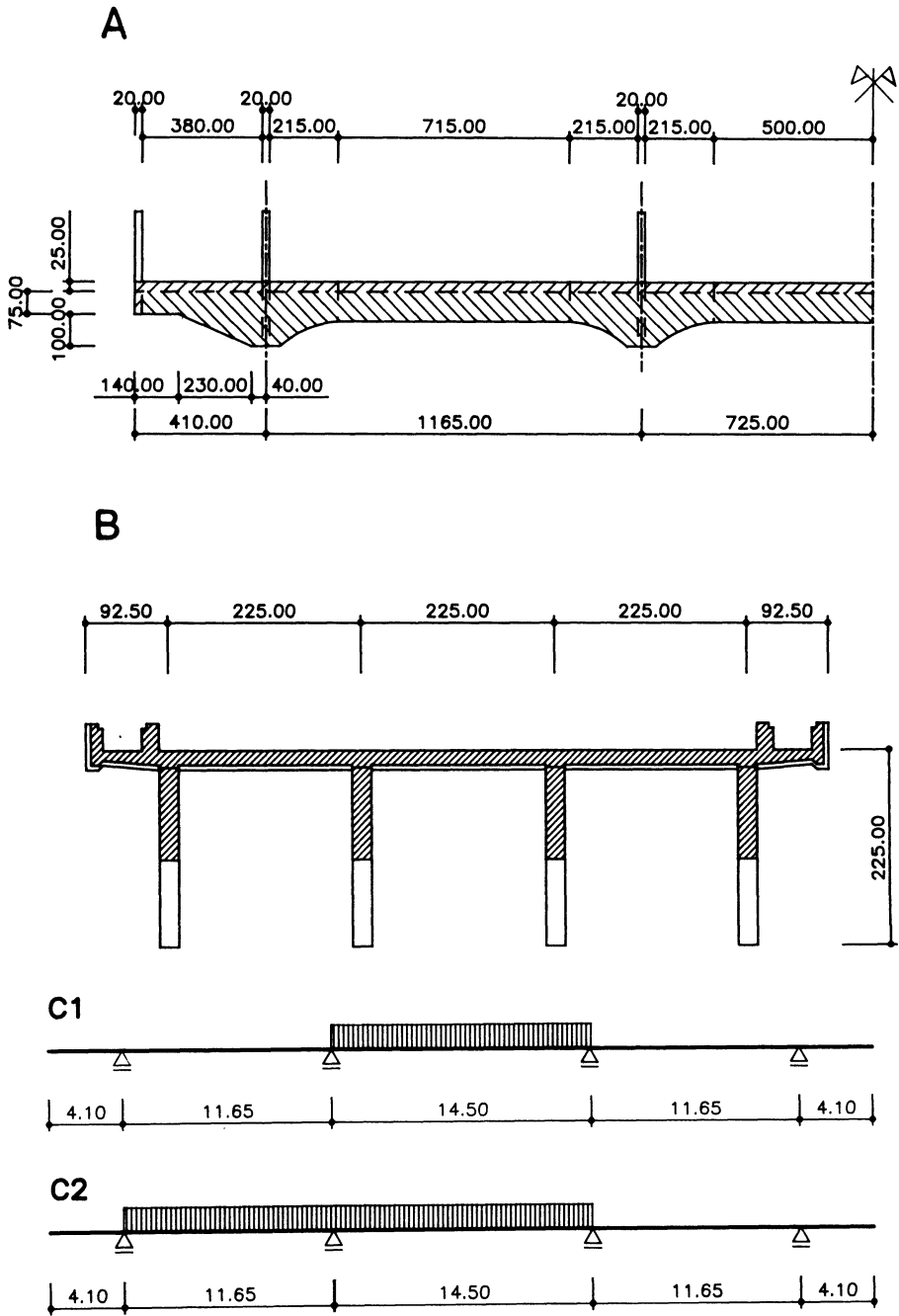


Fig. 15

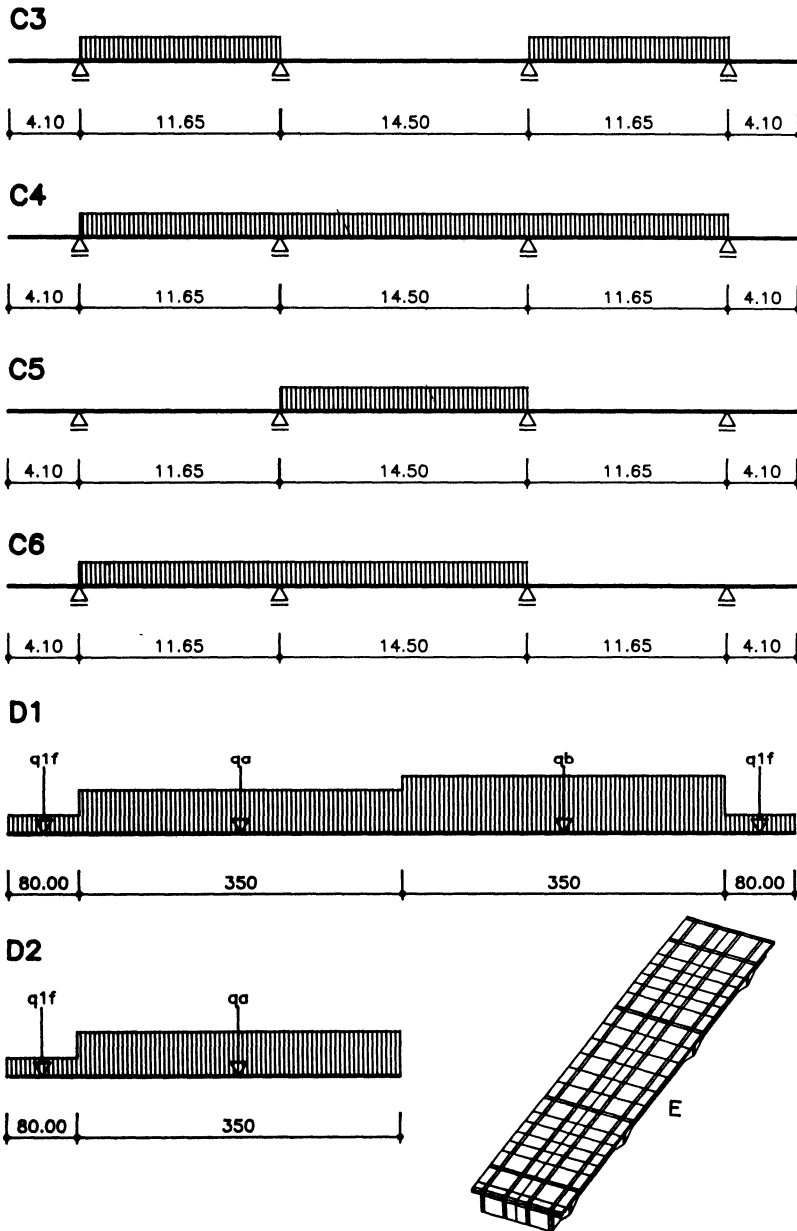


Fig. 15 Three span continuous reinforced concrete bridge.
 A - Longitudinal cross section.
 B - Transversal cross section.
 C - Longitudinal loading patterns.
 D - Transversal loading pattern.
 E - Finite element discretization.

The design of any section is then reduced to the standard one for a T-beam. It is remarkable that, being the model employed only for the search of deflections, the number of elements is very small: in fact the solution is within the deformation approach. Hence the application is highly effective.

On the other hand if a fully three-dimensional model is meant to work out the stress state and the material is non-homogeneous, the outcome needs to be interpreted. For instance a three-dimensional model of the highway overpass of figure 9 (solved above with thick plate elements) gives graphical results in terms of stress contours or contours of combinations of stress values (fig. 16).

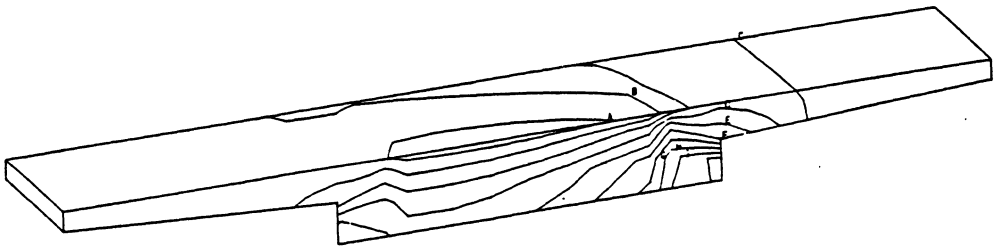


Fig. 16 Highway overpass. Contour of the shear stresses over a section at the intermediate support.

In conclusion the main difference between the use of a specific program and the use of a general purpose program is that in the first case the solution is conditional on a fixed model, which is assumed to be representative for both the preliminary calculation and the final design, while in the second case the modelling is fully free and can each time suit the design concept and the desired degree of precision. To make an example reference is made to the problem of figure 17, relating to a posttensioned concrete continuous slab bridge of three spans in a bend. To detail the corresponding finite element model to the limits of the method, a three-dimensional discretisation should be

employed, including the actual path of the tendons. The nodal forces equivalent to the prestressing force over any element can be computed as described in [19]. There are but many theoretical and practical reasons against such approach. From the practical point of view the model comes out to be complicated to be managed - in particular in the preliminary design phase, where changing the path of a tendon could lead to rework the model completely -, the computation is heavy - with consequences which are not negligible, especially in the handling of the results -, and the results are difficult to be interpreted. From the theoretical point of view, even if the program provides for the elastic-viscoplastic behaviour of three-dimensional continua, the experimental data are inadequate to lay down a three-axial characteristic relationship for stresses and strains and for their gradients. Following the above method leads rather to an investigation on the research side than to obtaining effective information for the design. A more direct and useful model is based on shell elements, combining the plate bending effects and the in-plane membrane stresses, and coded with non-linear constitutive relationships for layered materials. If this is the model, then the path of the tendons must be described materialising at each point their eccentricity with respect to the mid-plane of the plate. Figure 17 shows such type of application.

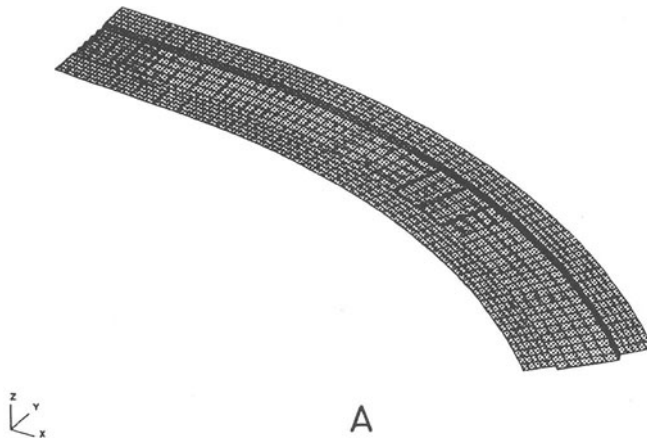


Fig. 17

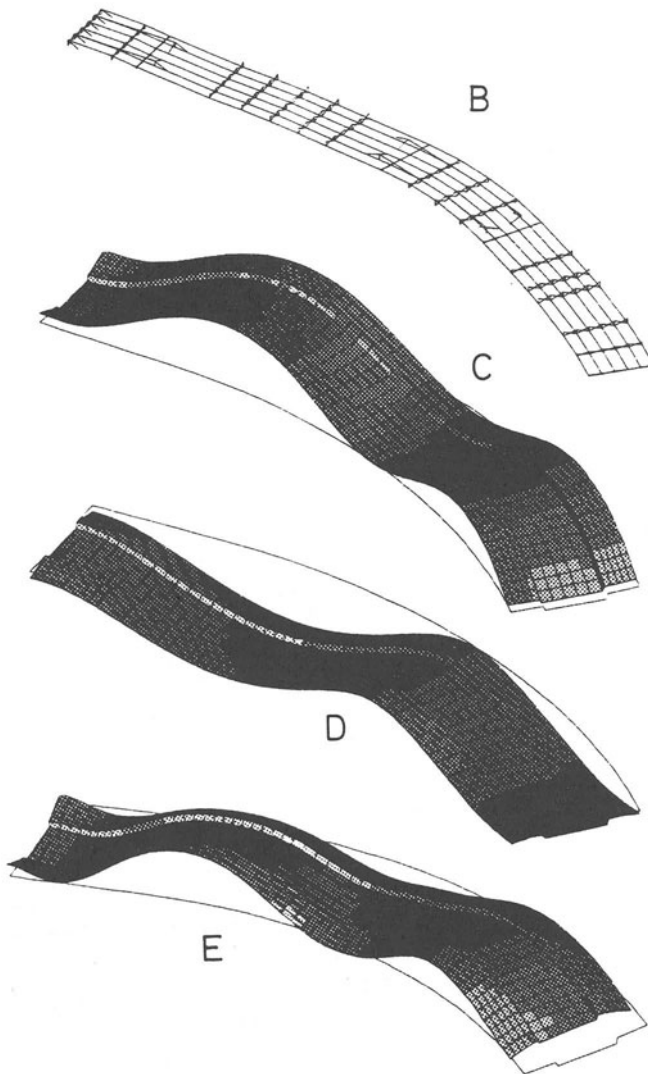


Fig. 17 Posttensioned concrete continuous slab bridge of three spans in a bend.

A - Finite element model of the slab.

B - Finite element model of the path of the tendons.

C - Prestressing force - Deformed configuration.

D - Dead load - Deformed configuration.

E - Superposition of C and D - Deformed configuration.

A further example (fig 18) illustrates the versatility of a general purpose program. It is an aluminium truss bridge with an upper orthotropic deck plate. The bridge has been designed to be employed provisionally over variable spans, which are obtained assembling a given number of elementary parts. The model reflects the same characteristics. Shell elements are employed for the deck plate, taking into account an orthotropic constitutive relationship, which has been obtained working out the load/displacement law on a detailed model of a portion. Then a mixed beam and shell model is set up for any elementary part of the bridge and for the end structures. Each one of these is handled as a substructure of a chain structure of variable size, the analysis of which becomes straightforward both with respect to static and dynamic loads.

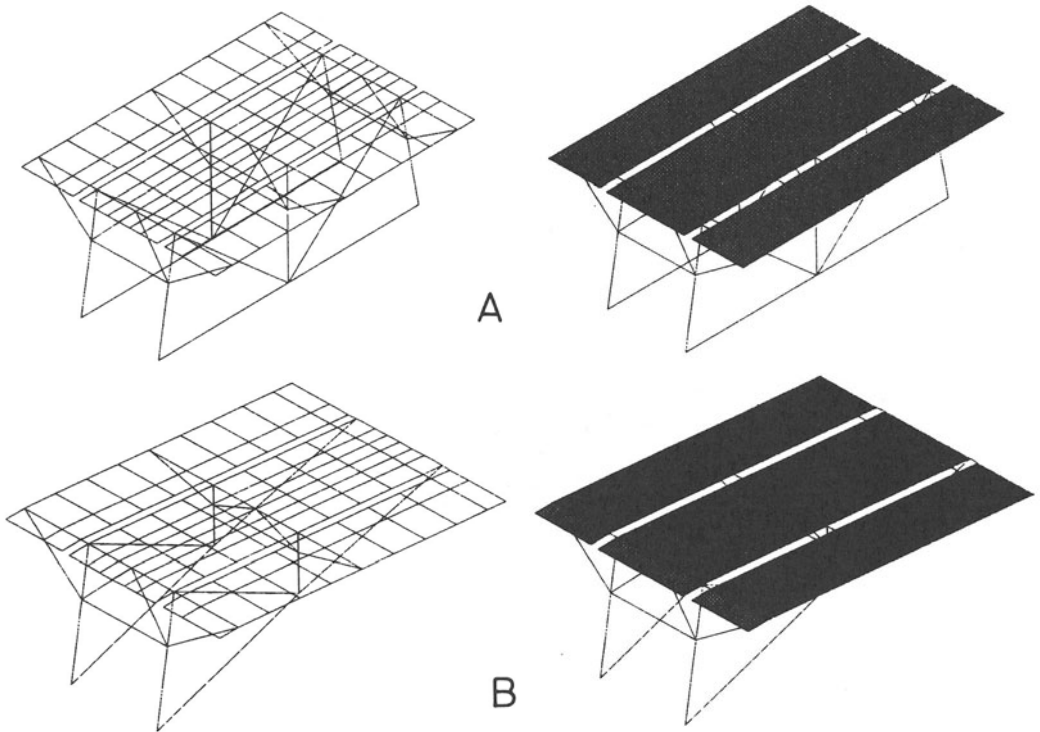


Fig. 18

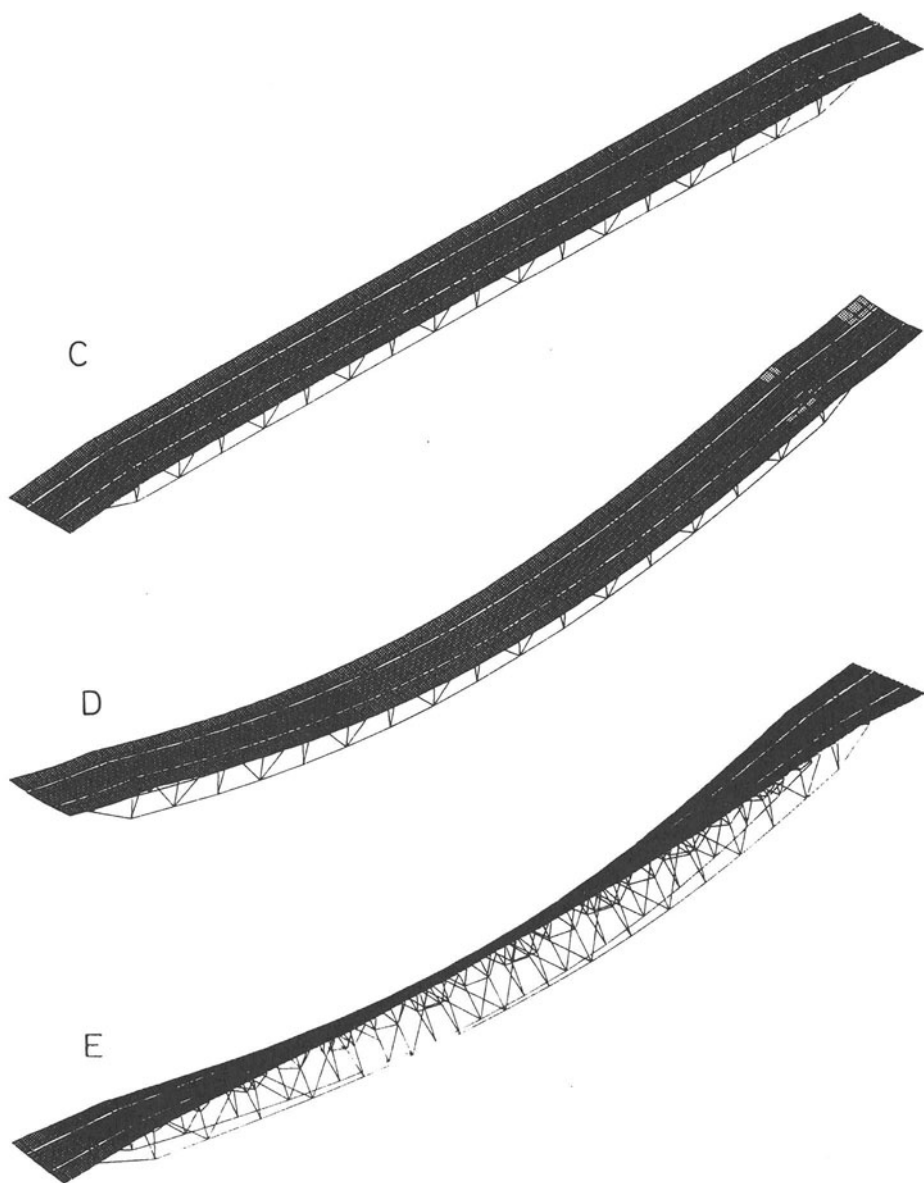


Fig. 18 Aluminium truss bridge with an upper orthotropic deck plate.
A - Finite element model of an intermediate component.
B - Finite element model of an end component.
C - Overall assembled structure.
D - Dead-load - Deformed configuration.
E - First free vibration frequency.

In favour of the application of a general purpose program, to work in an homogeneous computational environment, a practice normally takes place reducing the difference towards a specific program. In fact, whenever the application repeats itself, it turns out to be natural to code within a general purpose program a procedure for the automatic mesh generation and handling of the results, fixing once and for all a satisfactory model and the logical path of the use, including the references to specific standards. On the actual stage this is probably the most professional attitude. By the way the programs we are talking about make the internal coding of a procedure quite easy, allowing the different functions of a process to be directly addressed and stored in a journal file to be accessed afterwards for new applications.

6. CONCLUSIONS.

Some applications have been presented of the computer based structural analysis of given classes of bridges. Some other applications, while being coded for different specific purposes, suit quite well a number of cases. Eventually the general purpose finite element programs free the modelling of any structure, and hence of the bridge structures. The outline which is here proposed is not at all exhaustive of the subject nor gives definite categories. However the attitude is indirectly described with which the user of any actual computer program should face this kind of problems to get an effective solution in practice.

REFERENCES

1. Casellato A., Vescovi U., Vitaliani R., CALCOLO DI SOLETTE DA PONTE COME SERIE DI LASTRE CONTINUE COLLEGATE A TRAVI DEFORMABILI PER FLESSIONE E TORSIONE, Giornale del Genio Civile, ott-dic. 1976, 411-422.
2. Casellato A., Vitaliani R., Vescovi U., STRESS ANALYSIS OF BRIDGE SLABS WITH MICROCOMPUTERS, Proc. First Int. Conf. on Engineering Software for Microcomputers, Venezia, 2-5 aprile 1984, 119-133.
3. Cheung Y.K., THE FINITE STRIP METHOD IN THE ANALYSIS OF ELASTIC PLATES WITH TWO ENDS SIMPLY SUPPORTED, Proc. Inst. Civ. Eng. 40, 1968, 1-7.
4. Cheung Y.K., FOLDED PLATE STRUCTURES BY THE FINITE STRIP METHOD, Proc. A.M.S.C.E., 94, 1969, 2963-2979.

5. Grafton P.E., Strome P.R., ANALYSIS OF AXISYMMETRIC SHELLS BY THE DIRECT STIFFNESS METHOD, J.A.I.A.A. 1 1963, 2342-2347.
6. Ahmad S., Irons B.M., Zienkiewicz O.C., CURVED THICK SHELL AND MEMBRANE ELEMENTS WITH PARTICULAR REFERENCE TO AXISYMMETRIC PROBLEMS, Proc. 2nd Conf. on Matrix Methods in Structural Mechanics, Wright-Patterson Air Force Base, Ohio, 1968.
7. Loo Y.C., Cusens A.R., A REFINED FINITE STRIP METHOD FOR THE ANALYSIS OF ORTHOTROPIC PLATES, Proc. I.C.E., 48, 1971, 85-91.
8. Deist F.H., AN EXTENSION OF THE TWO-DIMENSIONAL FINITE ELEMENT METHOD TO REPETITIVE THREE-DIMENSIONAL SITUATIONS, The South African Mechanical Engineer, 140, 1969.
9. Zienkiewicz O.C., Too J.J.M., THE FINITE PRISM IN THE ANALYSIS OF THICK SIMPLY SUPPORTED BRIDGE BOXES, Proc. Inst. C.E., 53, 1972, 147-171.
10. Too J.J.M., TWO DIMENSION, PLATE, SHELL AND FINITE PRISM ISOPARAMETRIC ELEMENTS AND THEIR APPLICATIONS, Ph.D. Thesis, C/PH/14/71, Swansea 1971.
11. Zienkiewicz O.C., Cheung Y.K., THE FINITE ELEMENT METHOD FOR ANALYSIS OF ELASTIC ISOTROPIC AND ORTHOTROPIC SLABS, Proc. Inst. Civ. Eng. 28, 1964, 471-488.
12. Cheung Y.K., King I.P., Zienkiewicz O.C., SLAB BRIDGES WITH ARBITRARY SHAPE AND SUPPORT CONDITIONS : A GENERAL METHOD OF ANALYSIS BASED ON FINITE ELEMENTS, Proc. Inst. Civ. Eng. 40, 1968, 9-36.
13. Mindlin R.D., INFLUENCE OF ROTATORY INERTIA AND SHEAR ON FLEXURAL MOTIONS OF ISOTROPIC ELASTIC PLATES, J. Appl. Mech. 18, 1951, 31-38.
14. Hinton E., Owen D.R.J., FINITE ELEMENT PROGRAMMING, Academic Press, 1977.
15. Hinton E., Schrefler B.A., Natali A., A FINITE ELEMENT METHOD FOR VARIABLE THICKNESS PLATES, Proc. XXII ICES Conf., McGill University, Montreal, 1979.
16. Natali A., Odorizzi S., VARIABLE THICKNESS PLATES BOUNDED TO AN ELSTIC ISOTROPIC HALF SPACE : A FINITE ELEMENT APPROACH, Proc. XXI ICES Conf., Padova, 1978.
17. Hinton E., Razzaque A., Zienkiewicz O.C., Davies J.D., A SIMPLE FINITE ELEMENT SOLUTION FOR PLATES OF HOMOGENEOUS, SANDWICH AND CELLULAR CONSTRUCTION, Proc. Inst. Civ. Eng. 59, 1975, 43-46.

-
18. Schrefler B.A., Odorizzi S., Wood R.D., A TOTAL LAGRANGIAN GEOMETRICALLY NON-LINEAR ANALYSIS OF COMBINED BEAM AND CABLE STRUCTURES, *Computer and Structures*, 17, 1983, 115-127.
 19. Majorana C., Odorizzi S., Vitaliani R., ANALISI AD ELEMENTI FINITI DI MEMBRATURE TRIDIMENSIONALI PRESOLLECITATE, A COMPORTAMENTO ELASTO-VISCOPLASTICO, *La Prefabbricazione*, sett. 1984, 583-594.